

Thèse présentée pour obtenir le grade de
DOCTEUR DE L'ÉCOLE POLYTECHNIQUE

par

Hannes HÜBENER

**Second Harmonic Generation in Solids:
Theory and Simulation**

Soutenue le 24 Septembre 2010 devant le jury composé de :

Prof.	Friedhelm BECHSTEDT	Rapporteur
Prof.	Eric SURAUD	Rapporteur
Prof.	Silke BIERMANN	Examinatrice
Prof.	Benoit BOULANGER	Examineur
Dr.	Christian BROUDER	Examineur
Dr.	Valérie VÉNIARD	Directrice

Contents

1	Introduction	1
1.1	Second Harmonic Generation	2
1.2	Ab initio optical excitations	3
1.3	Calculations of Second Harmonic generation	5
1.4	This work	7
2	Second order TDDFT	10
2.1	Second order Response theory	10
2.2	Perturbation theory	11
2.2.1	Response functions	14
2.3	TDDFT	16
2.3.1	Interpretation of the solution	21
2.3.2	Graphical representation of the 2nd order Dyson Equation	24
2.4	Approximations	26
2.4.1	IPA	26
2.4.2	RPA	26
2.4.3	TDLDA	26
2.4.4	Quasiparticles	27
2.4.5	Excitons	28
3	Macroscopic response and local fields	31
3.1	Macroscopic average	31
3.2	Macroscopic response	32
3.3	Macroscopic response from TDDFT	36
3.3.1	Components of $\chi^{(2)}$	41
3.3.2	Macroscopic IPA response	44
4	Optical limit	46
4.1	perturbation theory in \mathbf{q}	48
4.1.1	$\mathbf{q} \rightarrow 0$ for $\chi_0^{(2)}$	49
4.2	Scissors shift	51
4.3	Exact optical transitions	52
4.3.1	Time reversal	54
4.3.2	Inversion	56
4.3.3	Time reversal and Inversion	57
4.4	Transverse vs. Longitudinal response	58

5	Spatial dispersion	61
5.1	Linear spatial dispersion	61
5.1.1	symmetry properties of tensors	62
5.2	SHG	64
5.2.1	Dipole case	65
5.2.2	Quadrupole case	66
6	Results	69
6.0.3	Structures	69
6.1	Independent (Quasi-)Particle Approximation	71
6.1.1	Transitions in c-SiC	71
6.2	Crystal Local Field effects	72
6.3	Exchange and correlation	75
6.3.1	ALDA	78
6.3.2	Long Range Kernel	79
6.4	GaAs spectrum as a Benchmark	82
7	A second order Bethe-Salpeter Equation	86
7.1	The equation	86
7.2	The non-interacting part L_{03}	89
7.3	The second order many-body kernel Ξ_3	89
7.4	Connection to Many Body Perturbation Theory	90
7.5	A g_{xc} from MBPT	91
8	Conclusions	94
A	Independent particle response function	96
B	Fourier Transforms	98
C	Degenerate perturbation theory	100
D	Derivation of the 2nd order Bethe-Salpter equation	109
E	Hedin's equations	117
F	Second order TDDFT and BSE	121

1 Introduction

Nonlinear optics is the field of research where a material is subjected to so intense light that its response to this light yields fundamentally different properties than observed in the more common optics that has been known and explored for centuries and is now referred to as linear optics. Since the light needs to be of high intensity, i.e. yield a high photon density, it was not until the advent of the laser in 1960 that nonlinear optics could be discovered, although there had been a theoretical prediction of two-photon absorption in 1931 [1]. In 1961 Franken et al. [2] used a laser with a wavelength of 6942 Å and observed an outgoing radiation with a wavelength of 3471 Å, i.e. with double the frequency. This was interpreted as the generation of the second harmonic in optical light, a phenomenon previously only known for radio waves.

The distinction between nonlinear and linear optics is made with respect to the intensity of the field. This means, while in linear optics the response of a material is proportional to the amplitude of the applied field, in nonlinear optics it is related to the square, the cube etc. of this field. Formally one can write down the polarization of the material expanded in terms of the field as [3, 4]

$$\mathbf{P} = \chi^{(1)}\mathbf{E} + \chi^{(2)}\mathbf{E}\mathbf{E} + \chi^{(3)}\mathbf{E}\mathbf{E}\mathbf{E} + \dots \quad (1.1)$$

where the term $\chi^{(1)}$ determines the linear optical response and all effects described by the other terms are referred to as nonlinear. Obviously, this one name refers to many effects in all orders, which can be fundamentally different. For example, second order effects are completely absent for materials with inversion symmetry and light that can be described within the dipole approximation, while third order effects are in principle always present. The susceptibilities $\chi^{(i)}$ are thus material dependent and while the efficiency of the effects can be very different for different materials, there is no material that does not exhibit any nonlinear properties. But even within one order, say the second or the third, one has a variety of effects of very different quality. Second order phenomena comprise not only the doubling of an incoming frequencies as encountered in second harmonic generation, but also the response with the sum or difference of two different incoming frequencies (sum/difference frequency generation), the splitting of one incoming photon into two outgoing ones (optical parametric amplification) or the creation of a DC field out of an intense AC field (optical rectification)[3, 4]. To third order, there are phenomena such as two photon absorption, third harmonic generation (or generally four wave mixing phenomena) and a nonlinear refractive index that can lead to the focalization of the laser inside the material by the material itself (self-focalization). A nonlinear optical process can be thought of as occurring in two steps: the intense light induces a nonlinear response in the material on a microscopic level that in turn

modifies the optical fields. The first step is related to the microscopic structure of the material and thus governed by quantum mechanics, while the second step is described by Maxwell's equations.

1.1 Second Harmonic Generation

In this thesis I will almost exclusively consider the case of second harmonic generation. The reason is, because on the one hand, it is one of the most widely used nonlinear optical effects and on the other hand because, being of lowest order, it is the simplest nonlinear effect to describe. Many considerations and the general formalism apply however also to other second order processes or can be readily generalized to third order. One can think of second harmonic generation in terms of a simple three level system, c.f. Fig. 1.1, where one of the two incoming photons excite an electron out of its equilibrium position to a higher lying state from which it gets excited by the second photon to a third and when subsequently relaxing to the groundstate it emits a single photon that then has twice the energy of the two incoming ones. The intermediate excited states are virtual states, i.e. they do not need to correspond to actual energy levels of the system. This is of course an oversimplification of what actually happens in the many-body electron system, where, for example, interactions between the electronic states have to be accounted for as well.

Second harmonic generation as an experimental tool has two main applications. One is to actually double the frequency of laboratory lasers and thus give access to other frequencies than the laser frequency. For this use it is particularly important that the second harmonics are generated with sufficient efficiency, which above all means that the phase matching condition $\mathbf{k}(2\omega) - \mathbf{k}(\omega) = 0$ between the lightvectors of incoming and outgoing field is fulfilled. Otherwise, second harmonic generation will still take place inside the material, but due to interference it would not be observable on the outside. Apart from phase matching, it is also important that the second harmonic susceptibility $\chi^{(2)}$ is as large as possible at the desired frequencies. This again is strongly material and frequency dependent and the search for high efficiency nonlinear crystals is still underway [5, 6]. The other main area of application is to use second harmonic generation as a probe. For systems with inversion symmetry second harmonic generation is dipole forbidden and therefore extremely sensitive to symmetry breaking. This makes it particularly suitable to probe surfaces or interfaces of centro-symmetric media, where the bulk will not contribute to the second harmonic light and one thus has a signal purely from the surface. The use of second harmonic generation is not limited to

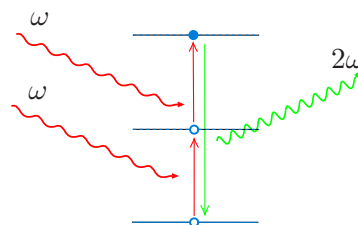


Figure 1.1: Model for second harmonic generation

these two fields and there are a variety of other circumstances where it is employed [7–18].

1.2 Ab initio optical excitations

The theoretical description of optical properties is based on the interaction of light with the electrons and nuclei of the material. This entails in principle the simultaneous quantum mechanical description of the light and the atoms that form the material with all their respective interactions. It is, however, sufficient to describe the light as a classical field and to assume that the dynamics of the electrons is decoupled from the dynamics of the nuclei, so that for the electronic system one can assume fixed ionic positions (Born-Oppenheimer approximation [19]). These two approximations leave essentially the mutual interaction of the electrons as they are excited by the light field as the most important effect. This can be formulated in terms of the Schrödinger equation

$$\left[\sum_{i=1}^{N_e} \left(-\frac{1}{2} \nabla_i^2 + V_{ext}(\mathbf{r}_i) \right) + \frac{1}{2} \sum_{i \neq j}^{N_e} v(|\mathbf{r}_i - \mathbf{r}_j|) \right] \Psi(\mathbf{r}_1, \dots, \mathbf{r}_N) = E \Psi(\mathbf{r}_1, \dots, \mathbf{r}_N) \quad (1.2)$$

where N_e is the number of electrons, that has the order of 10^{23} for macroscopic samples and v is the Coulomb interaction between the electrons. Solving this equation directly is not possible and not even necessarily desirable, because the sheer size of the solution in terms of many-body wavefunctions and energies would be impossible to manage. This fundamental problem that we know the equation that determines all properties of the material, but its solution is impossible to obtain, is commonly referred to as the many-body problem. For optical processes this system is then also subject to a time dependent excitation, which adds to the complexity. To tackle excitations of the many-body problem one usually separates it into the groundstate problem and the excited state problem that builds on the groundstate.

To describe electrons in a solid it is convenient to make the approximation that the electrons move independently of each other in the periodic potential created by the ions of the solid and the other electrons. This assumption allows one to describe the many-body system in terms of single particle energies and wavefunctions, the so called Bloch states [20], defined as

$$\left(-\frac{1}{2} \nabla^2 + V_{ext}(\mathbf{r}) \right) \psi_{n\mathbf{k}}(\mathbf{r}) = \varepsilon_{n\mathbf{k}} \psi_{n\mathbf{k}}(\mathbf{r}) \quad (1.3)$$

where $\psi_{n\mathbf{k}}(\mathbf{r}) = u_{n\mathbf{k}} e^{i\mathbf{k}\mathbf{r}}$. This formulation gives rise to the band structure of solids that gives the \mathbf{k} -dependence of the single particle eigenenergies $\varepsilon_{n\mathbf{k}}$. This reduces the groundstate many-body problem to two crucial steps, one is to obtain the single particle states and the other is to compensate the fact that one is using a single particle picture to describe a many-body problem. The first step is most commonly done by density functional theory (DFT), which passes from a description of the problem in

terms of wavefunctions to a framework where the electron density is the fundamental quantity. While this is in principle an exact theory, the many-body interactions are here approximated via an effective one particle potential, the exchange and correlation potential, that is not known exactly but approximation can be derived from fundamental models without adjustable parameters (i.e. LDA and GGA [21]). The resulting effective one particle states can be further refined with additional schemes (such as perturbative *GW* [22, 23]) which add to some extent many-body effects but one still has a description of the electronic system in terms of single particles. The second step, to incorporate many-body-effects beyond the single particle picture, is far less standardized than DFT but a rigorous framework for it exist in the many-body perturbation theory (MBPT) that relies on the many-body Green's function and a set of self consistent equations, Hedin's equations[24]. The crucial point is that in an *ab initio* approach one does not rely on free parameters even when one uses approximations, but rather has to derive expression and schemes that yield results that can be directly compared with experiments without further adjustment.

For optical excitations one is not interested in single particle properties like wavefunctions or energies, but rather in the response of the many-body system, i.e. its time dependent properties. By passing from the single particle quantities to the actual physical quantities, like for example the dielectric function, one has to account for the many-body effects along the way. It is here where the relevant physical approximations are made, since one can in principle choose which kind of many-body effect one wishes to include. One can, for example, consider the optical response of independent particles, which means that one does not include any further interaction. Beyond this, there are several approximations and different methods that have been applied with varying success. The two most important approaches for optical excitations are the Bethe-Salpeter equation (BSE) and the time dependent generalization of the density functional framework (TDDFT). The main difference between the two is that BSE is formulated in terms of the two-particle correlation function $L(\mathbf{r}_1, \mathbf{r}_2, \mathbf{r}_3, \mathbf{r}_4, \omega)$, which is a part of the two-particle Green's function, whereas TDDFT in response formulation gives the susceptibility $\chi(\mathbf{r}_1, \mathbf{r}_2, \omega)$. While the downside of the BSE approach is that one has to deal with a four-point quantity as compared to a two point one in TDDFT, its upside is that its ingredients have a clear physical interpretation, while in TDDFT all many-body effects are expressed in the effective kernel f_{xc} , whose exact expression is unknown.

This problem, of finding working approximations for the TDDFT kernel f_{xc} , has for a long time made it unsuitable for optical calculations, since existing approximation failed to produce viable results. This was assigned to the failure of properly describing the

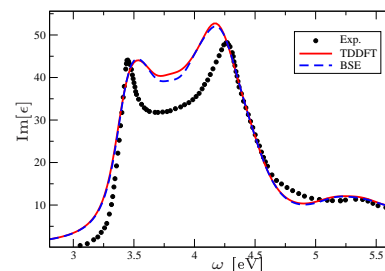


Figure 1.2: Absorption spectrum of bulk Si comparing experiment, BSE and TDDFT, as in [25].

electron-hole interaction (excitons) that is of great importance for optical processes. The BSE on the other hand, being a two particle correlation function, is perfectly suitable to describe this effect. By systematically comparing the two approaches it has been possible to derive an f_{xc} that does account for excitonic interaction and produces spectra of comparable quality to BSE [25–29], c.f. Fig. 1.2.

It is in this context that the work in this thesis is set and its motivation is to translate the success of TDDFT for linear optics into the nonlinear domain.

1.3 Calculations of Second Harmonic generation

The description of second harmonic generation based on band structure theory was developed shortly after the discovery of the effect. In 1962 Armstrong et al. [30] and Loudon [31] give expressions for the microscopic second harmonic susceptibility that are similar to those used today. Their equations allow an analysis of the susceptibility in terms of the frequency structure, i.e. the microscopic origin of the frequency doubling. Actual calculations based on this formulation have however been only of limited success for a long time. All early calculations are restricted to the static second harmonic coefficient [32–34], i.e. $\chi^{(2)}(\omega = 0)$, and with the absence of ab initio methods for the electronic structure strong approximations and assumptions had to be made. Aspnes further analyzed the formulation in 1972 [35] in terms of different gauges for the applied fields. His calculations, however, had to rely heavily on empirical data by interpolating matrix elements. Calculations made by Yong and Shen based on empirical pseudo-potentials missed the experimental values by orders of magnitude, but they showed that for the dispersion of $\chi^{(2)}(\omega)$ the \mathbf{k} -dependence of the matrix elements is crucial. In a later work in 1987 Moss et al. [36] used a semi-empirical tight-binding method to calculate static and frequency dependent second harmonic coefficients for a range of semi-conductors. While some of their static values are comparable to the experimental values their spectra are quite off the measured values, which the authors attribute to the deficiencies of the tight-binding approach. Although most works at that time were concerned with bulk semiconductor, the authors used this approach to calculate the second harmonic generation spectra for superlattices as well [37, 38].

The evolution of computational methods allowed the first ab initio calculation of second harmonic generation to be carried out by Levine and Allan in 1991 [39, 40] under consideration of quasi-particle effects. These are described by the *GW* method and have been found to open the DFT-LDA bandgap of simple semiconductors while leaving the wavefunctions largely unaffected. Levine and Allan thus incorporated the quasiparticle effect in their calculation by simply shifting the conduction bands (scissors shift). As results they give only static values for the second harmonic generation, however in very reasonable agreement with experimental values. They subsequently extended their formalism to account for crystal local field effects [41] and to frequency dependence [42]. At the same time Huang and Ching presented first-principle calculations of second harmonic spectra [43, 44] they relied on the formulas developed by Sipe and co-workers [36, 45] but used a more accurate scheme to calculate the band structures.

Also in the 1990's Sipe and co-workers further developed their formalism for an ab initio calculation of the independent particle second harmonic susceptibility [46, 47] that finally allowed them to perform an ab initio calculation of second harmonic spectra [48, 49]. While the agreement of their results with experimental spectra remained rather poor, this work is notable because in [48] they give a formulation of the independent particle response in the length gauge and optical limit that has since been widely used, e.g. in [50–58] among others. An alternative to the straightforward "sum over states" approach was suggested by Dal Corso et al. [59] relying on the "2n+1" theorem of perturbation theory [60]. This approach has the advantage that it does not need unoccupied states to evaluate the response and thus has advantageous scaling properties [61]. They also account self-consistently for local field effects. Most of the mentioned early ab initio approaches discuss the quality of the band structure and notice a strong dependence of the second harmonic spectra on the accuracy of the groundstate values. This together with the developing sophistication of DFT groundstate methods might be the reason for large discrepancies between single results and the overall unfavorable agreement with experiments might additionally be attributed to the fact that most approaches were only within the independent particle response.

Nonetheless, the independent particle response formulation of second harmonic generation was applied to a variety of materials and systems. Sharma and Ambrosch-Draxl applied a similar formulation to mono-layer InP/GaP (110) superlattices [62] and Lithium under pressure [56, 57]. Rashkeev and co-workers presented an efficient scheme [58] to evaluate the formulation given in [48] with a self-consistent linearized muffin-tin orbitals band structure method and applied it to III-V semiconductors [50], ternary pnictides [51], Ag-III-VI₂ compounds [52], I-III-VI₂ chalcopyrites [53] and Zn-IV-N₂ compounds [54]. Gavrilenko and co-workers applied the independent particle response to study group-III nitrides [55] and several surface and interface systems [63, 64]. Carbon nanotubes [65] and SiC nanotubes [66] have been studied by Guo and coworkers. More recently fluoride- [6] and borate-based crystals [5] have been studied within this approximation. While these approaches gradually improved the numerical description of second harmonic generation, the calculation remain non-trivial and the same level of accuracy encountered in linear optics has not yet been achieved.

Furthermore, there have been only few attempts to go beyond the independent particle approximation, where quasi-particle effects are almost always accounted for by the scissors approximation. Bechstedt and co-workers investigated the validity of this approach by comparing calculations with actual quasi-particle wavefunctions to results obtained with the scissors operator [67]. But in particular excitonic effects have been considered only by few authors. Chang et al. [68] proposed a method to include excitonic effects via wavefunctions that they represent as superpositions of pair excitations. Their formalism gives in principle the full frequency dependence but they only report calculations over a very short range. Leitsmann et al. [69] developed this formalism further and they use the excitonic wavefunctions obtained from a BSE calculation to construct the many-body $\chi^{(2)}$. This approach is clearly a conceptual improvement over the independent particle formulation, since here many-body effects are included in the wavefunctions that are

no longer of an independent particle system. The results they obtain give a qualitative agreement with experiments over a large spectral range. This work can be considered the most advanced, as far as sophistication of the theoretical formulation is concerned. Still, in this approach the crystal local field effects are only accounted for within the BSE calculation, which might be a limiting factor on the quality of the result.

Having exposed previous work done within the scope of solid state physics, it is worth to note that in the community of chemical physics nonlinear optical properties are calculated routinely for molecular systems. In this community one speaks of *hyperpolarizabilities* [70, 71] which is equivalent to the second order susceptibility of this work. TDDFT has been applied to calculate these quantities since the early days of this method [72, 73]. Subsequently the calculation of hyperpolarizabilities has been received much attention and a large body of work is available, e.g. [74–81]. This was facilitated by the implementation of hyperpolarizability features in widely used quantum chemistry codes, such as AdF [82] and others. There are however important differences between these calculations and the corresponding efforts in solids. First, on a practical level, for molecular polarizabilities the exchange-correlation functional used for the DFT groundstate is very important and many developments have been made in the chemistry community to go beyond the rather simple LDA approach, e. g. LB94 [83] or SOAP [84]. For optical properties solids, on the other hand, using functionals beyond LDA for the ground state calculation does not substantially improve the results. For the TDDFT exchange and correlation functionals the situation appears to be the inverse, where ALDA performs rather well for molecules but fails for solids, which is arguably the reason for the different levels of maturity TDDFT has gained in these two fields. Another important difference between solids and molecules for optical response calculations, is the fact that for molecules a microscopic description of the response is enough to model experiments, while for solids the connection between the microscopic and macroscopic world is non-trivial already in the linear case and one of the main results of this work is that they are even more involved when one considers second order processes. Therefore, the early and rapid success of TDDFT in the quantum chemistry community could not be easily translated to the solid state domain but it is nonetheless one of the motivations of this work to advance the description on nonlinear response in solids to a point where it is at least comparable with linear optics of solids and pave the way for further developments that might rival the accuracy achieved in chemistry calculations.

1.4 This work

While the independent particle formulation of second harmonic generation in solids can be considered to be well established, approaches that go beyond this approximation are not. Mainly for crystal local field effects and excitonic contributions there is a lack of systematic description for the second order. On the other hand, for linear optics these two effects can be considered to be well understood and their treatment fairly standardized. Especially within the TDDFT framework local field effects are routinely calculated and more recently the connection to the BSE had been made to account for excitons.

The main purpose of this work is to use the known concepts and experiences from linear optics and apply them to the second order case.

The description of the theoretical formulation starts in Chap. 2 with a revision of time-dependent perturbation theory which obviously is the basis for a response treatment. Then, the known linear TDDFT Dyson equation, where the connection between the independent and interacting particle response is made, needs to be generalized to second order, leading to a second order Dyson like equation that has been published only once [85] and never been applied. The structure of the equation allows to solve it analytically provided the linear response is known and thus can, to a certain extend, be related to the linear response, but it contains a higher order correlation part that only appears to second order. The most important difficulty lies in the numerical evaluation of the solution the TDDFT Dyson like equation. It gives the microscopic second order response of the electron density so that approximations concerning the many-body character have to be made at this level.

The relation between microscopic and macroscopic response given by Adler and Wiser [86, 87] is well known for linear optics, since it accounts for the crystal local field effects. For nonlinear response this connection is less studied and to our knowledge the analogue to the Adler and Wiser formulation has never been established for the nonlinear case. Consequently, such a relation is derived in Chap. 3 in a fairly general way for longitudinal and transverse fields. TDDFT, however can only give the response to longitudinal fields, which has to be taken into consideration when passing from microscopic to macroscopic quantities.

In the context of this thesis second harmonic generation is considered to be an optical effect, which means one has to consider a perturbation in the long wavelength limit. Therefore the theoretical formulation has to be taken in the limit $\mathbf{q} \rightarrow 0$, which calls for a rather lengthy expansion of the independent particle density response that is described in Chap. 4. To provide an alternative way to this expansion I propose a scheme that considers this limit numerically and thus provides an alternative route to the optical response. More specifically, I use the fact that for finite frequency the light wavevector is still finite and thus carry out the calculation with very small but finite \mathbf{q} .

This formulation in terms of finite \mathbf{q} allows to investigate the spatial dispersion of the optical response and thus gives also access to optical responses beyond the dipole limit. This is particularly interesting for second harmonic generation because it is dipole forbidden in centro-symmetric media. I explore this possibility in Chap. 5 with the example of bulk Si. This constitutes, to my knowledge, the first ab initio calculation of the second harmonic bulk quadrupole response. There are however intrinsic limitations in its formulation in terms of density response.

In Chap. 6 I will show a range of numerical results obtained in the standard formulation of the optical limit and with the various levels of approximation that the theory provides. The accuracy of the implementation is demonstrated in a benchmark test against the experimental spectrum of GaAs, where previous formulations have yielded results with only moderate success. I show that it is the interplay between local field and excitonic effects that can give a very good agreement of the calculation with the experiment; an

agreement that is almost as good as that for silicon absorption shown in Fig. 1.2. Finally, to follow the success of the Bethe-Salpeter equation for linear optics, I derive the analogous expression for second order response. The resulting equation accounts for all many-body effects that occur in second order processes of any kind, not only optical. It is, however, far more complex to solve and eventhough its ingredients are in principle known it its not clear if an actual implementation would be feasible. Nonetheless, in App. D.1 I sketch how such an implementation might be realized. Also, by exploiting the similar structure between the second order Bethe-Salpeter equation and the second order TDDFT Dyson like equation, I find an exact expression for the second order exchange and correlation kernel.

2 Second order TDDFT

The theoretical description of nonlinear optics to second order necessarily means one has to use perturbation theory to be able to account solely for the second order process. The behaviour of a physical system under the influence of an external perturbation is called its response. More precisely, it is the change in the expectation values of operators of the system when the perturbation is applied.

2.1 Second order Response theory

To introduce the concept of response functions, we formally expand an operator $\hat{A}(t)$ in terms of a small perturbation v in interaction picture:

$$\hat{A}(t)[v] = \hat{A}(t)_0 + \int d1 \frac{\delta \hat{A}(t)}{\delta v(1)} v(1) + \frac{1}{2!} \int d1 d2 \frac{\delta^2 \hat{A}(t)}{\delta v(1) \delta v(2)} v(1) v(2) + \dots \quad (2.1)$$

The expansion coefficients do not explicitly depend on the perturbing quantity, but are variation of the operator with respect to the perturbation. These quantities are the response functions. Their explicit form depends on the coupling between the system and the perturbation. We consider an interaction Hamiltonian where the perturbing field v couples with an operator \hat{O} in the form

$$\hat{H}_I(t) = \int d\mathbf{r} \hat{O}(\mathbf{r}, t) v(\mathbf{r}, t) . \quad (2.2)$$

From the Kubo response theory [88] the linear response function is known to take the general form

$$\chi_{AO}(1, 2) = -i\theta(t_1 - t_2) \langle [\hat{A}(1), \hat{O}(2)] \rangle \quad (2.3)$$

The theory can be generalized to higher orders (c.f. [89]) to yield the second order response function

$$\chi_{AOO}(1, 2, 3) = -\theta(t_1 - t_2)\theta(t_1 - t_3) T \langle [[\hat{A}(1), \hat{O}(2)], \hat{O}(3)] \rangle \quad (2.4)$$

where T is the time ordering operator¹.

¹The time ordering operator is defined by its action on a function of two time variables:
 $TF(t_2, t_3) = \Theta(t_2 - t_3)F(t_2, t_3) + \Theta(t_3 - t_2)F(t_3, t_2)$

2.2 Perturbation theory

It is clear that an expansion such as Eq. (2.1) can only be justified if the perturbation is small compared with the overall energies of the system, e.g. electron binding energy of a molecule or bond strength in a solid. That is to say, it is only valid within the scope of perturbation theory, from which the response functions are derived. To give a picture as comprehensive as possible, we will shortly expose here how this perturbation theory yields the response functions for the special case of electro-magnetic radiation coupled to a (many-body) electron system. When dealing with the interaction of the electron system of a solid with light one can usually separate the total Hamiltonian in a part describing the unperturbed electronic system and another part describing the coupling to the time dependent external perturbation

$$\hat{H} = \hat{H}_0 + \hat{H}_I(t). \quad (2.5)$$

This separation conveniently allows to define an interaction picture where the evolution of the states $|\Psi(t)\rangle$ is described by \hat{H}_I via the time dependent Schrödinger equation

$$\partial_t |\Psi(t)\rangle = -i\hat{H}_I(t)|\Psi(t)\rangle \quad (2.6)$$

with gives the integral equation

$$|\Psi(t)\rangle = |\Psi(t_0)\rangle - i \int_{t_0}^t dt_1 \hat{H}_I(t_1) |\Psi(t_1)\rangle. \quad (2.7)$$

Iterating this equation gives the dependence of the states to the orders of the interaction. We consider terms up to second order, thus

$$|\Psi(t)\rangle = |\Psi(t_0)\rangle - i \int_{t_0}^t dt_1 \hat{H}_I(t_1) |\Psi(t_0)\rangle - \int_{t_0}^t dt_1 \int_{t_0}^{t_1} dt_2 \hat{H}_I(t_1) \hat{H}_I(t_2) |\Psi(t_0)\rangle. \quad (2.8)$$

Using this expression for $|\Psi(t)\rangle$ in the expectation value of an operator $\langle \Psi(t) | \hat{A}(t) | \Psi(t) \rangle$ and keeping only terms up to second order in $\hat{H}_I(t)$ yields the response of the operator up to second order

$$\begin{aligned} \langle \hat{A}(t) \rangle &= \langle \hat{A}(t_0) \rangle + \delta \langle \hat{A}(t) \rangle^{(1)} + \delta \langle \hat{A}(t) \rangle^{(2)} \quad (2.9) \\ &= \langle \hat{A}(t_0) \rangle - i \int_{t_0}^t dt_1 \langle \Psi(t_0) | [\hat{A}(t), \hat{H}_I(t_1)] | \Psi(t_0) \rangle - \\ &\quad - \int_{t_0}^t dt_1 \int_{t_0}^{t_1} dt_2 \langle \Psi(t_0) | [[\hat{A}(t), \hat{H}_I(t_1)], \hat{H}_I(t_2)] | \Psi(t_0) \rangle \quad (2.10) \end{aligned}$$

This is the general result of second order time dependent perturbation theory. It can be generalized to n -th order, yielding increasingly nested commutators [90]. It gives, however, not yet the response functions, because the terms in Eq. (2.10) contain the perturbation itself.

To arrive at an explicit expression for the responses we have to use an explicit expression for \hat{H}_I . Here we consider the interaction Hamiltonian of an electron system with a general classical light field that can be written as

$$\hat{H}_I(t_1) = \int d\mathbf{r}_1 \left[\hat{\rho}(1)V_{per}(1) - \hat{\mathbf{j}}(1)\tilde{\mathbf{A}}_{per}(1) + \frac{1}{2}\hat{\rho}(1)\tilde{\mathbf{A}}_{per}^2(1) \right] \quad (2.11)$$

where 1 is shorthand for $\mathbf{r}_1 t_1$ and $\tilde{\mathbf{A}}_{per} \equiv \frac{1}{c}\mathbf{A}_{per}$ to keep the notation simple. This Hamiltonian contains the diamagnetic term $\hat{\rho}\mathbf{A}_{per}^2$ that is second order in the field and is thus neglected in first order response theory. We are, however, interested in the second order and therefore this term has to be included when evaluating the $\delta\langle\hat{A}(t)\rangle$ part of Eq. (2.10), while it gives third and fourth order contributions when used for the second order response $\delta\langle\hat{A}(t)\rangle^{(2)}$.

The quantities of interest here are the responses of electron- and current-density under the perturbation. We can use Eq. (2.10) together with the Hamiltonian (2.11) to get the first and second order responses of the total current composed of the para- and diamagnetic current $\hat{\mathbf{J}}(1) = \hat{\mathbf{j}}(1) + \hat{\rho}(1)\tilde{\mathbf{A}}_{per}(1)$ and the density $\hat{\rho}(1)$. To first order in the current we have

$$\delta\langle\hat{\mathbf{J}}(1)\rangle^{(1)} = \langle\hat{\rho}(1)\rangle\tilde{\mathbf{A}}_{per}(1) + i \int_{t_0}^{t_1} dt_2 \int d\mathbf{r}_2 \langle[\hat{\mathbf{j}}(1), \hat{\mathbf{j}}(2)]\rangle\tilde{\mathbf{A}}_{per}(2) - i \int_{t_0}^{t_1} dt_2 \int d\mathbf{r}_2 \langle[\hat{\mathbf{j}}(1), \hat{\rho}(1)]\rangle V_{per}(2) \quad (2.12)$$

where we can readily identify the response functions according to their definition Eq. (2.1), so that we can write:

$$\delta\langle\hat{\mathbf{J}}(1)\rangle^{(1)} = \int d^2\chi_{j\rho}(1, 2)V_{per}(2) + [\chi_{jj}(1, 2) + \delta(1, 2)\rho(2)]\tilde{\mathbf{A}}_{per}(2) \quad (2.13)$$

Similarly, we find the first order density response as

$$\delta\langle\hat{\rho}(1)\rangle^{(1)} = \int d^2\chi_{\rho\rho}(1, 2)V_{per}(2) + \chi_{\rho j}(1, 2)\tilde{\mathbf{A}}_{per}(2). \quad (2.14)$$

These are the well known first order responses. The second order responses, albeit more lengthy, are obtained in the same way. They are:

$$\begin{aligned} \delta\langle\hat{\mathbf{J}}(1)\rangle^{(2)} &= \int d^2\frac{1}{2}\chi_{j\rho}(1, 2)\tilde{\mathbf{A}}_{per}^2(2) + [\chi_{\rho j}(1, 2)\tilde{\mathbf{A}}_{per}(2) - \chi_{\rho\rho}(1, 2)V_{per}(2)]\tilde{\mathbf{A}}_{per}(1) + \\ &+ \frac{1}{2} \int d^2d^3 \left[\chi_{jjj}\tilde{\mathbf{A}}_{per}(2)\tilde{\mathbf{A}}_{per}(3) - \chi_{jj\rho}\tilde{\mathbf{A}}_{per}(2)V_{per}(3) - \right. \\ &\quad \left. - \chi_{jjj}V_{per}(2)\tilde{\mathbf{A}}_{per}(3) + \chi_{j\rho\rho}V_{per}(2)V_{per}(3) \right] \end{aligned} \quad (2.15)$$

and

$$\begin{aligned} \delta\langle\hat{\rho}(1)\rangle^{(2)} &= \frac{1}{2} \int d2 \chi_{\rho\rho}(1,2) \tilde{\mathbf{A}}_{per}^2(2) + \\ &+ \frac{1}{2} \int d2d3 \left[\chi_{\rho\mathbf{j}\mathbf{j}} \tilde{\mathbf{A}}_{per}(2) \tilde{\mathbf{A}}_{per}(3) - \chi_{\rho\mathbf{j}\rho} \tilde{\mathbf{A}}_{per}(2) V_{per}(3) - \right. \\ &\left. - \chi_{\rho\rho\mathbf{j}} V_{per}(2) \tilde{\mathbf{A}}_{per}(3) + \chi_{\rho\rho\rho} V_{per}(2) V_{per}(3) \right]. \end{aligned} \quad (2.16)$$

So, the changes in the electronic system are described by the correlations of the density and current density operator. These response functions are the central quantity of the microscopic description of the interaction of solids with light and their calculation is the central topic of this thesis.

These responses are given in terms of the general electromagnetic potentials V_{per} and $\tilde{\mathbf{A}}_{per}$ for which we can still choose a gauge. Here, it is convenient to take a gauge such that $V_{per} = 0$, which leaves only the vector potential as the perturbing quantity. The response then read

$$\delta\langle\hat{\mathbf{J}}(1)\rangle^{(2)} = \int d2d3 \left[\frac{1}{2} \chi_{\mathbf{j}\rho}(1,3) \delta(2,3) + \chi_{\rho\mathbf{j}}(3,2) \delta(1,3) + \frac{1}{2} \chi_{\mathbf{j}\mathbf{j}\mathbf{j}}(1,2,3) \right] \tilde{\mathbf{A}}_{per}(2) \tilde{\mathbf{A}}_{per}(3) \quad (2.17)$$

$$\delta\langle\hat{\rho}(1)\rangle^{(2)} = \int d2d3 \frac{1}{2} [\chi_{\rho\rho}(1,3) \delta(2,3) + \chi_{\rho\mathbf{j}\mathbf{j}}(1,2,3)] \tilde{\mathbf{A}}_{per}(2) \tilde{\mathbf{A}}_{per}(3). \quad (2.18)$$

Additionally we note that due to the continuity equation

$$\nabla_{\mathbf{r}_1} \hat{\mathbf{j}}(1) = \partial_{t_1} \rho(1) \quad (2.19)$$

knowledge of the current response implies the density response. Therefore we can focus on the current quantities without loss of generality. Writing Eq. (2.19) in momentum and frequency space (c.f. App. B) it reads

$$\mathbf{q} \cdot \hat{\mathbf{j}}(\mathbf{q}, \omega) = i\omega \rho(\mathbf{q}, \omega). \quad (2.20)$$

So we see that the density is actually proportional to the projection of $\hat{\mathbf{j}}$ along the direction of \mathbf{q} , i.e. the longitudinal projection of $\hat{\mathbf{j}}$. The density response can thus be expressed in terms of the current response, or vice versa, the longitudinal current response is proportional to the density response. Moreover, under the constraint that the perturbing field is purely longitudinal, this means that the second order longitudinal current response can be obtained from the second order density-density-density response function $\chi_{\rho\rho\rho}$.

2.2.1 Response functions

While their definition Eq. (2.3) and (2.4) together with the knowledge how to evaluate the expectation value is in principle all one would need to obtain response functions, in practice one has to make some transformations and assumptions to arrive at a quantity that can be calculated within existing computational schemes.

The definition of the response function can be cast in a more useful way by passing from the time domain to frequency space. Using the completeness relation in the definition of the linear response function Eq. (2.3), we obtain²

$$\chi_{AB}(1,2) = -\Theta(t_1-t_2) \sum_n \left(\langle \Psi_0 | \hat{A}_I(1) | \Psi_n \rangle \langle \Psi_n | \hat{B}_I(2) | \Psi_0 \rangle - \langle \Psi_0 | \hat{B}_I(2) | \Psi_n \rangle \langle \Psi_n | \hat{A}_I(1) | \Psi_0 \rangle \right). \quad (2.21)$$

The matrix elements of the operators in the interaction picture are

$$\langle \Psi_i | \hat{A}_I(t) | \Psi_j \rangle = \langle \Psi_i | e^{-i\hat{H}_0 t} \hat{A} e^{i\hat{H}_0 t} | \Psi_j \rangle = e^{-i(E_i - E_j)t} \langle \Psi_0 | \hat{A} | \Psi_i \rangle \quad (2.22)$$

so that the response function reads

$$\begin{aligned} \chi_{AB}(1,2) &= -\Theta(t_1 - t_2) \sum_n e^{-i(E_n - E_0)(t_1 - t_2)} \times \\ &\quad \times \left(\langle \Psi_0 | \hat{A} | \Psi_n \rangle \langle \Psi_n | \hat{B} | \Psi_0 \rangle - \langle \Psi_0 | \hat{B} | \Psi_n \rangle \langle \Psi_n | \hat{A} | \Psi_0 \rangle \right) \end{aligned}$$

and its Fourier transform (c.f. App. B) gives the spectral representation of the response function

$$\chi_{AB}(\mathbf{r}_1, \mathbf{r}_2, \omega) = \lim_{\eta \rightarrow 0^+} \sum_n \left(\frac{\langle \Psi_0 | \hat{A} | \Psi_n \rangle \langle \Psi_n | \hat{B} | \Psi_0 \rangle}{\omega - (E_n - E_0) + i\eta} - \frac{\langle \Psi_0 | \hat{B} | \Psi_n \rangle \langle \Psi_n | \hat{A} | \Psi_0 \rangle}{\omega + (E_n - E_0) + i\eta} \right). \quad (2.23)$$

²Here we write \hat{B} for the operator of the system instead of \hat{O} for the sake of readability. Likewise, in the second order we use the notation \hat{C} for the third operator of the response function.

To obtain an equivalent expression for the second order response, we follow exactly the same steps. The result is

$$\begin{aligned}
\chi_{ABC}(\mathbf{r}_1, \mathbf{r}_2, \mathbf{r}_3, \omega_1, \omega_2, \omega_3) = & \\
\lim_{\eta \rightarrow 0^+} \sum_{nm} \delta(\omega_1 - \omega_2 - \omega_3) & \left[\frac{\langle \Psi_0 | \hat{A} | \Psi_n \rangle \langle \Psi_n | \hat{B} | \Psi_m \rangle \langle \Psi_m | \hat{C} | \Psi_0 \rangle}{(E_0 - E_m + \omega_3 + i\eta)(E_0 - E_n + \omega_2 + \omega_3 + 2i\eta)} - \right. \\
& - \frac{\langle \Psi_0 | \hat{B} | \Psi_n \rangle \langle \Psi_n | \hat{A} | \Psi_m \rangle \langle \Psi_m | \hat{C} | \Psi_0 \rangle}{(E_0 - E_m + \omega_3 + i\eta)(E_n - E_m + \omega_2 + \omega_3 + 2i\eta)} - \\
& - \frac{\langle \Psi_0 | \hat{C} | \Psi_n \rangle \langle \Psi_n | \hat{A} | \Psi_m \rangle \langle \Psi_m | \hat{B} | \Psi_0 \rangle}{(E_n - E_0 + \omega_3 + i\eta)(E_n - E_m + \omega_2 + \omega_3 + 2i\eta)} + \\
& + \frac{\langle \Psi_0 | \hat{C} | \Psi_n \rangle \langle \Psi_n | \hat{B} | \Psi_m \rangle \langle \Psi_m | \hat{A} | \Psi_0 \rangle}{(E_n - E_0 + \omega_3 + i\eta)(E_m - E_0 + \omega_2 + \omega_3 + 2i\eta)} + \\
& \left. + \{2 \leftrightarrow 3\} \right]. \tag{2.24}
\end{aligned}$$

In this formulation we can already deduce some general properties of second order response. First, we notice that the three frequencies are not independent but linked through the delta function, which means that the response frequency ω_1 can be the sum of the two fundamental frequencies, i.e.

$$\chi_{ABC}(\omega_1, \omega_2, \omega_3) = \chi_{ABC}(\omega_2 + \omega_3, \omega_2, \omega_3) \tag{2.25}$$

This is the microscopic origin of the phenomenon of sum frequency generation, or in the case of $\omega_2 = \omega_3$ of second harmonic generation.

Regarding the spectral properties of the second order response function, we note that it has resonances at the fundamental frequencies as well as at their sum. In the case of second harmonic generation this means for each resonance at a frequency ω there will another resonance at $\omega/2$.

While its general structure shows some characteristics of the second order response, this form of the response function can only be used if the many-body wavefunctions and energies of the system are known. They are, however, not known and calculating them explicitly is unfeasible. To overcome the basic problem of obtaining the solutions of the many-body Hamiltonian is the motivation for many theories and calculatory schemes in the field of computational physics. Namely the density-functional theory (DFT) has been successfully employed to obtain the groundstate properties of interacting many-body systems. The basic idea is to exploit the fact that the density of electrons subject to some interacting potential is the same as the density of electrons in a non-interacting potential, called exchange-correlation potential, that uniquely represents the interacting potential [21].

This idea of mapping an interacting many-body system to a non-interacting one and thus confining the many-body problem to the search for the appropriate non-interacting potential is generalized to time dependent systems in the framework of time-dependent-

density-functional-theory (TDDFT), c.f. section 2.3. That is to say, that the response functions shown above are expressed in terms of a non-interacting system and the many-body character is included via the exchange correlation potential. So, the central quantities are the independent particle response functions. In App. A I outline how to pass from the responses in terms of many-body wavefunctions to the independent particle picture. The resulting response functions are:

$$\chi_{AB}^{(0)}(\mathbf{r}_1, \mathbf{r}_2, \omega) = \sum_{ij} (f_i - f_j) \frac{\langle \phi_i^*(\mathbf{r}_1) | \hat{a}(\mathbf{r}_1) | \phi_j(\mathbf{r}_1) \rangle \langle \phi_j^*(\mathbf{r}_2) | \hat{b}(\mathbf{r}_2) | \phi_i(\mathbf{r}_2) \rangle}{(\epsilon_i - \epsilon_j + \omega + i\eta)} \quad (2.26)$$

and

$$\begin{aligned} \chi_{ABC}^{(0)}(\mathbf{r}_1, \mathbf{r}_2, \mathbf{r}_3, \omega_2 + \omega_3, \omega_2, \omega_3) &= \sum_{ijk} \frac{\langle \phi_i^*(\mathbf{r}_1) | \hat{a}(\mathbf{r}_1) | \phi_j(\mathbf{r}_1) \rangle}{\epsilon_i - \epsilon_j + \omega_1 + \omega_2 + 2i\eta} \times \\ &\times \left[(f_i - f_k) \frac{\langle \phi_j^*(\mathbf{r}_2) | \hat{b}(\mathbf{r}_2) | \phi_k(\mathbf{r}_2) \rangle \langle \phi_k^*(\mathbf{r}_3) | \hat{c}(\mathbf{r}_3) | \phi_i(\mathbf{r}_3) \rangle}{(\epsilon_i - \epsilon_k + \omega_3 + i\eta)} + \right. \\ &+ (f_j - f_k) \frac{\langle \phi_j^*(\mathbf{r}_3) | \hat{c}(\mathbf{r}_3) | \phi_k(\mathbf{r}_3) \rangle \langle \phi_k^*(\mathbf{r}_2) | \hat{b}(\mathbf{r}_2) | \phi_i(\mathbf{r}_2) \rangle}{(\epsilon_k - \epsilon_j + \omega_3 + i\eta)} + \\ &\left. + \{3 \leftrightarrow 2\} \right] \quad (2.27) \end{aligned}$$

where \hat{a} , \hat{b} and \hat{c} are single electron operators, e.g. for $\hat{A} = \hat{\rho}$ we have $\hat{a}(\mathbf{r}) = \delta(\mathbf{r} - \mathbf{r}')$, and $\phi_i(\mathbf{r})$ one particle orbitals with eigenenergies ϵ_i and occupation numbers f_i . The explicit expression for $\chi_{\rho\rho\rho}^{(0)}$ is given in section 4 (Eq. (4.7)).

2.3 TDDFT

The generalization of Kohn and Sham's density functional theory (DFT) to time dependent system, i.e. time dependent density functional theory (TDDFT), by Runge and Gross is exposed in great detail in many works throughout the last 20 years [91]. Here, I will only roughly sketch the path from the static DFT to TDDFT, without going into the subtleties of the theory. Its generalization to second order response is readily obtain, once the first order response is established.

In DFT one constructs the electron density with wavefunctions obtained from a Hamiltonian with a non-interacting potential. By virtue of the Hohenberg-Kohn and Kohn-Sham theorems this density is identical to one obtained with an interacting potential and there is a one to one correspondence between the two potentials. The non-interacting wavefunctions do not have a rigorous physical meaning, but they are only used to build the electron density. Once the exact density is known, all other quantities of the real system

can be constructed, since they are regarded as functionals of the density.

$$\begin{array}{ccccccc}
 & \textit{Realsystem} & & \text{Kohn - Sham} & & \textit{fict.system} & \\
 \Psi_0 & \Rightarrow & \rho & \iff & \rho & \Rightarrow & V_{KS} \\
 \uparrow & & \downarrow & & \uparrow & & \downarrow \\
 \Psi_i & \Leftarrow & V_{ext} & & \phi_0 & \Leftarrow & \phi_i
 \end{array}$$

The non-interacting potential is called Kohn-Sham potential, V_{KS} , and is generally unknown, but can be further decomposed in the form

$$V_{KS}(\mathbf{r}) = V_{ext}(\mathbf{r}) + V_H(\mathbf{r}) + V_{xc}(\mathbf{r}) \quad (2.28)$$

where we have the external potential $V_{ext}(\mathbf{r})$, the Hartree potential defined with the Coulomb potential v as

$$V_H(\mathbf{r}) = \int d\mathbf{r}' \rho(\mathbf{r}') v(\mathbf{r} - \mathbf{r}') \quad (2.29)$$

and V_{xc} , the potential corresponding to the exchange and correlation energy,

$$V_{xc}(\mathbf{r}) = \frac{\delta E_{xc}(\mathbf{r})}{\delta \rho(\mathbf{r})} \quad (2.30)$$

of the system. It is this potential where the many-body effects are considered and consequently it is here where the physical approximations to the many-body problem are made.

The time dependent generalization of this theory is made by considering a time dependent external potential and thus all quantities of the system become time dependent. Analogously to the static case one defines a time-dependent Kohn Sham potential

$$V_{KS}(\mathbf{r}, t) = V_{ext}(\mathbf{r}, t) + V_H(\mathbf{r}, t) + V_{xc}(\mathbf{r}, t). \quad (2.31)$$

The time dependent density is then constructed from eigenstates of the time dependent Kohn-Sham equation

$$\left[-\frac{1}{2}\nabla^2 + V_{KS}(\mathbf{r}, t) \right] \phi_i(\mathbf{r}, t) = i\partial_t \phi_i(\mathbf{r}, t). \quad (2.32)$$

Again, if the exact Kohn-Sham potential was known, such a density would be exact. The point of TDDFT in response formulation is, that also the variation of this density would be the same whether it was obtained with respect to the interacting potential or to the corresponding non-interacting one [92]:

$$\delta\rho(1) = \int d2 \chi_{\rho\rho}(1, 2) \delta V_{per}(2) = \int d2 \chi_{\rho\rho}^{(0)}(1, 2) \delta V_{KS} \quad (2.33)$$

The response functions, however, are not the same. To relate the Kohn-Sham response functions $\chi_{\rho\rho}^{(0)}$ that connects the density with the non-interacting potential to the response function $\chi_{\rho\rho}$ that accounts for the interactions as well, is the objective of TDDFT in response formulation.

Starting point is the definition of the full response function

$$\chi_{\rho\rho}(1, 2) = \frac{\delta\rho(1)}{\delta V_{per}(2)} \quad (2.34)$$

in which we use the chain rule to obtain

$$\chi_{\rho\rho}(1, 2) = \int d3 \frac{\delta\rho(1)}{\delta V_{KS}(3)} \frac{\delta V_{KS}(3)}{\delta V_{per}(2)}. \quad (2.35)$$

Thus we have reformulated the response function to a product of the response of the non-interacting Kohn-Sham system and variation of the Kohn-Sham potential with respect to the perturbing potential. We define the response to the Kohn-Sham potential

$$\chi_{\rho\rho}^{(0)}(1, 2) = \frac{\delta\rho(1)}{\delta V_{KS}(2)}. \quad (2.36)$$

The variation of the Kohn-Sham potential with respect to the perturbing potential is

$$\frac{\delta V_{KS}(3)}{\delta V_{per}(2)} = \delta(3, 2) + \int d4 \frac{\delta(V_H(3) + V_{xc}(3))}{\delta\rho(4)} \frac{\delta\rho(4)}{\delta V_{per}(2)} \quad (2.37)$$

$$= \delta(3, 2) + \int d4 (v(3, 4) + f_{xc}(3, 4)) \chi_{\rho\rho}(4, 2), \quad (2.38)$$

where we defined the exchange and correlation kernel

$$f_{xc}(1, 2) = \frac{\delta V_{xc}(1)}{\delta\rho(2)}. \quad (2.39)$$

Now we can write down the full response as in Eq. (2.35)

$$\chi_{\rho\rho}(1, 2) = \chi_{\rho\rho}^{(0)}(1, 2) + \int d3 d4 \chi_{\rho\rho}^{(0)}(1, 3) (v(3, 4) + f_{xc}(3, 4)) \chi_{\rho\rho}(4, 2). \quad (2.40)$$

This is a Dyson equation for the response function $\chi_{\rho\rho}$ in terms of the interaction kernel $v + f_{xc}$, that can be solved by inversion. It is in principle exact, provided the correct exchange and correlation kernel is known. Since this kernel is defined as the functional derivative of the exchange and correlation potential, this theory suffers the same limitation as DFT, namely the fact that the true exchange and correlation potential is unknown and has to be approximated.

This treatment of the response function that amounts to reformulating it in terms of the independent particle response function and considering the many-body effects only through a kernel, can be readily generalized to higher order responses. This has been

sketched by Gross et. al. in [85]. Completely analogous to the linear case one starts with the definition of the response function, however, now one can make use of the linear result by realizing that the second order response is the variation of the first order response with respect to a another perturbing field.

$$\chi_{\rho\rho\rho}(1, 2, 3) = \frac{\delta^2\rho(1)}{\delta V_{per}(3)\delta V_{per}(2)} = \frac{\delta\chi_{\rho\rho}(1, 2)}{\delta V_{per}(3)} \quad (2.41)$$

Using the linear Dyson equation (2.40) for $\chi_{\rho\rho}$, we have

$$\chi_{\rho\rho\rho}(1, 2, 3) = \frac{\delta\chi_{\rho\rho}^{(0)}(1, 2)}{\delta V_{per}(3)} + \int d4d5 \frac{\delta\chi_{\rho\rho}^{(0)}(1, 4)}{\delta V_{per}(3)} f_{vxc}(4, 5)\chi_{\rho\rho}(5, 2) \quad (2.42)$$

$$+ \int d4d5 \chi_{\rho\rho}^{(0)}(1, 4) \frac{\delta f_{xc}(4, 5)}{\delta V_{per}(3)} \chi_{\rho\rho}(5, 2) + \quad (2.43)$$

$$+ \int d4d5 \chi_{\rho\rho}^{(0)}(1, 4) f_{vxc}(4, 5) \frac{\delta\chi_{\rho\rho}(5, 2)}{\delta V_{per}(3)}, \quad (2.44)$$

where we have written $f_{vxc}(4, 5) = v(4, 5) + f_{xc}(4, 5)$ for brevity. In the second term appears the variation of the kernel f_{xc} with respect to the perturbing field. This can be rewritten using the chain rule

$$\frac{\delta f_{xc}(4, 5)}{\delta V_{per}(3)} = \int d6 \frac{\delta f_{xc}(4, 5)}{\delta\rho(6)} \frac{\delta\rho(6)}{\delta V_{per}(3)} = \int d6 g_{xc}(4, 5, 6)\chi_{\rho\rho}(6, 3) \quad (2.45)$$

and we have defined a new quantity g_{xc} that is the second derivative of the exchange correlation potential and contains the higher order many-body effects. Furthermore, we define the second order Kohn-Sham response

$$\frac{\delta\chi_{\rho\rho}^{(0)}(1, 2)}{\delta V_{KS}(3)} = \frac{\delta\rho(1)}{\delta V_{KS}(3)\delta V_{KS}(2)} = \chi_{\rho\rho\rho}^{(0)}(1, 2, 3). \quad (2.46)$$

The full expression for $\chi_{\rho\rho\rho}$ can now be obtained by using the chain rule in Eq. (2.42) and Eq. (2.38), which finally yields

$$\begin{aligned} \chi_{\rho\rho\rho}(1, 2, 3) &= \chi_{\rho\rho\rho}^{(0)}(1, 2, 3) + \int d4d5 \chi_{\rho\rho\rho}^{(0)}(1, 4, 3) f_{vxc}(4, 5)\chi_{\rho\rho}(5, 2) \\ &+ \int d4d5 \chi_{\rho\rho\rho}^{(0)}(1, 2, 4) f_{vxc}(4, 5)\chi_{\rho\rho}(5, 3) + \\ &+ \int d4d5d6d7 \chi_{\rho\rho\rho}^{(0)}(1, 5, 4) f_{vxc}(5, 6)\chi_{\rho\rho}(6, 2) f_{vxc}(4, 7)\chi_{\rho\rho}(7, 3) + \\ &+ \int d4d5d6 \chi_{\rho\rho}^{(0)}(1, 4) g_{xc}(4, 5, 6)\chi_{\rho\rho}(6, 3)\chi_{\rho\rho}(5, 2) + \\ &+ \int d4d5 \chi_{\rho\rho}^{(0)}(1, 4) f_{vxc}(4, 5)\chi_{\rho\rho\rho}(5, 2, 3). \end{aligned} \quad (2.47)$$

This is the second order correspondent of the linear TDDFT Dyson equation (2.40). It is however different in the sense that one does not need to invert the whole equation to solve it. Only one term on the right hand side contains $\chi_{\rho\rho\rho}$, while all others either depend on the second order Kohn-Sham response $\chi_{\rho\rho\rho}^{(0)}$ or the second order kernel g_{xc} . We also note that the solution of the linear Dyson equation, i.e. $\chi_{\rho\rho}$, is required in order to get the full second order response. An interpretation of this structure might be given by considering that the physical process underlying the second order response fundamentally involves electrons making transitions between three levels. The Kohn-Sham response describes how they do so without interacting with each other, while the full Dyson equation takes into account their interactions. The repeated occurrence of $\chi_{\rho\rho}$ in the Dyson equation means that the underlying interaction is of linear nature, i.e. it involves only two levels or electrons. These two particle interactions can be seen as modulating the independent particle response $\chi_{\rho\rho}^{(0)}$ and only the term containing g_{xc} represents a true three body interaction.

Making use of the fact that the linear response has to be known in order to solve the second order case, we can solve the second order Dyson like equation (2.47) analytically. This is done by factorizing $\chi_{\rho\rho\rho}$ and rearranging the right hand side to give

$$\begin{aligned} \int d4d5 \left[\delta(1, 5) - \chi_{\rho\rho}^{(0)}(4, 5)f_{vxc}(4, 5) \right] \chi_{\rho\rho\rho}(5, 2, 3) = \\ = \int d4d5d6d7 \chi_{\rho\rho\rho}^{(0)}(1, 5, 4) [\delta(2, 5) + f_{vxc}(5, 6)\chi_{\rho\rho}(6, 2)] [\delta(3, 4) + f_{vxc}(4, 7)\chi_{\rho\rho}(7, 3)] \\ + \int d4d5d6 \chi_{\rho\rho}^{(0)}(1, 4)g_{xc}(4, 5, 6)\chi_{\rho\rho}(6, 3)\chi_{\rho\rho}(5, 2) . \end{aligned} \quad (2.48)$$

By using the linear Dyson equation (2.40) we can rewrite the terms in squared brackets as

$$\int d4 \left[\delta(1, 5) - \chi_{\rho\rho}^{(0)}(4, 5)f_{vxc}(4, 5) \right] = \int d6 \chi_{\rho\rho}^{(0)}(1, 6)\chi_{\rho\rho}^{-1}(6, 5) \quad (2.49)$$

and

$$\int d6 [\delta(2, 5) + f_{vxc}(5, 6)\chi_{\rho\rho}(6, 2)] = \int d8 \chi_0^{-1}(5, 8)\chi_{\rho\rho}(8, 2) \quad (2.50)$$

where we have used the shorthand $\chi_0^{-1} = \left[\chi_{\rho\rho}^{(0)} \right]^{-1}$. Inserting these expressions in Eq. (2.48), multiplying from left with the appropriate inverse and subsequently exchanging

the names of integral variables we arrive at the solution

$$\begin{aligned} \chi_{\rho\rho\rho}(1, 2, 3) = & \int d4\dots d9 \chi_{\rho\rho}(1, 8) \chi_0^{-1}(8, 9) \chi_{\rho\rho\rho}^{(0)}(9, 5, 4) \chi_0^{-1}(5, 6) \chi_{\rho\rho}(6, 2) \chi_0^{-1}(4, 7) \chi_{\rho\rho}(7, 3) + \\ & + \int d4d5d6d7 \chi_{\rho\rho}(1, 7) g_{xc}(7, 5, 6) \chi_{\rho\rho}(6, 2) \chi_{\rho\rho}(5, 3). \end{aligned} \quad (2.51)$$

This formulation has the advantage that once the linear response is known it only needs the inverse of the linear independent particle response and the second order independent particle response, $\chi_{\rho\rho\rho}^{(0)}$, to obtain the full $\chi_{\rho\rho\rho}$. It is also more handy to apply approximations on it, c.f. Chap. 7 where it is compared with the second order Bethe-Salpeter equation. We also give it in shorthand form

$$\chi^{(2)} = \chi^{(1)} \chi_0^{-1} \chi_0^{(2)} \chi_0^{-1} \chi^{(1)} \chi_0^{-1} \chi^{(1)} + \chi^{(1)} g_{xc} \chi^{(1)} \chi^{(1)}. \quad (2.52)$$

Alternatively, to avoid inverse quantities altogether, in Eq. (2.48) on the right hand side one can leave the terms in squared brackets and use the relation:

$$\int d8 \chi_{\rho\rho}(9, 8) \chi_0^{-1}(8, 7) = \int d8 [\delta(9, 7) + \chi_{\rho\rho}(9, 8) f_{vxc}(8, 7)] \quad (2.53)$$

for the inverse of Eq. (2.49). This yields the solution of the second order Dyson equation in the form

$$\begin{aligned} \chi_{\rho\rho\rho}(1, 2, 3) = & \int d4\dots d9 [\delta(1, 9) + \chi_{\rho\rho}(1, 8) f_{vxc}(8, 9)] \chi_{\rho\rho\rho}^{(0)}(9, 5, 4) \times \\ & \times [\delta(2, 5) + f_{vxc}(5, 6) \chi_{\rho\rho}(6, 2)] [\delta(3, 4) + f_{vxc}(4, 7) \chi_{\rho\rho}(7, 3)] + \\ & + \int d4d5d6d7 \chi_{\rho\rho}(1, 7) g_{xc}(7, 5, 6) \chi_{\rho\rho}(6, 2) \chi_{\rho\rho}(5, 3) \end{aligned} \quad (2.54)$$

with the short hand form:

$$\chi^{(2)} = \left[1 + \chi^{(1)} f_{vxc} \right] \chi_0^{(2)} \left[1 + f_{vxc} \chi^{(1)} \right] \left[1 + f_{vxc} \chi^{(1)} \right] + \chi^{(1)} g_{xc} \chi^{(1)} \chi^{(1)}. \quad (2.55)$$

2.3.1 Interpretation of the solution

This form actually gives some insight in the rather complex structure of the equation, when we introduce the concept of the dielectric function. The role of the dielectric function ϵ is to account for the screening of the perturbing potential by the induced field and thus connect the total with the perturbing potential:

$$V_{tot}(1) = \int d2 \epsilon^{-1}(1, 2) V_{per}(2). \quad (2.56)$$

where $V_{tot} = V_{per} + V_H$. Formally the screening can be defined by

$$\begin{aligned}\epsilon^{-1}(1, 2) &= \frac{\delta V_{tot}(1)}{\delta V_{per}(2)} = \delta(1, 3) + \int d3 \frac{\delta V_H(1)}{\delta \rho(3)} \frac{\delta \rho(3)}{\delta V_{per}(2)} \\ &= \delta(1, 3) + \int d3 v(1, 3) \chi_{\rho\rho}(3, 2).\end{aligned}\tag{2.57}$$

This definition assumes that the induced field is only due to the Hartree potential while the density response χ to the perturbing field contains exchange and correlation effects as well (c.f. Eqs. (2.33) and (2.40)). The screening of the perturbing potential can however be due to exchange and correlation effects as well so that one has to define the screening as the variation of a total potential that also contains V_{xc} :

$$\epsilon_{TE}^{-1}(1, 2) = \frac{\delta V_{KS}(1)}{\delta V_{per}(2)} = \delta(1, 3) + \int d3 (v(1, 3) + f_{xc}(1, 3)) \chi_{\rho\rho}(3, 2)\tag{2.58}$$

$$= \delta(1, 3) + \int d3 f_{vxc}(1, 3) \chi_{\rho\rho}(3, 2).\tag{2.59}$$

This case is called *test-electron* (TE) while the former is called *test-particle*, because they either describe an experiment with a quantum mechanically interacting probe (electron) or a classical particle.

We can use the test-electron screening to write the solution (Eq. (2.54) of the second order Dyson equation as

$$\chi^{(2)} = [\epsilon_{TE}^{-1}]^T \chi_0^{(2)} \epsilon_{TE}^{-1} \epsilon_{TE}^{-1} + \chi^{(1)} g_{xc} \chi^{(1)} \chi^{(1)}\tag{2.60}$$

where $[\epsilon_{TE}^{-1}]^T$ is the transposed of ϵ_{TE}^{-1} . The significance of the ϵ_{TE}^{-1} factors can be understood by considering that $\chi_0^{(2)}$ gives the response to V_{KS} while $\chi^{(2)}$ responds to V_{per} . Now the two ϵ_{TE}^{-1} on the right side of $\chi_0^{(2)}$ do nothing else but transform the applied perturbing potential V_{per} in a Kohn-Sham potential V_{KS} , since $V_{KS} = \epsilon_{TE}^{-1} V_{per}$.

The transpose ϵ_{TE}^{-1} to the left of the non-interacting $\chi_0^{(2)}$ is, however more involved. To understand its origin we reconsider the derivation of the second order Dyson equation using for the linear response

$$\chi^{(1)} = \chi_0^{(1)} \epsilon_{TE}^{-1}\tag{2.61}$$

from which follows

$$\chi^{(2)} = \frac{\delta\chi^{(1)}}{\delta V_{per}} = \frac{\delta\chi_0^{(1)}}{\delta V_{per}} \epsilon_{TE}^{-1} + \chi_0^{(1)} \frac{\delta\epsilon_{TE}^{-1}}{\delta V_{per}} \quad (2.62)$$

$$= \frac{\delta\chi_0^{(1)}}{\delta V_{KS}} \frac{\delta V_{KS}}{\delta V_{per}} \epsilon_{TE}^{-1} + \chi_0^{(1)} \frac{\delta}{\delta V_{per}} \left[1 + (v + f_{xc})\chi^{(1)} \right] \quad (2.63)$$

$$= \chi_0^{(2)} \epsilon_{TE}^{-1} \epsilon_{TE}^{-1} + \chi_0^{(1)} \frac{\delta f_{xc}}{\delta V_{per}} \chi^{(1)} + \chi_0^{(1)} (v + f_{xc}) \frac{\delta\chi^{(1)}}{\delta V_{per}} \quad (2.64)$$

$$= \chi_0^{(2)} \epsilon_{TE}^{-1} \epsilon_{TE}^{-1} + \chi_0^{(1)} \frac{\delta f_{xc}}{\delta \rho} \frac{\delta \rho}{\delta V_{per}} \chi^{(1)} + \chi_0^{(1)} (v + f_{xc}) \chi^{(2)} \quad (2.65)$$

$$= \chi_0^{(2)} \epsilon_{TE}^{-1} \epsilon_{TE}^{-1} + \chi_0^{(1)} g_{xc} \chi^{(1)} \chi^{(1)} + \chi_0^{(1)} (v + f_{xc}) \chi^{(2)} . \quad (2.66)$$

The last term in the last line can be combined with the left hand side of the equation and then yields the $[\epsilon_{TE}^{-1}]^T$ when inverted. From this derivation we see that this prefactor as well as the term with g_{xc} comes from the term $\frac{\delta\epsilon_{TE}^{-1}}{\delta V_{per}} = \frac{\delta^2 V_{KS}}{\delta V_{per} \delta V_{per}}$ in the first line. This can be interpreted as a second order screening and as such does not have analogous linear processes.

2.3.2 Graphical representation of the 2nd order Dyson Equation

The linear Dyson equation (2.40), consisting of three terms of only two point quantities, has a rather simple structure compared with the second order Dyson equation (2.47). Here, we have to deal with a mixture of two- and three-point quantities as well as with seven different terms. In order to get a clearer view of the structure of the equation and to show how the different terms are connected with each other, I will use here a set of diagrams in analogy with the Feynman diagrams. This might help to get a better view of the content of the equation and its constituting terms. It does of course not provide any further insight, that one might not get from the equation, but it might serve the intuition and as a mnemonic device.

The different quantities appearing in the equation are represented according to this table:

$\chi_0^{(1)}(1, 2)$	
$\chi^{(1)}(1, 2)$	
$f_{xc}(1, 2)$	
$\chi_0^{(2)}(1, 2, 3)$	
$\chi^{(2)}(1, 2, 3)$	
$g_{xc}(1, 2, 3)$	

With these symbols the linear Dyson equation takes this form

$$\begin{array}{c} 1 \\ \bullet \end{array} \text{---} \text{◇} \text{---} \begin{array}{c} 2 \\ \bullet \end{array} = \begin{array}{c} 1 \\ \bullet \end{array} \text{---} \text{◇} \text{---} \begin{array}{c} 2 \\ \bullet \end{array} + \begin{array}{c} 1 \\ \bullet \end{array} \text{---} \text{◇} \text{---} \begin{array}{c} 3 \\ \bullet \end{array} \text{---} \text{◇} \text{---} \begin{array}{c} 4 \\ \bullet \end{array} \text{---} \text{◇} \text{---} \begin{array}{c} 2 \\ \bullet \end{array}$$

Figure 2.1: Graphical representation of the linear TDDFT Dyson equation (2.40).

which, indeed, has a very simple structure and for this alone one would not need a graphical representation. Turning, however, to the second order Dyson equation, we obtain a far richer picture

$$\begin{array}{c} 1 \\ \bullet \end{array} \text{---} \text{◇} \text{---} \begin{array}{c} 2 \\ \bullet \\ 3 \\ \bullet \end{array} = \begin{array}{c} 1 \\ \bullet \end{array} \text{---} \text{◇} \text{---} \begin{array}{c} 2 \\ \bullet \\ 3 \\ \bullet \end{array} + \begin{array}{c} 1 \\ \bullet \end{array} \text{---} \text{◇} \text{---} \begin{array}{c} 4 \\ \bullet \end{array} \text{---} \text{◇} \text{---} \begin{array}{c} 5 \\ \bullet \end{array} \text{---} \text{◇} \text{---} \begin{array}{c} 2 \\ \bullet \\ 3 \\ \bullet \end{array} + \begin{array}{c} 1 \\ \bullet \end{array} \text{---} \text{◇} \text{---} \begin{array}{c} 4 \\ \bullet \end{array} \text{---} \text{◇} \text{---} \begin{array}{c} 5 \\ \bullet \end{array} \text{---} \text{◇} \text{---} \begin{array}{c} 2 \\ \bullet \\ 3 \\ \bullet \end{array} + \begin{array}{c} 1 \\ \bullet \end{array} \text{---} \text{◇} \text{---} \begin{array}{c} 5 \\ \bullet \end{array} \text{---} \text{◇} \text{---} \begin{array}{c} 6 \\ \bullet \end{array} \text{---} \text{◇} \text{---} \begin{array}{c} 2 \\ \bullet \\ 3 \\ \bullet \end{array} + \begin{array}{c} 1 \\ \bullet \end{array} \text{---} \text{◇} \text{---} \begin{array}{c} 4 \\ \bullet \end{array} \text{---} \text{◇} \text{---} \begin{array}{c} 5 \\ \bullet \end{array} \text{---} \text{◇} \text{---} \begin{array}{c} 6 \\ \bullet \end{array} \text{---} \text{◇} \text{---} \begin{array}{c} 2 \\ \bullet \\ 3 \\ \bullet \end{array} + \begin{array}{c} 1 \\ \bullet \end{array} \text{---} \text{◇} \text{---} \begin{array}{c} 4 \\ \bullet \end{array} \text{---} \text{◇} \text{---} \begin{array}{c} 5 \\ \bullet \end{array} \text{---} \text{◇} \text{---} \begin{array}{c} 6 \\ \bullet \end{array} \text{---} \text{◇} \text{---} \begin{array}{c} 2 \\ \bullet \\ 3 \\ \bullet \end{array} + \begin{array}{c} 1 \\ \bullet \end{array} \text{---} \text{◇} \text{---} \begin{array}{c} 4 \\ \bullet \end{array} \text{---} \text{◇} \text{---} \begin{array}{c} 5 \\ \bullet \end{array} \text{---} \text{◇} \text{---} \begin{array}{c} 6 \\ \bullet \end{array} \text{---} \text{◇} \text{---} \begin{array}{c} 2 \\ \bullet \\ 3 \\ \bullet \end{array}$$

Figure 2.2: Graphical representation of the second order TDDFT Dyson equation (2.47).

2.4 Approximations

2.4.1 IPA

The simplest approximation in the Dyson like equation (2.47) is done by neglecting all many-body effects by letting $f_{vxc} = 0$. Then, only the Kohn-Sham response is present therefore it is called the independent particle approximation (IPA):

$$\chi_{\rho\rho\rho}^{IPA}(1, 2, 3) = \chi_{\rho\rho\rho}^{(0)}(1, 2, 3) . \quad (2.67)$$

We will see in later chapters (c.f. chapter 6) that this approximation can represent important features of the response and thus is not as bad an approximation as its simplicity suggests.

2.4.2 RPA

Considering the Coulomb interaction while still neglecting exchange and correlation effects, i.e. by keeping v but letting $f_{xc} = 0$ the Dyson equation becomes

$$\begin{aligned} \chi_{\rho\rho\rho}^{RPA}(1, 2, 3) = & \chi_{\rho\rho\rho}^{(0)}(1, 2, 3) + \int d4d5 \chi_{\rho\rho\rho}^{(0)}(1, 4, 3)v(4, 5)\chi_{\rho\rho}(5, 2) \\ & + \int d4d5 \chi_{\rho\rho\rho}^{(0)}(1, 2, 4)v(4, 5)\chi_{\rho\rho}(5, 3) + \\ & + \int d4d5d6d7 \chi_{\rho\rho\rho}^{(0)}(1, 5, 4)v(5, 6)\chi_{\rho\rho}(6, 2)v(4, 7)\chi_{\rho\rho}(7, 3) + \\ & + \int d4d5 \chi_{\rho\rho}^{(0)}(1, 4)v(4, 5)\chi_{\rho\rho}^{RPA}(5, 2, 3) . \end{aligned} \quad (2.68)$$

and one speaks of the random phase approximations (RPA). This approximation already captures the important effect that the perturbation locally polarizes lattice atoms resulting in a field that itself can polarize other atoms and thus contribute to the overall perturbation. Since it is linked to the lattice structure and the fields are generally fast oscillating fields, this effect is commonly referred to as crystal *local field effect* (c.f. Chap. 3).

2.4.3 TDLDA

Apart from these two approximations that profit from what little is known exactly about the system, any further approximation has to concern the exchange and correlation kernel, which is unknown. Approximations to this kernel are made more in the spirit of educated guessing rather than in a rigorous way from exact expressions. One of the most commonly used TDDFT kernel is the time dependent generalization of the local density approximation (LDA) of DFT. Here, one assumes that $V_{xc}(\mathbf{r})$ only depends on the den-

sity at the point \mathbf{r} rather than on the environment as well. The time dependent version of this approximation, the time dependent local density approximation (TDLDA), uses the so called adiabatic local density approximation (ALDA) where $V_{xc}(\mathbf{r}, t)$ is taken to be the local density exchange and correlation potential calculated from the density at the time t

$$V_{xc}^{ALDA}(\mathbf{r}, t) = V_{xc}^{LDA}[\rho(\mathbf{r}, t)] . \quad (2.69)$$

The kernel for TDDFT derived from this approximation is then

$$f_{xc}^{TDLDA}(\mathbf{r}_1, t_1, \mathbf{r}_2, t_2) = \delta(\mathbf{r}_1 - \mathbf{r}_2)\delta(t_1 - t_2) \frac{\partial V_{xc}^{LDA}[\rho(\mathbf{r}_1, t_1)]}{\rho(\mathbf{r}_1, t_1)} . \quad (2.70)$$

From this approximation one can derive in the same spirit the second order g_{xc} . While the TDLDA works well for electron loss responses and other cases of finite momentum transfer, it fails to produce reliable results for the optical absorption of solids [93]. This failure has been attributed to the missing long range interaction in the local approximation. Long range interaction, however, is the hallmark of the Coulomb potential that in semiconductors leads to the formation of excitons which in turn are known to contribute important features to optical spectra. For this reason, TDLDA does not seem to be a good candidate as kernel for second order optical processes.

2.4.4 Quasiparticles

To go beyond the local density approximation one has to consider that the excitation of an electron in a solid will leave behind a hole that thus exerts an attractive force on its neighboring electrons, leading to a cloud of opposite charged particles around it and thus to a screening of the particle. This screening of the particle leads to a shift in the excitation energies and one refers to the particle and its screening together as a *quasiparticle*. The shifted energy spectrum is then attributed to this quasiparticle, which has the advantage that one can still think about it in terms of a single particle process. A TDDFT exchange and correlation kernel now has to fulfill two functions, first it should transform the Kohn-Sham single particle response into the response of quasiparticles and second it has to account for the actual two body interaction between the electron and the hole, i.e. the exciton. It has been shown [28] that one can split up the f_{xc} into two parts

$$f_{xc} = f_{xc}^{(1)} + f_{xc}^{(2)} \quad (2.71)$$

where $f_{xc}^{(1)}$ accounts for the quasiparticle effect and $f_{xc}^{(2)}$ for the excitonic effects. The quasiparticle formed by the screening of the hole is described within many-body

perturbation theory (MBPT) by the quasiparticle equation

$$[h_0(\mathbf{r}_1) + V_H(\mathbf{r}_1)] \phi_i(\mathbf{r}_1) + \int d\mathbf{r}_2 \Sigma(\mathbf{r}_1, \mathbf{r}_2, E_i) \phi_i(\mathbf{r}_2) = E_i \phi_i(\mathbf{r}_1) \quad (2.72)$$

where $\Sigma(\mathbf{r}_1, \mathbf{r}_2, E_i)$ is the so called self energy that accounts for the many-body effects and is the key quantity for which Hedin's equations [94] are formulated. The central idea is, instead of considering the bare Coulomb interaction v , one should formulate the self energy in terms of the screened potential W defined as

$$W(1, 2) = \int d3 \epsilon^{-1}(1, 3) v(3, 2) \quad (2.73)$$

where ϵ^{-1} is the time ordered screening

$$\epsilon^{-1}(1, 2) = \frac{\delta V_{tot}(1)}{\delta V_{per}(2)}. \quad (2.74)$$

This leads to a set of five self consistent equations (c.f App. E) for the Green's function. These equations are routinely solved within the GW approximation for the self energy which together with the quasiparticle equation (2.72) gives the quasiparticle energies and wavefunctions that can be used to construct a response function. It turns out that in many practical cases the quasiparticle effect amounts only to a shift of the conduction states in the band structure, which suggest that a calculation of the actual quasiparticle effect can be circumvented by just shifting the Kohn-Sham spectrum by the appropriate value. Indeed, it has been shown also for the case of second order response [67], that the application of such a scissors shift can reproduce the spectra. Therefore, one does not consider the exact form of $f_{xc}^{(1)}$, nor approximations to it, but either assumes the quasiparticle effect to be appropriately accounted for by shifting of the conduction states or uses the results of a quasiparticle calculation. Nevertheless, the simple scheme of shifting the conduction states has some implications for our formalism when we consider the optical limit (c.f. Chap. 4).

2.4.5 Excitons

Excitonic effects, being two particle processes, are correctly described by the Bethe-Salpeter equation (BSE), which gives the many-body two particle correlation function L . This quantity is closely related to the two body Green's function by its definition [95]

$$iL(1, 2, 3, 4) = G(1, 2)G(3, 4) - G_2(1, 3, 2, 4). \quad (2.75)$$

Thus, the two particle correlation function L describes those parts of two particle processes that go beyond their independent propagation that is represented by GG . In many-body perturbation theory, this quantity is also defined as the variation of the one

particle Green's function under the presence of a perturbing potential

$$L(1, 2, 3, 4) = -i \frac{G(1, 2)}{V_{per}(3, 4)} \quad (2.76)$$

while the single particle G is determined by the Dyson equation

$$G^{-1}(1, 2) = G_H^{-1}(1, 2) - V_{per}(1, 2) - \Sigma(1, 2) \quad (2.77)$$

where Σ is the self energy and G_H the Hartree Green's function [95, 96]. Combining the two equations yields the Bethe-Salpeter equation in the form [97]

$$iL(1, 2, 3, 4) = G(1, 3)G(4, 2) + \int d5678 G(1, 5)G(6, 2) [v(5, 7)\delta(5, 6)\delta(7, 8) + \Xi(5, 6, 7, 8)] L(7, 8, 3, 4) \quad (2.78)$$

where the many-body interaction kernel has been defined as

$$\Xi(5, 6, 7, 8) = i \frac{\delta \Sigma(5, 6)}{\delta G(7, 8)}. \quad (2.79)$$

The similarity between the Bethe-Salpeter equation (2.78) and the TDDFT Dyson equation (2.40) can be used by exploiting the fact that the density response function is the two point diagonal of the two body correlation function:

$$\chi_{\rho\rho}(1, 2) = \frac{\delta \rho(1)}{V_{per}(2)} = -i \frac{\delta G(1, 1^+)}{V_{per}(2, 2^+)} = L(1, 1^+, 2, 2^+). \quad (2.80)$$

In [96] it is shown how one obtains from this an exact expression for the two body correlation contribution to f_{xc} that can be linearized to yield

$$f_{xc}^{(2)}(1, 2) = \int d3456 P_0^{-1}(1, 3)G(3, 4)G(5, 3)W(4, 5)G(4, 6)G(6, 5)P_0^{-1}(6, 2) \quad (2.81)$$

where P_0^{-1} is the independent *quasi*particle polarizability and W the screened potential. This kernel has been shown to yield results for the absorption of solids that are almost identical with the Bethe-Salpeter result. There are different ways to derive this kernel, c.f. [25–29], each giving essentially the same result.

The main advantage of TDDFT with respect to BSE is that it deals only with 2-point quantities, that are numerically represented by two dimensional matrices, instead of 4-point quantities requiring much more computational resources. Implementations of the Eq. (2.81), that has been named the NANOQUANTA kernel, have however turned out to require computational effort that is close to the one required to solve the BSE. This is partly due to the fact that for BSE there exist well optimized methods of calculation but also due to the complex structure of the kernel. Therefore, a drastically simplified

kernel of the form.

$$f_{xc}(\mathbf{r}_1, \mathbf{r}_2) = -\frac{\alpha}{4\pi|\mathbf{r}_1 - \mathbf{r}_2|} \quad \text{and} \quad f_{xc}(\mathbf{q} + \mathbf{G}) = -\frac{\alpha}{|\mathbf{q} + \mathbf{G}|^2} \quad (2.82)$$

has been proposed [98]. The motivation for such a formulation is to explicitly introduce the long-range interaction, while α is a priori a parameter. One can, however, motivate this form of a kernel from the exact expression of Eq. (2.81) by considering the limiting behaviour of its constituents as $\mathbf{q} \rightarrow 0$. One finds that in this limit $P_0^{-1} \sim 1/q^2$ and $G \sim q$ while from the definition of the screening follows $W \sim \epsilon_\infty^{-1}/q^2$. This behaviour yields indeed the form of Eq. (2.82) as a reasonable approximation for the optical limit of the NANOQUANTA kernel. It does however also indicate that $\alpha \sim \epsilon_\infty^{-1}$, which has been confirmed by systematically comparing BSE results with results obtained with this kernel [99].

This kernel has been shown to reproduce results obtained with the Bethe-Salpeter equation on a qualitative and quantitative level. Indeed, the agreement can be viewed as remarkable given its simplicity and the computational cost saved with respect to the NANOQUANTA kernel or the BSE. Its downside, however, is the fact that α is a priori a parameter and can only be determined by comparison with a BSE result, thus comprising either its efficiency or the ab initio character of the calculation. Nevertheless, in this work I will use this kernel for the calculation of the second order response according the second order TDDFT Dyson like equation (2.47), because in this case its downside is somewhat less important. In most cases here we rely on established results from the linear case, where the value of α has already been confirmed by a BSE calculation. But even if such values are unknown, performing first a linear BSE calculation to determine them does not considerably increase the computational cost, since the second order calculation is already orders of magnitude larger than a linear BSE one.

3 Macroscopic response and local fields

In the previous chapter I have shown how one can use time-dependent perturbation theory together with density-functional-theory to obtain the second order microscopic response. To be able to interpret and predict experimental results, it is however important to be able to connect these microscopic quantities to the macroscopic world of the laboratory. The difference between these two responses comes from the fact that the charge distribution induced by the light field polarizes the crystal and thus induces an electric field that in turn modifies the charge distribution. Therefore the macroscopic and microscopic responses differ depending on the inhomogeneity of the system.

The connection between the microscopic and macroscopic quantities is made by means of a spatial average over a distance that is large compared with the lattice parameter a , following the argumentation of Ehrenreich [100], I will first show how such an average is taken and then proceed to relate the microscopic quantities to responses to macroscopic fields.¹

3.1 Macroscopic average

The microscopic potentials considered in Chap. 2.3 can be represented in momentum space as

$$V(\mathbf{r}, \omega) = \sum_{\mathbf{q}\mathbf{G}} V_{\mathbf{G}}(\mathbf{q}, \omega) e^{i(\mathbf{q}+\mathbf{G})\mathbf{r}}. \quad (3.1)$$

A macroscopic average now should be done by averaging over those parts of its decomposition that are periodic with respect to the lattice. We therefore rewrite Eq. (3.1) to yield explicitly these components

$$V(\mathbf{r}, \omega) = \sum_{\mathbf{q}} e^{i\mathbf{q}\mathbf{r}} \sum_{\mathbf{G}} V_{\mathbf{G}}(\mathbf{q}, \omega) e^{i\mathbf{G}\mathbf{r}} = \sum_{\mathbf{q}} e^{i\mathbf{q}\mathbf{r}} V(\mathbf{q}, \mathbf{r}, \omega) \quad (3.2)$$

where

$$V(\mathbf{q}, \mathbf{r}, \omega) = \sum_{\mathbf{G}} V_{\mathbf{G}}(\mathbf{q}, \omega) e^{i\mathbf{G}\mathbf{r}} \quad (3.3)$$

¹A mathematically more systematic way of obtaining macroscopic relations from microscopic quantities is taken by homogenization theory, where one expands all fields in powers of a/λ , where λ is the wavelength of the light field [101]. The advantage, apart from mathematical rigour, is that this approach also gives information about the corrections to the average, i.e. higher terms in the expansion.

is the lattice periodic part that has to be averaged. Integrating over the unit cell volume yields the macroscopic component $V_M(\mathbf{q}, \omega)$ of the potential

$$V_M(\mathbf{q}, \omega) = \frac{1}{\Omega_c} \int d\mathbf{r} V(\mathbf{q}, \mathbf{r}, \omega) = \sum_{\mathbf{G}} V_{\mathbf{G}}(\mathbf{q}, \omega) \frac{1}{\Omega_c} \int d\mathbf{r} e^{i\mathbf{G}\mathbf{r}} = V_{\mathbf{0}}(\mathbf{q}, \omega). \quad (3.4)$$

Thus the macroscopic average amounts to considering only the $\mathbf{G} = \mathbf{0}$ Fourier component of the field. In an intuitive physical picture this means that the components with $\mathbf{G} \neq \mathbf{0}$ are oscillating too fast to have influence on the macroscopic average.

3.2 Macroscopic response

The central quantity in optical measurements is the macroscopic polarization \mathbf{P}

$$\partial_{t_1} \mathbf{P}(1) = \mathbf{j}(1). \quad (3.5)$$

Its expansion in terms of the macroscopic total field defines the macroscopic linear and non-linear susceptibilities:

$$\mathbf{P}(1) = \chi_M(1, 2) \mathbf{E}_{\text{tot}}(2) + \chi_M(1, 2, 3) \mathbf{E}_{\text{tot}}(2) \mathbf{E}_{\text{tot}}(3) + \dots \quad (3.6)$$

where the microscopic total field contains the applied external field and contribution from the induced polarization of the system due to this perturbation. It is the effect of the induced field that makes the difference between the macroscopic and microscopic response and it is thus the main concern of this chapter.

To describe nonlinear optical experiments it is elementary to be able to distinguish between contributions according to their order in an expansion in terms of the total field in Eq. (3.6), e.g. the macroscopic polarization

$$\mathbf{P} = \mathbf{P}^{(1)} + \mathbf{P}^{(2)} + \dots \quad (3.7)$$

and we will find that the separation of orders in this expansion is not trivially obtained from the microscopic formulation, because one has to consider carefully how the external field induces a field in the medium thus giving rise to finite polarization. Starting point are the Maxwell equations

$$\begin{aligned} \nabla \cdot \mathbf{B} &= 0 & \nabla \times \mathbf{H} - \partial_t \mathbf{D} &= 4\pi \mathbf{j} \\ \nabla \cdot \mathbf{E} &= \rho & \nabla \times \mathbf{E} + \partial_t \mathbf{B} &= 0 \end{aligned} \quad (3.8)$$

where we will neglect the magnetization and use $\mathbf{H} = \mathbf{B}$. These Maxwell equations are true for the total field

$$\mathbf{E}_{\text{tot}} = \mathbf{E}_{\text{ext}} + \mathbf{E}_{\text{ind}}. \quad (3.9)$$

It follows the wave equation:

$$\nabla \times \nabla \times \mathbf{E}_{\text{tot}} + \partial_t^2 \mathbf{E}_{\text{tot}} = -4\pi \partial_t \mathbf{j}_{\text{tot}} . \quad (3.10)$$

Per definition the current is linked to the polarization via the time derivative thus it is this quantity where the definitions of the susceptibilities are made. The total current can be written as $\mathbf{j}_{\text{tot}} = \mathbf{j}_{\text{ext}} + \mathbf{j}_{\text{ind}}$. Considering only the external field, the Maxwell equations read:

$$\begin{aligned} \nabla \cdot \mathbf{B} &= 0 & \nabla \times \mathbf{B} - \partial_t \mathbf{E}_{\text{ext}} &= 4\pi \mathbf{j}_{\text{ext}} \\ \nabla \cdot \mathbf{E}_{\text{ext}} &= \rho_{\text{ext}} & \nabla \times \mathbf{E} + \partial_t \mathbf{B} &= 0 \end{aligned} \quad (3.11)$$

and the corresponding wave equation is

$$\nabla \times \nabla \times \mathbf{E}_{\text{ext}} + \partial_t^2 \mathbf{E}_{\text{ext}} = -4\pi \partial_t \mathbf{j}_{\text{ext}} . \quad (3.12)$$

Using the linearity of the Maxwell equations a similar equation follows for the induced field. Introducing the operator

$$\mathcal{O} = \nabla \times \nabla \times \bullet + \partial_t^2 \bullet \quad (3.13)$$

we can write it as

$$\mathbf{E}_{\text{ind}} = -4\pi \mathcal{O}^{-1} \partial_t \mathbf{j}_{\text{ind}} . \quad (3.14)$$

In terms of response theory we can formulate the perturbations of the induced current as

$$\partial_t \mathbf{j}_{\text{ind}}^{(1)}(1) = \int d2 \chi(1, 2) \mathbf{E}_{\text{ext}}(2) \quad (3.15)$$

$$\partial_t \mathbf{j}_{\text{ind}}^{(2)}(1) = \int d2 d3 \chi(1, 2, 3) \mathbf{E}_{\text{ext}}(2) \mathbf{E}_{\text{ext}}(3) . \quad (3.16)$$

This can also be regarded as definition of the response function χ to the external field. They can be derived from quantum mechanical perturbation theory and thus can be obtained from the quantum mechanical groundstate². We are, however, interested in the responses of the induced current to the total field, i.e. we would like to calculate response functions π like

$$\partial_t \mathbf{j}_{\text{ind}}^{(1)}(1) = \int d2 \pi(1, 2) \mathbf{E}_{\text{tot}}(2) \quad (3.17)$$

$$\partial_t \mathbf{j}_{\text{ind}}^{(2)}(1) = \int d2 d3 \pi(1, 2, 3) \mathbf{E}_{\text{tot}}(2) \mathbf{E}_{\text{tot}}(3) . \quad (3.18)$$

²Del Sole and Fiorino [102] point out that this is only true for groundstates where retardation effects of the electrons are accounted for. Since this is usually not the case, one has to include them in the perturbation, which I do later on in Eq. (3.39).

A microscopic formulation of these responses however, is not feasible because the induced field is a priori unknown and therefore we need to express them in terms of the known quantities χ .

To first order the relation between the two fields is

$$\begin{aligned} \mathbf{E}_{\text{tot}}(1) = \mathbf{E}_{\text{ext}}(1) + \mathbf{E}_{\text{ind}}(1) &= \mathbf{E}_{\text{ext}}(1) - 4\pi\mathcal{O}^{-1}(1)\partial_t\mathbf{j}_{\text{ind}}(1) \\ &= \left[\delta(1,2) - 4\pi\mathcal{O}^{-1}(1) \int d2\chi(1,2) \right] \mathbf{E}_{\text{ext}}(2). \end{aligned} \quad (3.19)$$

This equation become considerably more readable if we use the macroscopic average according to [100] as sketched in section 3.1, thus passing from the general variable 1 to $\mathbf{k} = \mathbf{q} + \mathbf{G}$ and taking only the $\mathbf{G} = \mathbf{0}$ component:³

$$\mathbf{E}_{\text{tot}}(\mathbf{q}) = [1 - 4\pi\mathcal{O}^{-1}(\mathbf{q})\chi(\mathbf{q}, \mathbf{q})] \mathbf{E}_{\text{ext}}(\mathbf{q}). \quad (3.20)$$

This is only possible because the external field is assumed to have only macroscopic components [102], i.e. on the right hand side of the equation we do take the average of a product. Inversion yields

$$\mathbf{E}_{\text{ext}}(\mathbf{q}) = [1 - 4\pi\mathcal{O}^{-1}(\mathbf{q})\chi(\mathbf{q}, \mathbf{q})]^{-1} \mathbf{E}_{\text{tot}}(\mathbf{q}) \quad (3.21)$$

Now, we would like to relate the second order response functions. The definition (3.16) can be averaged similarly as in Eq. (3.21)

$$\partial_t\mathbf{j}_{\text{ind}}^{(2)}(\mathbf{q}_1) = \sum_{\mathbf{q}_2\mathbf{q}_3} \chi(\mathbf{q}_1, \mathbf{q}_2, \mathbf{q}_3) \mathbf{E}_{\text{ext}}(\mathbf{q}_2) \mathbf{E}_{\text{ext}}(\mathbf{q}_3)$$

where again the fact that the external field is macroscopic was used. The external fields can be expressed in terms of the averaged total field \mathbf{E}_{tot} according to Eq. (3.21) and we have

$$\partial_t\mathbf{j}_{\text{ind}}^{(2)}(\mathbf{q}_1) = \sum_{\mathbf{q}_2\mathbf{q}_3} \chi(\mathbf{q}_1, \mathbf{q}_2, \mathbf{q}_3) [1 - 4\pi\mathcal{O}^{-1}(\mathbf{q}_2)\chi(\mathbf{q}_2, \mathbf{q}_2)]^{-1} \mathbf{E}_{\text{tot}}(\mathbf{q}_2) \times \quad (3.22)$$

$$\times [1 - 4\pi\mathcal{O}^{-1}(\mathbf{q}_3)\chi(\mathbf{q}_3, \mathbf{q}_3)]^{-1} \mathbf{E}_{\text{tot}}(\mathbf{q}_3) \quad (3.23)$$

This is a macroscopically averaged response to the total fields and thus can be regarded as the macroscopically averaged version of Eq. (3.18) and by comparison we can define the macroscopic average of π :

$$\begin{aligned} \langle \pi_{\mathbf{G}\mathbf{G}_1\mathbf{G}_2}(\mathbf{q}_1, \mathbf{q}_2, \mathbf{q}_3) \rangle &= \\ \chi(\mathbf{q}_1, \mathbf{q}_2, \mathbf{q}_3) [1 - 4\pi\mathcal{O}^{-1}(\mathbf{q}_2)\chi(\mathbf{q}_2, \mathbf{q}_2)]^{-1} [1 - 4\pi\mathcal{O}^{-1}(\mathbf{q}_3)\chi(\mathbf{q}_3, \mathbf{q}_3)]^{-1} \end{aligned} \quad (3.24)$$

³Here and in the following, microscopic quantities that are written to depend only on \mathbf{q} are assumed to be taken for $\mathbf{G} = \mathbf{0}$, e.g. $\chi(\mathbf{q}, \mathbf{q}) = \chi_{\mathbf{G}=\mathbf{0}, \mathbf{G}'=\mathbf{0}}(\mathbf{q}, \mathbf{q})$. Also the frequency dependence is not explicitly given to keep the equations readable but is always implicitly accounted for, because each \mathbf{q}_i is associated with the frequency ω_i .

Here we see how the induced fields enter into the macroscopically averaged response. Clearly the induced polarization, accounted for by $\chi(\mathbf{q}, \mathbf{q},)$ in the equation, modifies the second order microscopic response under the average.

To relate the two second order responses we had to use only the linear relation between the fields, because taking into account the induced field to second order would yield terms of higher than second order, when inserted into Eq. (3.16). However, an important point of the treatment is that, when considering the first order induced current, as in the definition (3.15), this argument does not hold, since we would like to account for all second order terms to achieve a proper ordering of the contributions in Eq. (3.7) and in general the relation between total and external field contains higher order terms. To second order we have

$$\mathbf{E}_{\text{tot}} = \mathbf{E}_{\text{ext}} + \mathbf{E}_{\text{ind}}^{(1)} + \mathbf{E}_{\text{ind}}^{(2)}. \quad (3.25)$$

That means, if in the context of second order perturbation, we want to express the first order response

$$\partial_t \mathbf{j}_{\text{ind}}^{(1)}(\mathbf{q}) = \chi(\mathbf{q}, \mathbf{q}) \mathbf{E}_{\text{ext}}(\mathbf{q}) \quad (3.26)$$

in terms of the total field, we have to take into account the nonlinear relation Eq. (3.25) between the two fields. Thus we have

$$\begin{aligned} \partial_t \mathbf{j}_{\text{ind}}^{(1)}(\mathbf{q}) &= \chi(\mathbf{q}, \mathbf{q}) \left[\mathbf{E}_{\text{tot}}(\mathbf{q}) - \mathbf{E}_{\text{ind}}^{(1)}(\mathbf{q}) - \mathbf{E}_{\text{ind}}^{(2)}(\mathbf{q}) \right] \\ &= \chi(\mathbf{q}, \mathbf{q}) \left[\mathbf{E}_{\text{tot}}(\mathbf{q}) + 4\pi \mathcal{O}^{-1}(\mathbf{q}) \partial_t \mathbf{j}_{\text{ind}}^{(1)}(\mathbf{q}) + 4\pi \mathcal{O}^{-1}(\mathbf{q}) \partial_t \mathbf{j}_{\text{ind}}^{(2)}(\mathbf{q}) \right] \end{aligned} \quad (3.27)$$

Solving for $\mathbf{j}_{\text{ind}}^{(1)}$ yields the first order current in terms of the total field

$$\begin{aligned} \partial_t \mathbf{j}_{\text{ind}}^{(1)}(\mathbf{q}) &= [1 - 4\pi \chi(\mathbf{q}, \mathbf{q}) \mathcal{O}^{-1}(\mathbf{q})]^{-1} \chi(\mathbf{q}, \mathbf{q}) \mathbf{E}_{\text{tot}} + \\ &\quad + 4\pi [1 - 4\pi \chi(\mathbf{q}, \mathbf{q}) \mathcal{O}^{-1}(\mathbf{q})]^{-1} \chi(\mathbf{q}, \mathbf{q}) \mathcal{O}^{-1}(\mathbf{q}) \partial_t \mathbf{j}_{\text{ind}}^{(2)} \end{aligned} \quad (3.28)$$

While the relation between the induced current and perturbing field, Eq. (3.26), is linear, the relation between the induced current and the total field, Eq. (3.27) is not, since in this context we want to keep all second order contributions. Thus when expressing Eq. (3.26) in terms of the total field, we find that this first order expression of the current contains higher order terms.

Now we can write down the proper macroscopic expansion of the polarization to second

order:

$$\begin{aligned}
\mathbf{P} &= \mathbf{P}^{(1)} + \mathbf{P}^{(2)} \\
&= -\frac{1}{\omega^2} \left\{ \partial_t \mathbf{j}_{\text{ind}}^{(1)}(\mathbf{q}) + \partial_t \mathbf{j}_{\text{ind}}^{(2)}(\mathbf{q}) \right\} \\
&= -\frac{1}{\omega^2} \left\{ [1 - 4\pi\chi(\mathbf{q}, \mathbf{q})\mathcal{O}^{-1}]^{-1} \chi(\mathbf{q}, \mathbf{q}) \mathbf{E}_{\text{tot}} + \right. \\
&\quad \left. + \left(1 + 4\pi [1 - 4\pi\chi(\mathbf{q}, \mathbf{q})\mathcal{O}^{-1}]^{-1} \chi(\mathbf{q}, \mathbf{q})\mathcal{O}^{-1} \right) \partial_t \mathbf{j}_{\text{ind}}^{(2)} \right\} \\
&= -\frac{1}{\omega^2} \left\{ [1 - 4\pi\chi(\mathbf{q}, \mathbf{q})\mathcal{O}^{-1}]^{-1} \chi(\mathbf{q}, \mathbf{q}) \mathbf{E}_{\text{tot}} + [1 - 4\pi\chi(\mathbf{q}, \mathbf{q})\mathcal{O}^{-1}]^{-1} \partial_t \mathbf{j}_{\text{ind}}^{(2)} \right\}
\end{aligned} \tag{3.29}$$

where in the last step we used

$$1 + 4\pi [1 - 4\pi\chi(\mathbf{q}, \mathbf{q})\mathcal{O}^{-1}(\mathbf{q})]^{-1} \chi(\mathbf{q}, \mathbf{q})\mathcal{O}^{-1}(\mathbf{q}) = [1 - 4\pi\chi(\mathbf{q}, \mathbf{q})\mathcal{O}^{-1}(\mathbf{q})]^{-1}. \tag{3.30}$$

Comparing Eq. (3.29) with the general expansion Eq. (3.6) and using Eq. (3.24) for second order the induced current we have the macroscopic susceptibilities

$$\epsilon_M = 1 - \frac{4\pi}{\omega^2} [1 - 4\pi\chi(\mathbf{q}, \mathbf{q})\mathcal{O}^{-1}(\mathbf{q})]^{-1} \chi(\mathbf{q}, \mathbf{q}) \tag{3.31}$$

$$\chi_M^{(2)}(\mathbf{q}, \mathbf{q}', \mathbf{q}'') = -\frac{4\pi}{\omega^2} \mathbf{M}(\mathbf{q}) \chi(\mathbf{q}, \mathbf{q}', \mathbf{q}'') \mathbf{N}(\mathbf{q}') \mathbf{N}(\mathbf{q}'') \tag{3.32}$$

where we have introduced the two very similar definitions

$$\mathbf{M}(\mathbf{q}) = [1 - 4\pi\chi(\mathbf{q}, \mathbf{q})\mathcal{O}^{-1}(\mathbf{q})]^{-1} \tag{3.33}$$

$$\mathbf{N}(\mathbf{q}) = [1 - 4\pi\mathcal{O}^{-1}(\mathbf{q})\chi(\mathbf{q}, \mathbf{q})]^{-1} \tag{3.34}$$

These are the general relations between the microscopic and macroscopic responses, where we have not made any assumptions on the nature of the external field except that it is macroscopic. In the context of TDDFT it is however important to notice that it can give only the longitudinal microscopic result whereas TDcurrentDFT can deal with transverse fields as well. I will discuss this point in more detail in Chap. 4.

3.3 Macroscopic response from TDDFT

To make the link between the scalar density response and our general result Eqs. (3.31) and (3.32) it is useful to consider the operator $\mathcal{O}(\mathbf{q})$ and its inverse in more detail. Fourier transform of the definition (3.13) yields

$$\mathcal{O}(\mathbf{q}, \omega) = \mathbf{q} \times \mathbf{q} \times -\omega^2 \mathbf{1} \tag{3.35}$$

Using the longitudinal and transverse projectors and their identity property⁴

$$P^L(\mathbf{q}) = \frac{\mathbf{q}\mathbf{q}}{q^2}, \quad P^T(\mathbf{q}) = -\frac{\mathbf{q}\times\mathbf{q}\times}{q^2}, \quad P^L(\mathbf{q}) + P^T(\mathbf{q}) = \mathbf{1} \quad (3.36)$$

this operator can be expressed as

$$\mathcal{O}(\mathbf{q}, \omega) = -\omega^2 P^L(\mathbf{q}) - (\omega^2 - q^2) P^T(\mathbf{q}) \quad (3.37)$$

and the inverse is readily obtained using the orthogonality of the projectors

$$\mathcal{O}^{-1}(\mathbf{q}, \omega) = -\frac{1}{\omega^2} P^L(\mathbf{q}) - \frac{1}{\omega^2 - q^2} P^T(\mathbf{q}). \quad (3.38)$$

With this expression we can consider the longitudinal and transverse part separately. Following the argumentation of Del Sole and Fiorino [102] we note that a microscopic response obtained from TDDFT can only account for longitudinal perturbations and it is therefore necessary to decompose the induced field into its longitudinal and transverse components and define the perturbing field as

$$\mathbf{E}_{\text{per}}(1) = \mathbf{E}_{\text{ext}}(1) + \mathbf{E}_{\text{ind}}^T(1) = \mathbf{E}_{\text{tot}}(1) - \mathbf{E}_{\text{ind}}^L(1) \quad (3.39)$$

so that the perturbation contains the transverse part of the induce field. It is the potential of this perturbing field in terms of which the microscopic response in Chap. 2.3 is formulated.

Now, to make the connection between this microscopic response and the macroscopic dielectric tensor ϵ_M (Eq. (3.31), we define the response function α for a perturbing field that contains the transverse part of the induced field:

$$\partial_t \mathbf{j}_{\text{ind}}^{(1)}(1) = \int d2 \alpha(1, 2) (\mathbf{E}_{\text{ext}}(2) + \mathbf{E}_{\text{ind}}^T(2)) = \int d2 \alpha(1, 2) (\mathbf{E}_{\text{per}}(2)). \quad (3.40)$$

This field has only macroscopic contributions (according to [102]) and can thus be expressed in terms of the external fields as

$$\mathbf{E}_{\text{per}}(\mathbf{q}) = [1 - 4\pi \mathcal{O}_T^{-1}(\mathbf{q}) \chi(\mathbf{q}, \mathbf{q})] \mathbf{E}_{\text{ext}}(\mathbf{q}). \quad (3.41)$$

By comparison with the definition (3.15) of χ we have:

$$\chi(\mathbf{q}, \mathbf{q}) = [1 + 4\pi \alpha(\mathbf{q}, \mathbf{q}) \mathcal{O}_T^{-1}(\mathbf{q})]^{-1} \alpha(\mathbf{q}, \mathbf{q}). \quad (3.42)$$

⁴The symbols P^L and P^T for the projectors should not be confused with the one for polarization \mathbf{P} .

Using the expression for $\chi(\mathbf{q}, \mathbf{q})$ in our result for the macroscopic dielectric tensor Eq. (3.31) yields

$$\begin{aligned}
\epsilon_M &= 1 - \frac{4\pi}{\omega^2} [1 - 4\pi\chi(\mathbf{q}, \mathbf{q})\mathcal{O}^{-1}(\mathbf{q})]^{-1} \chi(\mathbf{q}, \mathbf{q}) \\
&= 1 - \frac{4\pi}{\omega^2} [1 - 4\pi [1 + 4\pi\alpha(\mathbf{q}, \mathbf{q})\mathcal{O}_T^{-1}(\mathbf{q})]^{-1} \alpha(\mathbf{q}, \mathbf{q})\mathcal{O}^{-1}(\mathbf{q})]^{-1} \times \\
&\quad \times [1 + 4\pi\alpha(\mathbf{q}, \mathbf{q})\mathcal{O}_T^{-1}(\mathbf{q})]^{-1} \alpha(\mathbf{q}, \mathbf{q}) \\
&= 1 - \frac{4\pi}{\omega^2} [1 - 4\pi\alpha(\mathbf{q}, \mathbf{q})\mathcal{O}_L^{-1}(\mathbf{q})]^{-1} [1 + 4\pi\alpha(\mathbf{q}, \mathbf{q})\mathcal{O}_T^{-1}(\mathbf{q})] \times \\
&\quad \times [1 + 4\pi\alpha(\mathbf{q}, \mathbf{q})\mathcal{O}_T^{-1}(\mathbf{q})]^{-1} \alpha(\mathbf{q}, \mathbf{q}) \\
&= 1 - \frac{4\pi}{\omega^2} [1 - 4\pi\alpha(\mathbf{q}, \mathbf{q})\mathcal{O}_L^{-1}(\mathbf{q})]^{-1} \alpha(\mathbf{q}, \mathbf{q})
\end{aligned}$$

where we have used

$$\begin{aligned}
[1 - 4\pi\alpha(\mathbf{q}, \mathbf{q}) [1 + 4\pi\alpha(\mathbf{q}, \mathbf{q})\mathcal{O}_T^{-1}(\mathbf{q})]^{-1} \mathcal{O}^{-1}]^{-1} &= \\
&= [1 - 4\pi\alpha(\mathbf{q}, \mathbf{q})\mathcal{O}_L^{-1}(\mathbf{q})]^{-1} [1 + 4\pi\alpha(\mathbf{q}, \mathbf{q})\mathcal{O}_T^{-1}(\mathbf{q})] .
\end{aligned}$$

Now identifying $\mathcal{O}_L^{-1}(\mathbf{q}) = -\frac{1}{\omega^2} \frac{\mathbf{q}\mathbf{q}}{q\ q}$ (Eq. (3.38)) and defining $\tilde{\alpha} = -\frac{1}{\omega^2}\alpha$ we find

$$\epsilon_M = 1 + 4\pi \left[1 - 4\pi\tilde{\alpha}(\mathbf{q}, \mathbf{q}) \frac{\mathbf{q}\mathbf{q}}{q\ q} \right]^{-1} \tilde{\alpha}(\mathbf{q}, \mathbf{q}) \quad (3.43)$$

$$= 1 + 4\pi\tilde{\alpha}(\mathbf{q}, \mathbf{q}) \left[1 - 4\pi \frac{\mathbf{q}\mathbf{q}}{q\ q} \tilde{\alpha}(\mathbf{q}, \mathbf{q}) \right]^{-1} \quad (3.44)$$

which is exactly the result shown in [102]. The quasi-susceptibility $\tilde{\alpha}$ reads

$$\tilde{\alpha}(\mathbf{q}_1, \mathbf{q}_2, \omega) = -\frac{1}{\omega^2} [\chi_{\mathbf{j}\mathbf{j}}(\mathbf{q}_1, \mathbf{q}_2, \omega) - \rho(\mathbf{q}_1)\delta_{\mathbf{q}_1\mathbf{q}_2}] . \quad (3.45)$$

We note that the convenient redefinition of the response function $\alpha \rightarrow \tilde{\alpha}$ means that we are considering a response of the polarization, rather than $\partial_t \mathbf{j}$, since the two are related by a factor of ω^2 . The difference is that $\partial_t \mathbf{j}$ features in the wave equation (3.10), thus when regarding the response functions as a means to close Maxwell's equations it is convenient to keep this quantity, while when we are interested in the polarization and its expansion of the perturbing field (Eq. (3.6)) this redefinition is more convenient.

Using the same decomposition of the perturbing field as in Eq. (3.40) we define the second order response to the perturbing field, now directly for the polarization

$$\mathbf{P}_{\text{ind}}^{(2)}(1) = \int d2d3 \tilde{\alpha}(1, 2, 3) \mathbf{E}_{\text{per}}(2) \mathbf{E}_{\text{per}}(3). \quad (3.46)$$

With this definition, we obtain instead of the second order macroscopic susceptibility as in Eq. (3.32), the form

$$\begin{aligned} \chi_M^{(2)}(\mathbf{q}_1, \mathbf{q}_2, \mathbf{q}_3) &= -4\pi [1 - 4\pi\tilde{\alpha}(\mathbf{q}_1, \mathbf{q}_1)P^L(\mathbf{q}_1)]^{-1} \tilde{\alpha}(\mathbf{q}_1, \mathbf{q}_2, \mathbf{q}_3) \times \\ &\times [1 - 4\pi P^L(\mathbf{q}_2)\tilde{\alpha}(\mathbf{q}_2, \mathbf{q}_2)]^{-1} [1 - 4\pi P^L(\mathbf{q}_3)\tilde{\alpha}(\mathbf{q}_3, \mathbf{q}_3)]^{-1}. \end{aligned} \quad (3.47)$$

The advantage of this formulation is that now we can use the result of the second order perturbation theory of Chap. 2.2. Comparing the definition Eq. (3.46) and the second order microscopic perturbation response Eq. (2.17) yields the microscopic expression for $\tilde{\alpha}^{(2)}$

$$\tilde{\alpha}(\mathbf{q}_1, \mathbf{q}_2, \mathbf{q}_3) = -\frac{i}{\omega_1\omega_2\omega_3} \left[\frac{1}{2}\chi_{j\rho}(\mathbf{q}_1, \mathbf{q}_3)\delta_{\mathbf{q}_2\mathbf{q}_3} + \chi_{\rho j}(\mathbf{q}_2, \mathbf{q}_3)\delta_{\mathbf{q}_1\mathbf{q}_3} + \frac{1}{2}\chi_{jjj}(\mathbf{q}_1, \mathbf{q}_2, \mathbf{q}_3) \right]. \quad (3.48)$$

The linear responses $\chi_{j\rho}$ and $\chi_{\rho j}$ vanish in the optical limit and are therefore neglected in the following.

The link to TDDFT can now be made by considering only the longitudinal component of the the susceptibility. Formally one has to project along the directions of the \mathbf{q} :

$$\begin{aligned} \chi_M^{LLL}(\mathbf{q}_1, \mathbf{q}_2, \mathbf{q}_3) &= P^L(\mathbf{q}_1)\chi_M^{(2)}(\mathbf{q}_1, \mathbf{q}_2, \mathbf{q}_3)P^L(\mathbf{q}_2)P^L(\mathbf{q}_3) \\ &= -4\pi P^L(\mathbf{q}_1) [1 - 4\pi\tilde{\alpha}(\mathbf{q}_1, \mathbf{q}_1)P^L(\mathbf{q}_1)]^{-1} \tilde{\alpha}(\mathbf{q}_1, \mathbf{q}_2, \mathbf{q}_3) \times \\ &\times [1 - 4\pi P^L(\mathbf{q}_2)\tilde{\alpha}(\mathbf{q}_2, \mathbf{q}_2)]^{-1} P^L(\mathbf{q}_2) \times \\ &\times [1 - 4\pi P^L(\mathbf{q}_3)\tilde{\alpha}(\mathbf{q}_3, \mathbf{q}_3)]^{-1} P^L(\mathbf{q}_3). \end{aligned} \quad (3.49)$$

The longitudinal projections of the linear prefactors of $\tilde{\alpha}^{(2)}$ take a very simple form if we consider the identities

$$[1 - 4\pi\tilde{\alpha}(\mathbf{q}, \mathbf{q})P^L(\mathbf{q})]^{-1} = 1 + 4\pi \frac{\tilde{\alpha}(\mathbf{q}, \mathbf{q})}{1 - 4\pi\tilde{\alpha}(\mathbf{q}, \mathbf{q})^{LL}} P^L(\mathbf{q}) \quad (3.50)$$

$$[1 - 4\pi P^L(\mathbf{q})\tilde{\alpha}(\mathbf{q}, \mathbf{q})]^{-1} = 1 + 4\pi P^L(\mathbf{q}) \frac{\tilde{\alpha}(\mathbf{q}, \mathbf{q})}{1 - 4\pi\tilde{\alpha}(\mathbf{q}, \mathbf{q})^{LL}}. \quad (3.51)$$

In Eq. (3.49) these terms are multiplied with longitudinal projectors from the left and right respectively, so that there are three factors of the same form

$$P^L(\mathbf{q}) + 4\pi P^L(\mathbf{q}) \frac{\tilde{\alpha}(\mathbf{q}, \mathbf{q})}{1 - 4\pi\tilde{\alpha}(\mathbf{q}, \mathbf{q})^{LL}} P^L(\mathbf{q}) = \frac{P^L(\mathbf{q})}{1 - 4\pi\tilde{\alpha}(\mathbf{q}, \mathbf{q})^{LL}}. \quad (3.52)$$

We note that this is equal to the two sided longitudinal projection of the macroscopic dielectric tensor (Eq.(3.44))

$$\epsilon_M^{LL} = P^L(\mathbf{q})\epsilon_M P^L(\mathbf{q}) = \frac{P^L(\mathbf{q})}{1 - 4\pi\tilde{\alpha}(\mathbf{q}, \mathbf{q})^{LL}} \quad (3.53)$$

so that the longitudinal projection of the macroscopic second order susceptibility reads

$$\chi^{(2),LLL}(\mathbf{q}_1, \mathbf{q}_2, \mathbf{q}_3) = -4\pi\epsilon_M^{LL}(\mathbf{q}_1)\epsilon_M^{LL}(\mathbf{q}_2)\epsilon_M^{LL}(\mathbf{q}_3)P^L(\mathbf{q})\tilde{\alpha}(\mathbf{q}_1, \mathbf{q}_2, \mathbf{q}_3)P^L(\mathbf{q}_2)P^L(\mathbf{q}_3) \quad (3.54)$$

which leaves the projection of the microscopic response function to be considered.

As already noted in Chap. 2.2 the longitudinal projection of the current is related to the density via the continuity equation (2.20)

$$\mathbf{q} \cdot \hat{\mathbf{j}}(\mathbf{q}, \omega) = q P^L(\mathbf{q})\hat{\mathbf{j}}(\mathbf{q}, \omega) = i\omega\hat{\rho}(\mathbf{q}, \omega). \quad (3.55)$$

Using this relation to replace the projection of the current operators in the longitudinal projection of $\tilde{\alpha}(\mathbf{q}_1, \mathbf{q}_2, \mathbf{q}_3)$ (Eq. (3.48)) we find

$$P^L(\mathbf{q}_1)\tilde{\alpha}(\mathbf{q}_1, \mathbf{q}_2, \mathbf{q}_3)P^L(\mathbf{q}_2)P^L(\mathbf{q}_3) = \frac{1}{2} \frac{1}{(q_2 + q_3)q_2q_3} \chi_{\rho\rho\rho}(\mathbf{q}_1, \mathbf{q}_2, \mathbf{q}_3) \quad (3.56)$$

which is the quantity that is the result of the second order TDDFT Dyson equation. The final result for the longitudinal projection of the macroscopic second order susceptibility is thus, now also accounting for the frequency dependence

$$\begin{aligned} \chi^{(2),LLL}(\omega_2 + \omega_3, \omega_2, \omega_3, \mathbf{q}_2 + \mathbf{q}_3, \mathbf{q}_2, \mathbf{q}_3) &= -\frac{2\pi\chi_{\rho\rho\rho}(\omega_2 + \omega_3, \omega_2, \omega_3, \mathbf{q}_2 + \mathbf{q}_3, \mathbf{q}_2, \mathbf{q}_3)}{(q_2 + q_3)q_2q_3} \times \\ &\times \epsilon_M^{LL}(\omega_2 + \omega_3, \mathbf{q}_2 + \mathbf{q}_3)\epsilon_M^{LL}(\omega_2, \mathbf{q}_2)\epsilon_M^{LL}(\omega_3, \mathbf{q}_3) \end{aligned} \quad (3.57)$$

The simple TDDFT result $\chi_{\rho\rho\rho}$ therefore needs to be modulated by three different dielectric functions in order to obtain the macroscopic susceptibility. Moreover, here the limitation of TDDFT become appearant, since it can only provide the longitudinal component of the susceptibility. However, as far as optical processes, i.e. when $\mathbf{q} \rightarrow 0$, are concerned this limitation does not pose a problem to the applicability of TDDFT. The quantity \mathbf{q} defines the propagation direction of the field with respect to which the terms 'longitudinal' and 'transverse' are defined. Therefore, when one considers the limit of vanishing \mathbf{q} the longitudinal and transverse directions loose their definition and any direction is equivalent [103]. It is only in this limit that TDDFT can be applied rigorously. In Chap. 4 I will further discuss this limit and its range of validity as well as effects that occur beyond it.

It is interesting to note that Eq. (3.57) is similar to a result obtained by Armstrong and Bloembergen [30] in the Lorentz model. They find for cubic symmetry a relation between the macroscopic and microscopic susceptibilities of the form

$$\chi^{(2)}(\omega_1 + \omega_2) = N\beta(\omega_1 + \omega_2) \frac{\epsilon(\omega_1 + \omega_2) + 2}{3} \frac{\epsilon(\omega_1) + 2}{3} \frac{\epsilon(\omega_2) + 2}{3} \quad (3.58)$$

where β is their microscopic susceptibility.

3.3.1 Components of $\chi^{(2)}$

Having established that with TDDFT we can only get a scalar response, the problem arises that the second order susceptibility $\chi^{(2)}$ has in general 27 components, which have to be obtained from this scalar quantity. First, we note that for second harmonic generation only 18 of the 27 components are independent, since they are symmetric under exchange of the two perturbing fields, i.e. $\chi_{ijk} = \chi_{ikj}$. While this is true for all crystal systems, the symmetry operations of particular crystal systems also contribute to a reduction of the independent non-zero components. Table 3.1 lists these components by point group.

We note that 11 out of the 32, do not yield any second harmonic generation due to the inversion symmetry. For 4 others there is only one independent non-zero component and thus they pose no problem for a scalar response calculation. It can, however, not be obtained from any density response, but the polarization directions of the applied fields must be considered. A careful analysis of how the polarization enters into the equations yields not only the independent components of those 5 point groups but also a way to obtain the components of $\chi^{(2)}$ for point groups where more than one component is independently non-zero.

To this end we consider the longitudinal projection of $\chi^{(2)}$ like it appears in the macroscopic averaged second order response, Eq (3.57). The longitudinal projections are projections parallel to the propagation directions and can thus also be interpreted as projections along the polarization of longitudinal fields. Introducing the polarization vectors \mathbf{n}_1 and \mathbf{n}_2 of the perturbing field, we can write the longitudinal projection of the macroscopic second order susceptibility (3.57) as⁵

$$(\mathbf{n}_1 + \mathbf{n}_2)\chi^{(2)}\mathbf{n}_1\mathbf{n}_2 = \epsilon_M^{LL}(\mathbf{n}_1 + \mathbf{n}_2, 2\omega)\epsilon_M^{LL}(\mathbf{n}_1, \omega)\epsilon_M^{LL}(\mathbf{n}_2, \omega)\chi_{\rho\rho\rho}(\mathbf{n}_1 + \mathbf{n}_2, \mathbf{n}_1, \mathbf{n}_2, 2\omega, \omega) \quad (3.59)$$

which reads in terms of the tensor and vector components

$$\sum_{ijk} (n_{1_i} + n_{2_i})\chi_{ijk}n_{1_j}n_{2_k} = \epsilon_M(\mathbf{n}_1 + \mathbf{n}_2, 2\omega)\epsilon_M^{LL}(\mathbf{n}_1, \omega)\epsilon_M^{LL}(\mathbf{n}_2, \omega)\chi_{\rho\rho\rho}(\mathbf{n}_1 + \mathbf{n}_2, \mathbf{n}_1, \mathbf{n}_2, 2\omega, \omega). \quad (3.60)$$

This means that in order to obtain single tensor components we have to perform TDDFT calculations along different polarization directions.

There are four different kind of tensor components according to their index structure: the diagonals $\chi_{\alpha\alpha\alpha}^{(2)}$, two different block diagonals $\chi_{\alpha\alpha\beta}^{(2)}$ and $\chi_{\beta\alpha\alpha}^{(2)}$ and the off diagonals $\chi_{\alpha\beta\gamma}^{(2)}$. We also remember that for second harmonic generation the last two indices are interchangeable, i.e. $\chi_{\alpha\beta\gamma}^{(2)} = \chi_{\alpha\gamma\beta}^{(2)}$. As mentioned, depending on the symmetry, some

⁵Since $\chi^{(2)}$ only depends on two different \mathbf{q} we will call them in the following \mathbf{q}_1 and \mathbf{q}_2 instead of \mathbf{q}_2 and \mathbf{q}_3 .

#	Symbol		Components	Bravais
1	1	18	all	Triclinic
2	$\bar{1}$	0	—	
3-5	2	8	$xyz, xxy, yxx, yyy, yzz, yzx, zzy, zxy$	Monoclinic
6-9	m	9	$xxx, xyy, xxz, yyz, yyx,$ zxx, zyy, zzz, zzx	
10-15	2/m	0	—	
16-24	222	3	xyz, yzx, zxy	Orthorhombic
25-46	mm2	5	xxz, yyz, zxx, zyy, zzz	
47-74	mmm	0	—	
75-80	4	4	$xyz = -yxz, xxz = yyz, zxx = zyy, zzz$	Tetragonal
81-82	$\bar{4}$	4	$xyz = yxz, xxz = -yyz, zxx = -zyy, zxy$	
83-88	4/m	0	—	
89-98	422	1	$xyz = -yxz$	
99-110	4mm	3	$xxz = yyz, zxx = zyy, zzz$	
111-122	$\bar{4}2m$	2	$xyz = yxz, zxy$	
123-142	4/mmm	0	—	
143-146	3	6	$xxx = -xyy = -yyx, xyz = -yxz, xxz = yyz$ $yyy = -yxx = -xxy, zxx = zyy, zzz$	Trigonal
147-148	$\bar{3}$	0	—	
149-155	32	2	$xxx = -xyy = -yyx, xyz = -yxz$	
156-161	3m	4	$xxz = yyz, zxx = zyy, yyy = -yxx = -xxy, zzz$	
162-167	$\bar{3}2/m$	0	—	
168-173	6	4	$xyz = -yxz, xxz = yyz, zxx = zyy, zzz$	Hexagonal
174	$\bar{6}$	2	$xxx = -xyy = -yyx, yyy = -yxx = -xxy$	
175-176	6/m	0	—	
177-182	622	1	$xyz = -yxz$	
183-186	6mm	3	$xxz = yyz, zxx = zyy, zzz$	
187-190	$\bar{6}m2$	1	$yyy = -yxx = -xxy$	
192-194	6/mmm	0	—	
195-199	23	1	$xyz = yxz = zyx$	Cubic
200-206	2/m $\bar{3}$	0	—	
207-214	432	0	—	
215-220	$\bar{4}3m$	1	$xyz = yxz = zyx$	
221-230	m $\bar{3}m$	0	—	

Table 3.1: Components of the second order susceptibility $\chi^{(2)}$ for second harmonic generation. After Y. R. Shen [3] (p. 27)

components can be zero, which facilitates the solution of Eq. (3.60) for some symmetry groups. This also means that for some of the tensor components, it might be necessary to do a calculation with different polarizations, depending on the symmetry group of the crystal.

Components $\chi_{\alpha\alpha\alpha}$: For components of this form it is sufficient to perform a calculation with the polarizations in $\mathbf{n}_1 = \mathbf{n}_2 = \mathbf{e}_\alpha$, where \mathbf{e}_α is the unit vector in the cartesian direction α . Eq. (3.60) thus reads:

$$\chi_{\alpha\alpha\alpha} = \epsilon_M(\mathbf{e}_\alpha, 2\omega)\chi_{\rho\rho\rho}(\mathbf{e}_\alpha + \mathbf{e}_\alpha, \mathbf{e}_\alpha, \mathbf{e}_\alpha)\epsilon_M(\mathbf{e}_\alpha, \omega)\epsilon_M(\mathbf{e}_\alpha, \omega) \quad (3.61)$$

This is obviously true for any symmetry.

Components $\chi_{\alpha\alpha\beta}$: The components $\chi_{\alpha\alpha\beta}$ can be obtained by a calculation with the polarizations $\mathbf{n}_1 = \mathbf{e}_\alpha$ and $\mathbf{n}_2 = \mathbf{e}_\beta$. With this choice of polarization directions Eq. (3.60) reads

$$\chi_{\alpha\alpha\beta} + \chi_{\beta\beta\alpha} = \epsilon_M(\mathbf{e}_\alpha + \mathbf{e}_\beta, 2\omega)\chi_{\rho\rho\rho}(\mathbf{e}_\alpha + \mathbf{e}_\beta, \mathbf{e}_\alpha, \mathbf{e}_\beta)\epsilon_M(\mathbf{e}_\alpha, \omega)\epsilon_M(\mathbf{e}_\beta, \omega). \quad (3.62)$$

For most crystal symmetries only one of the components $\chi_{\alpha\alpha\beta}$ and $\chi_{\beta\beta\alpha}$ is non-zero, so that such a calculation directly yields the non-zero component. The exception are the symmetry groups '1', '2' and 'm', for which one has to perform an additional TDDFT calculations, with the polarizations $\mathbf{n}_1 = \mathbf{e}_\alpha$ and $\mathbf{n}_2 = -\mathbf{e}_\beta$ yielding Eq. (3.60) as

$$\chi_{\alpha\alpha\beta} - \chi_{\beta\beta\alpha} = \epsilon_M(\mathbf{e}_\alpha - \mathbf{e}_\beta, 2\omega)\chi_{\rho\rho\rho}(\mathbf{e}_\alpha - \mathbf{e}_\beta, \mathbf{e}_\alpha, -\mathbf{e}_\beta)\epsilon_M(\mathbf{e}_\alpha, \omega)\epsilon_M(-\mathbf{e}_\beta, \omega). \quad (3.63)$$

Adding or subtracting this from Eq. (3.62) yields the single component.

Components $\chi_{\alpha\beta\beta}$: Components of this shape are less easily obtained, since one has to use $\mathbf{n}_1 = \mathbf{e}_\alpha$ and $\mathbf{n}_2 = 1/\sqrt{2}(\mathbf{e}_\alpha + \mathbf{e}_\beta)$ which yields

$$\frac{1}{2}\chi_{\alpha\alpha\beta} + \frac{1}{2}\chi_{\alpha\beta\beta} + \frac{1+\sqrt{2}}{2}\chi_{\beta\beta\alpha} + \frac{1+\sqrt{2}}{2}\chi_{\beta\beta\beta} = \epsilon_M(\mathbf{n}_1 + \mathbf{n}_2, 2\omega)\chi_{\rho\rho\rho}(\mathbf{n}_1 + \mathbf{n}_2, \mathbf{n}_1, \mathbf{n}_2)\epsilon_M(\mathbf{n}_1, \omega)\epsilon_M(\mathbf{n}_2, \omega). \quad (3.64)$$

So depending on which of the other components are simultaneously non-zero one has to combine this with an additional calculation. For example, for the groups '6mm', '6', '4mm', '4', '4' and 'mm2' the $\chi_{\beta\beta\beta}$ and $\chi_{\beta\beta\alpha}$ components are zero, so that one has to combine this calculation only with the $\chi_{\alpha\alpha\beta}$ calculation to obtain the $\chi_{\alpha\beta\beta}$ component. For other symmetry groups their are more dependent components, so that one has to combine several calculations.

Components $\chi_{\alpha\beta\gamma}$: For the off diagonal elements there are symmetry groups ('4m3', '23', '622' and '422') where they are the only non-zero components. Then, it is sufficient

to do a single calculation with $\mathbf{n}_1 = \mathbf{n}_2 = \mathbf{e}_\alpha + \mathbf{e}_\beta + \mathbf{e}_\gamma$, yielding directly the component

$$\begin{aligned} \chi_{\alpha\beta\gamma} &= \epsilon_M(2(\mathbf{e}_\alpha + \mathbf{e}_\beta + \mathbf{e}_\gamma), 2\omega) \times \\ &\times \chi_{\rho\rho\rho}(2(\mathbf{e}_\alpha + \mathbf{e}_\beta + \mathbf{e}_\gamma), \mathbf{e}_\alpha + \mathbf{e}_\beta + \mathbf{e}_\gamma, \mathbf{e}_\alpha + \mathbf{e}_\beta + \mathbf{e}_\gamma) \epsilon_M(\mathbf{e}_\alpha + \mathbf{e}_\beta + \mathbf{e}_\gamma, \omega) \epsilon_M(\mathbf{e}_\alpha + \mathbf{e}_\beta + \mathbf{e}_\gamma, \omega) \end{aligned} \quad (3.65)$$

In the case of the symmetry groups '1', '2', '32', '3', ' $\overline{42m}$ ', '4', '222 and '6' there is no general applicable combination. Instead, one has to decide for each symmetry which is the best way to obtain the component.

For example for the χ_{xyz} component of group '3' is useful to choose $\mathbf{n}_1 = \mathbf{e}_x + \mathbf{e}_y + \mathbf{e}_z$ and $\mathbf{n}_2 = \mathbf{e}_y$ which yields

$$\chi_{xyz} + \chi_{xxx} = \epsilon_M(\mathbf{e}_\alpha + 2\mathbf{e}_\beta + \mathbf{e}_\gamma, 2\omega) \chi_{\rho\rho\rho}(\mathbf{e}_\alpha + 2\mathbf{e}_\beta + \mathbf{e}_\gamma, \mathbf{e}_\alpha + \mathbf{e}_\beta + \mathbf{e}_\gamma, \mathbf{e}_\beta) \epsilon_M(\mathbf{e}_\alpha + \mathbf{e}_\beta + \mathbf{e}_\gamma, \omega) \epsilon_M(\mathbf{e}_\beta, \omega) \quad (3.66)$$

From which one has to subtract χ_{xxx} , i.e. the result of a calculation of the form $\chi_{\alpha\alpha\alpha}$ to obtain the component.

In another example, for ' $\overline{42m}$ ' group, the choice $\mathbf{n}_1 = \mathbf{n}_2 = \mathbf{e}_x + \mathbf{e}_y + \mathbf{e}_z$ yields

$$8\chi_{xyz} + 4\chi_{zyx} = A \quad (3.67)$$

while a calculation with the polarizations $\mathbf{n}_1 = \mathbf{e}_x - \mathbf{e}_y + \mathbf{e}_z$ and $\mathbf{n}_2 = \mathbf{e}_x + \mathbf{e}_y + \mathbf{e}_z$ yields

$$4\chi_{xyz} + 4\chi_{zyx} = B \quad (3.68)$$

These can be combined to yield the components via

$$B - A = 4\chi_{xyz} \quad \text{and} \quad 2B - A = 4\chi_{zyx}. \quad (3.69)$$

Along these lines one can obtain the polarization directions for the off-diagonal components of the other symmetry groups as well.

The above outlined choices for \mathbf{n}_1 and \mathbf{n}_2 for which one performs the TDDFT are not necessarily unique to obtain the wanted components, there might be other, more practical combinations, depending on the specific component one wants to obtain.

3.3.2 Macroscopic IPA response

The result from this section, that in order to obtain the second macroscopic susceptibility one has to multiply the averaged microscopic second order density response function with three linear dielectric functions merits some closer consideration. Namely, I want to show what this means for the independent particle approximation, which is the one that has been used in the literature so far.

In this approximation one lets $f_{xc} = 0$ as well as neglects local fields by considering a $\chi_0^{(2)}$ with $\mathbf{G}_2 = \mathbf{G}_1 = \mathbf{G}_3 = \mathbf{0}$, so that the solution of the TDDFT Dyson equation (2.54)

reads

$$\begin{aligned} \chi_{\rho\rho\rho}(\mathbf{q}_1 + \mathbf{q}_2, \mathbf{q}_1, \mathbf{q}_2) &= [1 + \chi_{\rho\rho}(\mathbf{q}_1 + \mathbf{q}_2, \mathbf{q}_1 + \mathbf{q}_2)v(\mathbf{q}_1 + \mathbf{q}_2)] \chi_{\rho\rho\rho}^{(0)}(\mathbf{q}_1 + \mathbf{q}_2, \mathbf{q}_1, \mathbf{q}_2) \times \\ &\quad \times [1 + v(\mathbf{q}_1)\chi_{\rho\rho}(\mathbf{q}_1, \mathbf{q}_1)] [1 + v(\mathbf{q}_2)\chi_{\rho\rho}(\mathbf{q}_2, \mathbf{q}_2)] \end{aligned} \quad (3.70)$$

where the linear $\chi_{\rho\rho}$ obey the linear Dyson like equation (2.40) in the same approximation

$$\chi_{\rho\rho}(\mathbf{q}, \mathbf{q}) = \chi_{\rho\rho}^{(0)}(\mathbf{q}, \mathbf{q}) + \chi_{\rho\rho}^{(0)}(\mathbf{q}, \mathbf{q})v(\mathbf{q})\chi_{\rho\rho}(\mathbf{q}, \mathbf{q}). \quad (3.71)$$

Now, we note that within this approximation

$$[\epsilon^{LL}(\mathbf{q})]^{-1} = 1 + v(\mathbf{q})\chi_{\rho\rho} = 1 + \chi_{\rho\rho}v(\mathbf{q}) \quad (3.72)$$

so that the microscopic response $\chi_{\rho\rho\rho}$ reads

$$\chi_{\rho\rho\rho}(\mathbf{q}_1 + \mathbf{q}_2, \mathbf{q}_1, \mathbf{q}_2) = [\epsilon^{LL}(\mathbf{q}_1 + \mathbf{q}_2)]^{-1} \chi_{\rho\rho\rho}^{(0)}(\mathbf{q}_1 + \mathbf{q}_2, \mathbf{q}_1, \mathbf{q}_2) [\epsilon^{LL}(\mathbf{q}_1)]^{-1} [\epsilon^{LL}(\mathbf{q}_2)]^{-1}. \quad (3.73)$$

This form of the microscopic response, inserted in the macroscopic susceptibility (3.57), yields

$$\chi_{IPA}^{(2),LLL}(\mathbf{q}_1 + \mathbf{q}_2, \mathbf{q}_1, \mathbf{q}_2) = -\frac{2\pi}{(q_1 + q_2)q_1q_2} \chi_{\rho\rho\rho}^{(0)}(\mathbf{q}_1 + \mathbf{q}_2, \mathbf{q}_1, \mathbf{q}_2) \quad (3.74)$$

Thus, within the independent particle approximation, the macroscopic susceptibility is identical with the microscopic response to a non-interacting potential. While, this result agrees with physical intuition, it is not an obvious one when one considers the two equations, the TDDFT Dyson like equation (2.47) and the macroscopic relation (3.57). In this sense, it is at least a check of consistency of the theory.

4 Optical limit

For electromagnetic radiation the relation between light momentum vector \mathbf{q} and photon energy ω in vacuum is [104]

$$\mathbf{q} = \frac{\omega}{c}. \quad (4.1)$$

Visible light, as used in experiments like absorption, second harmonic generation or generally valence band spectroscopes, carries energy in the order of 1 or 10 eV which corresponds to a light wave vector of $\mathbf{q} \sim 10^{-3} \text{ \AA}^{-1}$ or a wavelength of $\lambda \sim 2\pi 10^3 \text{ \AA}$. On the other hand the typical length scale of the cell parameters in solids is of the order of 1 \AA , which means that the light wave is almost constant over the length of the cell. Therefore one considers for these kind of processes the long wavelength limit, i.e. $\lambda \rightarrow \infty$, or equivalently $\mathbf{q} \rightarrow 0$. This limit is also referred to as the *optical* limit.

This limit means that we are considering a field that does not propagate, which implies that the longitudinal and transverse direction are not longer distinguishable since they are defined with respect to the propagation direction [103]. It does however not mean that the field has no direction and the polarization is still defined. These points are important for our calculations, because they mean on the one hand that the longitudinal and transverse response are equivalent in the optical limit, while the polarization which determines the tensor components is well defined.

The limit is obtained formally by letting $\mathbf{q} \rightarrow 0$ in the response functions. There is however an important difference how this limit is carried out whether one considers the current response or the density response. To illustrate this I will here consider the linear case. The linear microscopic quasi-susceptibility $\tilde{\alpha}$ (3.45) depends on $\chi_{\mathbf{jj}}$:

$$\tilde{\alpha}(\mathbf{q}_1, \mathbf{q}_2, \omega) = -\frac{1}{\omega^2} [\chi_{\mathbf{jj}}(\mathbf{q}_1, \mathbf{q}_2, \omega) - \rho(\mathbf{q}_1)\delta_{\mathbf{q}_1 - \mathbf{q}_2}]. \quad (4.2)$$

and it can be shown [105] that¹

$$\lim_{\omega \rightarrow 0} \chi_{\mathbf{jj}} \sim \omega^2 \quad \text{and} \quad \lim_{\mathbf{q} \rightarrow 0} \chi_{\rho\rho} \sim q^2 \quad (4.3)$$

(for $\mathbf{G} = 0$) which means that the limit $\mathbf{q} \rightarrow 0$ of $\tilde{\alpha}$ is well behaved. On the other hand, when one wants to use TDDFT one has to express $\tilde{\alpha}$ in terms of the density response according to the relation [107, 108]

$$\chi_{\rho\rho}(\mathbf{q}, \mathbf{q}, \omega) = \frac{1}{\omega^2} \mathbf{q} \chi_{\mathbf{jj}}(\mathbf{q}, \mathbf{q}, \omega) \mathbf{q} \quad (4.4)$$

¹Note that there are numerous mathematical subtleties involved in this limit, c.f. [106]

which also means one considers only longitudinal fields and hence

$$\chi_{\mathbf{jj}}^{LL} = \frac{\omega^2}{q^2} \chi_{\rho\rho}(\mathbf{q}, \mathbf{q}, \omega). \quad (4.5)$$

In this case the limit of $\tilde{\alpha}$ is pathological because the denominator tends to zero in the same way as the numerator. To avoid this problem one has to expand $\chi_{\rho\rho}$ in terms of \mathbf{q} so that the leading term, which is proportional to q^2 cancels the denominator so that the limit can be taken safely. The same holds for the case $\omega \rightarrow 0$ for the current response, but which poses no problem in a $\chi_{\rho\rho}$ calculation.

The same reasoning holds for $\chi_{\rho\rho\rho}$ and $\chi_{\mathbf{jjj}}$ with the limiting behaviour

$$\lim_{\mathbf{q} \rightarrow 0} \chi_{\rho\rho\rho} \sim q^3 \quad \text{and} \quad \lim_{\omega \rightarrow 0} \chi_{\mathbf{jjj}} \sim \omega^3 \quad (4.6)$$

where the q^3 dependence of $\chi_{\rho\rho\rho}$ cancels with the prefactor $1/q_1 q_2 q_3$ in Eq. (3.57). In a TDDFT calculation the basic quantity is the non-interacting response function $\chi_{\rho\rho\rho}^{(0)}$ as given by Eq. 2.27. Using the real space representation for the density operator, Bloch functions for the single orbitals $|n_{\mathbf{k}}\rangle$ and subsequently passing to momentum space according to App. B yields the explicit expression for $\chi_{\rho\rho\rho}^{(0)}$:

$$\begin{aligned} \chi_0^{(2)}(\mathbf{q}' + \mathbf{q}'' + \mathbf{G}, \mathbf{q}' + \mathbf{G}', \mathbf{q}'' + \mathbf{G}'', \omega, \omega) = & \frac{2}{V} \sum_{n, n', n'', \mathbf{k}} \frac{\langle n_{\mathbf{k}} | -e^{i(\mathbf{q}' + \mathbf{q}'' + \mathbf{G})\mathbf{r}} | n_{\mathbf{k} + \mathbf{q}' + \mathbf{q}''} \rangle}{(E_{n, \mathbf{k}} - E_{n', \mathbf{k} + \mathbf{q}' + \mathbf{q}''} + 2\omega + 2i\eta)} \times \\ & \left[(f_{n, \mathbf{k}} - f_{n'', \mathbf{k} + \mathbf{q}'}) \frac{\langle n'_{\mathbf{k} + \mathbf{q}' + \mathbf{q}''} | e^{i(\mathbf{q}'' + \mathbf{G}'')\mathbf{r}'} | n''_{\mathbf{k} + \mathbf{q}'}) \langle n''_{\mathbf{k} + \mathbf{q}'} | e^{i(\mathbf{q}' + \mathbf{G}')\mathbf{r}''} | n_{\mathbf{k}} \rangle}{(E_{n, \mathbf{k}} - E_{n'', \mathbf{k} + \mathbf{q}'} + \omega + i\eta)} + \right. \\ & + (f_{n', \mathbf{k} + \mathbf{q}' + \mathbf{q}''} - f_{n'', \mathbf{k} + \mathbf{q}'}) \frac{\langle n'_{\mathbf{k} + \mathbf{q}' + \mathbf{q}''} | e^{i(\mathbf{q}'' + \mathbf{G}'')\mathbf{r}'} | n''_{\mathbf{k} + \mathbf{q}'}) \langle n''_{\mathbf{k} + \mathbf{q}'} | e^{i(\mathbf{q}' + \mathbf{G}')\mathbf{r}''} | n_{\mathbf{k}} \rangle}{(E_{n'', \mathbf{k} + \mathbf{q}'} - E_{n', \mathbf{k} + \mathbf{q}' + \mathbf{q}''} + \omega + i\eta)} + \\ & + (f_{n, \mathbf{k}} - f_{n'', \mathbf{k} + \mathbf{q}''}) \frac{\langle n'_{\mathbf{k} + \mathbf{q}' + \mathbf{q}''} | e^{i(\mathbf{q}' + \mathbf{G}')\mathbf{r}'} | n''_{\mathbf{k} + \mathbf{q}''}) \langle n''_{\mathbf{k} + \mathbf{q}''} | e^{i(\mathbf{q}'' + \mathbf{G}'')\mathbf{r}''} | n_{\mathbf{k}} \rangle}{(E_{n, \mathbf{k}} - E_{n'', \mathbf{k} + \mathbf{q}''} + \omega + i\eta)} + \\ & \left. + (f_{n', \mathbf{k} + \mathbf{q}' + \mathbf{q}''} - f_{n'', \mathbf{k} + \mathbf{q}''}) \frac{\langle n'_{\mathbf{k} + \mathbf{q}' + \mathbf{q}''} | e^{i(\mathbf{q}' + \mathbf{G}')\mathbf{r}'} | n''_{\mathbf{k} + \mathbf{q}''}) \langle n''_{\mathbf{k} + \mathbf{q}''} | e^{i(\mathbf{q}'' + \mathbf{G}'')\mathbf{r}''} | n_{\mathbf{k}} \rangle}{(E_{n'', \mathbf{k} + \mathbf{q}''} - E_{n', \mathbf{k} + \mathbf{q}' + \mathbf{q}''} + \omega + i\eta)} \right] \quad (4.7) \end{aligned}$$

I will now give some details about how the optical limit of this quantity is obtained via perturbation theory in \mathbf{q} . The fully general $\chi_{\rho\rho\rho}^{(0)}$ has \mathbf{q} dependence in the occupation numbers, the energies and the wavefunctions. We will henceforth only consider semiconductors (and insulators) and therefore neglect the momentum dependence of the Fermi factors, i.e. $f_{n, \mathbf{k} + \mathbf{q}} \rightarrow f_n$. The energies and wavefunctions however have to be expanded

in terms of \mathbf{q} . It turns out that we basically have to perform $\mathbf{k} \cdot \mathbf{p}$ perturbation theory to second order.

4.1 perturbation theory in \mathbf{q}

We have formulated the second order susceptibility $\chi_0^{(2)}$ in terms of Bloch functions $|\phi_{n,\mathbf{k}}\rangle$. These generally depend on \mathbf{q} , if we make the substitution $\mathbf{k} \rightarrow \mathbf{k} + \mathbf{q}$. In the limit $\mathbf{q} \rightarrow 0$ this means that we have to formulate a perturbation series in \mathbf{q} for Bloch functions. We start from the eigenvalue equation

$$H|\phi_{n,\mathbf{k}+\mathbf{q}}\rangle = \left[\frac{1}{2}p^2 + V_{\text{nl}} \right] |\phi_{n,\mathbf{k}+\mathbf{q}}\rangle \quad (4.8)$$

where $\mathbf{p} = i\nabla_r$ and V_{nl} is a generally non-local lattice periodic potential. Decomposing the Bloch functions into $|\phi_{n,\mathbf{k}+\mathbf{q}}\rangle = e^{i(\mathbf{k}+\mathbf{q})\mathbf{r}}|u_{n,\mathbf{k}+\mathbf{q}}\rangle$ we have

$$\left[-\frac{1}{2}k^2 - (\mathbf{k} + \mathbf{q}) \cdot \mathbf{p} + \frac{1}{2}(\mathbf{k} + \mathbf{q})^2 + \frac{1}{2}p^2 + e^{-i(\mathbf{k}+\mathbf{q})\mathbf{r}}V_{\text{nl}}e^{i(\mathbf{k}+\mathbf{q})\mathbf{r}} \right] |u_{n,\mathbf{k}+\mathbf{q}}\rangle. \quad (4.9)$$

Now, we expand the exponential as a series of \mathbf{q} and rearrange the terms according the order of \mathbf{q} :

$$\begin{aligned} h_{\mathbf{k}+\mathbf{q}} = & \frac{1}{2}p^2 - \mathbf{k} \cdot \mathbf{p} + e^{-i\mathbf{k}\mathbf{r}}V_{\text{nl}}e^{i\mathbf{k}\mathbf{r}} + \\ & + \mathbf{k} \cdot \mathbf{q} - \mathbf{q} \cdot \mathbf{p} + [e^{-i\mathbf{k}\mathbf{r}}V_{\text{nl}}e^{i\mathbf{k}\mathbf{r}}, i\mathbf{q}\mathbf{r}] + \\ & + \frac{1}{2}q^2 + i\mathbf{q}\mathbf{r}e^{-i\mathbf{k}\mathbf{r}}V_{\text{nl}}e^{i\mathbf{k}\mathbf{r}}i\mathbf{q}\mathbf{r} - \frac{1}{2}(\mathbf{q}\mathbf{r})^2 e^{-i\mathbf{k}\mathbf{r}}V_{\text{nl}}e^{i\mathbf{k}\mathbf{r}} - e^{-i\mathbf{k}\mathbf{r}}V_{\text{nl}}e^{i\mathbf{k}\mathbf{r}}\frac{1}{2}(\mathbf{q}\mathbf{r})^2 + \\ & + O(3). \end{aligned} \quad (4.10)$$

This Hamiltonian is readily transformed into a Hamiltonian for the full Bloch functions by multiplying with $e^{i\mathbf{k}\mathbf{r}}$, so that we have the perturbation Hamiltonians for the \mathbf{q} perturbation series:

$$H_{\mathbf{k}}^{(1)} = -\mathbf{q} \cdot \mathbf{p} + [V_{\text{nl}}, i\mathbf{q}\mathbf{r}] = i\mathbf{q}[H_{\mathbf{k}}, \mathbf{r}] = \mathbf{q}\mathbf{v} \quad (4.11)$$

$$H_{\mathbf{k}}^{(2)} = \frac{1}{2}q^2 + \frac{1}{2}[\mathbf{q}\mathbf{r}, [V_{\text{nl}}, \mathbf{q}\mathbf{r}]] = -\frac{i}{2}[\mathbf{q}\mathbf{v}, \mathbf{q}\mathbf{r}] \quad (4.12)$$

where we have used $[p^2, \mathbf{r}] = i\mathbf{p}$ and defined the generalized momentum operator

$$\mathbf{v} = \mathbf{p} + [V_{\text{nl}}, \mathbf{r}] \quad (4.13)$$

that is also called velocity operator. These two Hamiltonians are used within time dependent perturbation theory, c.f. App. C, to expand the matrix elements and energy denominators.

4.1.1 $\mathbf{q} \rightarrow 0$ for $\chi_0^{(2)}$

We now expand $\chi_0^{(2)}(\mathbf{q} + \mathbf{G}, \mathbf{q}' + \mathbf{G}', \mathbf{q}'' + \mathbf{G}'')$ in terms of \mathbf{q} to carry out the limit $\mathbf{q} \rightarrow 0$. Generally $\chi_0^{(2)}$ is a third rank tensor in terms of the \mathbf{G} vectors. For third rank tensors we classify four different parts

$$\text{head:} \quad \mathbf{G} = \mathbf{G}' = \mathbf{G}'' = 0 \quad (4.14)$$

$$\text{wings:} \quad \begin{cases} \mathbf{G} = \mathbf{G}' = 0 & \text{and } \mathbf{G}'' \neq 0 \\ \mathbf{G} = \mathbf{G}'' = 0 & \text{and } \mathbf{G}' \neq 0 \\ \mathbf{G}' = \mathbf{G}'' = 0 & \text{and } \mathbf{G} \neq 0 \end{cases} \quad (4.15)$$

$$\text{faces:} \quad \begin{cases} \mathbf{G} = 0 & \text{and } \mathbf{G}' \neq 0, \mathbf{G}'' \neq 0 \\ \mathbf{G}' = 0 & \text{and } \mathbf{G} \neq 0, \mathbf{G}'' \neq 0 \\ \mathbf{G}'' = 0 & \text{and } \mathbf{G} \neq 0, \mathbf{G}' \neq 0 \end{cases} \quad (4.16)$$

$$\text{body:} \quad \mathbf{G} \neq 0, \quad \mathbf{G}' \neq 0, \quad \mathbf{G}'' \neq 0 \quad (4.17)$$

We have to treat each of these cases separately, because the leading term of the head is proportional to q^3 while the faces and wings have a q and q^2 dependence respectively. This is due to the fact that for finite \mathbf{G} the leading order of an expansion in \mathbf{q} is independent of \mathbf{q} . In practice this means that for the faces we have to expand up to the first order, for the wings to second order and for the head to third order in \mathbf{q} . For second harmonic generation $\chi_0^{(2)}$ is symmetric under the exchange $\mathbf{q}' + \mathbf{G}' \leftrightarrow \mathbf{q}'' + \mathbf{G}''$ so that we have in total 6 different terms, of which the body does not need any expansion in \mathbf{q} . The exact expressions for all these terms are rather lengthy and we refer to App. C for details. Here we report only the result for the head, see Tab. 4.1, since it yields the dominating contribution in most of our calculations.

Here we have given the full expression, in practical calculations however, the terms containing the commutator turn out to be negligible and thus are not considered.

This expression is equivalent to the result of Hughes and Sipe [48], who are also using the length gauge and that is frequently used for IPA calculations also by other authors [50–58]. The difference between the two forms is that they did not consider non-locality of the potential. Another frequently employed formulation is in terms of the velocity operator [69] Eq. (4.13). The connection between the two formulations is made via the equation

$$\langle n\mathbf{k} | i\mathbf{r} | n'\mathbf{k}' \rangle = \frac{\langle n\mathbf{k} | \mathbf{v} | n'\mathbf{k}' \rangle}{E_{n\mathbf{k}} - E_{n'\mathbf{k}'}}. \quad (4.19)$$

The use of the length gauge has the additional complication that the matrix element of \mathbf{r} is ill defined in a crystal, which has to be carefully accounted for when using this representation.

$$\begin{aligned}
\chi_{\rho\rho\rho}^{(0),\text{head}}(\mathbf{q}, \mathbf{q}_1, \mathbf{q}_2) = & \frac{2}{V} \sum_{n, n', n'', \mathbf{k}} \left[\frac{(f_{n, \mathbf{k}} - f_{n'', \mathbf{k}})}{(\Delta_{nn'} + 2\tilde{\omega})(\Delta_{nn'} + \tilde{\omega})} + \frac{(f_{n', \mathbf{k}} - f_{n'', \mathbf{k}})}{(\Delta_{nn'} + 2\tilde{\omega})(\Delta_{n''n'} + \tilde{\omega})} + \right. \\
& \left. + 2 \frac{(f_{n, \mathbf{k}} - f_{n', \mathbf{k}})(\Delta_{n''n} + \Delta_{n''n'})}{\Delta_{nn'}^2(\Delta_{nn'} + 2\tilde{\omega})} - \frac{(f_{n, \mathbf{k}} - f_{n', \mathbf{k}})(\Delta_{n''n} + \Delta_{n''n'})}{2\Delta_{nn'}^2(\Delta_{nn'} + \tilde{\omega})} \right] \times \\
& \times \langle n_{\mathbf{k}} | -i(\mathbf{q}_1 + \mathbf{q}_2)\mathbf{r} | n'_{\mathbf{k}} \rangle \left[\langle n'_{\mathbf{k}} | i\mathbf{q}_2\mathbf{r} | n''_{\mathbf{k}} \rangle \langle n''_{\mathbf{k}} | i\mathbf{q}_1\mathbf{r} | n_{\mathbf{k}} \rangle + \langle n'_{\mathbf{k}} | i\mathbf{q}_1\mathbf{r} | n''_{\mathbf{k}} \rangle \langle n''_{\mathbf{k}} | i\mathbf{q}_2\mathbf{r} | n_{\mathbf{k}} \rangle \right] + \\
& + \frac{(f_{n, \mathbf{k}} - f_{n', \mathbf{k}})}{(\Delta_{n'n} + \tilde{\omega})(\Delta_{nn'} + \tilde{\omega})} \times \\
& \times \langle n''_{\mathbf{k}} | i(\mathbf{q}_1 + \mathbf{q}_2)\mathbf{r} | n_{\mathbf{k}} \rangle \left[\langle n_{\mathbf{k}} | i\mathbf{q}_1\mathbf{r} | n'_{\mathbf{k}} \rangle \langle n'_{\mathbf{k}} | i\mathbf{q}_2\mathbf{r} | n''_{\mathbf{k}} \rangle + \langle n_{\mathbf{k}} | i\mathbf{q}_2\mathbf{r} | n'_{\mathbf{k}} \rangle \langle n'_{\mathbf{k}} | i\mathbf{q}_1\mathbf{r} | n''_{\mathbf{k}} \rangle \right] + \\
& + \left[\frac{8(f_{n, \mathbf{k}} - f_{n', \mathbf{k}})}{\Delta_{nn'}^2(\Delta_{nn'} + 2\tilde{\omega})} - \frac{(f_{n, \mathbf{k}} - f_{n', \mathbf{k}})}{2\Delta_{nn'}^2(\Delta_{nn'} + \tilde{\omega})} \right] \times \\
& \times \langle n_{\mathbf{k}} | -i(\mathbf{q}_1 + \mathbf{q}_2)\mathbf{r} | n'_{\mathbf{k}} \rangle \left[\langle n'_{\mathbf{k}} | i\mathbf{q}_2\mathbf{r} | n_{\mathbf{k}} \rangle \Delta_{nn'}^{\mathbf{q}_1} + \langle n'_{\mathbf{k}} | i\mathbf{q}_1\mathbf{r} | n_{\mathbf{k}} \rangle \Delta_{nn'}^{\mathbf{q}_2} \right] + \\
& + \frac{(f_{n, \mathbf{k}} - f_{n', \mathbf{k}})\Delta_{n''n}}{\Delta_{nn'}(\Delta_{nn'} + \tilde{\omega})(\Delta_{n'n} + \tilde{\omega})} \times \\
& \times \left[-\langle n_{\mathbf{k}} | i\mathbf{q}_1\mathbf{r} | n'_{\mathbf{k}} \rangle \langle n'_{\mathbf{k}} | i\mathbf{q}_2\mathbf{r} | n''_{\mathbf{k}} \rangle \langle n''_{\mathbf{k}} | i(\mathbf{q}_1 + \mathbf{q}_2)\mathbf{r} | n_{\mathbf{k}} \rangle + \right. \\
& \quad + \langle n_{\mathbf{k}} | i(\mathbf{q}_1 + \mathbf{q}_2)\mathbf{r} | n'_{\mathbf{k}} \rangle \langle n'_{\mathbf{k}} | i\mathbf{q}_2\mathbf{r} | n''_{\mathbf{k}} \rangle \langle n''_{\mathbf{k}} | i\mathbf{q}_1\mathbf{r} | n_{\mathbf{k}} \rangle - \\
& \quad - \langle n_{\mathbf{k}} | i\mathbf{q}_2\mathbf{r} | n'_{\mathbf{k}} \rangle \langle n'_{\mathbf{k}} | i\mathbf{q}_1\mathbf{r} | n''_{\mathbf{k}} \rangle \langle n''_{\mathbf{k}} | i(\mathbf{q}_1 + \mathbf{q}_2)\mathbf{r} | n_{\mathbf{k}} \rangle + \\
& \quad \left. + \langle n_{\mathbf{k}} | i(\mathbf{q}_1 + \mathbf{q}_2)\mathbf{r} | n'_{\mathbf{k}} \rangle \langle n'_{\mathbf{k}} | i\mathbf{q}_1\mathbf{r} | n''_{\mathbf{k}} \rangle \langle n''_{\mathbf{k}} | i\mathbf{q}_2\mathbf{r} | n_{\mathbf{k}} \rangle \right] + \\
& + \left[\frac{(f_{n, \mathbf{k}} - f_{n', \mathbf{k}})}{\Delta_{nn'}^2(\Delta_{nn'} + \tilde{\omega})} - \frac{4(f_{n, \mathbf{k}} - f_{n', \mathbf{k}})}{\Delta_{nn'}^2(\Delta_{nn'} + 2\tilde{\omega})} \right] \times \\
& \times \langle n_{\mathbf{k}} | i(\mathbf{q}_1 + \mathbf{q}_2)\mathbf{r} | n'_{\mathbf{k}} \rangle \left[\langle n'_{\mathbf{k}} | -\frac{i}{2}[\mathbf{q}_1\mathbf{r}, \mathbf{q}_2\mathbf{v}] | n_{\mathbf{k}} \rangle + \langle n'_{\mathbf{k}} | -\frac{i}{2}[\mathbf{q}_2\mathbf{r}, \mathbf{q}_1\mathbf{v}] | n_{\mathbf{k}} \rangle \right] + \\
& + \frac{(f_{n, \mathbf{k}} - f_{n', \mathbf{k}})}{2\Delta_{nn'}^2(\Delta_{nn'} + \tilde{\omega})} \times \\
& + \left[\langle n_{\mathbf{k}} | [(\mathbf{q}_1 + \mathbf{q}_2)\mathbf{v}, i\mathbf{q}_2\mathbf{r}] | n'_{\mathbf{k}} \rangle \langle n'_{\mathbf{k}} | i\mathbf{q}_1\mathbf{r} | n_{\mathbf{k}} \rangle + \langle n_{\mathbf{k}} | [(\mathbf{q}_1 + \mathbf{q}_2)\mathbf{v}, i\mathbf{q}_1\mathbf{r}] | n'_{\mathbf{k}} \rangle \langle n'_{\mathbf{k}} | i\mathbf{q}_2\mathbf{r} | n_{\mathbf{k}} \rangle - \right. \\
& \quad \left. - \langle n_{\mathbf{k}} | i(\mathbf{q}_1 + \mathbf{q}_2)\mathbf{r} | n'_{\mathbf{k}} \rangle \langle n'_{\mathbf{k}} | [\mathbf{q}_2\mathbf{v}, i\mathbf{q}_1\mathbf{r}] | n_{\mathbf{k}} \rangle - \langle n_{\mathbf{k}} | i(\mathbf{q}_1 + \mathbf{q}_2)\mathbf{r} | n'_{\mathbf{k}} \rangle \langle n'_{\mathbf{k}} | [\mathbf{q}_1\mathbf{v}, i\mathbf{q}_2\mathbf{r}] | n_{\mathbf{k}} \rangle \right] \\
\end{aligned} \tag{4.18}$$

Table 4.1: Head of the leading order of the $\mathbf{k} \cdot \mathbf{p}$ expanded $\chi_{\rho\rho\rho}^{(0)}$, where we have used the shorthands $\tilde{\omega} = \omega + i\eta$, $\Delta_{nn'}^{\mathbf{q}} = \langle n_{\mathbf{k}} | \mathbf{q}\mathbf{v} | n_{\mathbf{k}} \rangle - \langle n'_{\mathbf{k}} | \mathbf{q}\mathbf{v} | n'_{\mathbf{k}} \rangle$ and $\Delta_{nn'} = E_{n_{\mathbf{k}}} - E_{n'_{\mathbf{k}}}$.

4.2 Scissors shift

As mentioned in Chap. 2.4.4 the application of the scissors shift to the band structure has some non-trivial implications in the second order case [109]. This is due to the fact that the scissors operator is a non-local operator and thus does not commute with the position operator, similar as the non-local potential. Formally the scissors operator reads

$$S = \Delta \sum_n (1 - f_n) |\phi_n\rangle \langle \phi_n| \quad (4.20)$$

where Δ is the energy shift, the sum runs over all states n and a finite band gap is assumed. The groundstate Hamiltonian of the $\mathbf{k} \cdot \mathbf{p}$ perturbation theory reads under consideration of the scissors operator

$$H_{SC} = \frac{1}{2} p^2 + V_{nl} + S \quad (4.21)$$

and the approximation is that this Hamiltonian has the same eigenstates as the one without the scissors operator

$$H_{LDA} = \frac{1}{2} p^2 + V_{nl} \quad (4.22)$$

which is the Hamiltonian we used in Eq. (4.8). Here the name H_{LDA} refers to the fact that it gives the wavefunctions that we obtain from the DFT groundstate calculation. The convenience of the scissors approximation is that we can keep using these wavefunctions even if the energies are shifted. This means that the matrix elements of the position operator do not change regardless of which Hamiltonian is used. The matrix elements of the velocity operator, however, do change under the scissors transformation, since the scissors operator is non-local S :

$$\mathbf{v}_{SC} = \mathbf{p} + [V_{nl} + S, \mathbf{r}]. \quad (4.23)$$

Using the relation between velocity and position matrix elements Eq. (4.19) and the fact the position matrix elements are invariant, we can write

$$\langle n\mathbf{k} | \mathbf{r} | n'\mathbf{k}' \rangle = \frac{\langle n\mathbf{k} | \mathbf{v} | n'\mathbf{k}' \rangle}{E_{n\mathbf{k}}^{LDA} - E_{n'\mathbf{k}'}^{LDA}} = \frac{\langle n\mathbf{k} | \mathbf{v}_{SC} | n'\mathbf{k}' \rangle}{E_{n\mathbf{k}}^{SC} - E_{n'\mathbf{k}'}^{SC}} \quad (4.24)$$

where $E_{n\mathbf{k}}^{SC}$ and $E_{n\mathbf{k}}^{LDA}$ are eigenenergies of the corresponding groundstate Hamiltonians, i.e. Eqs. (4.21) and (4.22) respectively. From Eq. (4.24) follows the relation

$$\langle n\mathbf{k} | \mathbf{v}_{SC} | n'\mathbf{k}' \rangle = \langle n\mathbf{k} | \mathbf{v} | n'\mathbf{k}' \rangle \frac{E_{n\mathbf{k}}^{SC} - E_{n'\mathbf{k}'}^{SC}}{E_{n\mathbf{k}}^{LDA} - E_{n'\mathbf{k}'}^{LDA}}, \quad (4.25)$$

which is trivially true for a zero scissors shift, i.e. $E_{n\mathbf{k}}^{SC} = E_{n\mathbf{k}}^{LDA}$, but can yield important changes in the response functions for large Δ .

The non-locality of S means it behaves the same as V_{nl} in our perturbation theory and thus the commutator terms in Eq. (4.18) contain this operator as well. While we have numerically verified that the potential commutators $[\mathbf{r}, \mathbf{p} + [\mathbf{r}, V_{nl}]]$ are negligible, we cannot make any general assumptions for $[\mathbf{r}, [\mathbf{r}, S]]$ and thus have to take them fully into account. Their contribution can be reexpressed in terms of shifted and non-shifted energies, similar to Eq. (4.25), but the algebra is somewhat lengthy. Therefore we give the final result, together with the $\mathbf{k} \cdot \mathbf{p}$ expressions for the wings and faces in appendix C.

4.3 Exact optical transitions

The expansion of $\chi_{\rho\rho\rho}^{(0)}$ in terms of \mathbf{q} to the leading order corresponds to the dipole approximation, i.e. $\mathbf{q} \rightarrow 0$. According to Eq. (4.1), however, every finite frequency corresponds to a finite \mathbf{q} . This means on the one hand, that the dipole approximation is only strictly valid for the static case $\omega \rightarrow 0$, but on the other hand it provides an alternative way to obtain $\chi_{\rho\rho\rho}^{(0)}$ by calculating it at the actual \mathbf{q} corresponding to finite frequencies. Such a treatment has two advantages. First one does not have to rely on the lengthy perturbation theory and second it provides a way to go beyond the dipole approximation by considering the actual \mathbf{q} dependence, c.f. Sec. 5.

As mentioned these \mathbf{q} are small so a numerical scheme has to be devised that can account for these very small difference in \mathbf{k} -points, since $\mathbf{q} = \mathbf{k}' - \mathbf{k}$. The sum over \mathbf{k} -points in Eq. (4.7) represents a discretization of the Brillouin zone into sample \mathbf{k} -points at which $\chi_{\rho\rho\rho}^{(0)}$ is evaluated. This discretization is usually done homogeneously, e.g. using the Monkhorst-Pack scheme [110], but it can also be carried out by sampling with random points. When one is interested in finite \mathbf{q} calculations this sampling has to be done under the restriction that differences between the resulting \mathbf{k} -points correspond to the desired \mathbf{q} , c.f. Fig. 4.1. This means that for very small \mathbf{q} a homogeneous sampling is not very efficient because one has to work with a much higher density of sampling points than necessary for convergence of the sum. Indeed, assuming that the size of the Brillouin zone is $\sim \text{\AA}^{-1}$ one needs 10^9 sampling points to be able to treat \mathbf{q} in the order of 10^{-3}\AA^{-1} , while convergence is usually achieved already with 10^3 points. Therefore one has to use a non-homogeneous sampling of the Brillouin zone, c.f. Fig. 4.1. The advantage of such a sampling is that the actual value of \mathbf{q} is not determined *a posteriori* as done for homogeneous sampling, but one can choose basically arbitrary values for \mathbf{q} . Moreover a non-homogeneous sampling can easily combined with a random sampling technique.

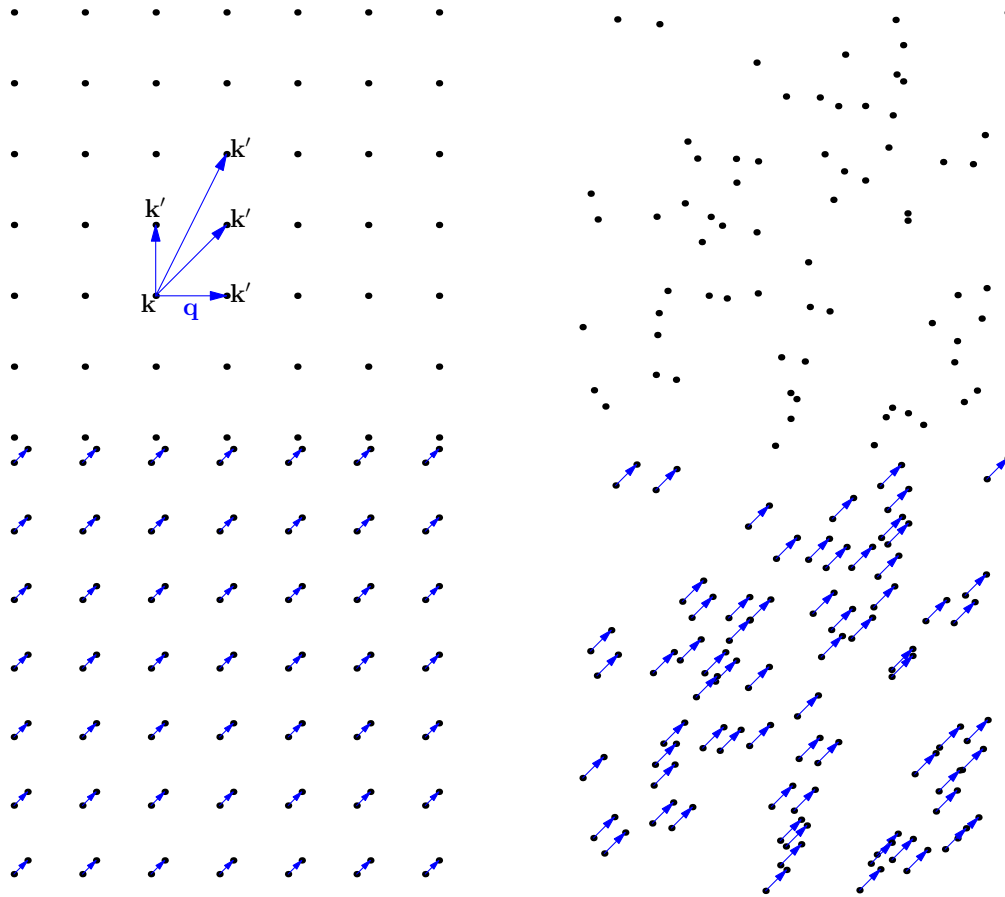


Figure 4.1: \mathbf{k} -points sampling schemes. **Top left:** Commonly used homogeneous grid with restricted set of possible \mathbf{q} vectors. **Top right:** Random sampling, where finite \mathbf{q} calculations are not possible, because all differences between \mathbf{k} -points are random. **Bottom left:** Inhomogeneous sampling done by shifting the homogeneous set by the target \mathbf{q} . **Bottom right:** Random sampling can be used by treating a set that contain for each random point one shifted by \mathbf{q} .

In practice one has to calculate matrix elements of the form

$$\tilde{\rho}_{\mathbf{k}n}^{\mathbf{k}'n'}(\mathbf{q} + \mathbf{G}) = \int d\mathbf{r} \phi_{\mathbf{k}n}(\mathbf{r}) e^{-i(\mathbf{q} + \mathbf{G})\mathbf{r}} \phi_{\mathbf{k}'n'}(\mathbf{r}). \quad (4.26)$$

so it is convenient to work with two different sets of Kohn-Sham wavefunctions, one corresponding to \mathbf{k} and one for \mathbf{k}' . This means that they can be generated separately, one shifted by \mathbf{q} with respect to the other. On the other hand this means that the implementation has to be able to manage two different \mathbf{k} -point sets. Since $\chi_{\rho\rho\rho}^{(0)}$ depends on two different \mathbf{q} , it turns out that one has to treat four different sets of \mathbf{k} -points, c.f. Fig. 4.2. Inspection of the \mathbf{q} dependent expression of $\chi_{\rho\rho\rho}^{(0)}$ Eq. (4.7) shows that one actually needs to calculate five different kinds of matrix elements corresponding to the

transitions shown in Fig. 4.2.

Another downside of this approach is the need for high numerical accuracy. When used to calculate responses near the optical limit, it must still hold that the $\chi_{\rho\rho\rho}^{(0)}$ is proportional to q^3 . Since $\chi_{\rho\rho\rho}^{(0)}$ is constructed by products of three matrix elements, these product have to be proportional to q^3 . If we think about the matrix elements as expanded in terms of q , i.e.

$$\tilde{\rho}(\mathbf{q}) = \tilde{\rho}^{(0)} + \tilde{\rho}^{(1)}q + \tilde{\rho}^{(2)}q^2 + \dots \quad (4.27)$$

it is apparent that in order to have a product of three of these proportional to q^3 one has to calculate each matrix element with an accuracy of the same order. This can be a serious numerical challenge when q is very small, e.g. for $q \sim 10^{-3}$ we need an accuracy up to 10^{-9} or 6 orders of magnitude, which is just the limit of single machine precision.

This approach is in a way a numerical brute force scheme where the exact cancellation achieved in the perturbative expansion has to be reached numerically. One can, however, use certain symmetry properties of the response function to improve the convergence even in this scheme. In particular time-reversal and, in case, inversion symmetry are crucial for convergence. Figure 4.3 illustrates which transitions are equivalent to a $(\mathbf{k}, n) \rightarrow (\mathbf{k} + \mathbf{q}, n')$ transition under these symmetries. The idea is to hardwire these symmetries into the numerical implementation by rewriting the equation for $\chi_{\rho\rho\rho}^{(0)}$ under consideration of these symmetry operations and then add it to the original expression. That is to say that if T is the unchanged summand of $\chi_{\rho\rho\rho}^{(0)}$ (Eq. (4.7)) and we apply analytically a symmetry operation i on this term giving T^i , we can implement $\chi_{\rho\rho\rho}^{(0)}$ in the form

$$\chi_{\rho\rho\rho}^{(0)} = \frac{2}{V} \sum_{nn'n'\mathbf{k}} \frac{1}{2} [T + T^i]. \quad (4.28)$$

Like this we can make sure that we include cancellations between terms due to the symmetry i that we might have missed otherwise because of the finite \mathbf{k} -point sampling etc.

4.3.1 Time reversal

Under timereversal symmetry for wavefunctions and eigenvalues of band n at point \mathbf{k} holds:

$$\phi_{n\mathbf{k}}(r) = \phi_{n-\mathbf{k}}^* \quad E_{n\mathbf{k}} = E_{n-\mathbf{k}} \quad (4.29)$$

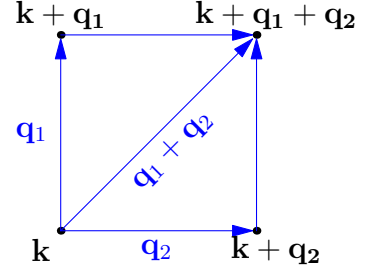


Figure 4.2: multigrid scheme

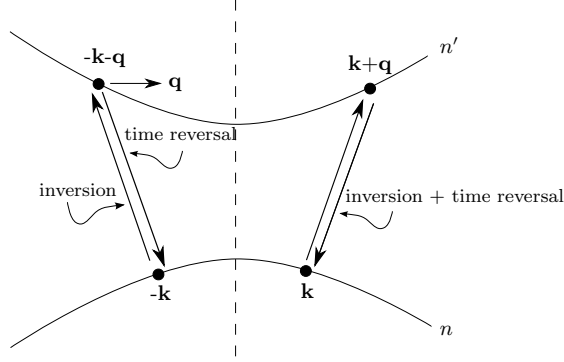


Figure 4.3: Schematic view of the different transitions in terms of which we reformulate $\chi_{\rho\rho\rho}^{(0)}$.

This means that we can write the matrix element $\tilde{\rho}_{n\mathbf{k},n'\mathbf{k}+\mathbf{q}}$ as

$$\tilde{\rho}_{n\mathbf{k},n'\mathbf{k}+\mathbf{q}}(\mathbf{q} + \mathbf{G}) = \int d\mathbf{r} e^{-i(\mathbf{q}+\mathbf{G})\mathbf{r}} \phi_{n\mathbf{k}}^*(\mathbf{r}) \phi_{n'\mathbf{k}+\mathbf{q}}(\mathbf{r}) \quad (4.30)$$

$$= \int d\mathbf{r} e^{-i(\mathbf{q}+\mathbf{G})\mathbf{r}} \phi_{n-\mathbf{k}}(\mathbf{r}) \phi_{n'-\mathbf{k}-\mathbf{q}}^*(\mathbf{r}) \quad (4.31)$$

$$= \int d\mathbf{r} e^{-i(\mathbf{q}+\mathbf{G})\mathbf{r}} \phi_{n'-\mathbf{k}-\mathbf{q}}^*(\mathbf{r}) \phi_{n-\mathbf{k}}(\mathbf{r}) \quad (4.32)$$

$$= \tilde{\rho}_{n'-\mathbf{k}-\mathbf{q},n-\mathbf{k}}(\mathbf{q} + \mathbf{G}) \quad (4.33)$$

from which we deduce that the transition $(n', -\mathbf{k} - \mathbf{q}) \rightarrow (n, -\mathbf{k})$ is the time reversed transition of $(n, \mathbf{k}) \rightarrow (n', \mathbf{k} + \mathbf{q})$, c.f. Fig. 4.3.

To make use of this property we take the full expression of $\chi_{\rho\rho\rho}^{(0)}$ (Eq. (4.7)) and replace in the sum $n \leftrightarrow n'$ and redefine the k -point parameter as

$$-\mathbf{K} = \mathbf{k} + \mathbf{q}_1 + \mathbf{q}_2 \quad \mathbf{k} + \mathbf{q}_1 = -\mathbf{K} - \mathbf{q}_2, \quad \mathbf{k} + \mathbf{q}_2 = -\mathbf{K} - \mathbf{q}_1, \quad \mathbf{k} = -\mathbf{K} - \mathbf{q}_1 - \mathbf{q}_2 \quad (4.34)$$

and sum over \mathbf{K} in stead of \mathbf{k} . We use these substitutions in $\chi_{\rho\rho\rho}^{(0)}$ and then apply the time reversal property Eq. (4.30) for the matrix elements and $E_{n\mathbf{k}} = E_{n-\mathbf{k}}$ for the energies.

We obtain:

$$\begin{aligned}
\chi_{\rho\rho\rho}^{(0),timerev} = & \frac{2}{V} \sum_{nn'n''\mathbf{k}} \frac{\langle n_{\mathbf{k}} | e^{-i(\mathbf{q}_1+\mathbf{q}_2+\mathbf{G})\mathbf{r}} | n'_{\mathbf{k}+\mathbf{q}_1+\mathbf{q}_2} \rangle}{(-E_{n\mathbf{k}} + E_{n'\mathbf{k}+\mathbf{q}_1+\mathbf{q}_2} + 2\omega + 2i\eta)} \times \\
& \times \left[(f_n - f_{n''}) \frac{\langle n'_{\mathbf{k}+\mathbf{q}_1+\mathbf{q}_2} | e^{i(\mathbf{q}_1+\mathbf{G}_1)\mathbf{r}} | n''_{\mathbf{k}+\mathbf{q}_2} \rangle \langle n''_{\mathbf{k}+\mathbf{q}_2} | e^{i(\mathbf{q}_2+\mathbf{G}_2)\mathbf{r}} | n_{\mathbf{k}} \rangle}{(-E_{n\mathbf{k}} + E_{n''\mathbf{k}+\mathbf{q}_2} + \omega + i\eta)} + \right. \\
& + (f_n - f_{n'}) \frac{\langle n'_{\mathbf{k}+\mathbf{q}_1+\mathbf{q}_2} | e^{i(\mathbf{q}_2+\mathbf{G}_2)\mathbf{r}} | n''_{\mathbf{k}+\mathbf{q}_1} \rangle \langle n''_{\mathbf{k}+\mathbf{q}_1} | e^{i(\mathbf{q}_1+\mathbf{G}_1)\mathbf{r}} | n_{\mathbf{k}} \rangle}{(-E_{n\mathbf{k}} + E_{n''\mathbf{k}+\mathbf{q}_1} + \omega + i\eta)} + \\
& + (f_{n'} - f_{n''}) \frac{\langle n'_{\mathbf{k}+\mathbf{q}_1+\mathbf{q}_2} | e^{i(\mathbf{q}_2+\mathbf{G}_2)\mathbf{r}} | n''_{\mathbf{k}+\mathbf{q}_1} \rangle \langle n''_{\mathbf{k}+\mathbf{q}_1} | e^{i(\mathbf{q}_1+\mathbf{G}_1)\mathbf{r}} | n_{\mathbf{k}} \rangle}{(-E_{n''\mathbf{k}+\mathbf{q}_1} + E_{n'\mathbf{k}+\mathbf{q}_1+\mathbf{q}_2} + \omega + i\eta)} + \\
& \left. + (f_{n'} - f_{n''}) \frac{\langle n'_{\mathbf{k}+\mathbf{q}_1+\mathbf{q}_2} | e^{i(\mathbf{q}_1+\mathbf{G}_1)\mathbf{r}} | n''_{\mathbf{k}+\mathbf{q}_2} \rangle \langle n''_{\mathbf{k}+\mathbf{q}_2} | e^{i(\mathbf{q}_2+\mathbf{G}_2)\mathbf{r}} | n_{\mathbf{k}} \rangle}{(-E_{n''\mathbf{k}+\mathbf{q}_2} + E_{n'\mathbf{k}+\mathbf{q}_1+\mathbf{q}_2} + \omega + i\eta)} \right] \quad (4.35)
\end{aligned}$$

which is the usual $\chi_{\rho\rho\rho}^{(0)}$ (Eq. (4.7)) with negative energy differences and we have replaced \mathbf{K} by \mathbf{k} for convenience. There is also a timereversal property for the \mathbf{k} dependence of the Fermi factors. Here we just suppress this dependence, since we deal with semi-conductors.

4.3.2 Inversion

Inversion symmetry is a symmetry property of the crystal system and does not hold in general. However, to treat Silicon we might want to include this symmetry property explicitly, because it is the crucial operation that lets $\chi_{\rho\rho\rho}^{(0)}$ vanish in the dipole approximation.

For any symmetry operation R we have ([111]):

$$\tilde{\rho}_{nR\mathbf{k},n'R(\mathbf{k}+\mathbf{q})}(\mathbf{q} + \mathbf{G}) = \tilde{\rho}_{n\mathbf{k},n'\mathbf{k}+\mathbf{q}}(R^{-1}(\mathbf{q} + \mathbf{G})) . \quad (4.36)$$

We consider the inversion operation

$$R = \begin{pmatrix} -1 & 0 & 0 \\ 0 & -1 & 0 \\ 0 & 0 & -1 \end{pmatrix} = R^{-1} \quad (4.37)$$

and we have for the matrix elements:

$$\tilde{\rho}_{n-\mathbf{k},n'-\mathbf{k}-\mathbf{q}}(\mathbf{q} + \mathbf{G}) = \tilde{\rho}_{n\mathbf{k},n'\mathbf{k}+\mathbf{q}}(-\mathbf{q} - \mathbf{G}) . \quad (4.38)$$

The energies do not change under the symmetry operation, i.e. $E_{\mathbf{n}\mathbf{k}} = E_{n-\mathbf{k}}$. We rewrite $\chi_{\rho\rho\rho}^{(0)}$ with the same substitutions Eqs. (4.34) and then use the symmetry property Eq. (4.38) of the system. Subsequently replacing \mathbf{K} by \mathbf{k} and expressing the result in terms of the matrix elements of the unchanged $\chi_{\rho\rho\rho}^{(0)}$ yields

$$\begin{aligned}
\chi_{\rho\rho\rho}^{(0),inv} = & \frac{2}{V} \sum_{nn'n''\mathbf{k}} \frac{\left(\langle n_{\mathbf{k}} | e^{-i(\mathbf{q}_1+\mathbf{q}_2+\mathbf{G})\mathbf{r}} | n'_{\mathbf{k}+\mathbf{q}_1+\mathbf{q}_2} \rangle\right)^*}{(-E_{n\mathbf{k}} + E_{n'\mathbf{k}+\mathbf{q}_1+\mathbf{q}_2} + 2\omega + 2i\eta)} \times \\
& \times \left[(f_n - f_{n''}) \frac{\left(\langle n'_{\mathbf{k}+\mathbf{q}_1+\mathbf{q}_2} | e^{i(\mathbf{q}_1+\mathbf{G}_1)\mathbf{r}} | n''_{\mathbf{k}+\mathbf{q}_2} \rangle\right)^* \left(\langle n''_{\mathbf{k}+\mathbf{q}_2} | e^{i(\mathbf{q}_2+\mathbf{G}_2)\mathbf{r}} | n_{\mathbf{k}} \rangle\right)^*}{(-E_{n\mathbf{k}} + E_{n''\mathbf{k}+\mathbf{q}_2} + \omega + i\eta)} + \right. \\
& + (f_n - f_{n''}) \frac{\left(\langle n'_{\mathbf{k}+\mathbf{q}_1+\mathbf{q}_2} | e^{i(\mathbf{q}_2+\mathbf{G}_2)\mathbf{r}} | n''_{\mathbf{k}+\mathbf{q}_1} \rangle\right)^* \left(\langle n''_{\mathbf{k}+\mathbf{q}_1} | e^{i(\mathbf{q}_1+\mathbf{G}_1)\mathbf{r}} | n_{\mathbf{k}} \rangle\right)^*}{(-E_{n\mathbf{k}} + E_{n''\mathbf{k}+\mathbf{q}_1} + \omega + i\eta)} + \\
& + (f_{n'} - f_{n''}) \frac{\left(\langle n'_{\mathbf{k}+\mathbf{q}_1+\mathbf{q}_2} | e^{i(\mathbf{q}_2+\mathbf{G}_2)\mathbf{r}} | n''_{\mathbf{k}+\mathbf{q}_1} \rangle\right)^* \left(\langle n''_{\mathbf{k}+\mathbf{q}_1} | e^{i(\mathbf{q}_1+\mathbf{G}_1)\mathbf{r}} | n_{\mathbf{k}} \rangle\right)^*}{(-E_{n''\mathbf{k}+\mathbf{q}_1} + E_{n'\mathbf{k}+\mathbf{q}_1+\mathbf{q}_2} + \omega + i\eta)} + \\
& \left. + (f_{n'} - f_{n''}) \frac{\left(\langle n'_{\mathbf{k}+\mathbf{q}_1+\mathbf{q}_2} | e^{i(\mathbf{q}_1+\mathbf{G}_1)\mathbf{r}} | n''_{\mathbf{k}+\mathbf{q}_2} \rangle\right)^* \left(\langle n''_{\mathbf{k}+\mathbf{q}_2} | e^{i(\mathbf{q}_2+\mathbf{G}_2)\mathbf{r}} | n_{\mathbf{k}} \rangle\right)^*}{(-E_{n''\mathbf{k}+\mathbf{q}_2} + E_{n'\mathbf{k}+\mathbf{q}_1+\mathbf{q}_2} + \omega + i\eta)} \right] \tag{4.39}
\end{aligned}$$

which is exactly the starting term Eq. (4.7) with a sign change in the energies and all matrix elements complex conjugated.

4.3.3 Time reversal and Inversion

To include both symmetry operations we need to obtain the time reversed version of $\chi_{\rho\rho\rho}^{(0),inv}$. To this end we take Eq. (4.39) and use the time reversal property Eq. (4.30) for the matrix elements and $E_{n\mathbf{k}} = E_{n-\mathbf{k}}$ for the energies. Then, replacing $n \leftrightarrow n'$ and making the substitutions

$$\begin{aligned}
-\mathbf{k}-\mathbf{q}_1-\mathbf{q}_2 = \mathbf{K} \quad & -\mathbf{k}-\mathbf{q}_1 = \mathbf{K}+\mathbf{q}_2, \quad & -\mathbf{k}-\mathbf{q}_2 = \mathbf{K}+\mathbf{q}_1, \quad & -\mathbf{k} = +\mathbf{K}+\mathbf{q}_1+\mathbf{q}_2
\end{aligned} \tag{4.40}$$

yields

$$\begin{aligned}
\chi_{\rho\rho\rho}^{(0),inv+timerev} = & \\
\frac{2}{V} \sum_{nn'n''\mathbf{k}} & \frac{\left(\langle n_{\mathbf{k}} | e^{-i(\mathbf{q}_1+\mathbf{q}_2+\mathbf{G})\mathbf{r}} | n'_{\mathbf{k}+\mathbf{q}_1+\mathbf{q}_2} \rangle\right)^*}{(E_{n\mathbf{k}} - E_{n'\mathbf{k}+\mathbf{q}_1+\mathbf{q}_2} + 2\omega + 2i\eta)} \times \\
& \times \left[(f_n - f_{n'}) \frac{\left(\langle n'_{\mathbf{k}+\mathbf{q}_1+\mathbf{q}_2} | e^{i(\mathbf{q}_1+\mathbf{G}_1)\mathbf{r}} | n''_{\mathbf{k}+\mathbf{q}_2} \rangle\right)^* \left(\langle n''_{\mathbf{k}+\mathbf{q}_2} | e^{i(\mathbf{q}_2+\mathbf{G}_2)\mathbf{r}} | n_{\mathbf{k}} \rangle\right)^*}{(E_{n\mathbf{k}} - E_{n''\mathbf{k}+\mathbf{q}_2} + \omega + i\eta)} + \right. \\
& + (f_n - f_{n'}) \frac{\left(\langle n'_{\mathbf{k}+\mathbf{q}_1+\mathbf{q}_2} | e^{i(\mathbf{q}_2+\mathbf{G}_2)\mathbf{r}} | n''_{\mathbf{k}+\mathbf{q}_1} \rangle\right)^* \left(\langle n''_{\mathbf{k}+\mathbf{q}_1} | e^{i(\mathbf{q}_1+\mathbf{G}_1)\mathbf{r}} | n_{\mathbf{k}} \rangle\right)^*}{(E_{n\mathbf{k}} - E_{n''\mathbf{k}+\mathbf{q}_1} + \omega + i\eta)} + \\
& + (f_{n'} - f_{n''}) \frac{\left(\langle n'_{\mathbf{k}+\mathbf{q}_1+\mathbf{q}_2} | e^{i(\mathbf{q}_2+\mathbf{G}_2)\mathbf{r}} | n''_{\mathbf{k}+\mathbf{q}_1} \rangle\right)^* \left(\langle n''_{\mathbf{k}+\mathbf{q}_1} | e^{i(\mathbf{q}_1+\mathbf{G}_1)\mathbf{r}} | n_{\mathbf{k}} \rangle\right)^*}{(E_{n''\mathbf{k}+\mathbf{q}_1} - E_{n'\mathbf{k}+\mathbf{q}_1+\mathbf{q}_2} + \omega + i\eta)} + \\
& \left. + (f_{n'} - f_{n''}) \frac{\left(\langle n'_{\mathbf{k}+\mathbf{q}_1+\mathbf{q}_2} | e^{i(\mathbf{q}_1+\mathbf{G}_1)\mathbf{r}} | n''_{\mathbf{k}+\mathbf{q}_2} \rangle\right)^* \left(\langle n''_{\mathbf{k}+\mathbf{q}_2} | e^{i(\mathbf{q}_2+\mathbf{G}_2)\mathbf{r}} | n_{\mathbf{k}} \rangle\right)^*}{(E_{n''\mathbf{k}+\mathbf{q}_2} - E_{n'\mathbf{k}+\mathbf{q}_1+\mathbf{q}_2} + \omega + i\eta)} \right] \quad (4.41)
\end{aligned}$$

which is the unchanged term with complex conjugated matrix elements.

All these terms can be directly included in the implementation by writing the terms under the same sum

$$\chi_{\rho\rho\rho}^{(0)} = \frac{2}{V} \sum_{nn'n''\mathbf{k}} \frac{1}{4} [T + T^{timerev} + T^{inv} + T^{inv+timerev}] \quad (4.42)$$

where T^i are the summands of the respective terms Eqs. (4.35),(4.39) and (4.41). Of course in case the system does not have inversion symmetry the last two terms cannot be included.

4.4 Transverse vs. Longitudinal response

For calculations with \mathbf{q} values that are finite but still in the optical range the statement that transverse and longitudinal response coincide is not true anymore, since it relies on the limit $\mathbf{q} \rightarrow 0$. Still the dipole limit is frequently employed to calculate optical spectra in a finite frequency range. The underlying assumption is that the longitudinal and transverse responses do not differ substantially in this range. Since it is an important assumption made in the formalism presented in this work, it should be to some extent quantified. The usual density matrix elements clearly cannot give the transverse response, instead one has to employ matrix elements of the current operator. This amounts to

calculating a $\chi_{\mathbf{jj}}^{(0)}$:

$$\chi_{\mathbf{jj}}^{(0)}(\mathbf{q} + \mathbf{G}, \omega) = \frac{2}{V} \sum_{\mathbf{k}n n'} (f_{n\mathbf{k}} - f_{n'\mathbf{k}+\mathbf{q}}) \frac{\tilde{\mathbf{j}}_{n\mathbf{k}, n'\mathbf{k}+\mathbf{q}}(\mathbf{q} + \mathbf{G}) \tilde{\mathbf{j}}_{n\mathbf{k}, n'\mathbf{k}+\mathbf{q}}^*(\mathbf{q} + \mathbf{G})}{(\epsilon_{n\mathbf{k}} - \epsilon_{n'\mathbf{k}+\mathbf{q}} + \omega + i\eta)} \quad (4.43)$$

where we have defined the current matrix elements $\tilde{\mathbf{j}}$ as

$$\tilde{\mathbf{j}}_{n\mathbf{k}, n'\mathbf{k}+\mathbf{q}}(\mathbf{q} + \mathbf{G}) = \int d\mathbf{r} e^{-i(\mathbf{q}+\mathbf{G})\mathbf{r}} \phi_{n\mathbf{k}}^*(\mathbf{r}) \frac{1}{2i} (\nabla - \nabla^\dagger) \phi_{n'\mathbf{k}+\mathbf{q}}(\mathbf{r}) \quad (4.44)$$

This is a 3×3 tensor in the (cartesian) components of the vector operator and it can be used to construct the full dielectric tensor (in the independent particle approximation) via

$$\epsilon(\mathbf{q}, \omega) = 1 - \frac{4\pi}{\omega^2} \chi_{\mathbf{jj}}^{(0)}(\mathbf{q}, \omega). \quad (4.45)$$

where we have neglected local field effects. This is in principle general if one takes the full $\chi_{\mathbf{jj}}$ instead of the non-interacting one as done in the framework of time dependent current density theory [105, 112–114]. The development of functionals and kernels that make use of the added information contained in the current density instead of the scalar electron density is still in a very early stage [115]. One can however translate any TDDFT kernel into TDcurrentDFT one by use of the continuity equation. Then, the two theories give exactly the same results for the longitudinal components of ϵ , while TDcurrentDFT may or may not contain additional information about the transverse components. Here, we will however only deal with the independent particle approximation, i.e. $v + f_{xc} = 0$, where the equivalence between the two formulations is trivial.

A direct comparison between longitudinal and transverse can be made by considering the full dielectric tensor $\epsilon(\mathbf{q})$ and decomposing it into its longitudinal and transverse constituents by applying the longitudinal and transverse projectors (c.f. Eq. (3.36))

$$P^L(\mathbf{q}) = \frac{\mathbf{q}\mathbf{q}}{q^2}, \quad P^T(\mathbf{q}) = -\frac{\mathbf{q} \times \mathbf{q} \times}{q^2} \quad (4.46)$$

to yield

$$\epsilon(\mathbf{q})^{LL} = P^L \epsilon(\mathbf{q}) P^L \quad \epsilon(\mathbf{q})^{TT} = P^T \epsilon(\mathbf{q}) P^T. \quad (4.47)$$

These terms take on a very simple form when \mathbf{q} points in a cartesian direction, e.g. $\mathbf{q} = q\mathbf{e}_x$ and we consider a system with cubic symmetry:

$$\epsilon(q\mathbf{e}_x)^{LL} = \begin{pmatrix} \epsilon_{xx} & 0 & 0 \\ 0 & 0 & 0 \\ 0 & 0 & 0 \end{pmatrix} \quad \epsilon(q\mathbf{e}_x)^{TT} = \begin{pmatrix} 0 & 0 & 0 \\ 0 & \epsilon_{yy} & 0 \\ 0 & 0 & \epsilon_{zz} \end{pmatrix} \quad (4.48)$$

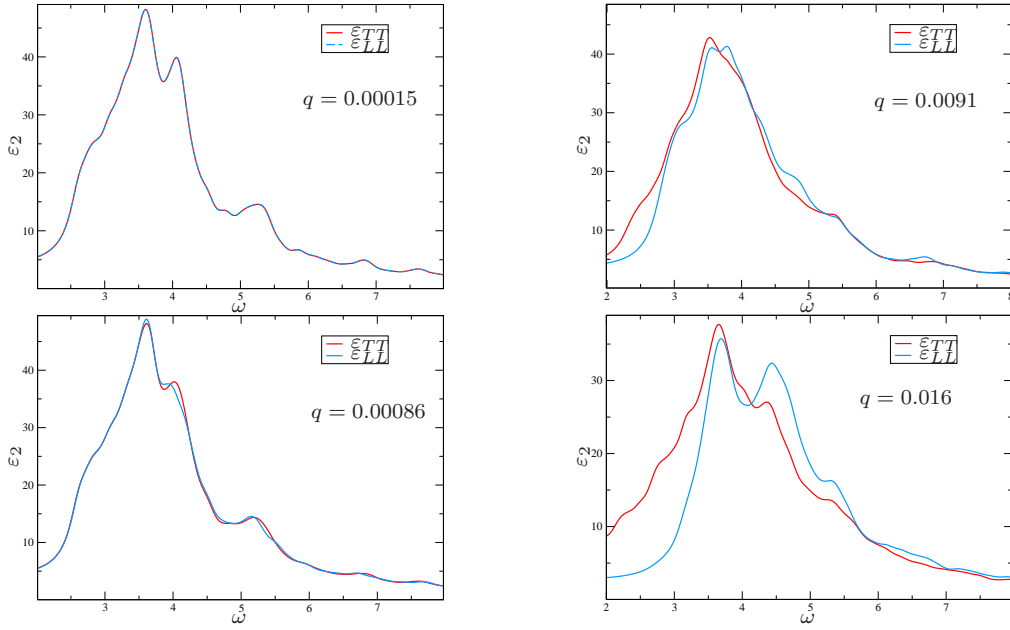


Figure 4.4: Comparison between the longitudinal and transverse dielectric function for Si with different \mathbf{q} values (in Bohr $^{-1}$).

where additionally holds $\epsilon_{yy} = \epsilon_{zz}$. Hence, in order to compare the longitudinal and transverse responses of a cubic system as a function of q we only need to consider the ϵ_{xx} and ϵ_{yy} component of $\epsilon(q\mathbf{e}_x)$, i.e. perform a calculation with $\mathbf{q} = q\mathbf{e}_x$ and subsequently compare the components. In Fig. 4.4 such a comparison is shown for Si. We find that in the optical range, i.e. $q \approx 10^{-3} \text{\AA}^{-1}$ the difference between the two polarization directions is not discernable. Only at values for $q \approx 10^{-2} \text{\AA}^{-1}$ differences occur. The energy carried by photons with the momentum is however, beyond 100 eV and thus far outside the range of valence band spectroscopy.

5 Spatial dispersion

The best known feature of second harmonic generation is that it vanishes for systems with inversion symmetry, which makes it a very useful symmetry selective tool. The vanishing of second harmonic generation is, however, only true in the dipole limit, i.e. $\mathbf{q} \rightarrow 0$. Since experiments, on the other hand, are usually performed at finite frequencies, this means that the actual dipole limit is never strictly reached and quadrupole contributions are in principle present in every measurement [116]. Therefore, when an experiment, e.g. at the surface of a centro-symmetric material, relies on the fact that the bulk does not contribute to second harmonic generation, it has to be very carefully performed in order to rule out quadrupole response from the bulk. The actual importance of the quadrupole contribution compared with, for example, surface dipole contributions is still a point of debate [117, 118], but is generally considered to be substantial [119–123]. There exist, to my knowledge, no published attempt at calculating this contribution within the ab initio framework, although numerous models are frequently employed, c.f. [124].

In this chapter I will explore the possibility to calculate second harmonic generation beyond the dipole limit using the facility of the multigrid approach described in Chap. 4.3 to treat \mathbf{q} -vectors of arbitrary length. This gives access to the spatial dispersion of the crystal that is intimately linked to multipole responses. I will discuss the concept of spatial dispersion briefly with examples from linear optics and then show how it can be used to obtain the quadrupole contributions to second harmonic generation.

5.1 Linear spatial dispersion

Spatial dispersion is the dependence of the dielectric function on the light wave vector [125]. It originates from the fact that the polarization at a point does not only depend on the field at this point but also on the field in its immediate neighborhood. This radius of non-locality a is usually very small, in solids it is of the order of the lattice constant. The amount of spatial dispersion one sees in the response depends on the ratio between the characteristic length a and the wavelength λ of the field. In the optical limit, when we look at very low energetic light, this ratio becomes very small and vanishes in the limit $\lim_{\lambda \rightarrow \infty}$ or equivalently $\lim_{\mathbf{q} \rightarrow 0}$. For finite optical frequencies it is safe to assume [125]

$$\frac{aq}{2\pi} = \frac{a}{\lambda} \ll 1. \quad (5.1)$$

The fact that the spatial dispersion is so small implies that it can be neglected in most cases and that in any case its effect will be visible only under special circumstances. But

it also allows for an expansion of the dielectric tensor in terms of the wave vector \mathbf{q} , because a sharply peaked response in real space is smooth in reciprocal space. We write the expansion as

$$\varepsilon_{ij}(\omega, \mathbf{q}) = \varepsilon_{ij}(\omega) + \gamma_{ijk}(\omega)q_k + \alpha_{ijkl}(\omega)q_kq_l + \dots \quad (5.2)$$

We note that the zeroth order in \mathbf{q} is the usual dielectric tensor with frequency dispersion. The higher order terms are the contribution of the non-locality to the full tensor. This expansion is the basis of the description of spatial dispersion, since it allows the discussion in terms of the tensors γ_{ijk} and α_{ijkl} .

5.1.1 symmetry properties of tensors

Although a crystal is not isotropic it does have some symmetry properties which according to von-Neumann's principle also hold for the dielectric tensor $\varepsilon(\omega, \mathbf{q})$. This means that for a given symmetry operation S that leaves the crystal unchanged the tensor must obey the relation

$$S^{-1}\varepsilon(\omega, S\mathbf{q})S = \varepsilon(\omega, \mathbf{q}). \quad (5.3)$$

Now, if we consider the special case of a vector \mathbf{q}_i that is invariant under one, or more, symmetry operations S_i of the crystal system, i.e.

$$S_i\mathbf{q}_i = \mathbf{q}_i \quad (5.4)$$

we can use the relation

$$S^{-1}\varepsilon(\omega, \mathbf{q}_i)S = \varepsilon(\omega, \mathbf{q}_i). \quad (5.5)$$

which yields a set of equations that express conditions on the tensor $\varepsilon(\omega, \mathbf{q}_i)$ and upon solving this set of equations we obtain information on the structure of the tensor. That is to say which components are equal and which vanish. This, however, is not a general property but only holds for the one \mathbf{q}_i (and its equivalent class) that fulfils Eq. (5.4). But nevertheless, it can be useful information when doing calculations for experiments that only use a few \mathbf{q} -directions.

When we consider spatial dispersion in optics we expand the tensor $\varepsilon(\omega, \mathbf{q})$ in terms of \mathbf{q}

$$\varepsilon(\omega, \mathbf{q}) = \sum_n \left. \frac{\partial^{(n)}\varepsilon(\omega, \mathbf{q})}{\partial \mathbf{q}^n} \right|_{\mathbf{q}_0} (\mathbf{q} - \mathbf{q}_0)^n \quad (5.6)$$

by introducing the quantities $\left. \frac{\partial^{(n)}\varepsilon(\omega, \mathbf{q})}{\partial \mathbf{q}^n} \right|_{\mathbf{q}_0}$ that are rank n tensor (γ_{ijk} , α_{ijkl} in Eq. (5.2)) and are independent of \mathbf{q} . Therefore, they possess the same symmetry properties as the crystal system and we can use the whole group of symmetry operations associated with the crystal to deduce the structure of the expansion tensors, i.e. to reduce them to their

dissimilar non-zero components. A rank n tensor transforms according to ([126, p. 761 ff])

$$\sum_{i_1 \dots i_n}^3 S_{\alpha_1 i_1} S_{\alpha_2 i_2} \dots S_{\alpha_n i_n} \chi_{i_1 \dots i_n} = \tilde{\chi}_{\alpha_1 \dots \alpha_n} \quad (5.7)$$

Under the conditions that the tensor is invariant under the symmetry operation we have

$$\tilde{\chi}_{\alpha_1 \dots \alpha_n} = \chi_{\alpha_1 \dots \alpha_n} \quad (5.8)$$

which yield our set of equations that we can use to reduce the number of components. When we neglect spatial dispersion we consider only the zeroth order in the expansion and our dielectric tensor has the properties a rank 2 tensor yields under the transformation with all crystal symmetries, e.g. in the cubic case it is diagonal with all elements equal. The higher order tensors, although invariant under the same symmetries, might however contribute components to the $\varepsilon(\omega, \mathbf{q})$ that are zero to zeroth order. In an example we consider cubic Silicon (O_h) where we have $\gamma_{ijk} = 0$ (due to inversion symmetry) and the second order tensor reduces to three components:

$$\alpha_1 = \alpha_{iiii} \quad \alpha_2 = \alpha_{ijij} \quad \alpha_3 = \alpha_{ijij} \quad (5.9)$$

Most significantly we have for the off diagonal element xy of the dielectric tensor

$$\varepsilon_{xy}(\omega, \mathbf{q}) = \alpha_3(\omega) q_x q_y \quad (5.10)$$

Here, the \mathbf{q} -dependence becomes clear, because this term is only non-zero if the \mathbf{q} has finite q_x and q_y components. Indeed, it is true for any such \mathbf{q} without any condition on its symmetry properties. We have for the xx -component

$$\varepsilon_{xx}(\omega, \mathbf{q}) = \varepsilon_{xx}(\omega) + \alpha_1(\omega) q_x q_x + \alpha_2(\omega) (q_y q_y + q_z q_z) . \quad (5.11)$$

That means to second order the y and z components of \mathbf{q} not only contribute to the response in x -direction but their contribution also has a different value than the one in x -direction.

It is important to note that this does not represent symmetry breaking nor does the \mathbf{q} introduce anisotropy to the system. Instead we think of spatial dispersion as a way of probing the anisotropy of the crystal. The expansion simply gives the ordering of the effect of the anisotropy in the different directions. To zeroth order the anisotropy does not appear, to first order, in the cubic case we do not have any further contribution and to second order the off diagonals become non-zero and the diagonals change depending on the direction of \mathbf{q} .

This is useful for the multi-grid approach described in Chap. 4.3 where, in principle, we calculate the full $\varepsilon(\omega, \mathbf{q})$, but having the knowledge of the structure of γ, α etc. we know for which component we can expect the largest effects and which directions yield equivalent spatial dispersion effects (up to a certain order). It also tells us which

components we can calculate using TDDFT, i.e. which components are longitudinal responses.

5.2 SHG

Spatial dispersion is particularly interesting in the case of second harmonic generation, where for systems with inversion symmetry it yields the leading order contribution. This is completely analogous to the linear case where the third rank tensor γ_{ijk} vanishes, but the fourth rank tensor α_{ijkl} is finite. The expansion of the second order polarization is commonly written as [119, 127, 128]

$$\mathbf{P}_i^{(2)}(\mathbf{r}, \omega) = \chi_{ijk} E_j(\mathbf{r}) E_k(\mathbf{r}) + \Gamma_{ijkl} E_j(\mathbf{r}) \nabla_k E_l(\mathbf{r}) + .. \quad (5.12)$$

which corresponds to an expansion of $\chi^{(2)}$ in terms of \mathbf{q}

$$\chi_{ijk}(\mathbf{q}, \omega) = \chi_{ijk}(\omega) + \chi_{ijkl}^Q(\omega) q_l + .. \quad (5.13)$$

where we have defined the quadrupolar second harmonic generation coefficient χ^Q ¹. As mentioned before the rank three tensor vanishes for inversion symmetry and for cubic systems the only non-zero components are

$$\alpha_1 = \chi_{iiii}^Q \quad \alpha_2 = \chi_{ijji}^Q \quad \alpha_3 = \chi_{iijj}^Q = \chi_{ijij}^Q \quad (5.14)$$

where in the last line we have used the fact that the polarization directions of the applied fields are interchangeable. These components are analogous to the linear case, only that here the indices have different meaning, i.e. the first three are polarization directions and only the last one is a propagation direction. With these definitions one can write down the general component of χ^Q as [129]

$$\chi_{ijkl}^Q = \alpha_1 \delta_{ij} \delta_{ik} \delta_{il} + \alpha_2 \delta_{il} \delta_{jk} (1 - \delta_{ij}) + \alpha_3 ((\delta_{ij} \delta_{kl} (1 - \delta_{ik}) + (\delta_{ik} \delta_{jl} (1 - \delta_{ij}))) \quad (5.15)$$

We note that the terms $\delta_{il} \delta_{jk}$, $\delta_{ij} \delta_{kl}$ and $\delta_{ik} \delta_{jl}$ are rank four invariant scalars which leaves them unchanged under any orthogonal transformation². This also means that they are unchanged under rotation of the coordinate system and hence they represent the isotropic contributions to χ^Q . These isotropic contributions do not give any additional information about the symmetry of the system and occur only as offsets in an angular dependent experiment. Therefore we rewrite Eq. (5.15) to separate these contributions

¹This definition differs from Γ_{ijkl} in the ordering of the indices. The latter is used in literature, but here I choose this definition because it is more consistent with the one used in [125].

²This can be seen by applying a transformation T on the tensor $\delta_{ij} \delta_{kl}$:

$$\sum_{ijkl} T_{\alpha i} T_{\beta j} T_{\gamma k} T_{\delta l} \delta_{ij} \delta_{kl} = \sum_{ik} T_{\alpha i} T_{\beta i} T_{\gamma k} T_{\delta k} = \sum_{ik} T_{i\alpha}^{-1} T_{\beta i} T_{k\gamma}^{-1} T_{\delta k} = \delta_{\alpha\beta} \delta_{\gamma\delta}$$

3.

$$\chi_{ijkl}^Q = \chi_{ijkl}^{Q,ai} + \chi_{ijkl}^{Q,iso} \quad (5.16)$$

$$= (\alpha_1 - \alpha_2 - 2\alpha_3)\delta_{ij}\delta_{ik}\delta_{il} + \alpha_2\delta_{il}\delta_{jk} + \alpha_3(\delta_{ij}\delta_{kl} + \delta_{ik}\delta_{jl}). \quad (5.17)$$

Hence the anisotropic part of χ^Q reads

$$\chi_{ijkl}^{Q,ai} = (\alpha_1 - \alpha_2 - 2\alpha_3)\delta_{ij}\delta_{ik}\delta_{il}. \quad (5.18)$$

which implies that only components of the form χ_{iiii}^Q have a non-vanishing anisotropic contribution.

The combination of the tensor components $(\alpha_1 - \alpha_2 - 2\alpha_3)$ can be obtained in the multigrid approach described in Sec. 4.3 by two different longitudinal calculations:

$$\chi_{\rho\rho\rho}(q\mathbf{e}_x) = \alpha_1 \quad (5.19)$$

$$\chi_{\rho\rho\rho}(q(\mathbf{e}_x + \mathbf{e}_y + \mathbf{e}_z)) = 3\alpha_1 + 6\alpha_2 + 12\alpha_3 \quad (5.20)$$

and the combinations of both yields the anisotropic coefficient

$$\chi_{iiii}^{Q,ai} = \frac{3}{2}\chi_{\rho\rho\rho}(q\mathbf{e}_x) - \frac{1}{6}\chi_{\rho\rho\rho}(q(\mathbf{e}_x + \mathbf{e}_y + \mathbf{e}_z)). \quad (5.21)$$

While the component $\alpha_1 = \chi_{iiii}^Q$ can be calculated as a longitudinal response as in Eq. (5.19) the two other components only appear as sums of the form of Eq. (5.20) in longitudinal calculations and cannot be separated by different choices of \mathbf{q} . This means, we cannot calculate the isotropic part for all components and this puts a serious limit to this approach. Still, we can calculate the isotropic part of χ_{iiii}^Q components via,

$$\chi_{iiii}^{Q,iso} = \alpha_2 + 2\alpha_3 = -\frac{1}{2}\chi_{\rho\rho\rho}(q\mathbf{e}_x) + \frac{1}{6}\chi_{\rho\rho\rho}(q(\mathbf{e}_x + \mathbf{e}_y + \mathbf{e}_z)). \quad (5.22)$$

5.2.1 Dipole case

In the expansion Eq. (5.13) the first term is independent of \mathbf{q} and thus corresponds to the dipole limit. While it is zero for systems with inversion symmetry it gives the leading order contribution for systems without such symmetry. In section 4.1 I have shown how these terms can be obtained from an analytical expansion of the fully \mathbf{q} -dependent $\chi_{\rho\rho\rho}^{(0)}$ while in section 4.3 I described how one can use the \mathbf{q} -dependence of $\chi_{\rho\rho\rho}^{(0)}$ to obtain its optical limit. Here, I will compare the two approaches for the example system of cubic SiC, that does not have inversion symmetry and hence the leading term in a \mathbf{q} -dependent calculation and the dipole expansion should give the same result.

Figure 5.1 shows on the left the direct comparison between a calculation where $\chi_{\rho\rho\rho}^{(0)}$ has been expanded up to dipole order, i.e. is expressed as in Eq. (4.18), and a \mathbf{q} -dependent calculation with $\mathbf{q} = 6 \times 10^{-4}(1, 1, 1)$, i.e. $q = 0.001$. The Brillouin zone is in both cases

³This is essentially the same expression given by Bloembergen et al. in [128].

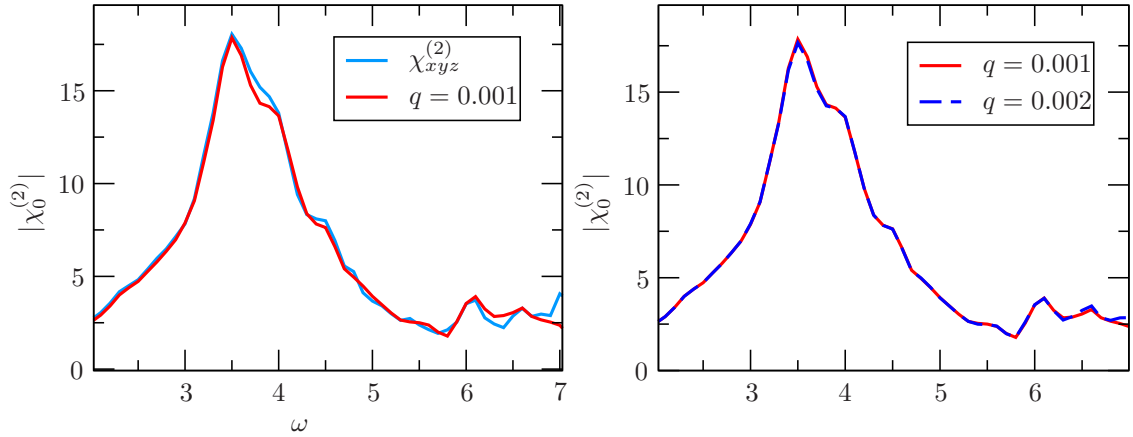


Figure 5.1: Comparison between analytical dipole expanded $\chi_{xyz}^{(0)}$ and a \mathbf{q} -dependent calculation with different \mathbf{q} values for cubic SiC. The differences between the dipole result and the q -dependent calculation are due to different convergence of the two methods.

sampled by a homogeneous grid of 4000 \mathbf{k} -points, which in the case of the \mathbf{q} -dependent calculation has been shifted by \mathbf{q} and $2\mathbf{q}$. The main difference in the calculation parameters is that in the case of the dipole calculation the basis size of the wavefunctions used for the matrix elements has 139 \mathbf{G} -vectors, while for the \mathbf{q} -dependent calculation one needs 3000 \mathbf{G} -vectors to represent the wavefunctions with the necessary accuracy. The overall agreement between the two calculation is rather good, with noticeable differences only in the high energy region and other small differences due to different convergence of the two methods. As an additional numerical test that this is indeed the dipole limit as well as to verify the stability of the numerical approach, we show on the right of Fig. 5.1 the comparison between the \mathbf{q} -dependent calculation for $\mathbf{q} = 6 \times 10^{-4}(1, 1, 1)$ and one with $\mathbf{q}' = 2\mathbf{q} = 1.2 \times 10^{-3}(1, 1, 1)$. We see that the resulting $\chi_0^{(2)}$ is indeed independent of q as must be in the dipole limit. Here, this check is trivial since the agreement with the analytical dipole expansion has already been shown, but in cases where one is interested in linear or quadratic dependencies on q , i.e. quadru- and octopole terms, this kind of analysis is crucial to ensure the calculation has been done with \mathbf{q} in the right range.

5.2.2 Quadrupole case

The q -dependence of the quadrupole response is linear and therefore a \mathbf{q} -dependent calculation should give results that scale linearly with q . Moreover, for centro-symmetric materials it is the leading order and thus the dependence should be such that the response vanishes for zero q . In Fig. 5.2 such calculations are shown for cubic Si with q values of 10^{-3} and 10^{-2} . Scaling of the latter calculation by a factors of 1/10 shows that the curves are identical up to this factor. The fact that there is a single factor of proportionality between the two curves means not only that the q -dependence is indeed

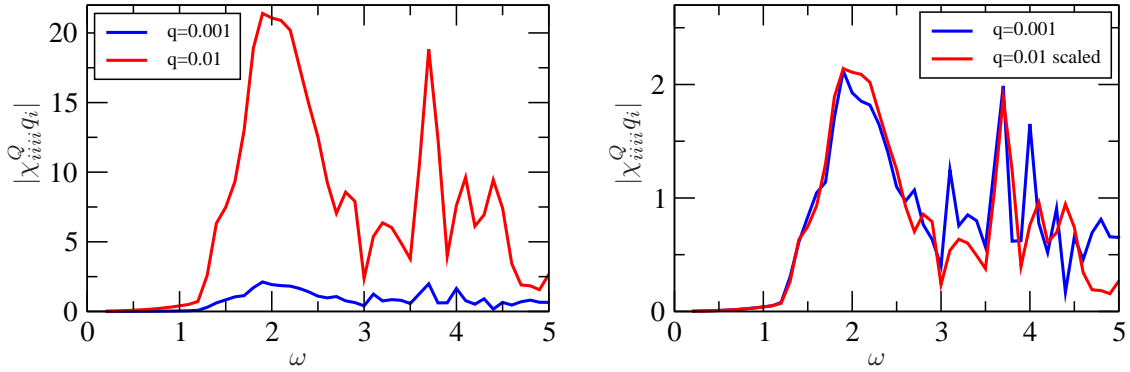


Figure 5.2: Comparison of two \mathbf{q} -dependent calculations of $\chi_{iiii}^Q q_i$ for Si with the two different $\mathbf{q} = 10^{-2}(0, 0, 1)$ and $\mathbf{q}' = 10^{-3}(1, 0, 0)$ (left panel). There is clearly a linear q -dependence, which can be seen on the right panel, where the \mathbf{q} calculation is scaled by a factor of 1/10. The different direction of \mathbf{q} and \mathbf{q}' is an additional convergence test.

linear but it also means that the results vanish for $q \rightarrow 0$, i.e. no offset at $q = 0$, as must be. The results have hence to be scaled by $1/q$ to yield the quadrupole tensor components defined in Eq. (5.13).

In Fig. 5.3 are shown the anisotropic contribution to the second harmonic quadrupole response of Si according to Eq. (5.21) as well as the isotropic contribution to the χ_{iiii}^Q components for comparison. We note that both components have large intensities, $\sim 10^3$, compared with the usual dipole contributions that are of the order of $\sim 10^1$. This, however, does not mean that the quadrupole response is orders of magnitude larger than the dipole. On the contrary, since the quadrupole response depends linearly on q , which in turn is connected with the frequency of the perturbing light via Eq. (4.1), and has values of 10^{-4} \AA^{-1} for optical light, the overall contribution will be rather small. The shape of the isotropic and anisotropic contribution is very similar, which is due to the fact that the responses Eq. (5.19) and (5.20) have very similar shape.

Furthermore, we note in Fig. 5.3 that the isotropic contribution to χ_{iiii}^Q is much smaller than the anisotropic one. We do not have any further information about the other two isotropic components, χ_{ijji}^Q and χ_{ijij}^Q , but one can at least assume that they will have the same order of magnitude.

Actual comparison with experiment is difficult in this form, since no pure bulk quadrupole spectra exist. But I would like to point out that Driscoll and Guidiotti [130] note a significantly strong second harmonic signal from bulk Si at $\lambda = 527 \text{ nm}$, which corresponds to $\omega = 2.3 \text{ eV}$ and thus to the main peak in Fig. 5.3.

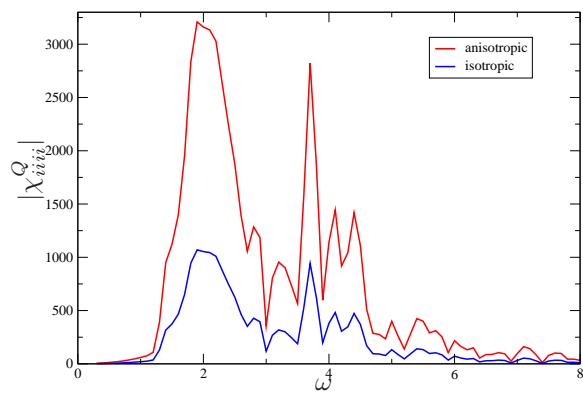


Figure 5.3: Anisotropic and isotropic contribution to the second harmonic quadrupole response of Si.

6 Results

In this chapter I will show some numerical results and test cases of the implementation of the formalism outlined in the previous chapters [131]. The main interest here is to investigate the influence of the local field and exchange and correlation effects on the second harmonic spectra. This is done for the example system of hexagonal silicon carbide (SiC), which exhibits polymorphism. The polymorphism is realized by different stacking orders of Si-C bi layers of either cubic (c) or hexagonal (h) types in the z -direction [132]. One can define the hexagonality H of the polytype by the ratio $H = h/(h + c)$. The polymorphism preserves the crystal symmetry thus allowing a direct comparison of the components of the susceptibility.

SiC polytypes have been studied extensively in the context of ab-initio calculations of SHG. Chen et al. [133] use a LDA+scissors scheme to calculate the static second harmonic coefficients in the independent particle approximation of various SiC polytypes and find a dependence of local field corrections on the hexagonality. In a later work [134] the same authors use a refined scheme to describe nonlinear local field effects for the static susceptibility and report an increase of xzx component, whereas the zzz decreases when local fields are accounted for. Rashkeev et al. [50] using a similar computational scheme as in [133], while neglecting local field and many body effects, are able to calculate the imaginary part of the frequency dependent second harmonic susceptibility, from which, through a Kramers-Kronig relation they infer the real part, which then enables them to construct the modulo of the susceptibility. Performing a transition by transition analysis of the spectra, they can assign single spectral features to single band transition, thereby suggesting SHG spectroscopy as a probe for electronic structure. The underlying assumption of these three works, that quasiparticle effects can accurately be described by a scissors operator is investigated in detail by Adolph and Bechstedt [135] by comparing this approach with a calculation where the optical matrix elements are corrected by a GW quasiparticle calculation. They find that the scissors operator approach gives very good agreement with the actual quasiparticle result for all polytypes under consideration. Then I will present the test case of GaAs, where a direct comparison of the calculated spectrum with experimental spectra is possible.

6.0.3 Structures

In this section I will briefly discuss the structures of the materials used in this chapter and also give some computational details concerning the parameters of the groundstate and response calculations. All groundstates are obtained with the ABINIT package [136], which gives the Kohn-Sham energies and wavefunctions in terms of a basis of plane waves. The LDA for the exchange and correlation potential is used and the atomic

core electrons are approximated by norm conserving pseudo-potentials of the Troullier-Martins form [137].

SiC

The purely cubic polytype of SiC has zincblende structure and can therefore be described by a unit cell with two atoms (primitive cell). I used the experimental cell parameter of $a = 8.24$ Bohr and an energy cut-off of 50 Ha for the plane wave basis. The irreducible Brillouin zone was sampled by 10 special \mathbf{k} -points, corresponding to a Monkhorst-Pack grid of 256 k -points in the full Brillouin zone.

The hexagonal polytypes $2h$, $4h$ and $6h$ have the $6mm$ (C_{6v}) symmetry and differ only in the stacking order of Si-C bilayers, c.f. Fig. 6.1. The primitive unit cells have 4, 8 and 12 atoms respectively and I used a cut off of 50 Ha for the basis of all polytypes. The experimental cell parameters are $a = 5.8$ Bohr for all compounds and $c = 9.37, 18.99$ for $2h$ and $4h$, while for $6h$ the theoretical lattice constants of $a = 5.7$ and $c = 28.39$ was used.

The calculation of the second harmonic spectra are done with a random sampling of

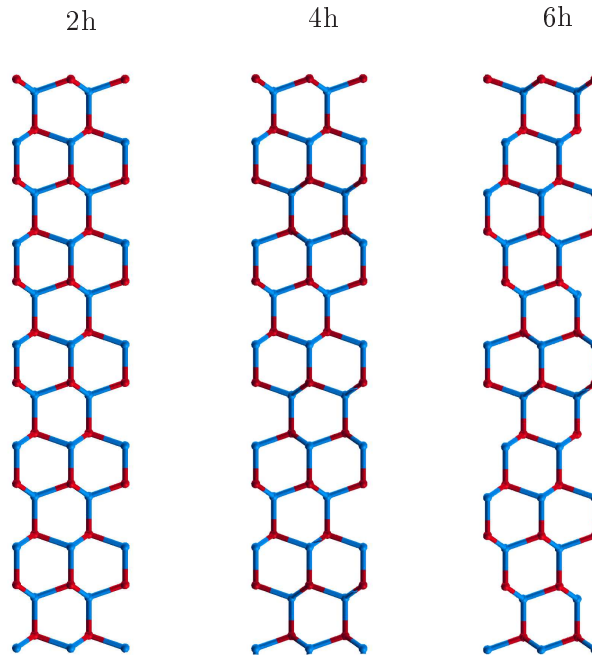


Figure 6.1: The $y - z$ -plane of the three hexagonal polytypes. They differ only in the stacking order of the Si-C bilayers. $2h$ -SiC has an $ABAB$ pattern, $4h$ -SiC an $ABAC$ and $6h$ -SiC has the stacking pattern $ABCACB$.

the Brillouin zone for the hexagonal polytypes. Convergence was reached with 1600

\mathbf{k} -points for 2h χ_{zzz} , 2400 for 2h χ_{xzx} , 2000 for 2h χ_{zxx} and 800 for all 4h and 6h components. Convergence of the local field effects with respect to the number of included \mathbf{G} vectors was reached with 23 for 2h χ_{xzx} , 59 for 2h χ_{zzz} , 37 for χ_{zxx} , 39 for 4h χ_{xzx} and χ_{zzz} , 51 for 4h χ_{zxx} and 43 for all 6h components. The number of conduction bands necessary for convergence in the considered energy range are 12, 24, 36 for the 2h, 4h and 6h components respectively. The basis size for the DFT wavefunctions was sufficiently converged with 300 for all polytypes.

GaAs

Gallium Arsenide also has the zincblende structure with the experimental lattice parameter of $a = 10.67$ Bohr and a cut off of 50 Ha is needed for a converged the groundstate density. For the second harmonic spectrum convergence is reached with 17575 \mathbf{k} -points to sample the Brillouin zone and 7 conduction bands. The local field effects on the second harmonic spectrum is converged with 65 \mathbf{G} vectors. This compound as the added complication that a pseudo potential description of Gallium needs the inclusion of d semicore states to accurately describe the electronic structure [138]. Therefore a pseudo potential with the valence configuration of $3d^{10}4s^24p^1$ is used for Gallium.

6.1 Independent (Quasi-)Particle Approximation

In the independent particle approximation the macroscopic susceptibility $\chi^{(2)}$ is just the head of the microscopic Kohn-Sham response function $\chi_{\rho\rho\rho}^{(0)}$, c.f. Eq. (3.74). The quasi-particle effects are accounted for by the scissors operator approach, which means one applies a rigid shift to all conduction bands, c.f. section 4.2. These two approximations are very similar in the sense that they do not explicitly take into account exchange and correlation effects. The quasi-particle shift of the band structure, does however, affect the spectrum substantially, since it leads to a shift of the resonances. While in the linear case this shift of the spectrum is more or less rigid [99] in the case of second harmonic generation it also leads to a redistribution of spectral weights.

Fig. 6.2 shows how the scissors shift changes the second harmonic spectra of SiC polytypes.

6.1.1 Transitions in c-SiC

The sum-over-states formulation for $\chi_{\rho\rho\rho}^{(0)}$ allows to do a transition resolved analysis of the second harmonic process, as already suggested by Lambrecht et. al. [50]. Here, I will briefly consider a decomposition of the transitions into valence-valence-conduction (vvc) and conduction-conduction-valence (ccv), which also contain the permutations, i.e. cvv and vcc. Fig. 6.3 left panel shows how these two types of transition contribute to the IPA spectrum of cubic SiC. The ccv transitions are clearly dominating the main peak at 3.5 eV, which could be explained by the fact that for a converged spectrum SiC needs 16 conduction bands on top of the 4 valence bands. Therefore, there are much more

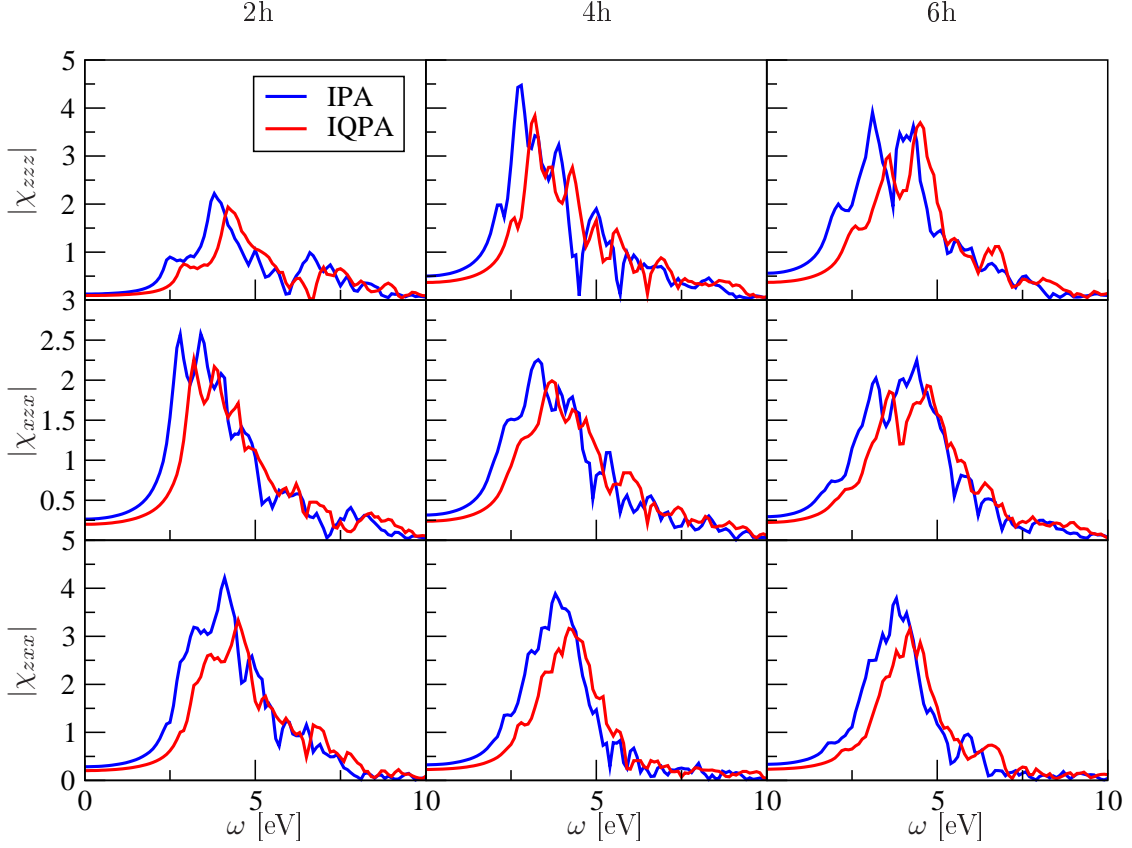


Figure 6.2: Effect of the scissors shift of 0.84 eV on the independent particle spectra of SiC hexagonal polytypes. All graphs show the modulus of the respective $\chi^{(2)}$ component in the independent particle approximation (IPA) and the independent quasi-particle approximation (IQPA), realized by a scissors shift as described in section 4.2.

ccv transitions presents. When we restrict the number of included conduction states to 2, Fig. 6.3 center panel, the contribution is only slightly reduced. It is essentially the transitions between the bands $6 \leftrightarrow 5 \leftrightarrow \{4, 3\}$ that make up the bigger part of the spectrum, and most notably the main resonance at 3.5 eV. The same analysis shows that the second peak, at 7 eV is only due to vvc transitions and, as shown in the right panel of Fig. 6.3, these are dominated by $3 \leftrightarrow 4 \leftrightarrow \{5, 6\}$.

6.2 Crystal Local Field effects

Local field effects enter into the macroscopic second harmonic susceptibility in two places. First the three macroscopic dielectric functions contain local field effects, and second the second order TDDFT Dyson like equation mixes \mathbf{G} -components of $\chi_{\rho\rho\rho}^{(2)}$ and $\chi_{\rho\rho}^{(1)}$. We

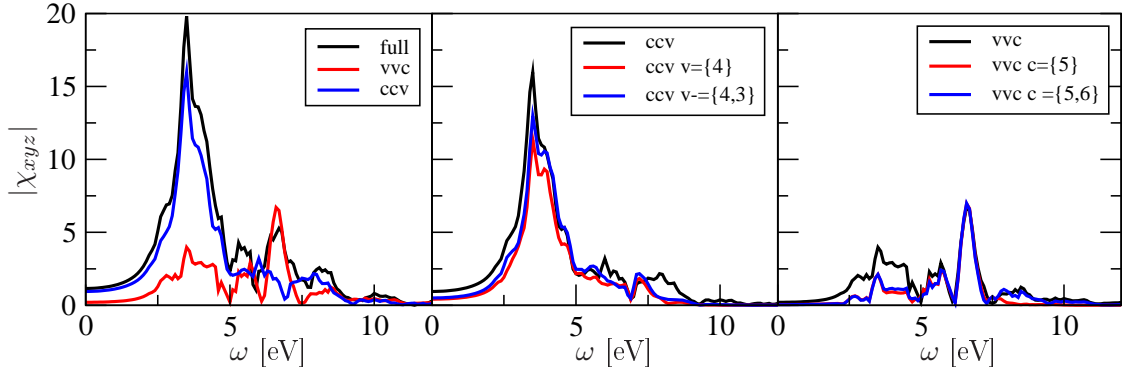


Figure 6.3: Analysis of transitions contributing to χ_{xyz} for cubic SiC. **left:** Contributions of vvc and ccv transitions to the spectrum, which is clearly dominated by ccv transitions for the peak at 3.5 eV, and by vvc transitions for the peak at 7 eV. **center:** Decomposition of the ccv transitions. The transitions $6 \leftrightarrow 5 \leftrightarrow \{4, 3\}$ are the most important for the main peak at 3.5 eV, with the $6 \leftrightarrow 5 \leftrightarrow 4$ transition accounting already for half of the peak intensity. **right:** Decomposition of the vvc transitions that make up the second peak at 7 eV. Here the transition $3 \leftrightarrow 4 \leftrightarrow 5$ accounts already for the full peak.

can write this more explicitly by using Eq. (2.60) for the solution of the Dyson equation and write explicitly the \mathbf{G} dependence. The macroscopic susceptibility then reads (in RPA):

$$\chi^{(2)} = \epsilon_M [\epsilon_{TE}^{-1}]^T_{\mathbf{0}\mathbf{G}} \left[\chi_{\rho\rho\rho}^{(0)} \right]_{\mathbf{G}\mathbf{G}_1\mathbf{G}_2} [\epsilon_{TE}^{-1}]_{\mathbf{G}_1\mathbf{0}} [\epsilon_{TE}^{-1}]_{\mathbf{G}_2\mathbf{0}} \epsilon_M \epsilon_M \quad (6.1)$$

with implicit sums over the \mathbf{G} vectors. While ϵ_M are scalars in this equation the ϵ_{TE} are \mathbf{G} -dependent and as such mix with the \mathbf{G} components of $\chi_{\rho\rho\rho}$.

First we consider the macroscopic dielectric functions ϵ_M that relate the microscopic response to the macroscopic susceptibility. These quantities also contain local field effects and are calculated according to [86, 87, 100]

$$\epsilon_M(\omega) = \lim_{\mathbf{q} \rightarrow 0} \frac{1}{\epsilon_{\mathbf{G}=0, \mathbf{G}=0}^{-1}(\mathbf{q}, \omega)} \quad (6.2)$$

where again a careful consideration of the \mathbf{G} dependence is crucial.

Therefore we have to consider the local field effects in the linear dielectric tensor as well. Due to the crystal symmetry the hexagonal polytypes have an optical anisotropy with two independent components of the dielectric tensor that are commonly denoted as $\epsilon_{\parallel} = \epsilon_{zz}$ and $\epsilon_{\perp} = \frac{1}{2}(\epsilon_{xx} + \epsilon_{yy})$. In Fig. 6.4 are shown the local field effects in these two components for the three polytypes. We can see a clear trend for the ϵ_{\perp} component, where the effect decreases with decreasing hexagonality and almost vanishes for the 6h polytype. The effect for ϵ_{zz} component, however, seems to be independent of the hexagonality, being of the same magnitude for all three polytypes. We also note that the relative local field effect in the ϵ_{zz} component is of the same size as for the ϵ_{\perp} in 2h.

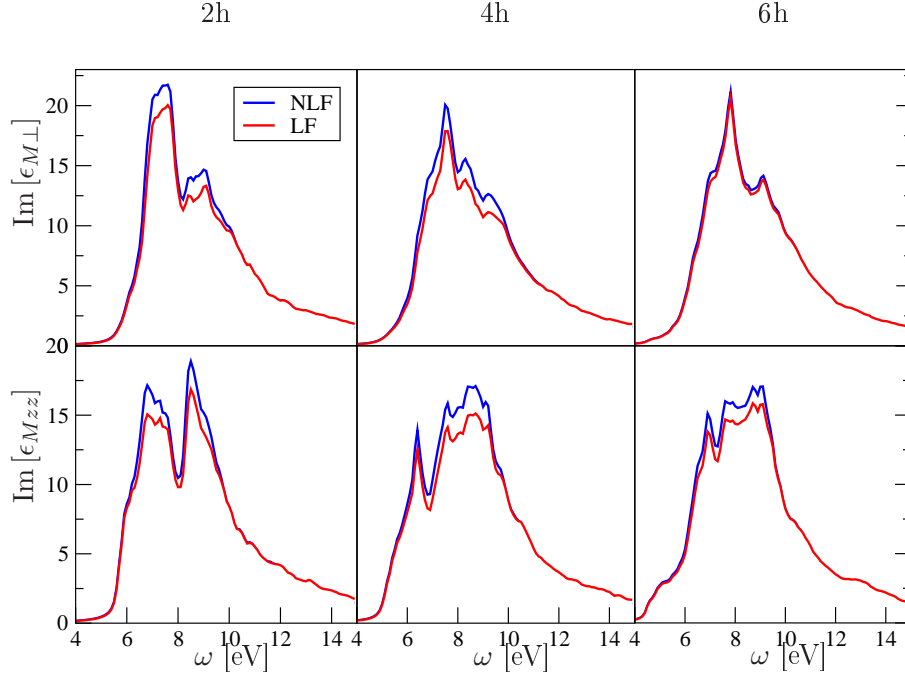


Figure 6.4: Influence of local fields on the imaginary part of the components of the linear dielectric tensor for the SiC polytypes 2h, 4h, 6h, where calculations accounting for local fields are denoted LF and those where they are neglected NLF. For the perpendicular component ϵ_{\perp} local field effects decrease with decreasing hexagonality and vanish for 6h, while the local field effect for the ϵ_{zz} component is independent of the hexagonality.

Since local field effects stem from the inhomogeneity of the crystal, it can be illustrating to link this dependence of the local field effect to the electronic densities of the different polytypes and thus explain the different behaviour in terms of the different electronic densities. Inhomogeneity of a density can be considered as the variation from a mean value. In order to quantify inhomogeneity in this sense I consider the Fourier transform of the density, which decomposes it into its constituent frequencies. The idea here is that for a homogeneous density only one Fourier component will be present, while inhomogeneous densities have a more complex decomposition.

A discrete Fourier transform is performed on the real space DFT densities for the different polytypes and the $(b_1, 0, 0)$ and $(0, b_2, 0) = (0, 0, b_3)$ directions which correspond to the z - and \perp -direction respectively. Inspection of the three dimensional Fourier transformed density shows, that indeed these directions yield the only significant contribution. Fig. 6.5 shows the comparison of the result for the three polytypes. First we note the strong dependence on hexagonality of the density in \perp -direction, where the values at the first \mathbf{G} decrease with decreasing hexagonality. Indeed, the 6h polytype exhibits no significant deviation from the maximum at $G = 0$ (not shown in the figure) and can thus be interpreted as being almost completely homogeneous. This behaviour is consistent with the absence of local field effects for this component of 6h. We find the same consistency

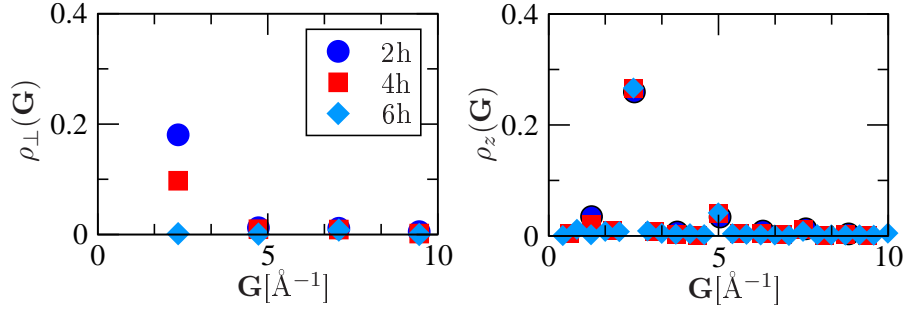


Figure 6.5: Fourier decomposition of the electronic densities of the three polytypes 2h, 4h and 6h along the directions \mathbf{b}_1 and $\mathbf{b}_2 = \mathbf{b}_3$ that correspond to the z - and \perp -direction respectively. The values are normalized with to the maximum of each transform, that occurs at $G = 0$ and is not shown here. The different number of points in b_1 -direction for the different polytypes is due to the different size of the unit cell in that direction.

for the z -direction where all densities show the same dispersion and no polytype related dependence is discernable in the spectra. Furthermore we note that the value of the peak at $G = 2.5 \text{ \AA}^{-1}$ is the same as for the peak for the 2h in \perp -direction at the same G values indicating the same importance of local field effects for the ϵ_{\perp} of 2h and the ϵ_{zz} for all polytypes. Also this corresponds to the observations we made for Fig. 6.4.

The analysis of the electronic density in terms of its Fourier components that give the frequency decomposition and thus a quantitative meaning to the concept of inhomogeneity is thus consistent with the influence of local field effects on the linear dielectric tensor. As far as the second harmonic susceptibility is concerned, however, it is not enough to consider only the linear ϵ that enter in Eq. (6.1), but also the contribution of the second order TDDFT Dyson like equation, where local field are also accounted for in the form of ϵ_{TE}^{-1} and their \mathbf{G} dependence. Figs. 6.6 and 6.7 show the components of the macroscopic second order susceptibility for the same polytypes as in Fig. 6.4. In Fig. 6.6 are shown the imaginary and real parts of the $\chi^{(2)}$ components. They are both equally affected by the local fields and thus the effect on the absolute values shown in Fig. 6.7 stem from both parts. While the influence of the local field on the zxz -component can be seen as roughly the same as for ϵ_{\perp} the overall trend is not as clear as in the linear case. This is partly due to the fact that zxz accounts for effects in two different crystallographic directions, but also due to the more complex mixing of effects in the Dyson equation. We also note that the zxz components increase due to the local fields as opposed to the decrease observed in the other components.

6.3 Exchange and correlation

To include exchange and correlation effects we have to make an approximation for f_{xc} in the TDDFT Dyson equation. As in the case of local field effects the exchange and correlation enter in several steps in the calculation of the macroscopic second order

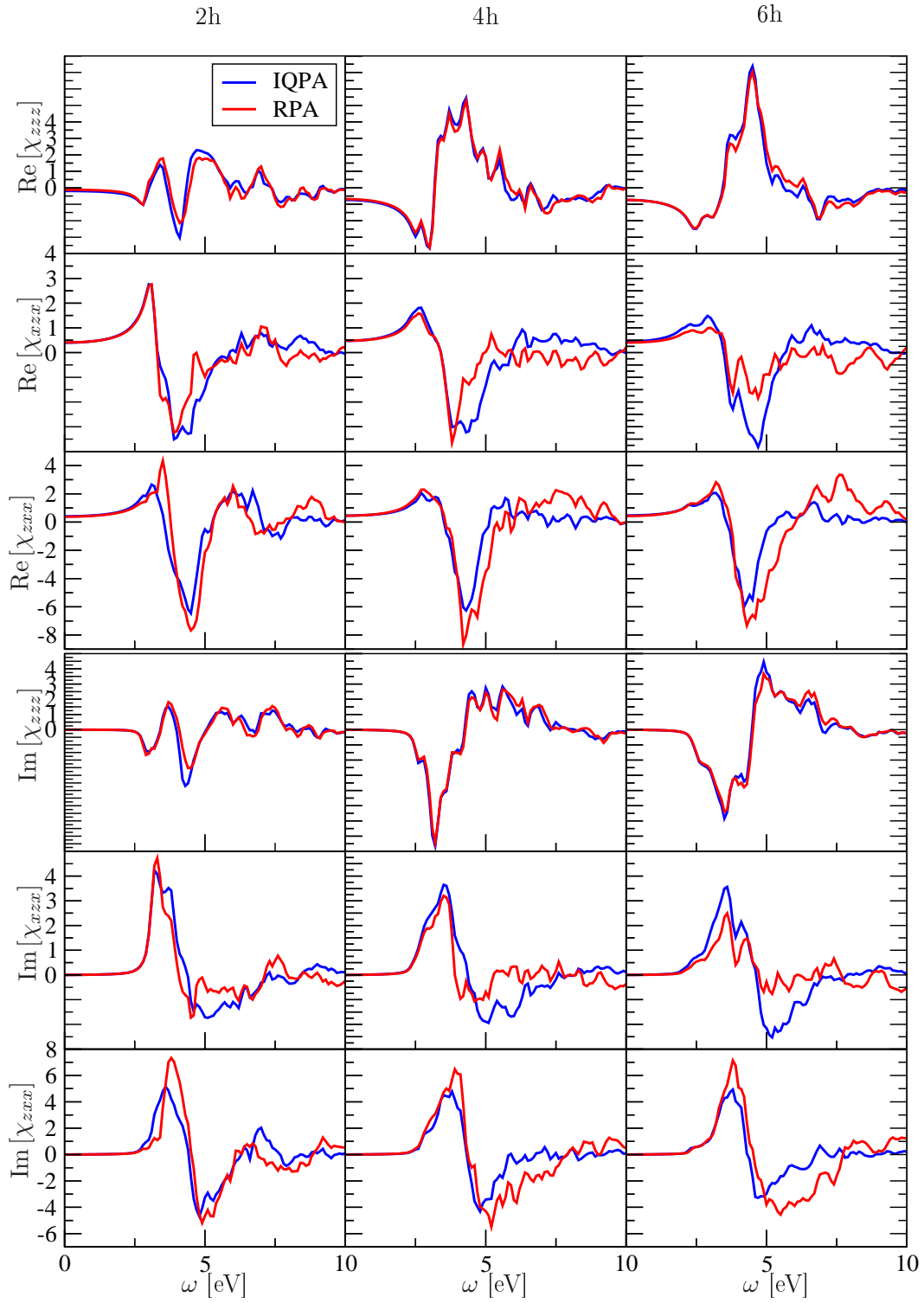


Figure 6.6: Comparison between a calculation including local field effects (RPA) and independent quasi-particle calculation (IQPA) where no local field effects are accounted. The effect is similar for the real and imaginary part for the components of the hexagonal SiC polytypes.

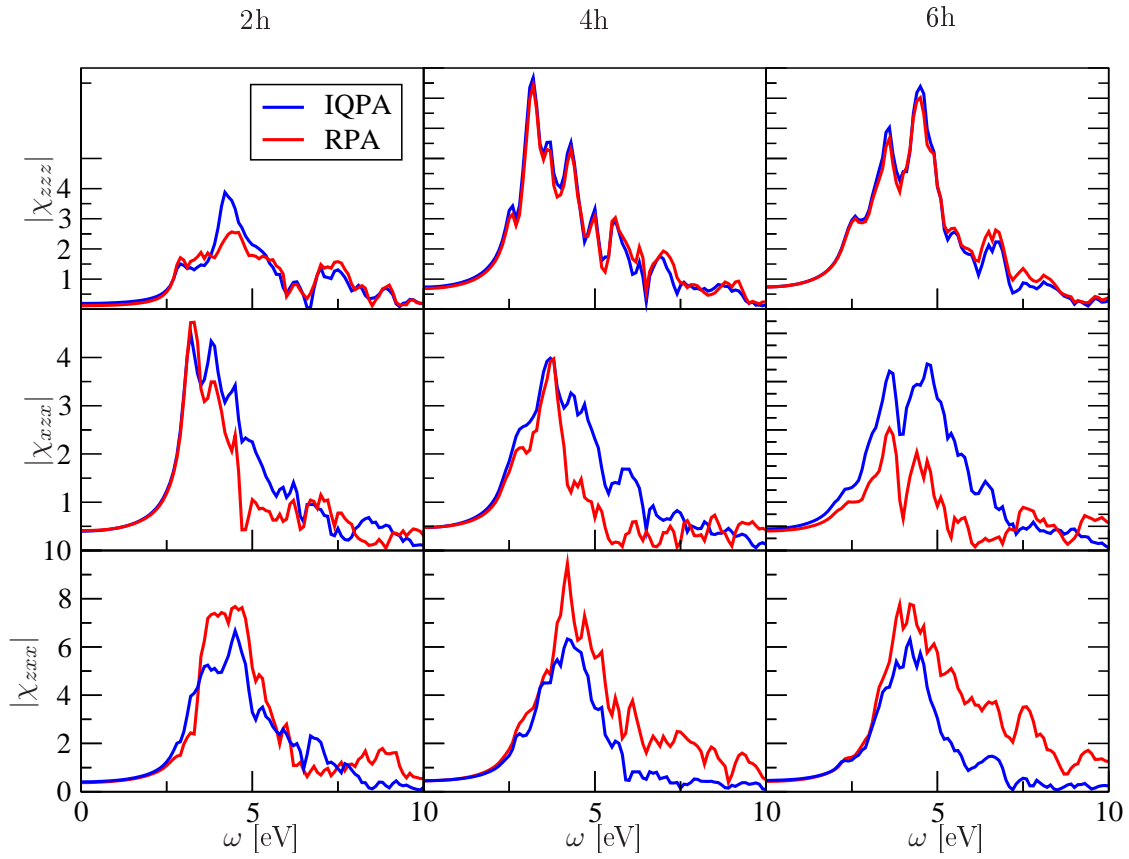


Figure 6.7: (As Fig.6.6. Shown here the absolute values of the $\chi^{(2)}$ components.)

susceptibility $\chi^{(2)}$. First, the DFT groundstate from which the independent particle responses $\chi_{\rho\rho}^{(0)}$ and $\chi_{\rho\rho\rho}^{(0)}$ are constructed, has to be obtained with some approximation for the exchange and correlation potential V_{xc} , here I always use the LDA. Next, in the second order Dyson equation (2.47) f_{xc} appears in several places, as well as in the calculation of the ϵ_M factors for the final expression for the macroscopic $\chi^{(2)}$.

6.3.1 ALDA

The time dependent generalization of the local density approximation (ALDA), c.f. Sec. 2.4.3, is known to be not sufficient to accurately describe optical absorption due to the lack of long range interaction in the $\mathbf{q} \rightarrow 0$ limit [93]. In Fig. 6.8 are shown the components of the second harmonic generation susceptibility obtained within the ALDA and compared to the results from the previous section (Fig. 6.7). While in both calculations local fields are accounted for, it is apparent that the additional contribution of exchange and correlation as described by ALDA leaves the spectra virtually unaffected.

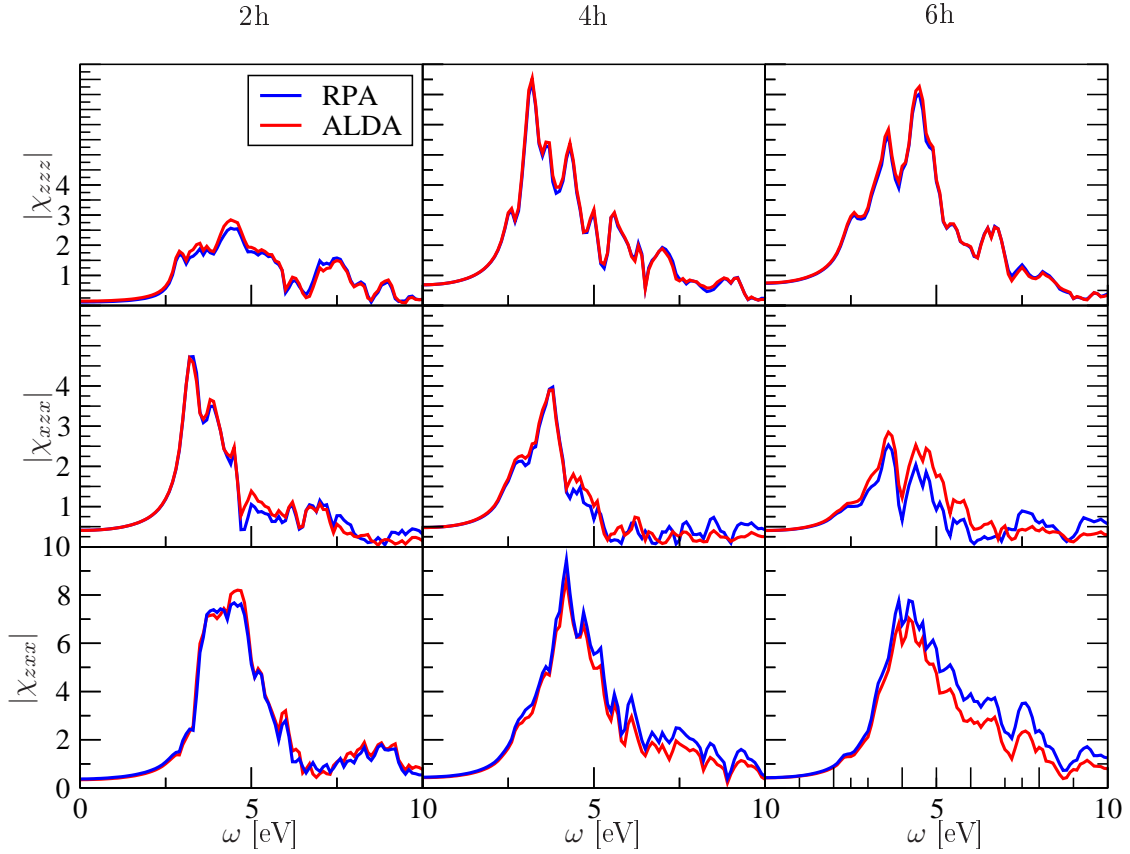


Figure 6.8: Effect of the adiabatic local density approximation (ALDA) on the second harmonic spectra of hexagonal SiC polytypes. The ALDA spectra are compared the RPA spectra (c.f. Fig. 6.7) and practically no change is discernable.

This weak influence of the local exchange and correlation effects on the second harmonic spectra can be attributed to the same lack of long range interaction that was already responsible for the failure of this approximation for optical absorption. On the one hand it means that the ϵ_M that appear in the expression for the macroscopic susceptibility are not accurately described and hence the nonlinear result suffers the same deficiencies present in linear ALDA results, and on the other hand the effect of the kernel in the second order Dyson equation seems to be not important. Here I show calculations where the ALDA kernel is combined with the scissors operator, i.e. quasiparticle corrections, which is in principle not consistent with the theory of the local density approximation. It is, however, well known, that ALDA fails to account for the quasiparticle shift and here I show it just to demonstrate that it has only very little influence on the shape and intensity of the spectrum.

6.3.2 Long Range Kernel

The known lack of long range interaction in the local density approximation can be corrected as described in chapter 2.4.5 by an effective kernel of the form $f_{xc} = -\alpha/q^2$ that mimics the effect of the Bethe-Salpeter equation. Therefore, I refer to this kind of calculation as *excitonic*. Fig. 6.9 shows the influence of the long range kernel with $\alpha = 0.5$ on the spectra of the hexagonal polytypes. The value for alpha is taken from Botti et al. [99] where it is used to fit the linear spectrum on the Bethe-Salpeter result.

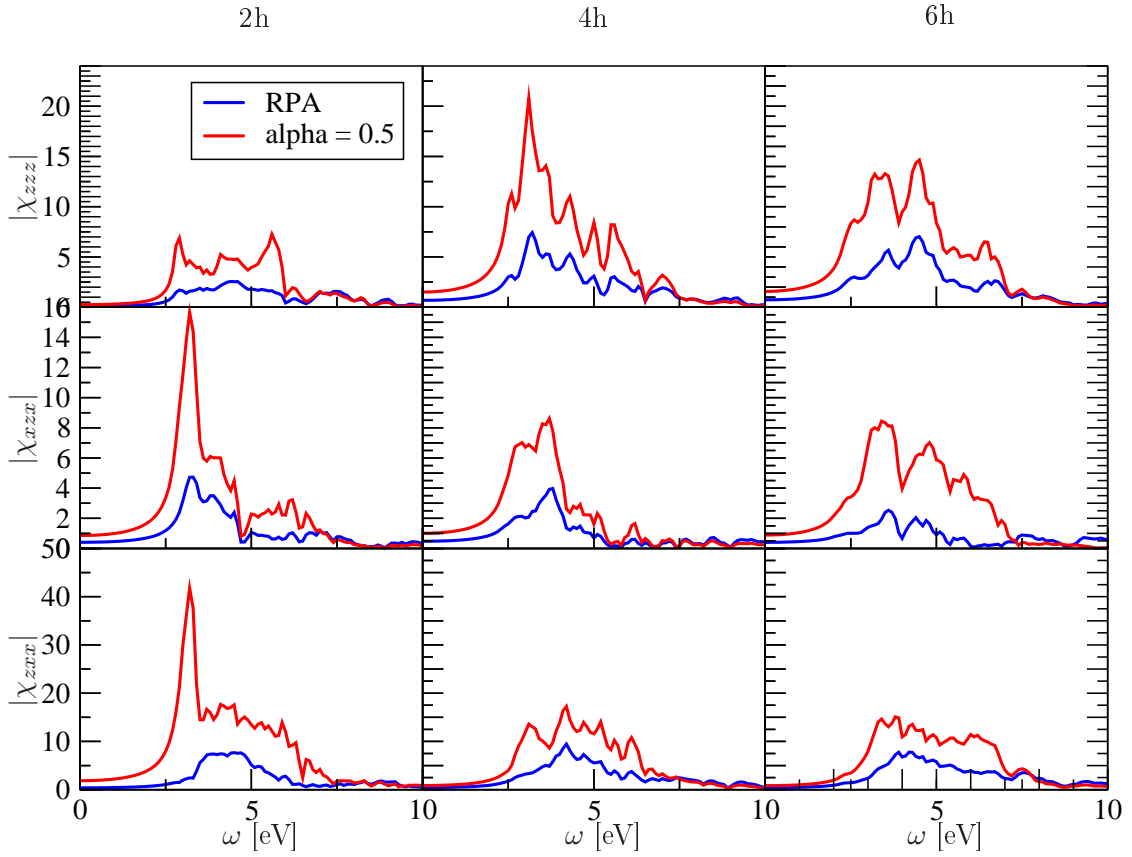


Figure 6.9: Effect of the effective long range kernel on the second harmonic spectra of hexagonal SiC polytypes. The excitonic spectra are compared the RPA spectra (c.f. Fig. 6.7) and show a considerable increase in intensity.

At this point it is interesting to compare the influence of the long range kernel on the linear and non-linear spectra. To this end I show in Fig. 6.10 the linear dielectric function for the hexagonal SiC polytypes calculated within the RPA and with the long range kernel. The effect is a strong increase in the first peak and a slight decrease for the higher energy part of the spectrum, but in general one can say that the effect does not result in a dramatic shift of intensity as seen for the non-linear spectra (Fig. 6.9). On the other hand, the influence of the long range kernel in the nonlinear Dyson like equation, i.e. on $\chi_{\rho\rho\rho}$, is shown in Fig. 6.11 and seen to be almost negligible. Therefore, one has to conclude that for second harmonic generation excitonic effects, as described by f_{xc} , almost exclusively enter via the macroscopic *linear* dielectric functions.

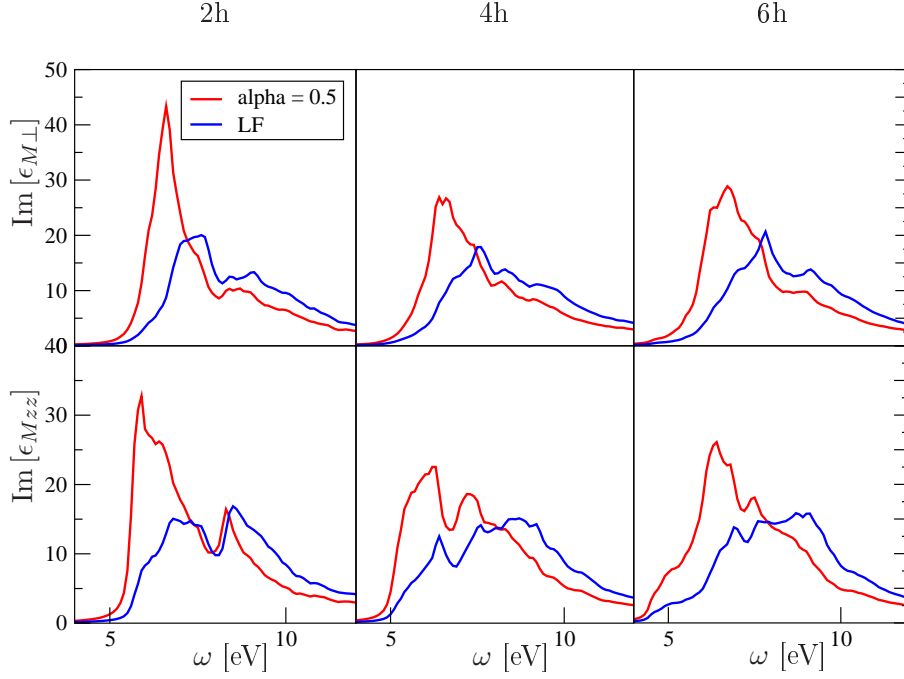


Figure 6.10: Influence of the long range kernel on the macroscopic dielectric function with $\alpha = 0.5$ for the direction along the stacking axis (ϵ_{zz}) and in plane (ϵ_{\perp}).

The behaviour of overall increase of $\chi^{(2)}$ can be understood by considering the limiting case of $\mathbf{G} = \mathbf{G}_1 = \mathbf{G}_2 = 0$ throughout the calculation but keeping f_{xc} . In this case it is possible to solve the TDDFT Dyson equation (2.47) analytically and thus obtain an expression for the effect of the kernel on the susceptibility. We find (here explicitly for the zzz -component)

$$\frac{\chi_{zzz}^{(2)}(\omega)}{\chi^{(0)}(2\mathbf{e}_z, \mathbf{e}_z, \mathbf{e}_z, 2\omega, \omega)} = A(\mathbf{e}_z, 2\omega)A(\mathbf{e}_z, \omega)A(\mathbf{e}_z, \omega) \quad (6.3)$$

where

$$A(\mathbf{q}, \omega) = 1 - \frac{\alpha}{4\pi} [\epsilon_M(\mathbf{q}, \omega) - 1]. \quad (6.4)$$

That means that when ϵ_M is smooth, the change of χ_{zzz} with the long range kernel is directly proportional to α . On the other hand when ϵ_M is changing significantly the change directly affects the long range contribution. This explains why in all spectra in Fig. 6.9 the low energy peaks are most prominently increased, because it is this feature in the ϵ_M that changes most. For the high energy range, when the ϵ_M are close to one, we do not see considerable change. This is consistent with the behaviour of Eq. (6.4) which is close to one when ϵ_M is close to one.

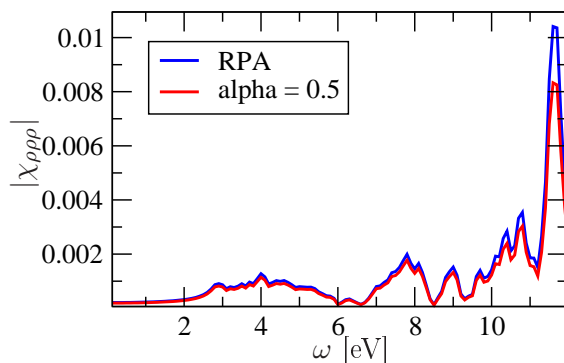


Figure 6.11: Influence of the long range kernel on the microscopic second harmonic susceptibility $\chi_{\rho\rho\rho}$ for 2h-SiC.

Fig. 6.11 also shows the importance of including the macroscopic dielectric functions ϵ_M in the final result, since the microscopic $\chi_{\rho\rho\rho}$ shown in the figure is not only order of magnitude off the independent particle and RPA results (c.f. Figs. 6.2 and 6.7) but the shape is very different also qualitatively. Most significantly so for the 2h case where the large peak of ϵ_M directly influences the $\chi^{(2)}$ components adding considerable qualitative features to the spectra.

6.4 GaAs spectrum as a Benchmark

While in the above sections I have used SiC polytypes to discuss some properties of this framework to calculate the second harmonic generation susceptibility, I will here present the case of GaAs where a detailed experimental spectrum is available. Bergfeld and Daum [139] measure the modulus of the second harmonic generation light in reflectance from a GaAs surface, which gives rise to an additional surface contribution that has been identified by the authors.

Fig. 6.12 shows step by step how the different levels of approximation in our framework perform in comparison to this experimental spectrum. The independent particle approximation has the lowest level of sophistication and indeed it gives a spectrum that, apart from an overall intensity, does not share many characteristics with the experiment. The application of a scissors shift of 0.8 eV, however, greatly improves the spectrum in comparison with the experiment, giving good positions of the peaks and also to some extent their relative intensity. The overall intensity is however too low compared with the experiment. The inclusion of local fields within the randomphase approximation has the effect of only further decreasing the intensity, as observed for some SiC components. Finally, when excitonic effects are included via the long range kernel the two spectra agree in terms of peak positions and intensity of the main peak, however the relative intensity in the calculated spectrum is not very good. Most significantly the low frequency part is far too high. This is partly due to the fact that the long range kernel used here is static, i.e. it is assumed that the value for α is the same for all frequencies. Especially

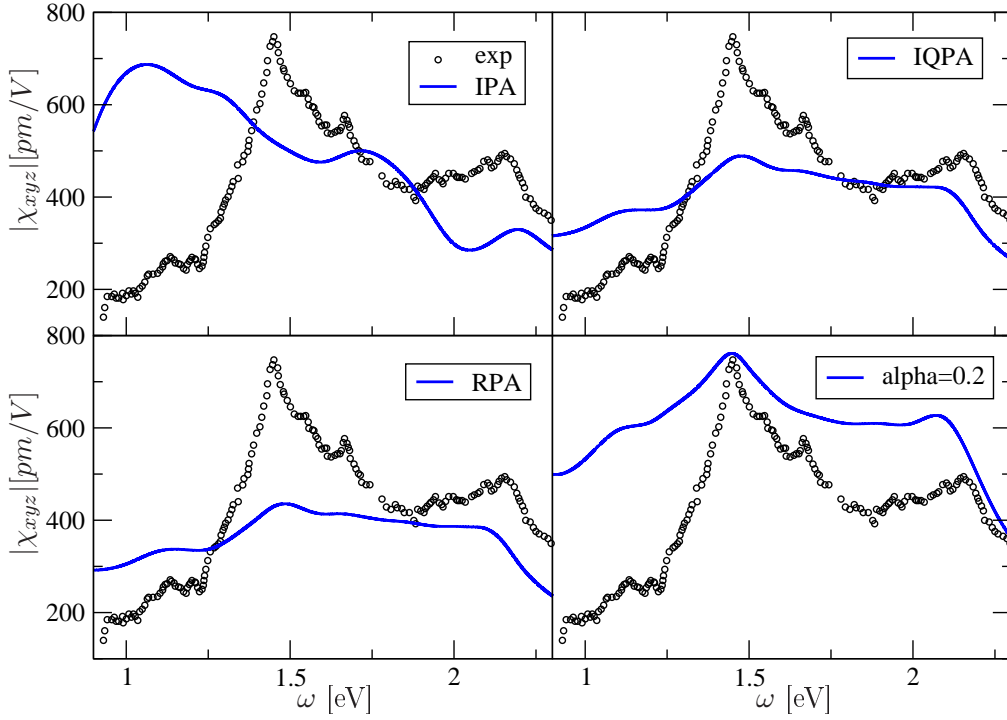


Figure 6.12: Calculated second harmonic spectrum of GaAs compared with the experimental one. Different levels of sophistication of the theory are shown, that gradually improve the comparison between the two (see text).

for the static limit ($\omega = 0$) this is not the case and it has been shown by Botti et al. [140] that a frequency dependence of the kernel can remedy this deficiency. To obtain a good static dielectric constant they use $\alpha = 0.05$, which in the case of our static second harmonic coefficient yields $|\chi_{xyz}(0)| = 216.54$ pm/V, which compares rather well with the experimental values that range between 166 [141] and 180 pm/V [142].

As shown in Fig. 6.11 the influence of the long range kernel is not very important for the microscopic $\chi_{\rho\rho\rho}$ and therefore most excitonic contributions to the spectrum stem from the macroscopic dielectric functions ϵ_M . On the other hand, the inclusion of long range interactions has proven to be crucial to obtain a good comparison with experiment. Consequently, the quality of description of the linear quantities determines to a great extent the quality of our calculated second harmonic spectrum. Fig. 6.13 compares the imaginary part of the ϵ_M used in the excitonic calculation shown in Fig. 6.12 to the experimental one measured by Studna and Aspnes [143]. While the overall agreement is very good, the two curves show considerable differences in the low energy range that is important for the second harmonic spectrum, i.e. from $\omega = 1$ to 2.5 eV. If instead of the calculated ϵ_M we use this experimental one in the calculation of χ_{xyz} , as also shown in Fig. 6.13, we get a much better agreement with the experimental spectrum.

Given that the experimental ϵ_M gives a much better χ_{xyz} than the calculated one and

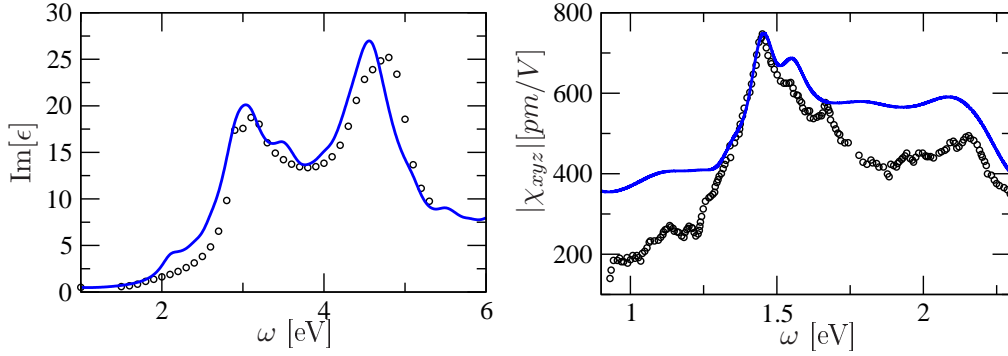


Figure 6.13: left: Calculated ϵ_M for GaAs compared with the experimental one. right: Comparison between the experimental χ_{xyz} and a calculation where the experimental ϵ_M has been used.

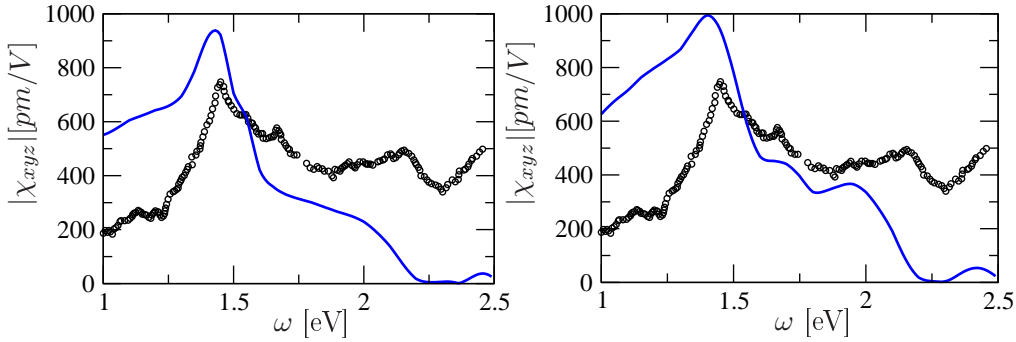


Figure 6.14: Calculation according to Eq. (6.5) with ϵ_M calculated (right) and the experimental ϵ_M (left).

the fact that the IQPA result is very close to the RPA one, c.f. Fig. 6.12, it is tempting to assume that one could get a similarly good result by neglecting the computationally costly local field calculation by making the approximation

$$\chi^{(2)} = \epsilon_M [\epsilon_{TE}^{-1}]_{\mathbf{00}}^T [\chi_{\rho\rho\rho}^{(0)}]_{\mathbf{000}} [\epsilon_{TE}^{-1}]_{\mathbf{00}} [\epsilon_{TE}^{-1}]_{\mathbf{00}} \epsilon_M \epsilon_M \quad (6.5)$$

where the test-particle dielectric functions are just $[\epsilon_{TE}^{-1}]_{\mathbf{00}} = 1 + (4\pi - \alpha)[\chi_{\rho\rho}]_{\mathbf{00}}$. The result of such calculations is shown in Fig. 6.14 where one time the experimental ϵ_M was used and in another calculation the usual ϵ_M from TDDFT. The result does not yield satisfactory agreement in either case. This means that although in the result they do not show a large effect compared with an IPA calculation, the finite \mathbf{G} components of $\chi_{\rho\rho\rho}$ are very important when combined with the ϵ_M , because there are substantial cancellation effects.

In summary we have seen for GaAs that already the IQPA yields a qualitative agreement with the experiment and the accounting for local field effects within RPA does not improve the spectrum. It is only when one wants to account for excitonic effects as well

that the local fields are important to achieve a quantitative agreement with experiments. Furthermore the accuracy of the ϵ_M over the whole frequency range used turn out to be very important for the macroscopic $\chi^{(2)}$.

7 A second order Bethe-Salpeter Equation

While the strength of TDDFT is to provide an efficient way to account for many body effects via the exchange and correlation term f_{xc} it is also its weakness, because its exact form is unknown and hence approximations rely to some extent on educated guessing rather than formal theory. On the other hand many-body perturbation theory does rigorously describe these effects and it is nowadays used almost routinely to calculate optical spectra of increasingly complex systems [144–146] via the Bethe-Salpeter equation, c.f. Sec. 2.4.5. The advantage of the Bethe-Salpeter equation is its ability to properly account for excitonic effects that are of great importance for optical absorption [93]. It is, as a computational framework, however, much heavier than TDDFT, because the two-body correlation function in terms of which it is formulated contains much more information than actually needed to describe optical spectroscopy [147]. In practice one therefore takes contractions of the two particle correlation function and thus discards a lot of information that is contained in this quantity. Some efforts have been made to capture the essential parts of this framework and translate them into TDDFT kernels, as described in Sec. 2.4.5, leading to the NANOQUANTA kernel and its simplification in form of the long range kernel I used in Chap. 6.

The Bethe-Salpeter equation does not only describe optical effects, but it gives, in its exact form, an equation for any kind of linear response [148]. This makes it a powerful tool to study a vast range of physical phenomena, not necessarily by solving it exactly but by providing a description that is at the same time exact and intuitive. Therefore, it could be interesting to find the generalization of the Bethe-Salpeter equation to second order responses. In this chapter I will outline how such a second order Bethe-Salpeter equation can be obtained, solved and related to second order response TDDFT.

7.1 The equation

The Bethe-Salpeter equation as described in section 2.4.5 provides an approach to many-body excitations within the framework of many-body perturbation theory [95]. More precisely it is an equation for the correlation part of the two-particle Green's function

that can be written using the Schwinger's functional derivative identity [95] as ¹

$$iL(1, 2, 3, 4) = \frac{\delta G(1, 2)}{\delta V_{per}(3, 4)} = -G(1, 3, 2, 4) + G(1, 2)G(3, 4) \quad (7.1)$$

where the product of the one-particle Green's functions GG describes the independent propagation of the two particles. The contraction of L yields the connection to the time ordered density response

$$\chi_{\rho\rho}(1, 2) = \frac{\delta\rho(1)}{\delta V_{per}(2)} = -i\frac{\delta G(1, 1^+)}{\delta V_{per}(2, 2^+)} = L(1, 1^+, 2, 2^+) . \quad (7.2)$$

For second harmonic generation and generally for any second order process in response formulation, we are interested in the response of the density to two perturbing fields and thus generalizing Eq. (7.2) we find the corresponding three-particle correlation function

$$\chi_{\rho\rho\rho}(1, 2, 3) = \frac{\delta^2\rho(1)}{\delta V_{per}(2)\delta V_{per}(3)} = -i\frac{\delta G(1, 1^+)}{\delta V_{per}(2, 2^+)\delta V_{per}(3, 3^+)} = L(1, 1^+, 2, 2^+, 3, 3^+) \quad (7.3)$$

which as a full six point quantity is defined as

$$L(1, 2, 3, 4, 5, 6) = -i\frac{\delta^2 G(1, 2)}{\delta V_{per}(5, 6)\delta V_{per}(3, 4)} = \frac{\delta L(1, 2, 3, 4)}{\delta V_{per}(5, 6)} . \quad (7.4)$$

This quantity can be interpreted as the correlation part of the three-particle Green's function, which is obtained from Eq. (7.1) by taking the functional derivative with respect to an additional non-local perturbing potential, c.f. App. D

$$\begin{aligned} iL(1, 2, 3, 4, 5, 6) = & -G(1, 3, 5, 2, 4, 6) - \\ & -G(1, 3, 2, 4)G(5, 6) - G(1, 5, 2, 6)G(3, 4) - G(3, 5, 4, 6)G(1, 2) + \\ & +2G(1, 2)G(3, 4)G(5, 6) \end{aligned} \quad (7.5)$$

There are not only the free propagations of three particles represented by the $G_1G_1G_1$ term but also the fully interacting propagation of pairs of particles with an independent third one represented by G_2G_1 . One can thus see from this equation that L_3 indeed represents the three-particle correlation part of G_3 .

A second order Bethe-Salpeter equation can now be derived from the linear Bethe-Salpeter equation (2.78) by carrying out the functional derivative in Eq. (7.4) as outlined

¹Here and in the following I use the notation $G_1 = G(\bullet, \bullet)$, $G_2 = G(\bullet, \bullet, \bullet, \bullet)$ etc., i.e. whether a quantity is second order, of two particles, of three particles etc. is determined by the number of variables.

in App. D. The final result reads, c.f. Eq. (D.11):

$$\begin{aligned}
L(1, 2, 3, 4, 5, 6) = & \\
& L_0(123456) + \\
& + \int d789\ 10 L_0(123478) \tilde{\Xi}(78910) L(9\ 10\ 56) + \\
& + \int d789\ 10 L_0(127856) \tilde{\Xi}(789\ 10) L(9\ 10\ 34) + \\
& + \int d789\ 10\ 11\ 12\ 13\ 14 L_0(1278\ 11\ 12) \tilde{\Xi}(11\ 12\ 13\ 14) L(13\ 14\ 56) \tilde{\Xi}(789\ 10) L(9\ 10\ 34) + \\
& + \int d789\ 10\ 11\ 12 L_0(1278) \Xi(789\ 10\ 11\ 12) L(11\ 12\ 56) L(9\ 10\ 34) \\
& + \int d789\ 10 L_0(1278) \tilde{\Xi}(789\ 10) L(9\ 10\ 3456)
\end{aligned} \tag{7.6}$$

where the non-interacting part L_{03} is defined as

$$iL_0(123456) = G(1, 5)G(6, 3)(4, 2) + G(1, 3)G(4, 5)(6, 2) \tag{7.7}$$

and the many-body interaction kernels are defined as

$$\tilde{\Xi}(1, 2, 3, 4) = v(1, 3)\delta(1, 2)\delta(3, 4) + i\frac{\delta\Sigma(1, 2)}{\delta G(3, 4)} \tag{7.8}$$

$$\Xi(1, 2, 3, 4, 5, 6) = i\frac{\delta^2\Sigma(1, 2)}{\delta G(5, 6)\delta G(3, 4)}. \tag{7.9}$$

Eq. (7.6) has exactly the same structure as the second order TDDFT Dyson like equation (2.47) only that here we have six-point quantities whereas second order response of TDDFT deals with three point quantities. Since it has the same structure, it can also be solved analytically assuming that the solution of the linear BSE, L_2 , is known, c.f Eq. (D.16). The solution reads in short hand

$$L_3 = L_2 L_{02}^{-1} L_{03} L_{02}^{-1} L_2 L_{02}^{-1} L_2 + L_2 \Xi_3 L_2 L_2 \tag{7.10}$$

or alternatively in analogy to Eq. (2.55)

$$L_3 = [1 + L_2 \Xi_2] L_{03} [1 + \Xi_2 L_2] [1 + \Xi_2 L_2] + L_2 \Xi_3 L_2 L_2. \tag{7.11}$$

In the form 7.10 the solution can in principle be obtained by combining the known two-particle quantities L_2 and L_{02}^{-1} with the three-particle quantities L_{03} and Ξ_3 . These quantities are however not obtained as straightforwardly and it is in these quantities where approximations have to be made or computational resources are needed.

7.2 The non-interacting part L_{03}

The three-particle non-interacting part of the second order Bethe-Salpeter equation is, according to Eq. (7.7), essentially the products of the three single-particle Green's functions combined in two different ways. Using the Lehmann representation of the single-particle Green's function [149]

$$iG(\mathbf{r}_1, \mathbf{r}_2, t_1 - t_2) = \sum_i [\Theta(t_1 - t_2)\Theta(\epsilon_i - \mu) - \Theta(t_2 - t_1)\Theta(\mu - \epsilon_i)] e^{-i\epsilon_i(t_1 - t_2)} \phi_i(\mathbf{r}_1)\phi_i^*(\mathbf{r}_2) \quad (7.12)$$

one can construct these products in terms of the electron addition and removal energies ϵ_i and the corresponding Lehmann amplitudes ϕ_i . Expressing the step functions containing the chemical potential μ in terms of electronic occupation numbers, i.e. $\Theta(\epsilon_i - \mu) = (1 - f_i)$ and $\Theta(\mu - \epsilon_i) = f_i$, as well as contracting the time variables $t_2 \rightarrow t_1$, $t_4 \rightarrow t_3$ and $t_6 \rightarrow t_5$ we can write L_{03} in frequency space as

$$\begin{aligned} L_0(\mathbf{r}_1, \mathbf{r}_2, \mathbf{r}_3, \mathbf{r}_4, \mathbf{r}_5, \mathbf{r}_6, \omega_2 + \omega_3, \omega_2, \omega_3) &= \sum_{ijk} \frac{\phi_i^*(\mathbf{r}_1)\phi_j(\mathbf{r}_2)}{(\epsilon_i - \epsilon_j + \omega_2 + \omega_3 + 2i\eta)} \times \\ &\times \left[(f_i - f_k) \frac{\phi_j^*(\mathbf{r}_5)\phi_k(\mathbf{r}_6)\phi_k^*(\mathbf{r}_3)\phi_i(\mathbf{r}_4)}{(\epsilon_i - \epsilon_k + \omega_2 + i\eta)} + (f_j - f_k) \frac{\phi_j^*(\mathbf{r}_5)\phi_k(\mathbf{r}_6)\phi_k^*(\mathbf{r}_3)\phi_i(\mathbf{r}_4)}{(\epsilon_k - \epsilon_j + \omega_3 + i\eta)} + \right. \\ &\left. (f_i - f_k) \frac{\phi_j^*(\mathbf{r}_3)\phi_k(\mathbf{r}_4)\phi_k^*(\mathbf{r}_5)\phi_i(\mathbf{r}_6)}{(\epsilon_i - \epsilon_k + \omega_3 + i\eta)} + (f_j - f_k) \frac{\phi_j^*(\mathbf{r}_3)\phi_k(\mathbf{r}_4)\phi_k^*(\mathbf{r}_5)\phi_i(\mathbf{r}_6)}{(\epsilon_k - \epsilon_j + \omega_2 + i\eta)} \right]. \end{aligned} \quad (7.13)$$

From this expression the analogy with the response of TDDFT becomes obvious once more, because a contraction of the space variables $\mathbf{r}_2 \rightarrow \mathbf{r}_1$, $\mathbf{r}_4 \rightarrow \mathbf{r}_3$ and $\mathbf{r}_6 \rightarrow \mathbf{r}_5$ and with the assumption that the Lehmann amplitudes are Kohn-Sham eigenstates and the energies the corresponding Kohn-Sham energies, this expression gives the independent particle response of TDDFT, Eq. (2.27). Also, this means that the independent (Kohn-Sham) particle response of TDDFT can in fact be represented as the contraction of L_{03} as

$$\chi_{\rho\rho\rho}^{(0)}(1, 2, 3) = L_0(1, 1, 2, 2, 3, 3) = -iG_0(1, 2)G_0(2, 3)G_0(3, 1) - iG_0(1, 3)G_0(3, 2)G_0(2, 1) \quad (7.14)$$

where G_{01} are Green's function constructed with Kohn-Sham energies and states.

7.3 The second order many-body kernel Ξ_3

The linear many-body interaction kernel is the variation of the self energy with respect to a single-particle Green's function. In practical applications of the BSE this self energy

is taken in the GW approximation, so that the kernel reads

$$\Xi(5, 6, 7, 8) = i \frac{\delta \Sigma(5, 6)}{\delta G(7, 8)} = - \frac{\delta G(5, 6) W(5, 6)}{\delta G(7, 8)} = -\delta(5, 7) \delta(6, 8) W(5, 6) - G(5, 6) \frac{\delta W(5, 6)}{\delta G(7, 8)}. \quad (7.15)$$

Additionally one assumes that the functional derivative of the screening with respect to the Green's function, $\delta W/\delta G$, which describes the change of the screening due to the excitation, is small and can thus be neglected, as shown by Hanke and Sham [150]. This assumption is however an ad hoc approximation and mainly justified pragmatically. In this approximation the second order kernel that is defined as

$$\Xi(1, 2, 3, 4, 5, 6) = i \frac{\delta^2 \Sigma(1, 2)}{\delta G(5, 6) \delta G(3, 4)} = \frac{\delta \Xi(1234)}{\delta G(5, 6)} \quad (7.16)$$

obviously vanishes as well. It does, however, not vanish *a priori* if one considers other approximations for the first order kernel, c.f. [148] for example.

Furthermore, even in *GW*, the assumption $\delta W/\delta G = 0$ could mean that one is missing important contribution and it might not be a good approximation when one is interested in second order processes. Especially, since the second order BSE is describing second order processes, the changing of the screening due to the excitation might be important.

7.4 Connection to Many Body Perturbation Theory

Many body perturbation theory is in the solid state community most commonly seen through the lens of Hedin's equations, c.f. App. E. It can therefore be illustrating to make the connection between the second order Bethe-Salpeter equation and these equations. Here, we are particularly interested in the second order polarizability, because it is closely related to $\chi^{(2)}$. More precisely, in the previous chapters, I have always considered $\chi_{\rho\rho\rho}$, which is a reducible quantity, since it contains the Coulomb interaction. In the context of many-body perturbation theory one seeks to separate this interaction from the other many-body interactions and thus considers the irreducible quantity P that is the variation of the density with respect to the total potential. In App. E.1 I show how these quantities are related in the second order case, and find ²:

$$\chi_2 = [1 + \chi_1 v] P_2 [1 + v \chi_1] [1 + v \chi_1] \quad (7.17)$$

$$= \chi_1 P_1^{-1} P_2 P_1^{-1} \chi_1 P_1^{-1} \chi_1 \quad (7.18)$$

$$P_2 = [1 - P_1 v] \chi_2 [1 - v P_1] [1 - v P_1] \quad (7.19)$$

$$= P_1 \chi_1^{-1} \chi_2 \chi_1^{-1} P_1 \chi_1^{-1} P_1 \quad (7.20)$$

²In this part I adopt a notation where $\chi_1 = \chi_{\rho\rho}$ and $\chi_2 = \chi_{\rho\rho\rho}$ to ensure readability of the equations and to make a clear distinction between first order and second order quantities.

These are the relations between second order reducible and irreducible quantities. While the linear relation has the form of a linear Dyson equation (E.12), we note that this relation has indeed the form of the second order Dyson like equation, similar to Eq. (2.54) and Eq. (7.11). The only difference is that there is no term corresponding to the second order interaction kernel, since the kernel between reducible and irreducible quantities is just the Coulomb interaction.

The second order irreducible polarizability P_2 can be expressed in the context of Hedin's equations as (c.f. App. E.1)

$$\begin{aligned}
P(1,2,3) = & +i \int d4567G(2,6)\Gamma(6,7,3)G(7,4)G(5,2)\Gamma(4,5,1) - \\
& +i \int d45G(2,4)G(5,6)\Gamma(6,7,3)G(7,2)\Gamma(4,5,1) - \\
& -i \int d45G(2,4)G(5,2)\frac{\delta\Gamma(4,5,1)}{\delta V_{\text{tot}}(3)}. \tag{7.21}
\end{aligned}$$

In the GW approximation one neglects vertex corrections and thus takes $\Gamma(1,2,3) = \delta(1,3)\delta(1,2)$. Applying this approximation to P yields the RPA. We thus have the second order RPA irreducible polarizability:

$$iP_0(1,2,3) = G(1,2)G(2,3)G(3,1) + G(1,3)G(3,2)G(2,1) \tag{7.22}$$

This is the same expression we have found for $\chi_{\rho\rho\rho}^{(0)}$ as a contraction of L_{03} , Eq. (7.14). Indeed, the RPA irreducible polarizability corresponds to the independent particle polarizability, since in both cases no interaction is present.

In the expression (7.21) for P_2 features the variation of the vertex function with respect to the total potential. This can be used as a motivation to define a second order vertex, which in turn is closely related to the second order Bethe-Salpeter equation, just like the linear vertex function is related to the linear BSE, as shown in [93].

7.5 A g_{xc} from MBPT

The similarity between the Bethe-Salpeter Equation and the fact that the contraction of L_2 yields the linear density response, has been used to derive an exact expression for the two-particle correlation part of the TDDFT kernel f_{xc} [98] as outlined in Chap. 2.4.5. Here, I will sketch how the second order Bethe-Salpeter equation can be used to derive a similar expression for g_{xc} .

Since the Coulomb interaction v is known and does not contribute directly to g_{xc} it is convenient to compare only the irreducible quantities in TDDFT and BSE. Combining Eq. (7.20) and the second order TDDFT Dyson like equation (2.52) yields the relation

between the irreducible polarizability and the independent particle response³:

$$P_2 = P_1 P_{01}^{-1} P_{02} P_{01}^{-1} P_1 P_{01}^{-1} P_1 + P_1 g_{xc} P_1 P_1 \quad (7.23)$$

where I have used the fact that $\chi_0 = P_0$. This equation can be solved for P_{02} which yields

$$P_{02} = P_{01} P_1^{-1} P_2 P_1^{-1} P_{01} P_1^{-1} P_{01} + P_{01} g_{xc} P_{01} P_{01}. \quad (7.24)$$

Exactly the same steps can be taken for the second order BSE, i.e. passing to irreducible quantities \tilde{L} , expressing them in terms of non-interacting quantities L_0 and solving for L_{03} :

$$L_{03} = L_{02} \tilde{L}_2^{-1} \tilde{L}_3 \tilde{L}_2^{-1} L_{02} \tilde{L}_2^{-1} L_{02} + L_{02} \Xi_3 L_{02} L_{02}. \quad (7.25)$$

Here I only give the shorthand notation, but it is understood that \tilde{L}_2 and \tilde{L}_3 are four and six-point quantities, while P_1 and P_2 are two and three point quantities.

The two equations can be combined by exploiting the similarity of the two independent particle responses L_{03} and P_{02} . As shown in Sec. 7.2 the three point contraction of L_{03} equals the independent density response and thus also P_{02} . It is however not practical to contract Eq. (7.25), because it prevents the possibility to eliminate \tilde{L}_3 at a later point. Instead we generalize Eq. (7.24) to six points, thus making all P and P_0 to trivially contractible four (4P) and six-point (6P) quantities, c.f. App. F.

Now using $L_{03} = {}^6P_{02}$ and $L_{02} = {}^4P_{01}$ the two equations can be combined and solved for the kernels

$$\Xi_3 - {}^6g_{xc} = \tilde{L}_2^{-1} \tilde{L}_3 \tilde{L}_2^{-1} \tilde{L}_2^{-1} - {}^4P_1^{-1} {}^6P_2 {}^4P_1^{-1} {}^4P_1^{-1}. \quad (7.26)$$

At this point we already note that even in the cases where $\Xi_3 = 0$, c.f. Sec. 7.3, the second order TDDFT kernel g_{xc} is still finite. Indeed it only vanishes if additionally ${}^6P_2 = \tilde{L}_3$ and ${}^4P_1 = \tilde{L}_2$, which is generally false and can only be achieved in oversimplified models. In particular this means that in the GW approximation with the additional assumption of $\delta W/\delta G = 0$, where $\Xi_3 = 0$, the second order TDDFT kernel g_{xc} generally does not vanish. That means that g_{xc} has to account for interactions that are not purely of second order in the sense of the Bethe-Salpeter interactions kernels, but are due to some non-trivial coupling of linear quantities.

We can now use the fact that P_2 is the three point contraction of \tilde{L}_3 and thus let ${}^6P_2|_{6 \rightarrow 3} = P_2 = \tilde{L}_3|_{6 \rightarrow 3}$. By solving equation (7.26) for L_3 and making this substitution we obtain

$$P_2 = (\tilde{L}_2 {}^4P_1^{-1} {}^6P_2 {}^4P_1^{-1} \tilde{L}_2 {}^4P_1^{-1} \tilde{L}_2)|_{6 \rightarrow 3} + (\tilde{L}_2 (\Xi_3 - {}^6g_{xc}) \tilde{L}_2 \tilde{L}_2)|_{6 \rightarrow 3}. \quad (7.27)$$

³Reminder on notation used: P_2 is the second order polarizability which cooresponds to the three particle correlation function L_3 .

where $6 \rightarrow 3$ indicates the pairwise contraction of the six free indices to three. This constitutes a Sham-Schlüter equation [96] for the kernels that now can be solved for g_{xc} . To keep track of the contracted quantities, it is necessary to explicitly account for the indices while proceeding, c.f. App. F. Therefore the resulting expression (F.9) lacks readability, so that here I give again only a shorthand, indicating left or right sided contractions of four point quantities as ${}_3|\bullet$ and $\bullet|_3$ respectively. Thus, Eq. (7.27) solved for g_{xc} reads

$$g_{xc} = P_1^{-1} \left[{}_3|\tilde{L}_2 {}^4P_1^{-1}|_3 P_2 {}_3|{}^4P_1^{-1} \tilde{L}_2|_3 {}_3|{}^4P_1^{-1} \tilde{L}_2|_3 - P_2 \right] P_1^{-1} P_1^{-1} + \\ + P_1^{-1} {}_3|\tilde{L}_2 \Xi_3 \tilde{L}_2|_3 \tilde{L}_2|_3 P_1^{-1} P_1^{-1}. \quad (7.28)$$

In comparison the corresponding expression of *linear* f_{xc} derived in this framework, c.f. Sec. 2.4.5, reads in this notation

$$f_{xc} = P_1^{-1} {}_3|{}^4P_1^{-1} \Xi_2 L_1|_3 P^{-1}. \quad (7.29)$$

To illustrate the notation in Eq. (7.28), we have, for example, quantities like

$${}_3|{}^4P_1^{-1} \tilde{L}_2|_3 = {}^4P^{-1}(1, 1, 3, 4) \tilde{L}(4, 3, 2, 2) \quad (7.30)$$

from which we can see again that only if ${}^4P_1 = \tilde{L}_2$ one can follow $g_{xc} = \Xi_3|_{6 \rightarrow 3}$. Instead, Eq. (7.28) gives the exact expression for a TDDFT kernel that reproduces a P_2 such that $P(1, 2, 3) = \tilde{L}(1, 1, 2, 3, 3,)$, i.e. a second order irreducible polarizability that accounts for all three-particle many-body interactions. The advantage is that one does not have to solve the six point second order Bethe-Salpeter equation, as outlined in App. D.1, but can keep the three point formalism described in the preceding part of this thesis. The downside is that apart from having to perform a linear BSE calculation first to obtain \tilde{L}_2 the actual knowledge of the kernel g_{xc} as in Eq. (7.28) implies knowledge of P_2 and is therefore not possible. For calculation purposes one has to make approximation on this equation, particularly on P_2 . The most straightforward would be to let $P_2 \rightarrow P_{02}$.

8 Conclusions

This work has been concerned with the ab initio calculation of the material dependent second harmonic generation susceptibility $\chi^{(2)}$. The central result is its expression containing exchange and correlation effects in terms of the second order density response $\chi_{\rho\rho\rho}$ and the macroscopic dielectric function from linear response ϵ_M , c.f. Eq. (3.57):

$$\chi^{(2),LLL} = -\frac{2\pi}{2q^3} \epsilon_M^{LL} \chi_{\rho\rho\rho} \epsilon_M^{LL} \epsilon_M^{LL} . \quad (8.1)$$

In this expression, local field effects and exchange and correlation effects are contained in the $\chi_{\rho\rho\rho}$ and the ϵ_M alike. It turns out that for the influence of the local fields there is rather subtle cancellation effect between the local fields accounted for in $\chi_{\rho\rho\rho}$ and those in ϵ_M . For SiC polytypes, the influence of local fields is traced back to the inhomogeneity of the electron density, where the effect varies with component and polytype.

The agreement with experimental data has been shown to depend on the inclusion of exchange and correlation effects, here in form of an effective kernel that mimics the excitonic interaction. This kernel leads to good agreement of peak intensity between the spectra, but is not completely accurate over the whole frequency range. We traced this problem back to small differences between the calculated ϵ_M and the experimental one, showing that when we use the experimental ϵ_M in our calculation of $\chi^{(2)}$, we obtain excellent agreement with the experimental result. This means on the one hand that the accuracy of the linear ϵ_M is of great importance for a nonlinear calculation, but on the other hand that many important contributions are stemming from linear processes.

The numerical implementation of this formalism allows for realistic calculations of second harmonic spectra. Pending optimization, it can be used for surfaces and interfaces alike, where second harmonic generation is of great interest. Also, it can be used to make more quantitative predictions of the second harmonic intensity of materials and thus be applied to systematically improve second harmonic crystals.

TDDFT can also be used to calculate the quadrupole second harmonic generation, which is the leading order for centro-symmetric materials. However, the fact that one only deals with a density response means that one can not calculate all components separately but only superpositions. This could in principle be overcome by considering current matrix elements, but the density formalism used in this work can yield the full anisotropic, i.e. directional dependent, contribution of this effect and thus might still be valuable.

Finally, from a more formal point of view, second harmonic generation is a process involving three electronic states and thus can be described by the three-particle Green's function, or more precisely, its three-particle correlation part. This is done by a second

order generalization of the Bethe-Salpeter equation. While a solution of this equation is readily obtained formally, a numerical implementation does not seem feasible at the moment. Still, by comparing this equation with the second order TDDFT Dyson like equation, one can gain some insight into the properties of the second order exchange and correlation kernel g_{xc} .

On a more general note, I found that second order variations as described by the TDDFT Dyson equation or Bethe-Salpeter can be solved analytically when the corresponding first order is known. From this observation one could formulate the following conjecture:

Conjecture: Let S be a first order variational quantity that is related to its non-interacting expression S_0 via an interaction kernel K as

$$S = S_0 + S_0 K S. \quad (8.2)$$

The second order variation R of this quantity is then related to its non-interaction expression R_0 via

$$R = [1 + SK] R_0 [1 + KS] [1 + KS] + S \kappa S S \quad (8.3)$$

$$= S S_0^{-1} R_0 S_0^{-1} S S_0^{-1} S + S \kappa S S \quad (8.4)$$

where κ is the variation of the interaction kernel K .

A Independent particle response function

The spectral representation of the linear and second order response functions, Eq. (2.23) and (2.24), are given in terms of many body wavefunctions and many body excitations energies. These quantities are not feasibly computed and thus, as a first approximation and starting point for further computational schemes, one constructs the response functions with wavefunctions and energies of non-interacting particles. Here, I will outline how to pass from the many body response functions to the single, independent, particle ones by example of the second order response function. The same reasoning can of course be applied to the first order case, which however is much simpler and has been shown in other places, e.g. [151].

The operators in the matrix elements of Eq. (2.24) read in second quantization formulation (c.f. [152])

$$\hat{A} = \int d\mathbf{r} \psi^\dagger(\mathbf{r}) \hat{a}(\mathbf{r}) \psi(\mathbf{r}) \quad (\text{A.1})$$

where $\hat{a}(\mathbf{r})$ is the single particle operator and $\psi(\mathbf{r})$ and $\psi^\dagger(\mathbf{r})$ are the field operators that can be represented by single particle orbitals as

$$\psi^\dagger(\mathbf{r}) = \sum_i \phi_i^*(\mathbf{r}) \hat{a}_i^\dagger \quad \text{and} \quad \psi(\mathbf{r}) = \sum_i \phi_i(\mathbf{r}) \hat{a}_i. \quad (\text{A.2})$$

The operators \hat{a}_i^\dagger and \hat{a}_i create and annihilate a particle in the state i . With this representation the many body operator reads

$$\hat{A} = \sum_{ij} \langle \phi_i | \hat{a}(\mathbf{r}) | \phi_j \rangle \hat{a}_i^\dagger \hat{a}_j. \quad (\text{A.3})$$

We consider the first term of Eq. (2.24) with this formulation

$$\begin{aligned} \sum_{nm} \frac{\langle \Psi_0 | \hat{A} | \Psi_n \rangle \langle \Psi_n | \hat{B} | \Psi_m \rangle \langle \Psi_m | \hat{C} | \Psi_0 \rangle}{(E_0 - E_m + \omega_3 + i\eta)(E_0 - E_n + \omega_2 + \omega_3 + 2i\eta)} = \\ \sum_{nmijklrs} \frac{\langle \phi_i | \hat{a}(\mathbf{r}_1) | \phi_j \rangle \langle \phi_k | \hat{b}(\mathbf{r}_2) | \phi_l \rangle \langle \phi_r | \hat{c}(\mathbf{r}_3) | \phi_s \rangle \langle \Psi_0 | \hat{a}_i^\dagger \hat{a}_j | \Psi_n \rangle \langle \Psi_n | \hat{a}_k^\dagger \hat{a}_l | \Psi_m \rangle \langle \Psi_m | \hat{a}_r^\dagger \hat{a}_s | \Psi_0 \rangle}{(E_0 - E_m + \omega_3 + i\eta)(E_0 - E_n + \omega_2 + \omega_3 + 2i\eta)} \end{aligned} \quad (\text{A.4})$$

the creation and annihilation operators now impose conditions on the excited many body states $|\Psi_n\rangle$ and $|\Psi_m\rangle$ so that the matrix elements do not vanish. For a non-interacting

groundstate we can convince ourselves that the first matrix element $\langle \Psi_0 | \hat{a}_i^\dagger \hat{a}_j | \Psi_n \rangle$ is only non-zero if $|\Psi_n\rangle = \hat{a}_j^\dagger \hat{a}_i | \Psi_0 \rangle$ due to the orthogonality of the states. Similarly, the last matrix element $\langle \Psi_m | \hat{a}_r^\dagger \hat{a}_s | \Psi_0 \rangle$ demands that $|\Psi_m\rangle = \hat{a}_r^\dagger \hat{a}_s | \Psi_0 \rangle$. This makes the sums over n and m obsolete and the many body excitation energies get replaced by the corresponding single particle energies, i.e. $E_0 - E_n = \epsilon_i - \epsilon_j$ and $E_0 - E_m = \epsilon_s - \epsilon_r$. Thus we have

$$\begin{aligned} & \sum_{nm} \frac{\langle \Psi_0 | \hat{A} | \Psi_n \rangle \langle \Psi_n | \hat{B} | \Psi_m \rangle \langle \Psi_m | \hat{C} | \Psi_0 \rangle}{(E_0 - E_m + \omega_3 + i\eta)(E_0 - E_n + \omega_2 + \omega_3 + 2i\eta)} = \\ & \sum_{ijklrs} \langle \phi_i | \hat{a}(\mathbf{r}_1) | \phi_j \rangle \langle \phi_k | \hat{b}(\mathbf{r}_2) | \phi_l \rangle \langle \phi_r | \hat{c}(\mathbf{r}_3) | \phi_s \rangle \times \\ & \times \frac{\langle \Psi_0 | \hat{a}_i^\dagger \hat{a}_j \hat{a}_k^\dagger \hat{a}_l | \Psi_0 \rangle \langle \Psi_0 | \hat{a}_i^\dagger \hat{a}_j \hat{a}_k^\dagger \hat{a}_l \hat{a}_r^\dagger \hat{a}_s | \Psi_0 \rangle \langle \Psi_0 | \hat{a}_s^\dagger \hat{a}_r \hat{a}_l^\dagger \hat{a}_i | \Psi_0 \rangle}{(\epsilon_s - \epsilon_r + \omega_3 + i\eta)(\epsilon_i - \epsilon_j + \omega_2 + \omega_3 + 2i\eta)} \end{aligned} \quad (\text{A.5})$$

The operators in the central matrix element now imply that either $k = s \wedge r = j \wedge l = i$ or $k = j \wedge s = i \wedge l = r$, i.e.

$$\langle \Psi_0 | \hat{a}_i^\dagger \hat{a}_j \hat{a}_k^\dagger \hat{a}_l \hat{a}_r^\dagger \hat{a}_s | \Psi_0 \rangle = \langle \Psi_0 | \hat{a}_i^\dagger \hat{a}_j \hat{a}_s^\dagger \hat{a}_l \hat{a}_r^\dagger \hat{a}_i | \Psi_0 \rangle + \langle \Psi_0 | \hat{a}_i^\dagger \hat{a}_j \hat{a}_j^\dagger \hat{a}_r \hat{a}_l^\dagger \hat{a}_i | \Psi_0 \rangle \quad (\text{A.6})$$

We now make use of the anti-commuting property of the operators while rearranging them to the form $\hat{a}_i^\dagger \hat{a}_i = \hat{n}_i$, that is to say to give occupation number operators:

$$\begin{aligned} & \sum_{nm} \frac{\langle \Psi_0 | \hat{A} | \Psi_n \rangle \langle \Psi_n | \hat{B} | \Psi_m \rangle \langle \Psi_m | \hat{C} | \Psi_0 \rangle}{(E_0 - E_m + \omega_3 + i\eta)(E_0 - E_n + \omega_2 + \omega_3 + 2i\eta)} = \\ & = \sum_{ijs} \langle \phi_i | \hat{a}(\mathbf{r}_1) | \phi_j \rangle \langle \phi_s | \hat{b}(\mathbf{r}_2) | \phi_i \rangle \langle \phi_j | \hat{c}(\mathbf{r}_3) | \phi_s \rangle \times \\ & \quad \times \frac{\langle \Psi_0 | \hat{n}_i (1 - \hat{n}_j) | \Psi_0 \rangle \langle \Psi_0 | \hat{n}_i (1 - \hat{n}_j) \hat{n}_s | \Psi_0 \rangle \langle \Psi_0 | \hat{n}_s (1 - \hat{n}_j) | \Psi_0 \rangle}{(\epsilon_s - \epsilon_j + \omega_3 + i\eta)(\epsilon_i - \epsilon_j + \omega_2 + \omega_3 + 2i\eta)} + \\ & + \sum_{ijr} \langle \phi_i | \hat{a}(\mathbf{r}_1) | \phi_j \rangle \langle \phi_j | \hat{b}(\mathbf{r}_2) | \phi_r \rangle \langle \phi_r | \hat{c}(\mathbf{r}_3) | \phi_i \rangle \times \\ & \quad \times \frac{\langle \Psi_0 | \hat{n}_i (1 - \hat{n}_j) | \Psi_0 \rangle \langle \Psi_0 | \hat{n}_i (1 - \hat{n}_j) (1 - \hat{n}_r) | \Psi_0 \rangle \langle \Psi_0 | \hat{n}_i (1 - \hat{n}_r) | \Psi_0 \rangle}{(\epsilon_i - \epsilon_r + \omega_3 + i\eta)(\epsilon_i - \epsilon_j + \omega_2 + \omega_3 + 2i\eta)} \\ & = \sum_{ijk} \frac{f_i (1 - f_j) f_k \langle \phi_i | \hat{a}(\mathbf{r}_1) | \phi_j \rangle \langle \phi_k | \hat{b}(\mathbf{r}_2) | \phi_i \rangle \langle \phi_j | \hat{c}(\mathbf{r}_3) | \phi_k \rangle}{(\epsilon_k - \epsilon_j + \omega_3 + i\eta)(\epsilon_i - \epsilon_j + \omega_2 + \omega_3 + 2i\eta)} + \\ & + \frac{f_i (1 - f_j) (1 - f_k) \langle \phi_i | \hat{a}(\mathbf{r}_1) | \phi_j \rangle \langle \phi_j | \hat{b}(\mathbf{r}_2) | \phi_k \rangle \langle \phi_k | \hat{c}(\mathbf{r}_3) | \phi_i \rangle}{(\epsilon_i - \epsilon_k + \omega_3 + i\eta)(\epsilon_i - \epsilon_j + \omega_2 + \omega_3 + 2i\eta)} \end{aligned} \quad (\text{A.7})$$

where in the last step we used $\langle \Psi_0 | \hat{n}_i | \Psi_0 \rangle = f_i$ and that this expectation value of the occupation operator is either 1 or 0.

B Fourier Transforms

When dealing with first and second order response we have to take the Fourier-transforms of functions of two or three variables, for which we need to define the Fourier transform. For one point functions we use the definitions

$$\tilde{f}(\mathbf{k}, \omega) = \int d\mathbf{r} dt e^{-i(\mathbf{k}\cdot\mathbf{r}-\omega t)} f(\mathbf{r}, t) \quad (\text{B.1})$$

$$f(\mathbf{r}, t) = \frac{1}{(2\pi)^4} \int d\mathbf{k} d\omega e^{i(\mathbf{k}\cdot\mathbf{r}-\omega t)} \tilde{f}(\mathbf{k}, \omega) \quad (\text{B.2})$$

When dealing with functions of two variables, especially response function, these definitions have to carefully generalized. here we will shortly demonstrate this by considering a two time linear response function and its transformation into frequency space. The transformation into momentum space as well as the generalization to second order is done analogously. Considering a first order response function defined in real time by

$$f(t_1) = \int dt_2 \chi(t_1, t_2) V_{per}(t_2) \quad (\text{B.3})$$

which we would like to express in Fourier space as

$$f(\omega_1) = \int d\omega_2 \chi(\omega_1, \omega_2) V_{per}(\omega_2). \quad (\text{B.4})$$

Starting by substituting the perturbing field in terms of its Fourier transform we have

$$f(t_1) = \frac{1}{2\pi} \int dt_2 \chi(t_1, t_2) \int d\omega_2 e^{-\omega_2 t_2} V_{per}(\omega_2) \quad (\text{B.5})$$

and performing now the Fourier transform of the whole expression according to

$$f(\omega) = \int dt e^{i\omega t} f(t) \quad (\text{B.6})$$

we have

$$f(\omega_1) = \frac{1}{2\pi} \int d\omega_2 dt_1 dt_2 e^{i\omega_1 t_1} \chi(t_1, t_2) e^{-\omega_2 t_2} V_{per}(\omega_2). \quad (\text{B.7})$$

Comparison with Eq. (B.4) yields the rule for Fourier transforming linear response functions:

$$\chi(\omega_1, \omega_2) = \frac{1}{2\pi} \int dt_1 dt_2 e^{i\omega_1 t_1} \chi(t_1, t_2) e^{-\omega_2 t_2}. \quad (\text{B.8})$$

For the transformation into the momentum space of a periodic crystal we find analogously

$$\chi(\mathbf{r}_1, \mathbf{r}_2) = \frac{1}{V} \sum_{\mathbf{q}, \mathbf{G}_1, \mathbf{G}_2} e^{i(\mathbf{q} + \mathbf{G}_1) \cdot \mathbf{r}_1} \chi(\mathbf{q} + \mathbf{G}_1, \mathbf{q} + \mathbf{G}_2) e^{-i(\mathbf{q} + \mathbf{G}_2) \cdot \mathbf{r}_2} \quad (\text{B.9})$$

$$\chi(\mathbf{q} + \mathbf{G}_1, \mathbf{q} + \mathbf{G}_2) = \frac{1}{V} \int_V d\mathbf{r}_1 d\mathbf{r}_2 e^{-i(\mathbf{q} + \mathbf{G}_1) \cdot \mathbf{r}_1} \chi(\mathbf{r}_1, \mathbf{r}_2) e^{i(\mathbf{q} + \mathbf{G}_2) \cdot \mathbf{r}_2} \quad (\text{B.10})$$

where we used the periodicity of the lattice and V is the volume of solid (c.f. [153]). The second order response functions follow in the same way and we have:

$$\chi(\omega_1, \omega_2, \omega_3) = \frac{1}{2\pi} \int dt_1 dt_2 dt_3 e^{i\omega_1 t_1} \chi(t_1, t_2, t_3) e^{-i\omega_2 t_2} e^{-i\omega_3 t_3} \quad (\text{B.11})$$

and

$$\begin{aligned} \chi(\mathbf{r}_1, \mathbf{r}_2, \mathbf{r}_3) = \\ \frac{1}{V} \sum_{\substack{\mathbf{q}_1, \mathbf{q}_2, \mathbf{q}_3 \\ \mathbf{G}_1, \mathbf{G}_2, \mathbf{G}_3}} e^{i(\mathbf{q}_1 + \mathbf{G}_1) \cdot \mathbf{r}_1} \chi(\mathbf{q}_1 + \mathbf{G}_1, \mathbf{q}_2 + \mathbf{G}_2, \mathbf{q}_3 + \mathbf{G}_3) e^{-i(\mathbf{q}_2 + \mathbf{G}_2) \cdot \mathbf{r}_2} e^{-i(\mathbf{q}_3 + \mathbf{G}_3) \cdot \mathbf{r}_3} \end{aligned} \quad (\text{B.12})$$

C Degenerate perturbation theory

The important difference to usual perturbation theory is, that as we are dealing with eigenenergies from real band structures, we need to account for the degeneracy of bands. This is text book knowledge, so we just state the results. They are similar to non-degenerate ones, only that the sums exclude those states that belong to the subspace D of states that have degenerate energies. (We denote the non-degenerate energies and states by E_n and $|\psi_n\rangle$ respectively.)

Energies

$$\epsilon_n^{(1)} = \langle \psi_n | H^{(1)} | \psi_n \rangle \quad (\text{C.1})$$

$$\epsilon_n^{(2)} = \sum_{m \notin D_n} \frac{|\langle \psi_n | H^{(1)} | \psi_m \rangle|^2}{E_n - E_m} + \langle \psi_n | H^{(2)} | \psi_n \rangle \quad (\text{C.2})$$

Note that this kind of expression is only possible if ψ_n diagonalize the perturbation, which here is the case, because ψ_n are Bloch functions and the perturbing Hamiltonian is Eq. (4.11). Now we can insert this $\mathbf{k} \cdot \mathbf{p}$ -perturbed Hamiltonian Eq. (4.11):

$$\epsilon_n^{(1)} = \langle \psi_n | \mathbf{q}\mathbf{v} | \psi_n \rangle \quad (\text{C.3})$$

$$\epsilon_n^{(2)} = \sum_{m \notin D_n} \frac{|\langle \psi_n | \mathbf{q}\mathbf{v} | \psi_m \rangle|^2}{E_n - E_m} - \frac{i}{2} \langle \psi_n | [\mathbf{q}\mathbf{v}, \mathbf{q}\mathbf{r}] | \psi_n \rangle \quad (\text{C.4})$$

States

$$|\Psi_n^{(1)}\rangle = \sum_{m \notin D_n} \frac{\langle \psi_m | H^{(1)} | \psi_n \rangle}{E_n - E_m} |\psi_m\rangle \quad (\text{C.5})$$

$$|\Psi_n^{(2)}\rangle = \sum_{m, p \notin D_n} \frac{\langle \psi_m | H^{(1)} | \psi_p \rangle \langle \psi_p | H^{(1)} | \psi_n \rangle}{(E_n - E_p)(E_n - E_m)} |\psi_m\rangle + \sum_{m \notin D_n} \frac{\langle \psi_m | H^{(2)} | \psi_n \rangle}{(E_n - E_m)} |\psi_m\rangle \quad (\text{C.6})$$

$$- \langle \psi_n | H^{(1)} | \psi_n \rangle \sum_{m \notin D} \frac{\langle \psi_m | H^{(1)} | \psi_n \rangle}{(E_n - E_m)^2} |\psi_m\rangle - \frac{1}{2} \sum_{m \notin D_n} \frac{|\langle \psi_m | H^{(1)} | \psi_n \rangle|^2}{(E_n - E_m)^2} |\psi_n\rangle \quad (\text{C.7})$$

Again, we insert the $\mathbf{k} \cdot \mathbf{p}$ -perturbed Hamiltonian:

$$|\Psi_n^{(1)}\rangle = \sum_{m \notin D_n} \frac{\langle \psi_m | \mathbf{qV} | \psi_n \rangle}{E_n - E_m} |\psi_m\rangle \quad (\text{C.8})$$

$$|\Psi_n^{(2)}\rangle = \sum_{m, p \notin D_n} \frac{\langle \psi_m | \mathbf{qV} | \psi_p \rangle \langle \psi_p | \mathbf{qV} | \psi_n \rangle}{(E_n - E_p)(E_n - E_m)} |\psi_m\rangle + \sum_{m \notin D_n} \frac{\langle \psi_m | -\frac{i}{2} [\mathbf{qV}, \mathbf{qF}] | \psi_n \rangle}{(E_n - E_m)} |\psi_m\rangle \quad (\text{C.9})$$

$$- \langle \psi_n | \mathbf{qV} | \psi_n \rangle \sum_{m \notin D} \frac{\langle \psi_m | \mathbf{qV} | \psi_n \rangle}{(E_n - E_m)^2} |\psi_m\rangle - \frac{1}{2} \sum_{m \notin D_n} \frac{|\langle \psi_m | \mathbf{qV} | \psi_n \rangle|^2}{(E_n - E_m)^2} |\psi_n\rangle \quad (\text{C.10})$$

In $\chi_{\rho\rho\rho}^{(0)}$ there are three different kinds matrix elements and denominators:

$$a_{nn'}(\mathbf{q}) = \langle n_{\mathbf{k}} | e^{-i(\mathbf{q}' + \mathbf{q}'' + \mathbf{G})\mathbf{r}} | n_{\mathbf{k} + \mathbf{q}' + \mathbf{q}''} \rangle \quad (\text{C.11})$$

$$b_{n'n''}(\mathbf{q}'' + \mathbf{G}'') = \langle n'_{\mathbf{k} + \mathbf{q}' + \mathbf{q}''} | e^{i(\mathbf{q}'' + \mathbf{G}'')\mathbf{r}'} | n''_{\mathbf{k} + \mathbf{q}'} \rangle \quad (\text{C.12})$$

$$c_{n''n}(\mathbf{q}' + \mathbf{G}') = \langle n''_{\mathbf{k} + \mathbf{q}'} | e^{i(\mathbf{q}' + \mathbf{G}')\mathbf{r}''} | n_{\mathbf{k}} \rangle \quad (\text{C.13})$$

$$(\text{C.14})$$

and three different denominators:

$$E_{Ann'} = E_{n, \mathbf{k}} - E_{n', \mathbf{k} + \mathbf{q}' + \mathbf{q}''} + 2\omega + 2i\eta \quad (\text{C.15})$$

$$E_{Bn'n''}(\mathbf{q}') = E_{n, \mathbf{k}} - E_{n'', \mathbf{k} + \mathbf{q}'} + \omega + i\eta \quad (\text{C.16})$$

$$E_{Cnm''}(\mathbf{q}') = E_{n'', \mathbf{k} + \mathbf{q}'} - E_{n', \mathbf{k} + \mathbf{q}' + \mathbf{q}''} + \omega + i\eta \quad (\text{C.17})$$

$$(\text{C.18})$$

So we can write:

$$\begin{aligned} \chi_{\rho\rho\rho}^{(0)}(\mathbf{q}' + \mathbf{q}'' + \mathbf{G}, \mathbf{q}' + \mathbf{G}', \mathbf{q}'' + \mathbf{G}'', \omega, \omega) &= \frac{2}{V} \sum_{n, n', n'', \mathbf{k}} a_{nn'}(\mathbf{q}) E_{Ann'} \times \\ &[(f_{n\mathbf{k}} - f_{n''\mathbf{k}}) b_{n'n''}(\mathbf{q}'' + \mathbf{G}'') c_{n''n}(\mathbf{q}' + \mathbf{G}') E_{Cnm''}(\mathbf{q}') + \\ &+ (f_{n'\mathbf{k}} - f_{n''\mathbf{k}}) b_{n'n''}(\mathbf{q}'' + \mathbf{G}'') c_{n''n}(\mathbf{q}' + \mathbf{G}') E_{Bn'n''}(\mathbf{q}') + \\ &+ (f_{n\mathbf{k}} - f_{n''\mathbf{k}}) b_{n'n''}(\mathbf{q}' + \mathbf{G}') c_{n''n}(\mathbf{q}'' + \mathbf{G}'') E_{Cnm''}(\mathbf{q}') + \\ &+ (f_{n'\mathbf{k}} - f_{n''\mathbf{k}}) b_{n'n''}(\mathbf{q}' + \mathbf{G}') c_{n''n}(\mathbf{q}'' + \mathbf{G}'') E_{Bn'n''}(\mathbf{q}'')] \end{aligned} \quad (\text{C.19})$$

In order to carry out the perturbative expansion we apply the perturbation theory to all these six terms separately up to second order¹:

a-matrix elements

$$a_{nn'}^{(0)} = \delta_{nn'} \quad (\text{C.20})$$

$$a_{nn'}^{(0)}(\mathbf{G}) = \langle n_{\mathbf{k}} | e^{-i\mathbf{G}\mathbf{r}} | n'_{\mathbf{k}} \rangle \quad (\text{C.21})$$

$$a_{nn'}^{(1)}(\mathbf{q}) = \frac{\langle n_{\mathbf{k}} | (\mathbf{q}' + \mathbf{q}'') \mathbf{v} | n'_{\mathbf{k}} \rangle}{E_{n',\mathbf{k}} - E_{n,\mathbf{k}}} \quad (\text{C.22})$$

$$a_{nn'}^{(1)}(\mathbf{G}) = \sum_{m \notin D_{n'}} \frac{\langle m_{\mathbf{k}} | (\mathbf{q}' + \mathbf{q}'') \mathbf{v} | n'_{\mathbf{k}} \rangle \langle n_{\mathbf{k}} | e^{-i\mathbf{G}\mathbf{r}} | m_{\mathbf{k}} \rangle}{E_{n',\mathbf{k}} - E_{m,\mathbf{k}}} \quad (\text{C.23})$$

b-matrix elements

$$b_{n'n''}^{(0)} = \delta_{n'n''} \quad (\text{C.24})$$

$$b_{n'n''}^{(0)}(\mathbf{G}) = \langle n'_{\mathbf{k}} | e^{i\mathbf{G}\mathbf{r}'} | n''_{\mathbf{k}} \rangle \quad (\text{C.25})$$

$$b_{n'n''}^{(1)}(\mathbf{q}') = \frac{\langle n'_{\mathbf{k}} | \mathbf{q}' \mathbf{v} | n''_{\mathbf{k}} \rangle}{E_{n',\mathbf{k}} - E_{n'',\mathbf{k}}} \quad (\text{C.26})$$

$$\begin{aligned} b_{n'n''}^{(1)}(\mathbf{q}' + \mathbf{G}') &= \sum_{m \notin D_{n''}} \frac{\langle m_{\mathbf{k}} | \mathbf{q}'' \mathbf{v} | n''_{\mathbf{k}} \rangle \langle n'_{\mathbf{k}} | e^{i\mathbf{G}'\mathbf{r}'} | m_{\mathbf{k}} \rangle}{E_{n'',\mathbf{k}} - E_{m,\mathbf{k}}} + \\ &+ \sum_{m \notin D_{n'}} \frac{\langle n'_{\mathbf{k}} | (\mathbf{q}' + \mathbf{q}'') \mathbf{v} | m_{\mathbf{k}} \rangle \langle m_{\mathbf{k}} | e^{i\mathbf{G}'\mathbf{r}'} | n''_{\mathbf{k}} \rangle}{E_{n',\mathbf{k}} - E_{m,\mathbf{k}}} \end{aligned} \quad (\text{C.27})$$

¹In principle one would need them up to third order, but it turns out that all terms containing third order matrix elements or denominators vanish due to the occupation number. The same holds for second order of a .

$$\begin{aligned}
b_{n'n''}^{(2)}(\mathbf{q}'') &= \sum_{p \notin D_{n''}} \frac{\langle n'_k | \mathbf{q}' \mathbf{v} | p_k \rangle \langle p_k | \mathbf{q}' \mathbf{v} | n''_k \rangle}{(E_{n'',k} - E_{p,k})(E_{n'',k} - E_{n',k})} - \frac{\langle n''_k | \mathbf{q}' \mathbf{v} | n''_k \rangle \langle n'_k | \mathbf{q}' \mathbf{v} | n''_k \rangle}{(E_{n'',k} - E_{n',k})^2} + \\
&+ \frac{\langle n'_k | -\frac{i}{2} [\mathbf{q}' \mathbf{r}, \mathbf{q}' \mathbf{v}] | n''_k \rangle}{E_{n'',k} - E_{n',k}} + \\
&+ \sum_{p \notin D_{n'}} \frac{\langle n'_k | (\mathbf{q}' + \mathbf{q}'') \mathbf{v} | p_k \rangle \langle p_k | (\mathbf{q}' + \mathbf{q}'') \mathbf{v} | n''_k \rangle}{(E_{n',k} - E_{p,k})(E_{n',k} - E_{n'',k})} - \frac{\langle n'_k | (\mathbf{q}' + \mathbf{q}'') \mathbf{v} | n''_k \rangle \langle n'_k | (\mathbf{q}' + \mathbf{q}'') \mathbf{v} | n''_k \rangle}{(E_{n',k} - E_{n'',k})^2} + \\
&+ \frac{\langle n'_k | -\frac{i}{2} [(\mathbf{q}' + \mathbf{q}'') \mathbf{r}, (\mathbf{q}' + \mathbf{q}'') \mathbf{v}] | n''_k \rangle}{E_{n',k} - E_{n'',k}} + \\
&+ \sum_{m \notin D_{n'}, \notin D_{n''}} \frac{\langle n'_k | (\mathbf{q}' + \mathbf{q}'') \mathbf{v} | m_k \rangle \langle m_k | \mathbf{q}' \mathbf{v} | n''_k \rangle}{(E_{n',k} - E_{m,k})(E_{n'',k} - E_{m,k})} - \\
&- \frac{1}{2} \delta_{n'n''} \left[\sum_{m \notin D_{n''}} \frac{|\langle m_k | \mathbf{q}' \mathbf{v} | n''_k \rangle|^2}{(E_{n'',k} - E_{m,k})^2} - \sum_{m \notin D_{n'}} \frac{|\langle n'_k | (\mathbf{q}' + \mathbf{q}'') \mathbf{v} | m_k \rangle|^2}{(E_{n',k} - E_{m,k})^2} \right]
\end{aligned} \tag{C.28}$$

c-matrix elements

$$c_{n''n}^{(0)} = \delta_{n''n} \tag{C.29}$$

$$c_{n''n}^{(0)}(\mathbf{G}) = \langle n''_k | e^{i\mathbf{G}\mathbf{r}''} | n_k \rangle \tag{C.30}$$

$$c_{n''n}^{(1)}(\mathbf{q}') = \frac{\langle n''_k | \mathbf{q}' \mathbf{v} | n_k \rangle}{E_{n'',k} - E_{n,k}} \tag{C.31}$$

$$c_{n''n}^{(1)}(\mathbf{q}' + \mathbf{G}') = \sum_{m \notin D_n} \frac{\langle n''_k | \mathbf{q}' \mathbf{v} | m_k \rangle \langle m_k | e^{i\mathbf{G}'\mathbf{r}''} | n_k \rangle}{E_{n'',k} - E_{m,k}} \tag{C.32}$$

$$\begin{aligned}
c_{n''n}^{(2)}(\mathbf{q}') &= \sum_{p \notin D_{n''}} \frac{\langle p_k | \mathbf{q}' \mathbf{v} | n_k \rangle \langle n''_k | \mathbf{q}' \mathbf{v} | p_k \rangle}{(E_{n'',k} - E_{p,k})(E_{n'',k} - E_{n,k})} + \\
&+ \frac{\langle n''_k | -\frac{i}{2} [\mathbf{q}' \mathbf{r}, \mathbf{q}' \mathbf{v}] | n_k \rangle}{E_{n'',k} - E_{n,k}} - \langle n''_k | \mathbf{q}' \mathbf{v} | n''_k \rangle \frac{\langle n''_k | \mathbf{q}' \mathbf{v} | n_k \rangle}{(E_{n'',k} - E_{n,k})^2} - \\
&- \frac{1}{2} \sum_{m \notin D_{n''}} \frac{|\langle m_k | \mathbf{q}' \mathbf{v} | n''_k \rangle|^2}{(E_{n'',k} - E_{m,k})^2} \delta_{n''n}
\end{aligned} \tag{C.33}$$

$$\begin{aligned}
c_{n''n}^{(2)}(\mathbf{q}' + \mathbf{G}') &= \sum_{m,p \notin D_{n''}} \frac{\langle p_{\mathbf{k}} | \mathbf{q}' \mathbf{v} | m_{\mathbf{k}} \rangle \langle n''_{\mathbf{k}} | \mathbf{q}' \mathbf{v} | p_{\mathbf{k}} \rangle}{(E_{n'',\mathbf{k}} - E_{p,\mathbf{k}})(E_{n'',\mathbf{k}} - E_{m,\mathbf{k}})} \langle m_{\mathbf{k}} | e^{i\mathbf{G}' \mathbf{r}''} | n_{\mathbf{k}} \rangle + \\
&+ \sum_{m \notin D_{n''}} \frac{\langle n''_{\mathbf{k}} | -\frac{i}{2} [\mathbf{q}' \mathbf{r}, \mathbf{q}' \mathbf{v}] | m_{\mathbf{k}} \rangle}{E_{n'',\mathbf{k}} - E_{m,\mathbf{k}}} \langle m_{\mathbf{k}} | e^{i\mathbf{G}' \mathbf{r}''} | n_{\mathbf{k}} \rangle - \\
&- \langle n''_{\mathbf{k}} | \mathbf{q}' \mathbf{v} | n''_{\mathbf{k}} \rangle \sum_{m \notin D_{n''}} \frac{\langle n''_{\mathbf{k}} | \mathbf{q}' \mathbf{v} | m_{\mathbf{k}} \rangle}{(E_{n'',\mathbf{k}} - E_{m,\mathbf{k}})^2} \langle m_{\mathbf{k}} | e^{i\mathbf{G}' \mathbf{r}''} | n_{\mathbf{k}} \rangle - \\
&- \frac{1}{2} \sum_{m \notin D_{n''}} \frac{|\langle m_{\mathbf{k}} | \mathbf{q}' \mathbf{v} | n''_{\mathbf{k}} \rangle|^2}{(E_{n'',\mathbf{k}} - E_{m,\mathbf{k}})^2} \langle n''_{\mathbf{k}} | e^{i\mathbf{G}' \mathbf{r}''} | n_{\mathbf{k}} \rangle
\end{aligned} \tag{C.34}$$

Denominators

$$E_{Ann'}^{(0)} = \frac{1}{(E_{n,\mathbf{k}} - E_{n',\mathbf{k}} + 2\omega + 2i\eta)} \tag{C.35}$$

$$E_{Ann'}^{(1)} = \frac{E_{n'}^{(1)}(\mathbf{q}' + \mathbf{q}'')}{(E_{n,\mathbf{k}} - E_{n',\mathbf{k}} + 2\omega + 2i\eta)^2} \tag{C.36}$$

$$E_{Bn''n'}^{(0)} = \frac{1}{(E_{n'',\mathbf{k}} - E_{n',\mathbf{k}} + \omega + i\eta)} \tag{C.37}$$

$$E_{Bn''n'}^{(1)}(\mathbf{q}') = \frac{E_{n'}^{(1)}(\mathbf{q}' + \mathbf{q}'') - E_{n''}^{(1)}(\mathbf{q}')}{(E_{n'',\mathbf{k}} - E_{n',\mathbf{k}} + \omega + i\eta)^2} \tag{C.38}$$

$$E_{Cnm''}^{(0)} = \frac{1}{(E_{n,\mathbf{k}} - E_{n'',\mathbf{k}} + \omega + i\eta)} \tag{C.39}$$

$$E_{Cnm''}^{(1)}(\mathbf{q}') = \frac{E_{n''}^{(1)}(\mathbf{q}')}{(E_{n,\mathbf{k}} - E_{n'',\mathbf{k}} + \omega + i\eta)^2} \tag{C.40}$$

where $E_n^{(1)}(\mathbf{q}) = \langle n_{\mathbf{k}} | \mathbf{q} \mathbf{v} | n_{\mathbf{k}} \rangle$.

We note that here all matrix elements are in terms of $\mathbf{v} = \mathbf{p} + [V_{nl}, \mathbf{r}]$. For our implementation we pass to matrix elements of the position operator \mathbf{r} , using the relation

$$\langle n_{\mathbf{k}} | \mathbf{r} | n'_{\mathbf{k}} \rangle = \frac{\mathbf{v}}{E_{n\mathbf{k}} - E_{n'\mathbf{k}}}. \tag{C.41}$$

C.1 Head

The head of $\chi_{\rho\rho\rho}^{(0)}$ including the scissors approximation as described in section 4.2 reads:

$$\begin{aligned}
\chi_{\rho\rho\rho}^{(0),head}(\mathbf{q}, \mathbf{q}_1, \mathbf{q}_2) &= \frac{2}{V} \sum_{n,n',n'',\mathbf{k}} \left[\frac{(f_{n,\mathbf{k}} - f_{n',\mathbf{k}})}{(\Delta_{nn'}^{SC} + 2\omega')(\Delta_{nn'}^{SC} + \omega')} + \frac{(f_{n',\mathbf{k}} - f_{n'',\mathbf{k}})}{(\Delta_{nn'}^{SC} + 2\omega')(\Delta_{n''n'}^{SC} + \omega')} + \right. \\
&\quad \left. + 2 \frac{(f_{n,\mathbf{k}} - f_{n',\mathbf{k}})(\Delta_{n''n}^{LDA} + \Delta_{n''n'}^{LDA})}{\Delta_{nn'}^{LDA} \Delta_{nn'}^{SC} (\Delta_{nn'}^{SC} + 2\omega')} - \frac{(f_{n,\mathbf{k}} - f_{n',\mathbf{k}})(\Delta_{n''n}^{LDA} + \Delta_{n''n'}^{LDA})}{2\Delta_{nn'}^{LDA} \Delta_{nn'}^{SC} (\Delta_{nn'}^{SC} + \omega')} \right] \times \\
&\quad \times \langle n_{\mathbf{k}} | -i(\mathbf{q}_1 + \mathbf{q}_2)\mathbf{r} | n'_{\mathbf{k}} \rangle [\langle n'_{\mathbf{k}} | i\mathbf{q}_2\mathbf{r} | n''_{\mathbf{k}} \rangle \langle n''_{\mathbf{k}} | i\mathbf{q}_1\mathbf{r} | n_{\mathbf{k}} \rangle + \langle n'_{\mathbf{k}} | i\mathbf{q}_1\mathbf{r} | n''_{\mathbf{k}} \rangle \langle n''_{\mathbf{k}} | i\mathbf{q}_2\mathbf{r} | n_{\mathbf{k}} \rangle] + \\
&\quad + \frac{(f_{n,\mathbf{k}} - f_{n',\mathbf{k}})}{(\Delta_{n'n}^{SC} + \omega')(\Delta_{nn'}^{SC} + \omega')} \times \\
&\quad \times \langle n''_{\mathbf{k}} | i(\mathbf{q}_1 + \mathbf{q}_2)\mathbf{r} | n_{\mathbf{k}} \rangle [\langle n_{\mathbf{k}} | i\mathbf{q}_1\mathbf{r} | n'_{\mathbf{k}} \rangle \langle n'_{\mathbf{k}} | i\mathbf{q}_2\mathbf{r} | n''_{\mathbf{k}} \rangle + \langle n_{\mathbf{k}} | i\mathbf{q}_2\mathbf{r} | n'_{\mathbf{k}} \rangle \langle n'_{\mathbf{k}} | i\mathbf{q}_1\mathbf{r} | n''_{\mathbf{k}} \rangle] + \\
&\quad + \left\{ \frac{8(f_{n,\mathbf{k}} - f_{n',\mathbf{k}})}{(\Delta_{nn'}^{SC})^2 (\Delta_{nn'}^{SC} + 2\omega')} - \frac{(f_{n,\mathbf{k}} - f_{n',\mathbf{k}})}{2(\Delta_{nn'}^{SC})^2 (\Delta_{nn'}^{SC} + \omega')} + \right. \\
&\quad \left. + \left[\frac{4(f_{n,\mathbf{k}} - f_{n',\mathbf{k}})}{\Delta_{n'n}^{SC} (\Delta_{nn'}^{SC} + 2\omega')} + \frac{(f_{n,\mathbf{k}} - f_{n',\mathbf{k}})}{2\Delta_{n'n}^{SC} (\Delta_{nn'}^{SC} + \omega')} \right] \left[\frac{1}{\Delta_{nn'}^{SC}} - \frac{1}{\Delta_{nn'}^{LDA}} \right] \right\} \times \\
&\quad \times \langle n_{\mathbf{k}} | -i(\mathbf{q}_1 + \mathbf{q}_2)\mathbf{r} | n'_{\mathbf{k}} \rangle [\langle n'_{\mathbf{k}} | i\mathbf{q}_2\mathbf{r} | n_{\mathbf{k}} \rangle \Delta_{nn'}^{\mathbf{q}_1} + \langle n'_{\mathbf{k}} | i\mathbf{q}_1\mathbf{r} | n_{\mathbf{k}} \rangle \Delta_{nn'}^{\mathbf{q}_2}] + \\
&\quad + \frac{(f_{n,\mathbf{k}} - f_{n',\mathbf{k}})\Delta_{n''n}^{LDA}}{\Delta_{nn'}^{LDA} (\Delta_{nn'}^{SC} + \omega')(\Delta_{n'n}^{SC} + \omega')} \times \\
&\quad \times [-\langle n_{\mathbf{k}} | i\mathbf{q}_1\mathbf{r} | n'_{\mathbf{k}} \rangle \langle n'_{\mathbf{k}} | i\mathbf{q}_2\mathbf{r} | n''_{\mathbf{k}} \rangle \langle n''_{\mathbf{k}} | i(\mathbf{q}_1 + \mathbf{q}_2)\mathbf{r} | n_{\mathbf{k}} \rangle + \\
&\quad + \langle n_{\mathbf{k}} | i(\mathbf{q}_1 + \mathbf{q}_2)\mathbf{r} | n'_{\mathbf{k}} \rangle \langle n'_{\mathbf{k}} | i\mathbf{q}_2\mathbf{r} | n''_{\mathbf{k}} \rangle \langle n''_{\mathbf{k}} | i\mathbf{q}_1\mathbf{r} | n_{\mathbf{k}} \rangle - \\
&\quad - \langle n_{\mathbf{k}} | i\mathbf{q}_2\mathbf{r} | n'_{\mathbf{k}} \rangle \langle n'_{\mathbf{k}} | i\mathbf{q}_1\mathbf{r} | n''_{\mathbf{k}} \rangle \langle n''_{\mathbf{k}} | i(\mathbf{q}_1 + \mathbf{q}_2)\mathbf{r} | n_{\mathbf{k}} \rangle + \\
&\quad + \langle n_{\mathbf{k}} | i(\mathbf{q}_1 + \mathbf{q}_2)\mathbf{r} | n'_{\mathbf{k}} \rangle \langle n'_{\mathbf{k}} | i\mathbf{q}_1\mathbf{r} | n''_{\mathbf{k}} \rangle \langle n''_{\mathbf{k}} | i\mathbf{q}_2\mathbf{r} | n_{\mathbf{k}} \rangle] + \\
&\quad + \left[\frac{(f_{n,\mathbf{k}} - f_{n',\mathbf{k}})}{\Delta_{nn'}^{LDA} \Delta_{nn'}^{SC} (\Delta_{nn'}^{SC} + \omega')} - \frac{4(f_{n,\mathbf{k}} - f_{n',\mathbf{k}})}{\Delta_{nn'}^{LDA} \Delta_{nn'}^{SC} (\Delta_{nn'}^{SC} + 2\omega')} \right] \times \\
&\quad \times \langle n_{\mathbf{k}} | i(\mathbf{q}_1 + \mathbf{q}_2)\mathbf{r} | n'_{\mathbf{k}} \rangle \left[\langle n'_{\mathbf{k}} | -\frac{i}{2}[\mathbf{q}_1\mathbf{r}, \mathbf{q}_2\mathbf{v}] | n_{\mathbf{k}} \rangle + \langle n'_{\mathbf{k}} | -\frac{i}{2}[\mathbf{q}_2\mathbf{r}, \mathbf{q}_1\mathbf{v}] | n_{\mathbf{k}} \rangle \right] + \\
&\quad + \frac{(f_{n,\mathbf{k}} - f_{n',\mathbf{k}})}{2\Delta_{nn'}^{LDA} \Delta_{nn'}^{SC} (\Delta_{nn'}^{SC} + \omega')} \times \\
&\quad + [\langle n_{\mathbf{k}} | [(\mathbf{q}_1 + \mathbf{q}_2)\mathbf{v}, i\mathbf{q}_2\mathbf{r}] | n'_{\mathbf{k}} \rangle \langle n'_{\mathbf{k}} | i\mathbf{q}_1\mathbf{r} | n_{\mathbf{k}} \rangle + \langle n_{\mathbf{k}} | [(\mathbf{q}_1 + \mathbf{q}_2)\mathbf{v}, i\mathbf{q}_1\mathbf{r}] | n'_{\mathbf{k}} \rangle \langle n'_{\mathbf{k}} | i\mathbf{q}_2\mathbf{r} | n_{\mathbf{k}} \rangle - \\
&\quad - \langle n_{\mathbf{k}} | i(\mathbf{q}_1 + \mathbf{q}_2)\mathbf{r} | n'_{\mathbf{k}} \rangle \langle n'_{\mathbf{k}} | [\mathbf{q}_2\mathbf{v}, i\mathbf{q}_1\mathbf{r}] | n_{\mathbf{k}} \rangle - \langle n_{\mathbf{k}} | i(\mathbf{q}_1 + \mathbf{q}_2)\mathbf{r} | n'_{\mathbf{k}} \rangle \langle n'_{\mathbf{k}} | [\mathbf{q}_1\mathbf{v}, i\mathbf{q}_2\mathbf{r}] | n_{\mathbf{k}} \rangle] \\
\end{aligned} \tag{C.42}$$

C.2 Wings

C.2.1 $G \neq 0$:

$$\begin{aligned}
\chi_{\rho\rho\rho}^{(0),wing1}(\mathbf{G}, \mathbf{q}_1, \mathbf{q}_2) &= \frac{2}{V} \sum_{n,n',n'',\mathbf{k}} (f_{n,\mathbf{k}} - f_{n',\mathbf{k}}) \left\{ \langle n_{\mathbf{k}} | e^{-i\mathbf{G}\mathbf{r}} | n'_{\mathbf{k}} \rangle \langle n'_{\mathbf{k}} | i\mathbf{q}_1 \mathbf{r} | n_{\mathbf{k}} \rangle \Delta_{nn'}^{\mathbf{q}_2} \times \right. \\
&\times \left[\frac{1}{(\Delta_{nn'}^{SC})^2 (\Delta_{nn'}^{SC} + \omega')} + \frac{2}{\Delta_{nn'}^{LDA} \Delta_{nn'}^{SC} (\Delta_{nn'}^{SC} + \omega')} + \right. \\
&\quad \left. \left. + \frac{2}{\Delta_{nn'}^{SC} (\Delta_{nn'}^{SC} + 2\omega') (\Delta_{nn'}^{SC} + \omega')} + \frac{2}{\Delta_{nn'}^{LDA} (\Delta_{nn'}^{SC} + 2\omega') (\Delta_{nn'}^{SC} + \omega')} \right] + \right. \\
&+ \frac{2 \langle n_{\mathbf{k}} | i\mathbf{q}_2 \mathbf{r} | n''_{\mathbf{k}} \rangle \langle n''_{\mathbf{k}} | e^{-i\mathbf{G}\mathbf{r}} | n'_{\mathbf{k}} \rangle \langle n'_{\mathbf{k}} | i\mathbf{q}_1 \mathbf{r} | n_{\mathbf{k}} \rangle}{(\Delta_{nn'}^{SC} + \omega') (\Delta_{n'n}^{SC} + \omega')} + \\
&+ \langle n_{\mathbf{k}} | e^{-i\mathbf{G}\mathbf{r}} | n'_{\mathbf{k}} \rangle \langle n'_{\mathbf{k}} | i\mathbf{q}_1 \mathbf{r} | n''_{\mathbf{k}} \rangle \langle n''_{\mathbf{k}} | i\mathbf{q}_2 \mathbf{r} | n_{\mathbf{k}} \rangle \times \\
&\times \left[\frac{2(\Delta_{n''n}^{SC} + \Delta_{n'n''}^{SC})}{(\Delta_{nn'}^{SC})^2 (\Delta_{nn'}^{SC} + 2\omega')} - \frac{(\Delta_{n''n}^{SC} + \Delta_{n'n''}^{SC})}{(\Delta_{nn'}^{SC})^2 (\Delta_{nn'}^{SC} + \omega')} - \frac{(\Delta_{n''n}^{SC} + \Delta_{n'n''}^{SC})}{\Delta_{nn'}^{SC} (\Delta_{nn'}^{SC} + 2\omega') (\Delta_{nn'}^{SC} + \omega')} \right] + \\
&+ \langle n_{\mathbf{k}} | e^{-i\mathbf{G}\mathbf{r}} | n'_{\mathbf{k}} \rangle \langle n'_{\mathbf{k}} | i\mathbf{q}_2 \mathbf{r} | n''_{\mathbf{k}} \rangle \langle n''_{\mathbf{k}} | i\mathbf{q}_1 \mathbf{r} | n_{\mathbf{k}} \rangle \times \\
&\times \left[\frac{(\Delta_{n''n}^{LDA} + \Delta_{n'n''}^{LDA})}{\Delta_{nn'}^{LDA} \Delta_{nn'}^{SC} (\Delta_{nn'}^{SC} + \omega')} + \frac{(\Delta_{n''n}^{LDA} + \Delta_{n'n''}^{LDA})}{\Delta_{nn'}^{LDA} (\Delta_{nn'}^{SC} + 2\omega') (\Delta_{nn'}^{SC} + \omega')} \right] \left. \right\} + \\
&+ \langle n_{\mathbf{k}} | e^{-i\mathbf{G}\mathbf{r}} | n'_{\mathbf{k}} \rangle \langle n'_{\mathbf{k}} | i\mathbf{q}_2 \mathbf{r} | n''_{\mathbf{k}} \rangle \langle n''_{\mathbf{k}} | i\mathbf{q}_1 \mathbf{r} | n_{\mathbf{k}} \rangle \times \\
&\times \left[\frac{(f_{n,\mathbf{k}} - f_{n'',\mathbf{k}})}{(\Delta_{nn'}^{SC} + 2\omega') (\Delta_{nn''}^{SC} + \omega')} + \frac{(f_{n',\mathbf{k}} - f_{n'',\mathbf{k}})}{(\Delta_{nn'}^{SC} + 2\omega') (\Delta_{n''n'}^{SC} + \omega')} \right] + \\
&+ \frac{(f_{n,\mathbf{k}} - f_{n',\mathbf{k}}) \langle n_{\mathbf{k}} | e^{-i\mathbf{G}\mathbf{r}} | n'_{\mathbf{k}} \rangle \langle n'_{\mathbf{k}} | [\mathbf{q}_1 \mathbf{v}, i\mathbf{q}_2 \mathbf{r}] | n_{\mathbf{k}} \rangle}{\Delta_{nn'}^{LDA} \Delta_{nn'}^{SC} (\Delta_{nn'}^{SC} + 2\omega')} + \\
&+ \{ \mathbf{q}_1 \leftrightarrow \mathbf{q}_2 \}
\end{aligned} \tag{C.43}$$

C.2.2 $\mathbf{G}_1 \neq 0$:

$$\begin{aligned}
\chi_{\rho\rho\rho}^{(0),wing2}(\mathbf{q}_1 + \mathbf{q}_2, \mathbf{G}_1, \mathbf{q}_2) &= \frac{2}{V} \sum_{n,n',n'',\mathbf{k}} \langle n_{\mathbf{k}} | i(\mathbf{q}_1 + \mathbf{q}_2)\mathbf{r} | n'_{\mathbf{k}} \rangle \langle n'_{\mathbf{k}} | e^{i\mathbf{G}_1\mathbf{r}} | n_{\mathbf{k}} \rangle \Delta_{nn'}^{\mathbf{q}_2} \times \\
&\times \left[-\frac{2(f_{n,\mathbf{k}} - f_{n',\mathbf{k}})}{\Delta_{nn'}^{SC}(\Delta_{nn'}^{SC} + 2\omega')(\Delta_{nn'}^{SC} + \omega')} - \frac{(f_{n,\mathbf{k}} - f_{n',\mathbf{k}})}{(\Delta_{nn'}^{SC})^2(\Delta_{nn'}^{SC} + \omega')} - \frac{(f_{n,\mathbf{k}} - f_{n',\mathbf{k}})}{\Delta_{nn'}^{LDA}\Delta_{nn'}^{SC}(\Delta_{nn'}^{SC} + \omega')} \right] - \\
&- \frac{(f_{n,\mathbf{k}} - f_{n',\mathbf{k}}) \langle n_{\mathbf{k}} | i\mathbf{q}_2\mathbf{r} | n'_{\mathbf{k}} \rangle \langle n'_{\mathbf{k}} | e^{i\mathbf{G}_1\mathbf{r}} | n_{\mathbf{k}} \rangle \Delta_{nn'}^{\mathbf{q}_1+\mathbf{q}_2}}{\Delta_{nn'}^{LDA}\Delta_{nn'}^{SC}(\Delta_{nn'}^{SC} + \omega')} - \\
&- (f_{n,\mathbf{k}} - f_{n',\mathbf{k}}) \frac{\langle n_{\mathbf{k}} | e^{i\mathbf{G}_1\mathbf{r}} | n'_{\mathbf{k}} \rangle \left[\langle n'_{\mathbf{k}} | i(\mathbf{q}_1 + \mathbf{q}_2)\mathbf{r} | n_{\mathbf{k}} \rangle \Delta_{nn'}^{\mathbf{q}_2} + \langle n'_{\mathbf{k}} | i\mathbf{q}_2\mathbf{r} | n_{\mathbf{k}} \rangle \Delta_{nn'}^{\mathbf{q}_2+\mathbf{q}_2} \right]}{2\Delta_{nn'}^{LDA}\Delta_{nn'}^{SC}(\Delta_{nn'}^{SC} + \omega')} + \\
&+ (f_{n,\mathbf{k}} - f_{n',\mathbf{k}}) \frac{\Delta_{n''n'}^{LDA}}{\Delta_{nn'}^{LDA}} \frac{\langle n_{\mathbf{k}} | i\mathbf{q}_2\mathbf{r} | n''_{\mathbf{k}} \rangle \langle n''_{\mathbf{k}} | i(\mathbf{q}_1 + \mathbf{q}_2)\mathbf{r} | n'_{\mathbf{k}} \rangle \langle n'_{\mathbf{k}} | e^{i\mathbf{G}_1\mathbf{r}} | n_{\mathbf{k}} \rangle}{\Delta_{nn'}^{SC}(\Delta_{nn'}^{SC} + \omega')} + \\
&+ (f_{n,\mathbf{k}} - f_{n',\mathbf{k}}) \frac{\Delta_{n''n}^{LDA}}{\Delta_{nn'}^{LDA}} \frac{\langle n_{\mathbf{k}} | i(\mathbf{q}_1 + \mathbf{q}_2)\mathbf{r} | n''_{\mathbf{k}} \rangle \langle n''_{\mathbf{k}} | i\mathbf{q}_2\mathbf{r} | n'_{\mathbf{k}} \rangle \langle n'_{\mathbf{k}} | e^{i\mathbf{G}_1\mathbf{r}} | n_{\mathbf{k}} \rangle}{\Delta_{nn'}^{SC}(\Delta_{nn'}^{SC} + \omega')} + \\
&+ (f_{n,\mathbf{k}} - f_{n',\mathbf{k}}) \frac{\langle n_{\mathbf{k}} | e^{i\mathbf{G}_1\mathbf{r}} | n'_{\mathbf{k}} \rangle}{\Delta_{nn'}^{SC}(\Delta_{nn'}^{SC} + \omega')} \times \\
&\quad \times \left[\langle n'_{\mathbf{k}} | i(\mathbf{q}_1 + \mathbf{q}_2)\mathbf{r} | n''_{\mathbf{k}} \rangle \langle n''_{\mathbf{k}} | i\mathbf{q}_2\mathbf{r} | n_{\mathbf{k}} \rangle - \langle n'_{\mathbf{k}} | i\mathbf{q}_2\mathbf{r} | n''_{\mathbf{k}} \rangle \langle n''_{\mathbf{k}} | i(\mathbf{q}_1 + \mathbf{q}_2)\mathbf{r} | n_{\mathbf{k}} \rangle \right] - \\
&- 2(f_{n,\mathbf{k}} - f_{n',\mathbf{k}}) \frac{\langle n_{\mathbf{k}} | i(\mathbf{q}_1 + \mathbf{q}_2)\mathbf{r} | n'_{\mathbf{k}} \rangle}{\Delta_{nn'}^{SC}(\Delta_{nn'}^{SC} + 2\omega')} \times \\
&\quad \times \left[\langle n'_{\mathbf{k}} | e^{i\mathbf{G}_1\mathbf{r}} | n''_{\mathbf{k}} \rangle \langle n''_{\mathbf{k}} | i\mathbf{q}_2\mathbf{r} | n_{\mathbf{k}} \rangle - \langle n'_{\mathbf{k}} | i\mathbf{q}_2\mathbf{r} | n''_{\mathbf{k}} \rangle \langle n''_{\mathbf{k}} | e^{i\mathbf{G}_1\mathbf{r}} | n_{\mathbf{k}} \rangle \right] + \\
&+ (f_{n,\mathbf{k}} - f_{n',\mathbf{k}}) \frac{\langle n_{\mathbf{k}} | i\mathbf{q}_2\mathbf{r} | n'_{\mathbf{k}} \rangle}{2\Delta_{nn'}^{SC}(\Delta_{nn'}^{SC} + \omega')} \times \\
&\quad \times \left[\langle n'_{\mathbf{k}} | i(\mathbf{q}_1 + \mathbf{q}_2)\mathbf{r} | n''_{\mathbf{k}} \rangle \langle n''_{\mathbf{k}} | e^{i\mathbf{G}_1\mathbf{r}} | n_{\mathbf{k}} \rangle - \langle n'_{\mathbf{k}} | e^{i\mathbf{G}_1\mathbf{r}} | n''_{\mathbf{k}} \rangle \langle n''_{\mathbf{k}} | i(\mathbf{q}_1 + \mathbf{q}_2)\mathbf{r} | n_{\mathbf{k}} \rangle \right] - \\
&- \langle n_{\mathbf{k}} | i(\mathbf{q}_1 + \mathbf{q}_2)\mathbf{r} | n'_{\mathbf{k}} \rangle \left[\langle n'_{\mathbf{k}} | e^{i\mathbf{G}_1\mathbf{r}} | n''_{\mathbf{k}} \rangle \langle n''_{\mathbf{k}} | i\mathbf{q}_2\mathbf{r} | n_{\mathbf{k}} \rangle + \langle n'_{\mathbf{k}} | i\mathbf{q}_2\mathbf{r} | n''_{\mathbf{k}} \rangle \langle n''_{\mathbf{k}} | e^{i\mathbf{G}_1\mathbf{r}} | n_{\mathbf{k}} \rangle \right] \times \\
&\quad \times \left[\frac{(f_{n,\mathbf{k}} - f_{n'',\mathbf{k}})}{(\Delta_{nn'}^{SC} + 2\omega')(\Delta_{nn'''}^{SC} + \omega')} + \frac{(f_{n',\mathbf{k}} - f_{n'',\mathbf{k}})}{(\Delta_{nn'}^{SC} + 2\omega')(\Delta_{n''n'}^{SC} + \omega')} \right]
\end{aligned} \tag{C.44}$$

The case $\mathbf{G}_2 \neq 0$ follows from this one by exchanging $\mathbf{G}_1 \leftrightarrow \mathbf{G}_2$ and $\mathbf{q}_1 \leftrightarrow \mathbf{q}_2$.

C.3 Faces

C.3.1 $\mathbf{G} = 0$:

$$\begin{aligned}
\chi_{\rho\rho\rho}^{(0),face1}(\mathbf{q}_1 + \mathbf{q}_2, \mathbf{G}_1, \mathbf{G}_2) &= \frac{2}{V} \sum_{n,n',n'',\mathbf{k}} (f_{n,\mathbf{k}} - f_{n',\mathbf{k}}) \frac{\langle n_{\mathbf{k}} | i(\mathbf{q}_1 + \mathbf{q}_2)\mathbf{r} | n''_{\mathbf{k}} \rangle}{(\Delta_{nn'}^{SC} + \omega')(\Delta_{n'n}^{SC} + \omega')} \times \\
&\times [\langle n''_{\mathbf{k}} | e^{i\mathbf{G}_1\mathbf{r}} | n'_{\mathbf{k}} \rangle \langle n'_{\mathbf{k}} | e^{i\mathbf{G}_2\mathbf{r}} | n_{\mathbf{k}} \rangle + \langle n''_{\mathbf{k}} | e^{i\mathbf{G}_2\mathbf{r}} | n'_{\mathbf{k}} \rangle \langle n'_{\mathbf{k}} | e^{i\mathbf{G}_1\mathbf{r}} | n_{\mathbf{k}} \rangle] - \\
&- \langle n_{\mathbf{k}} | i(\mathbf{q}_1 + \mathbf{q}_2)\mathbf{r} | n'_{\mathbf{k}} \rangle [\langle n'_{\mathbf{k}} | e^{i\mathbf{G}_1\mathbf{r}} | n''_{\mathbf{k}} \rangle \langle n''_{\mathbf{k}} | e^{i\mathbf{G}_2\mathbf{r}} | n_{\mathbf{k}} \rangle + \langle n'_{\mathbf{k}} | e^{i\mathbf{G}_2\mathbf{r}} | n''_{\mathbf{k}} \rangle \langle n''_{\mathbf{k}} | e^{i\mathbf{G}_1\mathbf{r}} | n_{\mathbf{k}} \rangle] \times \\
&\times \left[\frac{(f_{n,\mathbf{k}} - f_{n',\mathbf{k}})}{(\Delta_{nn'}^{SC} + 2\omega')(\Delta_{nn''}^{SC} + \omega')} + \frac{(f_{n',\mathbf{k}} - f_{n'',\mathbf{k}})}{(\Delta_{nn'}^{SC} + 2\omega')(\Delta_{n'n''}^{SC} + \omega')} \right]
\end{aligned} \tag{C.45}$$

C.3.2 $\mathbf{G}_1 = 0$:

$$\begin{aligned}
\chi_{\rho\rho\rho}^{(0),face2}(\mathbf{G}, \mathbf{q}_1, \mathbf{G}_2) &= \frac{2}{V} \sum_{n,n',n'',\mathbf{k}} \left[\frac{(f_{n,\mathbf{k}} - f_{n'',\mathbf{k}})}{(\Delta_{nn'}^{SC} + 2\omega)(\Delta_{nn''}^{SC} + \omega)} + \frac{(f_{n',\mathbf{k}} - f_{n'',\mathbf{k}})}{(\Delta_{nn'}^{SC} + 2\omega)(\Delta_{n'n''}^{SC} + \omega)} \right] \times \\
&\times \langle n_{\mathbf{k}} | e^{-i\mathbf{G}\mathbf{r}} | n'_{\mathbf{k}} \rangle \left[\langle n'_{\mathbf{k}} | e^{i\mathbf{G}_2\mathbf{r}'} | n''_{\mathbf{k}} \rangle \langle n''_{\mathbf{k}} | \mathbf{q}_1\mathbf{r} | n_{\mathbf{k}} \rangle + \langle n'_{\mathbf{k}} | \mathbf{q}_1\mathbf{r} | n''_{\mathbf{k}} \rangle \langle n''_{\mathbf{k}} | e^{i\mathbf{G}_2\mathbf{r}'} | n_{\mathbf{k}} \rangle \right] + \\
&+ \frac{2(f_{n,\mathbf{k}} - f_{n',\mathbf{k}}) \langle n_{\mathbf{k}} | e^{-i\mathbf{G}\mathbf{r}} | n'_{\mathbf{k}} \rangle}{\Delta_{nn'}^{SC}(\Delta_{nn'}^{SC} + 2\omega)} \left[\langle n''_{\mathbf{k}} | \mathbf{q}_1\mathbf{r} | n_{\mathbf{k}} \rangle \langle n'_{\mathbf{k}} | e^{i\mathbf{G}_2\mathbf{r}'} | n''_{\mathbf{k}} \rangle - \langle n'_{\mathbf{k}} | \mathbf{q}_1\mathbf{r} | n''_{\mathbf{k}} \rangle \langle n''_{\mathbf{k}} | e^{i\mathbf{G}_2\mathbf{r}'} | n_{\mathbf{k}} \rangle \right] + \\
&+ \frac{4(f_{n,\mathbf{k}} - f_{n',\mathbf{k}}) \langle n_{\mathbf{k}} | e^{-i\mathbf{G}\mathbf{r}} | n'_{\mathbf{k}} \rangle \langle n'_{\mathbf{k}} | e^{i\mathbf{G}_2\mathbf{r}'} | n_{\mathbf{k}} \rangle \Delta_{nn'}^{\mathbf{q}_1}}{\Delta_{nn'}^{SC}(\Delta_{nn'}^{SC} + 2\omega)(\Delta_{nn'}^{SC} + \omega)} + \\
&+ \frac{(f_{n,\mathbf{k}} - f_{n',\mathbf{k}}) \langle n_{\mathbf{k}} | e^{-i\mathbf{G}\mathbf{r}} | n'_{\mathbf{k}} \rangle \langle n'_{\mathbf{k}} | e^{i\mathbf{G}_2\mathbf{r}'} | n_{\mathbf{k}} \rangle \Delta_{nn'}^{\mathbf{q}_1}}{(\Delta_{nn'}^{SC})^2(\Delta_{nn'}^{SC} + \omega)} + \\
&+ \frac{(f_{n,\mathbf{k}} - f_{n',\mathbf{k}}) \langle n'_{\mathbf{k}} | e^{i\mathbf{G}_2\mathbf{r}'} | n_{\mathbf{k}} \rangle}{\Delta_{nn'}^{SC}(\Delta_{nn'}^{SC} + \omega)} \left[\langle n_{\mathbf{k}} | e^{-i\mathbf{G}\mathbf{r}} | n''_{\mathbf{k}} \rangle \langle n''_{\mathbf{k}} | \mathbf{q}_1\mathbf{r} | n'_{\mathbf{k}} \rangle - \langle n_{\mathbf{k}} | \mathbf{q}_1\mathbf{r} | n''_{\mathbf{k}} \rangle \langle n''_{\mathbf{k}} | e^{-i\mathbf{G}\mathbf{r}} | n'_{\mathbf{k}} \rangle \right]
\end{aligned} \tag{C.46}$$

The case $\mathbf{G}_2 = 0$ follows from this one by exchanging $\mathbf{G}_1 \leftrightarrow \mathbf{G}_2$ and $\mathbf{q}_1 \leftrightarrow \mathbf{q}_2$.

D Derivation of the 2nd order Bethe-Salpeter equation

In this appendix I give the detailed derivation of the second order Bethe-Salpeter equation discussed in chapter 2.4.5.

The second order BSE is formulated in terms of the three-particle correlation function L_3 that is related to the three-particle Green's function via Schwingers functional derivative identity, Eq. (7.1) and its derivative¹:

$$\begin{aligned}
iL(1, 2, 3, 4, 5, 6) &= \frac{\delta^2 G(1, 2)}{\delta V(3, 4)\delta V(5, 6)} = -\frac{\delta G(1, 3, 2, 4)}{\delta V(5, 6)} + \frac{\delta G(1, 2)G(3, 4)}{\delta V(5, 6)} \\
&= -\frac{\delta G(1, 3, 2, 4)}{\delta V(5, 6)} + \frac{\delta G(1, 2)}{\delta V(5, 6)}G(3, 4) + G(1, 2)\frac{\delta G(3, 4)}{\delta V(5, 6)} \\
&= -\frac{\delta G(1, 3, 2, 4)}{\delta V(5, 6)} - \\
&\quad -G(1, 5, 2, 6)G(3, 4) + G(1, 2)G(5, 6)G(3, 4) \\
&\quad -G(1, 2)G(3, 5, 4, 6) + G(1, 2)G(3, 4)G(5, 6) \\
&= -G(1, 3, 5, 2, 4, 6) - \\
&\quad -G(1, 3, 2, 4)G(5, 6) - G(1, 5, 2, 6)G(3, 4) - G(3, 5, 4, 6)G(1, 2) + \\
&\quad +2G(1, 2)G(3, 4)G(5, 6) \tag{D.1}
\end{aligned}$$

where I used Schwinger's relation for G_3

$$\frac{\delta G(1, 3, 2, 4)}{\delta V(5, 6)} = G(1, 3, 5, 2, 4, 6) + G(1, 3, 2, 4)G(5, 6). \tag{D.2}$$

¹In this section the potential V always represents the *perturbing* potential V_{per} as opposed to the *total* potential.

To obtain a Bethe-Salpeter like equation for this quantity we simply have to derive the first order BSE (2.78):

$$\begin{aligned}
\frac{\delta L(1, 2, 3, 4)}{\delta V(5, 6)} &= \\
&= \frac{\delta}{\delta V(5, 6)} [-iG(1, 3)G(4, 2)] + \\
&\quad + \frac{\delta}{\delta V(5, 6)} \left[\int d789 10 (-i)G(1, 7)G(8, 2) \times \right. \\
&\quad \quad \times \left. \left[v(7, 9)\delta(7, 8)\delta(9, 10) + i\frac{\delta\Sigma(7, 8)}{\delta G(9, 10)} \right] (-i)\frac{\delta G(9, 10)}{\delta V(3, 4)} \right] \\
&= (-i)\frac{\delta G(1, 3)}{\delta V(5, 6)}G(4, 2) + (-i)G(1, 3)\frac{\delta G(4, 2)}{V(5, 6)} + \\
&\quad + \int d789 10 (-i)\frac{\delta G(1, 7)}{\delta V(5, 6)}G(8, 2) \left[v(7, 9)\delta(7, 8)\delta(9, 10) + i\frac{\delta\Sigma(7, 8)}{\delta G(9, 10)} \right] (-i)\frac{\delta G(9, 10)}{\delta V(3, 4)} \\
&\quad + \int d789 10 (-i)G(1, 7)\frac{\delta G(8, 2)}{\delta V(5, 6)} \left[v(7, 9)\delta(7, 8)\delta(9, 10) + i\frac{\delta\Sigma(7, 8)}{\delta G(9, 10)} \right] (-i)\frac{\delta G(9, 10)}{\delta V(3, 4)} \\
&\quad + \int d789 10 (-i)G(1, 7)G(8, 2)i\frac{\delta}{\delta V(5, 6)} \left[\frac{\delta\Sigma(7, 8)}{\delta G(9, 10)} \right] (-i)\frac{\delta G(9, 10)}{\delta V(3, 4)} \\
&\quad + \int d789 10 (-i)G(1, 7)G(8, 2) \times \\
&\quad \quad \times \left[v(7, 9)\delta(7, 8)\delta(9, 10) + i\frac{\delta\Sigma(7, 8)}{\delta G(9, 10)} \right] (-i)\frac{\delta^2 G(9, 10)}{\delta V(5, 6)\delta V(3, 4)} \\
&\hspace{15em} \text{(D.3)}
\end{aligned}$$

We note the repeated occurrence of first order quantities known from first order BSE. The only new term is the second derivative of the self energy in the second last line. In this term we use the chain rule and get

$$\frac{\delta}{\delta V(5, 6)} \left[\frac{\delta\Sigma(7, 8)}{\delta G(9, 10)} \right] = \int d11 12 \frac{\delta}{\delta G(11, 12)} \left[\frac{\delta\Sigma(7, 8)}{\delta G(9, 10)} \right] \frac{\delta G(11, 12)}{\delta V(5, 6)} \quad \text{(D.4)}$$

Analogously to the first order case, we define the six-point kernel:

$$\Xi(1, 2, 3, 4, 5, 6) = i\frac{\delta^2\Sigma(1, 2)}{\delta G(5, 6)\delta G(3, 4)} \quad \text{(D.5)}$$

and to keep the notation compact we also define a first order kernel that contains the coulomb potential:

$$\tilde{\Xi}(1, 2, 3, 4) = v(1, 3)\delta(1, 2)\delta(3, 4) + \Xi(1, 2, 3, 4) \quad \text{(D.6)}$$

Now inserting the known first order quantities we can write

$$\begin{aligned}
\frac{\delta L(1, 2, 3, 4)}{\delta V(5, 6)} &= L(1, 3, 5, 6)G(4, 2) + G(1, 3)L(4, 2, 5, 6) + \\
&+ \int d789 10 L(1, 7, 5, 6)G(8, 2)\tilde{\Xi}(7, 8, 9, 10)L(9, 10, 3, 4) + \\
&+ \int d789 10 G(1, 7)L(8, 2, 5, 6)\tilde{\Xi}(7, 8, 9, 10)L(9, 10, 3, 4) + \\
&+ \int d789 10 11 12 L_0(1, 2, 7, 8)\Xi(7, 8, 9, 10, 11, 12)L(11, 12, 5, 6)L(9, 10, 3, 4) \\
&+ \int d789 10 L_0(1, 2, 7, 8)\tilde{\Xi}(7, 8, 9, 10)\frac{\delta L(9, 10, 3, 4)}{\delta V(5, 6)}
\end{aligned} \tag{D.7}$$

This is in principle already a second order BSE. We note that at this point we do not need any six-point quantities other than the kernel.

To make the connection to the TDDFT Dyson equation and to avoid explicit reference to the one-particle Green's function G , we define

$$iL'_0(1, 2, 3, 4, 5, 6) = G(1, 3)G(4, 2)G(5, 6) \tag{D.8}$$

and insert the full first order expressions for the L_2 (Eq. (2.78)) in the above equation. Recalling the definition for $L_3 = \delta L_2 / \delta V$ we have ²

$$\begin{aligned}
L(123456) = & L'_0(135642) + L'_0(425613) + \\
& + \int d789\ 10 L'_0(137842) \tilde{\Xi}(78910) L(9\ 10\ 56) + \\
& + \int d789\ 10 L'_0(427813) \tilde{\Xi}(78910) L(9\ 10\ 56) + \\
& + \int d789\ 10 L'_0(175682) \tilde{\Xi}(789\ 10) L(9\ 10\ 34) + \\
& + \int d789\ 10 L'_0(825617) \tilde{\Xi}(789\ 10) L(9\ 10\ 34) + \\
& + \int d789\ 10\ 11\ 12\ 13\ 14 L'_0(17\ 11\ 12\ 82) \tilde{\Xi}(11\ 12\ 13\ 14) L(13\ 14\ 56) \tilde{\Xi}(789\ 10) L(9\ 10\ 34) + \\
& + \int d789\ 10\ 11\ 12\ 13\ 14 L'_0(82\ 11\ 12\ 17) \tilde{\Xi}(11\ 12\ 13\ 14) L(13\ 14\ 56) \tilde{\Xi}(789\ 10) L(9\ 10\ 34) + \\
& + \int d789\ 10\ 11\ 12 L_0(1278) \Xi(789\ 10\ 11\ 12) L(11\ 12\ 56) L(9\ 10\ 34) \\
& + \int d789\ 10 L_0(1278) \tilde{\Xi}(789\ 10) L(9\ 10\ 3456).
\end{aligned} \tag{D.9}$$

We note that the eight first terms are in fact pairs of terms with the same structure. This is due to the symmetry in the perturbing fields, i.e. it doesent make a physical difference if the $V(5, 6)$ field is applied before the $V(3, 4)$ field or vice versa. We can see that by exchanging the indices $3 \leftrightarrow 5$ and $4 \leftrightarrow 6$ in the equation. We therefore define an L_0 such that it accounts for these two possibilities:

$$iL_0(123456) = iL'_0(135642) + iL'_0(425613) = G(1, 5)G(6, 3)(4, 2) + G(1, 3)G(4, 5)(6, 2) \tag{D.10}$$

²To keep the equation readable I drop the separating commas between variables, relying on the readers goodwill to distinguish.

with this the second order BSE reads:

$$\begin{aligned}
L(123456) = & \\
& L_0(123456) + \\
& + \int d78910 L_0(123478) \tilde{\Xi}(78910) L(91056) + \\
& + \int d78910 L_0(127856) \tilde{\Xi}(78910) L(91034) + \\
& + \int d7891011121314 L_0(12781112) \tilde{\Xi}(11121314) L(131456) \tilde{\Xi}(78910) L(91034) + \\
& + \int d789101112 L_0(1278) \Xi(789101112) L(111256) L(91034) \\
& + \int d78910 L_0(1278) \tilde{\Xi}(78910) L(9103456).
\end{aligned} \tag{D.11}$$

To formally solve the second order BSE we rearrange it to

$$\begin{aligned}
\int d78910 \left[\delta(1,7) \delta(7,9) \delta(2,8) \delta(8,10) - L_0(1278) \tilde{\Xi}(78910) \right] L(9103456) = \\
= \int d7\dots14 L_0(12781112) \left[\delta(7,3) \delta(8,4) + \tilde{\Xi}(78910) L(91034) \right] \times \\
\times \left[\delta(5,11) \delta(6,12) + \tilde{\Xi}(11121314) L(131456) \right] + \\
+ \int d789101112 L_0(1278) \Xi(789101112) L(111256) L(91034).
\end{aligned} \tag{D.12}$$

Now we can use the linear BSE to write for the factor on the left hand side

$$\int d78 \left[\delta(1,9) \delta(2,10) - L_0(1278) \tilde{\Xi}(78910) \right] = \int d78 L_0(1278) L^{-1}(87109) \tag{D.13}$$

as well as to rewrite the two linear factors on the right hand side according to

$$\int d56 \left[\delta(3,1) \delta(4,2) + \tilde{\Xi}(1256) L(5634) \right] = \int d56 L_0^{-1}(2165) L(5634) \tag{D.14}$$

so that the second order BSE can be written as

$$\begin{aligned}
\int d78910 L_0(1278) L^{-1}(87109) L(9103456) = \\
= \int d7\dots14 L_0(12781112) L_0^{-1}(87109) L(91034) L_0^{-1}(12111413) L(131456) + \\
+ \int d789101112 L_0(1278) \Xi(789101112) L(111256) L(91034)
\end{aligned}$$

(D.15)

Now multiplying from the left with $\int d12\ 15\ 16L(17\ 18\ 15\ 16)L_0^{-1}(16\ 15\ 21)$ and renaming the indices $17 \leftrightarrow 1$ and $18 \leftrightarrow 2$ we have the final result

$$\begin{aligned}
L(123456) &= \\
&= \int d7\dots 18L(12\ 15\ 16)L_0^{-1}(16\ 15\ 18\ 17)L_0(17\ 18\ 78\ 11\ 12)\times \\
&\quad \times L_0^{-1}(8, 7\ 10\ 9)L(9\ 10\ 34)L_0^{-1}(12\ 11\ 14\ 13)L(13\ 14\ 56)+ \\
&\quad + \int d789\ 10\ 11\ 12\ 15\ 16L(12\ 15\ 16)\Xi(15\ 16\ 9\ 10\ 11\ 12)L(11\ 12\ 56)L(9\ 10\ 34)
\end{aligned}
\tag{D.16}$$

D.1 Solving the 2nd order BSE

In this section I will give a quick sketch how the solution of the second order Bethe-Salpeter equation might be evaluated in practice using the known scheme for solving the first order BSE.

In order to simplify the notation and the evaluation of the solution (D.16) we assume for the moment that Ξ_3 is indeed vanishing and we define the quantities

$$F(1234) = \int d56L(1256)L_0^{-1}(6543) \tag{D.17}$$

$$I(1234) = \int d56L_0^{-1}(2165)L(5634) \tag{D.18}$$

so that the solution reads

$$L(123456) = \int d7\dots 12F(1278)L_0^{(2)}(789\ 10\ 11\ 12)I(9\ 10\ 34)I(11\ 12\ 56). \tag{D.19}$$

The linear BSE is customarily solved in the linear transition space $(n\mathbf{k}) \leftrightarrow (n'\mathbf{k}')$, where the linear quantities are matrices. In this space the second order quantities are three dimensional arrays. Note that in principle one could define a second order transition space $(n\mathbf{k}) \leftrightarrow (n'\mathbf{k}') \leftrightarrow (n''\mathbf{k}'')$, where second order quantities are diagonal, but the product with the linear quantities in such a representation is not straightforward. We will therefore solve the equation in the linear transition space. Here, we are only interested in optic (i.e. vertical transitions), so we can drop the \mathbf{k} index and henceforth assume an implicit sum over all \mathbf{k} -points.

The definition of the transition space is such that L_{02} is diagonal, i.e. for any L_2

$$L(1234) = \sum_{n_1 n_2 n_3 n_4} \phi_{n_1}(1)\phi_{n_2}^*(2)\phi_{n_3}^*(3)\phi_{n_4}(4)L_{(n_1 n_2)}^{(n_3 n_4)} \tag{D.20}$$

and

$$L_{(n_1 n_2)}^{(n_3 n_4)} = \int d1234 \phi_{n_1}^*(1) \phi_{n_2}(2) \phi_{n_3}(3) \phi_{n_4}^*(4) L(1234). \quad (\text{D.21})$$

Inserting the real space representation of L_{02}

$$L_0(1234) = \sum_{ij} (f_i - f_j) \frac{\phi_i(1) \phi_j^*(2) \phi_i^*(3) \phi_j(4)}{\epsilon_i - \epsilon_j + \omega} \quad (\text{D.22})$$

yields

$$L_{0(n_1 n_2)}^{(n_3 n_4)} = (f_1 - f_2) \frac{\delta(n_1, n_3) \delta(n_2, n_4)}{\epsilon_1 - \epsilon_2 + \omega} \quad (\text{D.23})$$

Analogously, we define for the 6-point quantities:

$$L(123456) = \sum_{n_1 n_2 n_3 n_4 n_5 n_6} \phi_{n_1}(1) \phi_{n_2}^*(2) \phi_{n_3}^*(3) \phi_{n_4}(4) \phi_{n_5}^*(5) \phi_{n_6}(6) L_{(n_1 n_2)}^{(n_3 n_4)} \quad (\text{D.24})$$

and

$$L_{(n_1 n_2)}^{(n_3 n_4)} = \int d123456 \phi_{n_1}^*(1) \phi_{n_2}(2) \phi_{n_3}(3) \phi_{n_4}^*(4) \phi_{n_5}(5) \phi_{n_6}^*(6) L(123456) \quad (\text{D.25})$$

inserting the real space representation of L_{03}

$$\begin{aligned} L_0(123456) &= \sum_{ijk} \frac{\phi_i(\mathbf{r}_1) \phi_j^*(\mathbf{r}_2)}{(\epsilon_i - \epsilon_j + \omega_2 + \omega_3 + 2i\eta)} \times \\ &\quad \times \left[(f_i - f_k) \frac{\phi_j^*(\mathbf{r}_5) \phi_k(\mathbf{r}_6) \phi_k^*(\mathbf{r}_3) \phi_i(\mathbf{r}_4)}{(\epsilon_i - \epsilon_k + \omega_2 + i\eta)} + (f_j - f_k) \frac{\phi_j^*(\mathbf{r}_5) \phi_k(\mathbf{r}_6) \phi_k^*(\mathbf{r}_3) \phi_i(\mathbf{r}_4)}{(\epsilon_k - \epsilon_j + \omega_3 + i\eta)} + \right. \\ &\quad \left. (f_i - f_k) \frac{\phi_j^*(\mathbf{r}_3) \phi_k(\mathbf{r}_4) \phi_k^*(\mathbf{r}_5) \phi_i(\mathbf{r}_6)}{(\epsilon_i - \epsilon_k + \omega_3 + i\eta)} + (f_j - f_k) \frac{\phi_j^*(\mathbf{r}_3) \phi_k(\mathbf{r}_4) \phi_k^*(\mathbf{r}_5) \phi_i(\mathbf{r}_6)}{(\epsilon_k - \epsilon_j + \omega_2 + i\eta)} \right] \quad (\text{D.26}) \end{aligned}$$

yields

$$\begin{aligned} L_{0(n_1 n_2)}^{(n_3 n_4)} &= \frac{1}{(\epsilon_i - \epsilon_j + \omega_2 + \omega_3 + 2i\eta)} \times \\ &\quad \times \left[(f_1 - f_3) \frac{\delta(n_2, n_5) \delta(n_3, n_6) \delta(n_1, n_4)}{(\epsilon_1 - \epsilon_3 + \omega_2 + i\eta)} + (f_2 - f_3) \frac{\delta(n_2, n_5) \delta(n_3, n_6) \delta(n_1, n_4)}{(\epsilon_3 - \epsilon_2 + \omega_3 + i\eta)} + \right. \\ &\quad \left. (f_1 - f_4) \frac{\delta(n_2, n_3) \delta(n_4, n_5) \delta(n_1, n_6)}{(\epsilon_1 - \epsilon_4 + \omega_3 + i\eta)} + (f_2 - f_4) \frac{\delta(n_2, n_3) \delta(n_4, n_5) \delta(n_1, n_6)}{(\epsilon_4 - \epsilon_2 + \omega_2 + i\eta)} \right] \quad (\text{D.27}) \end{aligned}$$

With this notation the solution of the second order BSE reads

$$L \begin{pmatrix} n_5 n_6 \\ n_3 n_4 \\ n_1 n_2 \end{pmatrix} = \sum_{n_7 \dots n_{12}} F \begin{pmatrix} n_7 n_8 \\ n_1 n_2 \end{pmatrix} L_0 \begin{pmatrix} n_7 n_8 \\ n_9 n_{10} \\ n_{11} n_{12} \end{pmatrix} I \begin{pmatrix} n_3 n_4 \\ n_9 n_{10} \end{pmatrix} I \begin{pmatrix} n_5 n_6 \\ n_{11} n_{12} \end{pmatrix} \quad (\text{D.28})$$

The convenience of the representation in transition space is that one can assign to each pair of indices $(n_j n_k)$ a single index i , i.e $i \leftrightarrow (n_j n_k)$, so that we have to evaluate the rank three matrix equation

$$L_{ijk} = \sum_{lmn} F_{il} L_0 lmn I_{mj} I_{nk}. \quad (\text{D.29})$$

The second order polarizability χ_2 is then obtained from this result via

$$\chi(123) = L(112233) = \sum_{ijk} \phi_{i_1}(1) \phi_{i_2}^*(1) \phi_{j_1}^*(2) \phi_{j_2}(2) \phi_{k_1}^*(3) \phi_{k_2}(3) L_{ijk}. \quad (\text{D.30})$$

The method outlined here to evaluate the three-particle correlation function can be implemented on top of existing schemes to solve the linear BSE, provided they give L_2 in transition space. While the linear BSE is now almost routinely solved for systems with increasing complexity, it is however not clear if this method to obtain the three-particle correlation function is feasible in terms of computational resources because the scaling of the six-point quantity is very unfavorable.

E Hedin's equations

Hedin's equations are a set of self-consistent many-body equations that in principle give the exact single particle Green's function. They read:

$$\Sigma(1, 2) = i \int d34 G(1, 4) W(3, 1) \Gamma(4, 2, 3) \quad (\text{E.1})$$

$$G(1, 2) = G_H(1, 2) + \int d34 G_H(1, 3) \Sigma(3, 4) G(4, 2) \quad (\text{E.2})$$

$$\Gamma(1, 2, 3) = \delta(1, 2) \delta(1, 3) + \int d4567 \frac{\delta \Sigma(1, 2)}{\delta G(4, 5)} G(4, 6) G(7, 5) \Gamma(6, 7, 3) \quad (\text{E.3})$$

$$P(1, 2) = -i \int d34 G(2, 3) G(4, 2) \Gamma(3, 4, 1) \quad (\text{E.4})$$

$$W(1, 2) = v(1, 2) + \int d34 v(1, 2) P(3, 4) W(4, 2) \quad (\text{E.5})$$

While these equations form a closed set of equations, it is in practice not possible to solve them exactly so that many different approximations have been made to solve them at least partly.

In the following I will give the definitions of the constituent quantities of Hedin's equations, without going into detail about their physical motivation, which has been done in many other places [24, 96, 154]. The Hartree Green's function G_H can be defined from

$$\left[i \frac{\partial}{\partial t_1} - h_0(1) - V_H(1, 2) \right] G_H(1, 2) = \delta(1, 2) \quad (\text{E.6})$$

where $h_0(1) = -\nabla_1^2/2 + V_{ext}$ is the single particle Hamiltonian and V_H is the Hartree potential.

The self energy Σ is introduced to closed the equation of motion [95] of the Green's function by letting

$$i \int d3 v(1^+, 3) \frac{\delta G(1, 2)}{\delta V_{per}(3)} = \int d3 \Sigma(1, 3) G(3, 2) \quad (\text{E.7})$$

and is most commonly approximated as $\Sigma = GW$, where the screened interaction W reads

$$W(1, 2) = \int d3 \epsilon^{-1}(1, 2) v(3, 2). \quad (\text{E.8})$$

and ϵ^{-1} is the (time ordered) screening

$$\epsilon^{-1}(1, 2) = \frac{\delta V_{\text{tot}}(1)}{\delta V_{\text{per}}(2)} = \delta_{1,2} + \int d3v(1, 3)\chi(3, 2). \quad (\text{E.9})$$

The vertex Γ contains the higher order corrections to the self energy and is defined as

$$\Gamma(1, 2, 3) = -\frac{\delta G^{-1}(1, 2)}{\delta V_{\text{tot}}(3)}. \quad (\text{E.10})$$

The irreducible polarizability P is closely related to the reducible polarizability χ_1 , Eq. (2.34), and is defined as

$$P(1, 2) = \frac{\delta \rho(1)}{V_{\text{tot}}(2)} \quad (\text{E.11})$$

so it is the variation of the density with respect to the total instead the perturbing potential, as in the case of χ_1 . Their relation obeys the Dyson equation

$$\chi(1, 2) = P(1, 2) + \int d34P(1, 3)v(3, 4)\chi(4, 2). \quad (\text{E.12})$$

E.1 Second order Irreducible Polarizability

For the second order χ_2 , which in this context is called the second order reducible polarizability, one can derive the analogous second order irreducible polarizability P_2 . Starting from the definition of χ_2

$$\chi(1, 2, 3) = \frac{\delta^2 \rho(1)}{\delta V_{\text{per}}(3)\delta V_{\text{per}}(2)} \quad (\text{E.13})$$

we can make the connection to the irreducible quantities in Hedin's equations. We use the chainrule to obtain derivative with respect to the total potential:

$$\begin{aligned} \chi(1, 2, 3) &= \frac{\delta \rho(1)}{\delta V_{\text{per}}(3)} \left[\int d4 \frac{\delta \rho(1)}{\delta V_{\text{tot}}(4)} \frac{\delta V_{\text{tot}}(4)}{\delta V_{\text{per}}(2)} \right] \\ &= \int d45 \frac{\delta}{\delta V_{\text{tot}}(5)} \left[\frac{\delta \rho(1)}{\delta V_{\text{tot}}(4)} \frac{\delta V_{\text{tot}}(4)}{\delta V_{\text{per}}(2)} \right] \frac{\delta V_{\text{tot}}(5)}{\delta V_{\text{per}}(3)} \\ &= \int d45 \frac{\delta^2 \rho(1)}{\delta V_{\text{tot}}(5)\delta V_{\text{tot}}(4)} \frac{\delta V_{\text{tot}}(4)}{\delta V_{\text{per}}(2)} \frac{\delta V_{\text{tot}}(5)}{\delta V_{\text{per}}(3)} + \\ &\quad + \int d45 \frac{\delta \rho(1)}{\delta V_{\text{tot}}(4)} \frac{\delta^2 V_{\text{tot}}(4)}{\delta V_{\text{tot}}(5)\delta V_{\text{per}}(2)} \frac{\delta V_{\text{tot}}(5)}{\delta V_{\text{per}}(3)} \\ &= \int d45 \frac{\delta^2 \rho(1)}{\delta V_{\text{tot}}(5)\delta V_{\text{tot}}(4)} \frac{\delta V_{\text{tot}}(4)}{\delta V_{\text{per}}(2)} \frac{\delta V_{\text{tot}}(5)}{\delta V_{\text{per}}(3)} + \int d4 \frac{\delta \rho(1)}{\delta V_{\text{tot}}(4)} \frac{\delta^2 V_{\text{tot}}(4)}{\delta V_{\text{per}}(3)\delta V_{\text{per}}(2)} \end{aligned}$$

Now we use the definitions of the screening ϵ^{-1} , Eq. (E.9), the linear irreducible polarizability P_1 , Eq. (E.11) and define the second order irreducible polarizability as

$$P(1, 2, 3) = \frac{\delta^2 \rho(1)}{\delta V_{\text{tot}}(3) \delta V_{\text{tot}}(2)} \quad (\text{E.14})$$

so we can write

$$\chi(1, 2, 3) = \int d45 P(1, 4, 5) \epsilon^{-1}(4, 2) \epsilon^{-1}(5, 3) + \int d4 P(1, 4) \frac{\delta^2 V_{\text{tot}}(4)}{\delta V_{\text{per}}(3) \delta V_{\text{per}}(2)}. \quad (\text{E.15})$$

Using again Eq. (E.9) for ϵ^{-1} in this expression and carrying out

$$\frac{\delta^2 V_{\text{tot}}(4)}{\delta V_{\text{per}}(3) \delta V_{\text{per}}(2)} = \frac{\delta \epsilon^{-1}(4, 2)}{\delta V_{\text{per}}(3)} = \int d5 v(4, 5) \chi(5, 2, 3) \quad (\text{E.16})$$

we obtain

$$\begin{aligned} \chi(1, 2, 3) = & \int d4567 P(1, 4, 5) [\delta(4, 2) + v(4, 6) \chi(6, 2)] [\delta(5, 3) + v(5, 7) \chi(7, 3)] + \\ & + \int d45 P(1, 4) v(4, 5) \chi(5, 2, 3). \end{aligned} \quad (\text{E.17})$$

In analogy with the Dyson like equation for $\chi^{(2)}$ (2.47) this can be formally solved by using the first order Dyson equation for the reducible polarizability (E.12) in steps similar to Eqs. (2.48)-(2.55). The final relations are

$$\begin{aligned} \chi(1, 2, 3) = & \\ & \int d4567 [\delta(1, 9) + \chi(1, 8) v(8, 9)] P(9, 4, 5) [\delta(4, 2) + v(4, 6) \chi(6, 2)] [\delta(5, 3) + v(5, 7) \chi(7, 3)] \end{aligned} \quad (\text{E.18})$$

and

$$\begin{aligned} P(1, 2, 3) = & \\ & \int d4567 [\delta(1, 9) - v(8, 9) P(1, 8)] \chi(9, 4, 5) [\delta(4, 2) - v(4, 6) P(6, 2)] [\delta(5, 3) - v(5, 7) P(7, 3)] \end{aligned} \quad (\text{E.19})$$

or alternatively expressed with inverse linear quantities

$$\begin{aligned} \chi(1, 2, 3) = & \int d4\dots d9 \chi(1, 8) P^{-1}(8, 9) P(9, 5, 4) P^{-1}(5, 6) \chi(6, 2) P^{-1}(4, 7) \chi(7, 3) \\ P(1, 2, 3) = & \int d4\dots d9 P(1, 8) \chi^{-1}(8, 9) \chi(9, 5, 4) \chi^{-1}(5, 6) P(6, 2) \chi^{-1}(4, 7) P(7, 3). \end{aligned} \quad (\text{E.20})$$

These are the relations between reducible and irreducible quantities for the second order case.

The second order irreducible polarizability (E.14) contains all many body interactions and can be obtained from Hedin's equation for the first order, Eq. (E.4), by deriving with respect to V_{tot} :

$$P(1, 2, 3) = \frac{\delta^2 \rho(1)}{\delta V_{\text{tot}}(3) \delta V_{\text{tot}}(2)} = \frac{\delta P(1, 2)}{V_{\text{tot}}(3)} \quad (\text{E.21})$$

$$= -i \int d45 \frac{\delta G(2, 4)}{\delta V_{\text{tot}}(3)} G(5, 2) \Gamma(4, 5, 1) - \quad (\text{E.22})$$

$$-i \int d45 G(2, 4) \frac{\delta G(5, 2)}{\delta V_{\text{tot}}(3)} \Gamma(4, 5, 1) - \quad (\text{E.23})$$

$$-i \int d45 G(2, 4) G(5, 2) \frac{\delta \Gamma(4, 5, 1)}{\delta V_{\text{tot}}(3)}. \quad (\text{E.24})$$

The derivative of G with respect to the total field can be expressed in terms of the vertex. To this end we take the derivative of the identity

$$\int d3 G^{-1}(1, 3) G(3, 2) = \delta(1, 2) \quad (\text{E.25})$$

with respect to the total field

$$\int d3 G^{-1}(1, 3) \frac{\delta G(3, 2)}{\delta V_{\text{tot}}(4)} = - \int d3 \frac{\delta G^{-1}(1, 3)}{\delta V_{\text{tot}}(4)} G(3, 2) \quad (\text{E.26})$$

and it follows

$$\frac{\delta G(1, 2)}{\delta V_{\text{tot}}(3)} = - \int d45 G(1, 4) \frac{\delta G^{-1}(4, 5)}{\delta V_{\text{tot}}(3)} G(5, 2). \quad (\text{E.27})$$

Furthermore we use the definition of the irreducible vertex function, Eq. (E.10) so we have for our second order irreducible polarizability

$$P(1, 2, 3) = +i \int d4567 G(2, 6) \Gamma(6, 7, 3) G(7, 4) G(5, 2) \Gamma(4, 5, 1) - \quad (\text{E.28})$$

$$+i \int d45 G(2, 4) G(5, 6) \Gamma(6, 7, 3) G(7, 2) \Gamma(4, 5, 1) - \quad (\text{E.29})$$

$$-i \int d45 G(2, 4) G(5, 2) \frac{\delta \Gamma(4, 5, 1)}{\delta V_{\text{tot}}(3)}. \quad (\text{E.30})$$

F Second order TDDFT and BSE

In this appendix I will give some details concerning the derivation of the second order many body exchange and correlation kernel g_{xc} as described in Sec. 7.5.

To combine the second order Bethe Salpeter equation and the TDDFT Dyson like equation we have to represent the TDDFT equation in terms of four and six point quantities, written as 4P and 6P . The Dyson like equation for the irreducible polarizability reads:

$$\begin{aligned} {}^6P(1, 2, 3, 4, 5, 6) = & \int d7..19 {}^4P(1, 2, 7, 8) {}^4P_0^{-1}(8, 7, 10, 9) {}^6P_0(9, 10, 11, 12, 13, 14) \times \\ & \times {}^4P_0^{-1}(12, 11, 16, 17) {}^4P(16, 17, 3, 4) {}^4P_0^{-1}(14, 13, 19, 18) {}^4P(18, 19, 5, 6) + \\ & + \int d7..12 {}^4P(1, 2, 7, 8) {}^6g_{xc}(7, 8, 9, 10, 11, 12) {}^4P(9, 10, 3, 4) {}^4P(11, 12, 5, 6) \end{aligned} \quad (\text{F.1})$$

where

$${}^6g_{xc}(7, 8, 9, 10, 11, 12) = \delta(7, 8)\delta(9, 10)\delta(11, 12)g_{xc}(7, 9, 11) \quad (\text{F.2})$$

and the linear quantities obey the four point Dyson equation, like

$${}^4P(1, 2, 3, 4) = \int d5678 {}^4P_0(1, 2, 5, 6) [\delta(3, 5)\delta(4, 6) + \delta(5, 6)\delta(7, 8)f(5, 7)P(7, 8, 3, 4)] \quad (\text{F.3})$$

so that

$$\int d12 {}^4P_0^{-1}(10, 9, 2, 1) {}^4P(1, 2, 3, 4) = \int d78 [\delta(3, 9)\delta(4, 10) + \delta(9, 10)\delta(7, 8)f(9, 7)P(7, 8, 3, 4)] \quad (\text{F.4})$$

so that when one takes the contraction $P(1, 1, 2, 2, 3, 3)$ of Eq. (F.1) it collapses to

$$\begin{aligned} P(1, 2, 3) = & \int d456789P(1, 4)P_0^{-1}(4, 5)P_0(5, 6, 7)P_0^{-1}(6, 8)P(8, 2)P_0^{-1}(7, 9)P(9, 2) + \\ & + \int d45P(1, 4)g_{xc}(4, 5, 6)P(5, 2)P(6, 3). \end{aligned} \quad (\text{F.5})$$

With this definitions the 'Sham-Schlüter' equation (7.27) reads

$$\begin{aligned}
& \int d7..12\tilde{L}^{-1}(1278)\tilde{L}(789\ 10\ 11\ 12)\tilde{L}^{-1}(10\ 9\ 34)\tilde{L}^{-1}(12\ 11\ 56)- \\
& \int d7..12{}^4P^{-1}(1278){}^6P(789\ 10\ 11\ 12){}^4P^{-1}(10\ 9\ 34){}^4P^{-1}(12\ 11\ 56) = \quad (F.6) \\
& = \Xi(123456) - {}^6g_{xc}(123456)
\end{aligned}$$

and can be solved for \tilde{L}_3 to yield

$$\begin{aligned}
& \tilde{L}(13\ 14\ 15\ 16\ 17\ 18) = \\
& = \int d1..12\tilde{L}(13\ 14\ 21){}^4P^{-1}(1278){}^6P(789\ 10\ 11\ 12){}^4P^{-1}(10\ 9\ 34)\tilde{L}(43\ 15\ 16)\times \\
& \quad \times {}^4P^{-1}(12\ 11\ 56)\tilde{L}(65\ 17\ 18)+ \quad (F.7) \\
& + \int d1..6\tilde{L}(13\ 14\ 21) [\Xi(123456) - {}^6g_{xc}(123456)] \tilde{L}(43\ 15\ 16)\tilde{L}(65\ 17\ 18).
\end{aligned}$$

Now, to use the property $\tilde{L}(13\ 13\ 15\ 15\ 17\ 17) = P(13, 15, 17)$ we carry out this contraction, as well as collapsing all redundant indices and obtain

$$\begin{aligned}
& P(13, 15, 17) = \\
& = \int d1..12\tilde{L}(13\ 13\ 21){}^4P^{-1}(1277)P(79\ 11){}^4P^{-1}(9\ 9\ 34)\tilde{L}(43\ 15\ 15)\times \\
& \quad \times {}^4P^{-1}(11\ 11\ 56)\tilde{L}(65\ 17\ 17)+ \quad (F.8) \\
& + \int d1..6\tilde{L}(13\ 13\ 21)\Xi(123456)\tilde{L}(43\ 15\ 15)\tilde{L}(65\ 17\ 17)- \\
& - \int d135\tilde{L}(13\ 13\ 11)g_{xc}(135)\tilde{L}(33\ 15\ 15)\tilde{L}(55\ 17\ 17).
\end{aligned}$$

The diagonal \tilde{L}_2 in the last term are in fact P_1 quantities, so that we obtain solving this equation for g_{xc}

$$\begin{aligned}
& g_{xc}(1, 2, 3) = \\
& = \int d4..15P^{-1}(1, 4) \left[\tilde{L}(4456){}^4P^{-1}(6577)P_2(7, 8, 9){}^4P^{-1}(88\ 11\ 10)\tilde{L}(10\ 11\ 12\ 12) \times \right. \\
& \quad \left. \times {}^4P^{-1}(99\ 14\ 13)\tilde{L}(13\ 14\ 15\ 15) - P_2(4, 12, 15) \right] P^{-1}(12, 2)P^{-1}(15, 3)+ \\
& + \int d4..12P^{-1}(1, 4)\tilde{L}(4456)\Xi(6587\ 10\ 9)\tilde{L}(78\ 11\ 11)\tilde{L}(9\ 10\ 12\ 12)P^{-1}(12, 2)P^{-1}(12, 3). \quad (F.9)
\end{aligned}$$

List of Publications

- Ab-initio calculation of Second Harmonic Generation in solids
H. Hübener, E. Luppi and V. Vénard
Physica Status Solidi (b), **247**, 1984 (2010)
- Ab initio second-order nonlinear optics in solids
E. Luppi, H. Hübener and V. Vénard
Journal of Chemical Physics, **132**, 241104 (2010)
- First-principles calculation of Second Harmonic Generation for cubic semiconductors using Time-Dependent Density-Functional Theory
E. Luppi, H. Hübener and V. Vénard
(submitted to Physical Review B)
- Local Fields and Excitons in Second Harmonic Generation of SiC polytypes
H. Hübener, E. Luppi and V. Vénard
(in preparation, to be submitted to Physical Review B)
- Ab initio tool for second-order nonlinear optical properties: 2light code
E. Luppi, H. Hübener and V. Vénard
(in preparation, to be submitted to Computer Physics Communications)
- Second order exchange and correlation effects described by a generalized Bethe-Salpeter equation
H. Hübener
(in preparation, to be submitted to Physical Review A)
- Second harmonic generation in bulk Si from ab initio calculations
H. Hübener, R. Hambach, E. Luppi and V. Vénard
(in preparation, to be submitted to Physical Review B)

Acknowledgements

I am happy to acknowledge my deep gratitude to my supervisor **Valérie Vényard**, to whom I owe the existence of this thesis and its is essentially her ideas that are presented here. I am thankful for the rigour and consequence with which she has followed this project and by being always available for discussion and ideas she created a very pleasant working atmosphere.

An almost equal amount of thank is due to **Eleonora Luppi**, who very thoroughly followed the coding process, was always available for questions and thus crucially contributed to this work.

I also would like to thank **Ralf Hambach** with whom I shared a great many long discussions on a variety of topics and who was always ready to critically asses new ideas, follow them through when they seemed reasonable and pushing for their realization. His unforgiving rigour and toughness to convince prevented me from making many mistake, but led to the realization of the multigrid approach and many other formal ideas in this thesis.

To **Matteo Gatti** I owe the chapter on the second order Bethe-Salpeter equation, because it was he who repeatedly pointed me in the right directions, who taught me the little I know on this subject and who guided me through the development of this idea.

I also enjoyed many discussion with **Arjan Berger**, whose implementation of current response I used in parts of this work and who was always willing to write down definitions and sketch derivations. I also appreciated him as a great source of trivia.

Lucia Reining provided usefull comments and discussions on many-body perturbation theory and other fundamental topics and pointed me in new directions. I am thankful to her for creating an atmosphere of scientific honesty and relevance and in general a very collegial working spirit.

With **Francesco Sottile** I had many discussions on technicalities and fundamentals I a greatly appreciated his openness for ideas and their critical assessment.

Special thanks goes to **France Pochard** who worked the miracle of keeping me out of any administrative hassle and kept any paperwork at a surprisingly small minimum.

Furthermore I want to thank **Federico Iori, Julien Vidal, Alberto Zobelli, Pina Romaniello, Irene Aguilera, Matteo Guzzo, Andrea Cucca, Christine Giorgetti, Silvana Botti, Lorenzo Sponza, Hansi Weissker, Xochitl Lopez-Lozano, Gaëlle Bruant** and all of the above for the friendly atmosphere, the many entertaining coffee breaks, dinner occasions and conference trips and many technical help and — last but not least — **Giovanna Lani** for being a surprisingly pleasant office mate.

I also would like to thank the referees **Prof. Eric Suraud** and **Prof. Friedhelm Bechstedt** for taking the trouble of reading this manuscript and the latter also for several very usefull discussions throughout the course of this project.

Bibliography

- [1] M. Göppert-Mayer, *Annalen der Physik* **401** (1931).
- [2] P. A. Franken and *et al.*, *Phys. Rev. Lett.* **7**, 118 (1961).
- [3] Y. R. Shen, *Principles of Nonlinear Optics*, Series in Pure and Applied Optics (Wiley, Hoboken, 2003).
- [4] R. W. Boyd, *Nonlinear Optics* (Academic Press, San Diego, 1992).
- [5] C. Chen, Z. Lin, and Z. Wang, *Applied Physics B: Lasers and Optics* **80**, 1 (2005).
- [6] Y. Tong, X. Y. Meng, Z. Z. Wang, C. Chen, and M.-H. Lee, *Journal of Applied Physics* **98**, 033504 (pages 7) (2005).
- [7] C. Manzo, A. Savoia, D. Paparo, and L. Marrucci, *Molecular Crystals and Liquid Crystals* **454**, 91 (2006).
- [8] R. Ehlert, K. Jinhee, L. Loumakos, O. Sahria, A. A. Demkov, and M. Downer, *J. Opt. Soc. Am. B* (2010).
- [9] J. Proce, Y. Q. An, and M. Downer, *physica status solidi (c)* **5**, 2667 (2008).
- [10] Y. D. Glinka, N. H. Tolk, X. Liu, Y. Sasaki, and J. K. Furdyna, *Applied Physics Letters* **91**, 231104 (pages 3) (2007).
- [11] M. M. Albert and N. H. Tolk, *Phys. Rev. B* **63**, 035308 (2000).
- [12] Y. Takimoto, F. D. Vila, and J. J. Rehr, *J. Chem. Phys.* **127**, 154114 (2007).
- [13] L. Frediani, H. Ågren, L. Ferrighi, and K. Ruud, *J. Chem. Phys.* **123**, 144117 (2005).
- [14] J. Salafsky, *J. Chem. Phys.* **125**, 074701 (2006).
- [15] M. Oh-e, H. Yokoyama, S. Yorozya, K. Akagi, M. A. Belkin, and Y. R. Shen, *Phys. Rev. Lett.* **93**, 267402 (2004).
- [16] S. A. Mitchell, R. A. McAloney, D. Moffatt, N. Mora-Diez, and M. Z. Zgierski, *J. Chem. Phys.* **122**, 114707 (2005).
- [17] D. A. Hammons and *et al.*, *Opt. Commun.* **156** , 328 (1998).
- [18] A. Lupei and *et al.*, *Phys. Rev. B* **65**, 224518 (2002).

- [19] M. Born and R. Oppenheimer, *Ann. Phys.* **84**, 457 (1927).
- [20] F. Bloch, *Z. Phys.* **52**, 553 (1928).
- [21] R. Martin, *Electronic Structure* (Cambridge University Press, Cambridge, 2004).
- [22] M. S. Hybertsen and S. G. Louie, *Phys. Rev. B* **34**, 5390 (1986).
- [23] R. W. Godby, M. Schlüter, and L. J. Sham, *Phys. Rev. B* **37**, 10159 (1988).
- [24] L. Hedin and S. Lundqvist, in *Solid State Physics*, edited by F. Turnbull (Academic Press, New York, 1969) Vol. 23, p.1.
- [25] F. Sottile, V. Olevano, and L. Reining, *Phys. Rev. Lett.* **91**, 056402 (2003).
- [26] G. Adragna, R. Del Sole, and A. Marini, *Phys. Rev. B* **68**, 165108 (2003).
- [27] A. Marini and R. Del Sole, *Phys. Rev. Lett.* **91**, 176402 (2003).
- [28] R. Stubner, I. V. Tokatly, and O. Pankratov, *Phys. Rev. B* **70**, 245119 (2004).
- [29] F. Bruneval, F. Sottile, V. Olevano, R. Del Sole, and L. Reining, *Phys. Rev. Lett.* **94**, 186402 (2005).
- [30] J. A. Armstrong, N. Bloembergen, J. Ducuing, and P. S. Pershan, *Phys. Rev.* **127**, 1918 (1962).
- [31] R. Loudon, *Proceedings of the Physical Society* **80**, 952 (1962).
- [32] M. I. Bell, in *Electronic Density of States*, edited by L. H. Bennett (U. S. GPO, Washington, D. C., 1971), *Natl. Bur. Std. (U. S.) Spec. Publ. No. 323*, p. 757.
- [33] P. N. Butcher and T. P. McLean, *Proceedings of the Physical Society* **81**, 219 (1963).
- [34] P. N. Butcher and T. P. McLean, *Proceedings of the Physical Society* **83**, 579 (1964).
- [35] D. E. Aspnes, *Phys. Rev. B* **6**, 4648 (1972).
- [36] D. J. Moss, J. E. Sipe, and H. M. van Driel, *Phys. Rev. B* **36**, 9708 (1987).
- [37] E. Ghahramani, D. J. Moss, and J. E. Sipe, *Phys. Rev. Lett.* **64**, 2815 (1990).
- [38] E. Ghahramani, D. J. Moss, and J. E. Sipe, *Phys. Rev. B* **43**, 8990 (1991).
- [39] Z. H. Levine and D. C. Allan, *Phys. Rev. Lett.* **66**, 41 (1991).
- [40] Z. H. Levine and D. C. Allan, *Phys. Rev. B* **44**, 12781 (1991).
- [41] Z. H. Levine and D. C. Allan, *Phys. Rev. B* **48**, 7783 (1990).

- [42] Z. H. Levine, Phys. Rev. B **49**, 4532 (1994).
- [43] M.-Z. Huang and W. Y. Ching, Phys. Rev. B **45**, 8738 (1992).
- [44] M.-Z. Huang and W. Y. Ching, Phys. Rev. B **47**, 9464 (1993).
- [45] D. J. Moss, E. Ghahramani, J. E. Sipe, and H. M. van Driel, Phys. Rev. B **41**, 1542 (1990).
- [46] J. E. Sipe and E. Ghahramani, Phys. Rev. B **48**, 11705 (1993).
- [47] C. Aversa and J. E. Sipe, Phys. Rev. B **52**, 14636 (1995).
- [48] J. L. P. Hughes and J. E. Sipe, Phys. Rev. B **53**, 10751 (1996).
- [49] J. L. P. Hughes and J. E. Sipe, Phys. Rev. B **58**, 7761 (1998).
- [50] S. N. Rashkeev, W. R. L. Lambrecht, and B. Segall, Phys. Rev. B **57**, 9705 (1998).
- [51] S. N. Rashkeev, S. Limpijumnong, and W. R. L. Lambrecht, Phys. Rev. B **59**, 2737 (1999).
- [52] S. N. Rashkeev and W. R. L. Lambrecht, Applied Physics Letters **77**, 190 (2000).
- [53] S. N. Rashkeev and W. R. L. Lambrecht, Phys. Rev. B **63**, 165212 (2001).
- [54] T. R. Paudel and W. R. L. Lambrecht, Phys. Rev. B **79**, 245205 (2009).
- [55] V. I. Gavrilenko and R. Q. Wu, Phys. Rev. B **61**, 2632 (2000).
- [56] S. Sharma, J. K. Dewhurst, and C. Ambrosch-Draxl, Phys. Rev. B **67**, 165332 (2003).
- [57] R. E. Alonso, S. Sharma, C. Ambrosch-Draxl, C. O. Rodriguez, and N. E. Christensen, Phys. Rev. B **73**, 064101 (2006).
- [58] S. N. Rashkeev, W. R. L. Lambrecht, and B. Segall, Phys. Rev. B **57**, 3905 (1998).
- [59] A. Dal Corso and F. Mauri, Phys. Rev. B **50**, 5756 (1994).
- [60] P. W. Langhoff, S. T. Epstein, and M. Karplus, Rev. Mod. Phys. **44**, 602 (1972).
- [61] A. Dal Corso, F. Mauri, and A. Rubio, Phys. Rev. B **53**, 15638 (1996).
- [62] S. Sharma and C. Ambrosch-Draxl, Physica Scripta **T109**, 128 (2004).
- [63] V. I. Gavrilenko, Phys. Rev. B **77**, 155311 (2008).
- [64] V. Gavrilenko, physica status solidi (a) **188**, 1267 (2001).
- [65] G. Y. Guo, K. C. Chu, D.-s. Wang, and C.-g. Duan, Phys. Rev. B **69**, 205416 (2004).

- [66] I. J. Wu and G. Y. Guo, *Phys. Rev. B* **78**, 035447 (2008).
- [67] B. Adolph and F. Bechstedt, *Phys. Rev. B* **57**, 6519 (1998).
- [68] E. C. Chang, E. L. Shirley, and Z. H. Levine, *Phys. Rev. B* **65**, 035205 (2001).
- [69] R. Leitsmann, W. G. Schmidt, P. H. Hahn, and F. Bechstedt, *Phys. Rev. B* **71**, 195209 (2005).
- [70] D. R. Kanis, M. A. Ratner, and T. J. Marks, *Chemical Reviews* **94**, 195 (1994).
- [71] J. E. Rice and N. C. Handy, *Int. J. Quantum Chem.* **43**, 91 (1992).
- [72] G. D. Mahan and K. R. Subbaswamy, *Local Density Theory of Polarizability* (Plenum, New York, 1990).
- [73] J. Guan, P. Duffy, J. T. Carter, D. P. Chong, K. C. Casida, M. E. Casida, and M. Wrinn, *The Journal of Chemical Physics* **98**, 4753 (1993).
- [74] S. J. A. van Gisbergen, J. G. Snijders, and E. J. Baerends, *The Journal of Chemical Physics* **109**, 10657 (1998).
- [75] S. J. A. van Gisbergen, J. G. Snijders, and E. J. Baerends, *The Journal of Chemical Physics* **109**, 10644 (1998).
- [76] B. Champagne, E. A. Perpete, S. J. A. van Gisbergen, E.-J. Baerends, J. G. Snijders, C. Soubra-Ghaoui, K. A. Robins, and B. Kirtman, *The Journal of Chemical Physics* **109**, 10489 (1998).
- [77] S. Tretiak and S. Mukamel, *Chemical Reviews* **102**, 3171 (2002).
- [78] P. Salek, O. Vahtras, T. Helgaker, and H. Agren, *The Journal of Chemical Physics* **117**, 9630 (2002).
- [79] S. Tretiak and V. Chernyak, *The Journal of Chemical Physics* **119**, 8809 (2003).
- [80] Z. Rinkevicius, P. C. Jha, C. I. Oprea, O. Vahtras, and H. Agren, *The Journal of Chemical Physics* **127**, 114101 (2007).
- [81] P. Romaniello, M. C. D'Andria, and F. Lelj, *The Journal of Physical Chemistry A* **114**, 5838 (2010).
- [82] S. van Gisbergen, J. Snijders, and E. Baerends, *Computer Physics Communications* **118**, 119 (1999).
- [83] R. van Leeuwen and E. J. Baerends, *Phys. Rev. A* **49**, 2421 (1994).
- [84] M. Gruning, O. Gritsenko, S. van Gisbergen, and E. Baerends, *The Journal of Chemical Physics* **116**, 9591 (2002).

- [85] E. Gross, J. Dobson, and M. Petersilka, in *Density-functional theory of time-dependent phenomena* (Springer, 1996), vol. 181 of *Topics in Current Chemistry*, pp. 81–172.
- [86] S. L. Adler, Phys. Rev. **126**, 413 (1962).
- [87] N. Wiser, Phys. Rev. **129**, 62 (1963).
- [88] R. Kubo, J. Phys. Soc. Japan **12**, 570 (1957).
- [89] R. van Leeuwen, *Introduction to time-dependent density functional theory*, URL <http://www.tddft.org/TDDFT2006/2006tddft/docs/school/vanLeeuwen-I+II.pdf> (2006).
- [90] J. D. Franson and M. M. Donegan, Phys. Rev. A **65**, 052107 (2002).
- [91] M. A. L. Marques, C. A. Ullrich, F. Nogueira, A. Rubio, K. Burke, and E. K. U. Gross (eds.) *Time-Dependent Density Functional Theory*, vol. 706 of *Lecture Notes in Physics* (Springer, Berlin / Heidelberg, 2006).
- [92] E. Runge and E. K. U. Gross, Phys. Rev. Lett. **52**, 997 (1984).
- [93] G. Onida, L. Reining, and A. Rubio, Rev. Mod. Phys. **74**, 601 (2002).
- [94] L. Hedin, Phys. Rev. **139**, A796 (1965).
- [95] G. Strinati, Rivista del Nuovo Cimento **11** (1988).
- [96] M. Gatti, Ph.D. thesis, Ecole Polytechnique (2007).
- [97] E. E. Salpeter and H. A. Bethe, Phys. Rev. **84**, 1232 (1951).
- [98] L. Reining, V. Olevano, A. Rubio, and G. Onida, Phys. Rev. Lett. **88**, 066404 (2002).
- [99] S. Botti, F. Sottile, N. Vast, V. Olevano, L. Reining, H.-C. Weissker, A. Rubio, G. Onida, R. D. Sole, and R. W. Godby, Phys. Rev. B **69**, 155112 (2004).
- [100] H. Ehrenreich, in *The Optical Properties of solids*, edited by J. Tauc (Academic, New York, 1966), Proceedings of the International School of Physics "Enrico Fermi", p. 106.
- [101] C. Brouder and S. Rossano, Eur. Phys. J. B **45**, 19 (2005).
- [102] R. Del Sole and E. Fiorino, Phys. Rev. B **29**, 4631 (1984).
- [103] D. Pines and P. Nozieres, *The Theory of Quantum Liquids*, vol. I (Addison-Wesley, New York, 1989).
- [104] J. D. Jackson *Classical Electrodynamics* (Wiley, 1998) .

- [105] P. Romaniello, Ph.D. thesis, Rijksuniversiteit Groningen (2006).
- [106] E. Cancès and M. Lewin, *Arch. Rational Mech. Anal.* **197**, 139 (2010).
- [107] P. M. Platzmann and P. A. Wolff, *Waves and Interactions in Solid State Plasma* (Academic Press, New York, 1973).
- [108] O. V. Dolgov and E. G. Maksimov, in *The Dielectric Function of Condensed Systems*, edited by L. V. Keldysh, D. A. Kirzhnits, and A. A. Maradudin (North-Holland, Amsterdam, 1989), Modern Problems in Condensed Matter Sciences.
- [109] F. Nastos, B. Olejnik, K. Schwarz, and J. E. Sipe, *Phys. Rev. B* **72**, 045223 (2005).
- [110] H. J. Monkhorst and J. D. Pack, *Phys. Rev. B* **13**, 5188 (1976).
- [111] S. Albrecht, Ph.D. thesis, Ecole Polytechnique (1999).
- [112] J. A. Berger, Ph.D. thesis, Rijksuniversiteit Groningen (2006).
- [113] G. Vignale and W. Kohn, *Phys. Rev. Lett.* **77**, 2037 (1996).
- [114] G. Vignale, *Phys. Rev. B* **70**, 201102 (2004).
- [115] M. Gatti (to be published)(2011).
- [116] N. Bloembergen, *Applied Physics B: Lasers and Optics* **68**, 289 (1999).
- [117] M. Falasconi, L. C. Andreani, A. M. Malvezzi, M. Patrini, V. Mulloni, and L. Pavesi, *Surface Science* **481**, 105 (2001).
- [118] Y. Shen, *Applied Physics B: Lasers and Optics* **68**, 295 (1999).
- [119] J. E. Sipe, D. J. Moss, and H. M. van Driel, *Phys. Rev. B* **35**, 1129 (1987).
- [120] P. Guyot-Sionnest, W. Chen, and Y. R. Shen, *Phys. Rev. B* **33**, 8254 (1986).
- [121] P. Guyot-Sionnest and Y. R. Shen, *Phys. Rev. B* **38**, 7985 (1988).
- [122] H. J. Peng, E. J. Adles, J.-F. T. Wang, and D. E. Aspnes, *Phys. Rev. B* **72**, 205203 (2005).
- [123] S. A. Yang, X. Li, A. D. Bristow, and J. E. Sipe, *Phys. Rev. B* **80**, 165306 (2009).
- [124] D. E. Aspnes, *physica status solidi (b)* **247**, 1873 (2009).
- [125] V. M. Agranovich and V. L. Ginzburg, *Crystal Optics with Spatial Dispersion and Excitons*, Springer Series in Solid State Science (Springer, Berlin, 1984).
- [126] C. Giacovazzo, H. Monaco, G. Artioli, D. Viterbo, G. Ferraris, G. Gilli, G. Zanotti, and M. Catti, *Fundamentals of Crystallography*, IUCr Texts in Crystallography (Oxford University Press, Oxford, 2002).

- [127] P. S. Pershan, Phys. Rev. **130**, 919 (1963).
- [128] N. Bloembergen, R. K. Chang, S. S. Jha, and C. H. Lee, Phys. Rev. **174**, 813 (1968).
- [129] J. H. Burnett, Z. H. Levine, E. L. Shirley, and J. H. Bruning, Journal of Microlithography, Microfabrication, and Microsystems **1**, 213 (2002).
- [130] T. A. Driscoll and D. Guidotti, Phys. Rev. B **28**, 1171 (1983).
- [131] H. Hübener, E. Luppi and V. Véniard, (to be published) (2011).
- [132] W. R. L. Lambrecht, S. Limpijumnong, S. N. Rashkeev, and B. Segall, physica status solidi (b) **202**, 5 (1997).
- [133] J. Chen, Z. H. Levine, and J. W. Wilkins, Phys. Rev. B **50**, 11514 (1994).
- [134] J. Chen, L. Jönsson, J. W. Wilkins, and Z. H. Levine, Phys. Rev. B **56**, 1787 (1997).
- [135] B. Adolph and F. Bechstedt, Phys. Rev. B **62**, 1706 (2000).
- [136] X. Gonze *et al.*, <http://www.abinit.org>.
- [137] N. Troullier and J. L. Martins, Phys. Rev. B **43**, 1993 (1991).
- [138] O. A. von Lilienfeld and P. A. Schultz, Phys. Rev. B **77**, 115202 (2008).
- [139] S. Bergfeld and W. Daum, Phys. Rev. Lett. **90**, 036801 (2003).
- [140] S. Botti and *et al.*, Phys. Rev. B **72**, 125203 (2005).
- [141] B. F. Levine and C. G. Bethea, Appl. Phys. Lett. **20**, 272 (1972).
- [142] D. A. Roberts, IEEE, J. Quantum Electron, **28**, 2057 (1992).
- [143] D. Aspnes and A. A. Studna, Phys. Rev. B **27**, 985 (1983).
- [144] A. Schleife, C. Rödl, F. Fuchs, J. Furthmüller, and F. Bechstedt, Phys. Rev. B **80**, 035112 (2009).
- [145] M. Gatti, I. V. Tokatly, and A. Rubio, Phys. Rev. Lett. **104**, 216404 (2010).
- [146] M. Palumbo, C. Hogan, F. Sottile, P. Bagala, and A. Rubio, The Journal of Chemical Physics **131** (2009).
- [147] M. Gatti, V. Olevano, L. Reining, and I. V. Tokatly, Phys. Rev. Lett. **99**, 057401 (2007).
- [148] G. Baym and L. P. Kadanoff, Phys. Rev. **124**, 287 (1961).

- [149] S. Boffi, *Da Heisenberg a Landau, Introduzione alla fisica dei sistemi a molte particelle*, Quaderni di fisica teorica (Bibliopolis, 2004).
- [150] W. Hanke and L. J. Sham, Phys. Rev. Lett. **43**, 387 (1979).
- [151] F. Sottile, Ph.D. thesis, Ecole Polytechnique (2003).
- [152] W. Nolting, *Viel-Teichen-Theorie*, vol. 7 of *Grundkurs Theoretische Physik* (Springer, Berlin, 2005).
- [153] F. Bruneval, Ph.D. thesis, Ecole Polytechnique (2005).
- [154] W. G. Aulbur, L. Jönsson, , and J. W. Wilkins, Solid State Phys. **54** (2006).